

CHARACTERIZATION OF REACTANTS, REACTION MECHANISMS, AND REACTION
PRODUCTS IN ATMOSPHERIC WATER DROPLETS:
Fog, Cloud, Dew, and Rain Water Chemistry

Final Report
ARB Contract No. A2-048-32

by

Michael R. Hoffmann, Daniel J. Jacob, Jed M. Waldman, J. W. Munger, and
Richard C. Flagan

Environmental Engineering Science
W. M. Keck Laboratories
California Institute of Technology
Pasadena, California 91125

April 1985

The statements and conclusions in this report are those of the contractor and not necessarily those of the California Air Resources Board. The mention of commercial products, their source or their use in connection with material reported herein is not to be considered as either an actual or implied endorsement of such products.

ABSTRACT

This report is a summary of our findings from a two-year study of the chemical composition of fogwater in California. Fogwater was sampled at a number of sites with a rotating arm collector, which was developed in our laboratory and collects representative samples. Field investigations in the Los Angeles basin, the San Gabriel Mountains, and the San Joaquin Valley revealed very high ionic concentrations in polluted fogs, often coupled with very high acidities. Fogs and stratus in the Los Angeles basin typically had pH values ranging from 2 to 4. Acidities were not as high in the San Joaquin Valley, mostly because of scavenging by the fogs of ammonia from agricultural sources. We showed that fogwater deposits efficiently on surfaces during fog events; this deposition was observed to be an important pollutant sink during stagnation episodes in the San Joaquin Valley, but at the same time it could be an important source of acid input to surfaces in some areas. By comparing our data to previous case studies of health-threatening pollution events, we find evidence that suspended "acid fog" can constitute a hazard to public health.

Insight into the oxidation of S(IV) to S(VI), which is the major aqueous-phase source of acidity, was gained from field data, laboratory studies, and model development. Kinetic experiments showed that H_2O_2 was an important oxidant at low pH, and we predicted that metal-catalyzed autoxidation could also be an important source of sulfate. However, we found that the extreme acidities observed in fogs (below pH 3) require condensation on preexistent acidic nuclei and scavenging of gaseous nitric acid. Stabilization of S(IV) in the fog was observed, and this was attributed to the formation of S(IV)-aldehyde adducts.

TABLE OF CONTENTS

<u>Section</u>	<u>Title</u>	<u>Page</u>
Abstract		i
List of Figures		ii
List of Tables		xi
Chapter I	RESEARCH OBJECTIVES AND ACCOMPLISHMENTS	I-1
Chapter II	OVERVIEW, RESULTS, AND DISCUSSION	II-1
Chapter III	RECOMMENDATIONS FOR FUTURE RESEARCH	III-1
Chapter IV	REFERENCES	IV-1
Appendix I	CHEMICAL COMPOSITION OF FOGWATER COLLECTED ALONG THE CALIFORNIA COAST	I-1
Appendix II	FOGWATER CHEMISTRY IN AN URBAN ATMOSPHERE	II-1
Appendix III	KINETICS AND MECHANISMS OF THE CATALYTIC OXIDATION OF DISSOLVED SULFUR DIOXIDE IN AQUEOUS SOLUTION: AN APPLICATION TO NIGHT- TIME FOG WATER CHEMISTRY	III-1
Appendix IV	A DYNAMIC MODEL FOR THE PRODUCTION OF H^+ , NO_3^- , and SO_4^{2-} IN URBAN FOG	IV-1
Appendix V	ACID FOG/COMMENT ON ACID FOG	V-1
Appendix VI	A FIELD INVESTIGATION OF PHYSICAL AND CHEMICAL MECHANISMS AFFECTING POLLUTANT CONCENTRATIONS IN FOG DROPLETS	VI-1
Appendix VII	AEROSOL COMPOSITION IN A STAGNANT AIR MASS IMPACTED BY DENSE FOGS	VII-1
Appendix VIII	THE OCCURRENCE OF BISULFITE-ALDEHYDE ADDITION PRODUCTS IN FOG- AND CLOUDWATER	VIII-1
Appendix IX	CHEMICAL CHARACTERIZATION OF STRATUS CLOUD- WATER AND ITS ROLE AS A VECTOR FOR POLLUTANT DEPOSITION IN A LOS ANGELES FOREST	IX-1
Appendix X	FOGWATER COLLECTOR DESIGN AND CHARACTERIZATION	X-1

TABLE OF CONTENTS
(continued)

<u>Section</u>	<u>Title</u>	<u>Page</u>
Appendix XI	KINETICS AND MECHANISM OF THE OXIDATION OF AQUATED SULFUR DIOXIDE BY HYDROGEN PEROXIDE AT LOW pH	XI-1
Appendix XII	KINETICS AND MECHANISM OF THE FORMATION OF HYDROXYMETHANESULFONIC ACID AT LOW pH	XII-1

LIST OF FIGURES

<u>Figure</u>		<u>Page</u>
Appendix I		
1	Fogwater sampling sites.	I-22
2a	Fogwater concentrations at Del Mar. pH Values and liquid water contents (g m^{-3} , in parentheses) are indicated on top of each data bar.	I-23
2b	Source contributions to the fogwater loading at Del Mar; contributions from soil dust, fly ash, and exhaust were not determined for the last sample.	I-24
Appendix II		
1	Map of fog sampling sites in Southern California. Los Angeles area sites are indicated on the inset.	II-2
2	A schematic flow diagram indicating fog sample-handling protocol and analytical procedures.	II-3
3	Ionic composition as a function of time in sequential fog samples. Sampling interval is indicated by the width of each bar. The times of fog formation and dissipation are indicated by arrows.	II-6
4(a-h)	Nondimensional concentrations of individual ions in fog collected on December 7-8, 1981, at the Lennox sampling site.	II-7
5(a-h)	Nondimensional concentrations of individual ions in fog collected on November 23-24, 1981, at the Pasadena sampling site.	II-8
6	A schematic diagram depicting the temperature and humidity dependence for fog formation and the apparent link between atmospheric gas phase and water phase chemistry.	II-9
7	Plot of nitrate and sulfate equivalent concentrations in fogwater. Dashed lines indicate 2.5:1 and 1:1 ratios.	II-10
8	Plot of sodium and chloride concentrations. Dashed line indicates the NaCl ratio in seawater.	II-10

LIST OF FIGURES (continued)

<u>Figure</u>		<u>Page</u>
Appendix III		
1	Schematic representation of the proposed catalytic reaction mechanism starting with the Co(II)-TSP sulfite complex as the active catalytic center.	III-12
2	Speciation of Fe(III) vs pH in aqueous solution as a function of the stability constant $FeSO_3^+$ as determined with SURFEQL. Other species that form are listed on the right side of the figure.	III-23
3	Speciation of S(IV) vs pH for the conditions on the far right of the figure as determined by SURFEQL.	III-23
4	Speciation of Fe(III) perturbed by iron(III)oxalato complexes as a function of pH and stability constant (β_1) of the $FeSO_3^+$.	III-24
5	Speciation of Fe(III), S(IV), Cu(II) and Mn(II) in fog water as a function of pH.	III-24
6	Sulfate formed, pH and total S(IV) for the fog water as a function of time after fog formation, under conditions typical of the Los Angeles atmosphere.	III-29
7	Sulfate formed and pH for the fog water as a function of time after fog formation, when $Fe^{3+} = 20 \mu eq-L^{-1}$ and $Mn^{2+} = 1 \mu eq-L^{-1}$ which are the lows observed in the Los Angeles fog water, or when no synergism for iron- and manganese-catalyzed oxidation mechanisms is considered.	III-29
8	Sulfate formed and pH for the fog water as a function of time after fog formation, when $H_2O_2 = 5$ ppb in the pre-fog gas phase, or when the temperature is 25 C.	III-30
9	Sulfate formed and pH for the fog water as a function of time after fog formation, when condensation takes place on HNO_3 ACCN, or on NaOH ACCN.	III-30
10	Sulfate formed, pH and nitrate for the fog water as a function of time after fog formation when ozone is in excess of NO , and sulfate formed under conditions of a NO_x -free atmosphere.	III-31

LIST OF FIGURES (continued)

<u>Figure</u>		<u>Page</u>
	Appendix IV	
1(a,b)	(a) Profile versus time of total sulfate in the fog-water and of the individual contributions to the total sulfate aerosol and different S(IV) oxidants. (b) Profile of pH versus time.	IV-5
2(a,b)	(a) Speciation of Fe(III) in the fogwater as a function of time under conditions of Table 3, with liquid water content = 0.1 g m^{-3} and temperature = 10°C . (b) Speciation of Mn(II) in the fogwater as a function of time under conditions of Table 3, with liquid water content = 0.1 g m^{-3} and temperature = 10°C .	IV-5
3(a,b)	(a) Concentrations of S(IV) species in the fogwater as a function of time under conditions of Table 3, with liquid water content = 0.1 g m^{-3} and temperature = 10°C . (b) Same as (a) but with no formaldehyde in the atmosphere.	IV-6
4(a,b)	Profile versus time of total sulfate and of the individual contributions to the total sulfate of sulfate aerosol and different S(IV) oxidants. (b) Profile of pH versus time.	IV-6
5	Concentration of S(IV) species in the fogwater as a function of time.	IV-7
6(a,b)	(a) Profile versus time of total sulfate and of the individual contributions to the total sulfate of sulfate aerosol and different S(IV) oxidants. (b) Profile of pH versus time.	IV-7
7	Speciation of Fe(III) in the fogwater as a function of time under conditions of Table 3, with liquid water content = 0.1 g m^{-3} and temperature = 1°C .	IV-7
8	Concentrations of S(IV) species in the fogwater as a function of time under conditions of Table 3, with liquid water content = 0.1 g m^{-3} and temperature = 1°C .	IV-8
9	Liquid water content profile versus time chosen for the simulation of a fog event in the Los Angeles basin.	IV-8
10(a-c)	Profiles versus time of the concentrations of the major ions in the fogwater under conditions of Table 3, with liquid water content as given in Figure 9 and temperature = 10°C . (a) Nitrate and ammonium ions. (b) Total sulfate and individual contributions of the different sulfate production mechanisms. (c) pH.	IV-9

LIST OF FIGURES (continued)

<u>Figure</u>		<u>Page</u>
11	Speciation of Fe(III) in the fogwater as a function of time under conditions of Table 3, with liquid water content as given in Figure 9 and temperature = 10°C.	IV-10
12	Concentrations of S(IV) species in the fogwater as a function of time under conditions of Table 3, with liquid water content as given in Figure 9 and temperature = 10°C.	IV-10
Appendix VI		
1	The Central Valley of California.	VI-2
2	Evolution of fogwater concentrations over the course of the 7 January 1983 fog event at Bakersfield.	VI-5
3	Fogwater and aerosol loadings of NH_4^+ , NO_3^- , SO_4^{2-} , and H^+ (fogwater) measured at Bakersfield during the period 30 December 1982 - 15 January 1983.	VI-6
4	Evolution of fogwater ionic loadings over the course of the 7 January fog event.	VI-7
5	Frequency distribution of the pseudo first-order rate constant for S(VI) in-fog production, $k(\% \text{ h}^{-1})$.	VI-10
6	Evolution of the sulfate equivalent fraction in the fogwater and in the aerosol at Bakersfield during the period 30 December 1982 - 15 January 1983.	VI-10
7	pH frequency distribution for $n = 108$ fogwater samples collected at Bakersfield during the period 30 December 1982 - 15 January 1983. Results are compared to those obtained in the Los Angeles basin for fogs ($n = 45$) and stratus clouds ($n = 156$).	VI-11
8	Frequency distribution of the non-neutralized fraction of the acidity, as expressed by $[\text{H}^+]/([\text{NO}_3^-]+[\text{SO}_4^{2-}])$, for $n = 108$ fogwater samples collected at Bakersfield during the period 30 December 1982 - 15 January 1983.	VI-12

LIST OF FIGURES (continued)

<u>Figure</u>		<u>Page</u>
Appendix VII		
1	Fogwater and aerosol loadings of NH_4^+ , NO_3^- , SO_4^{2-} and H^+ measured at Bakersfield during December 1982 - January 1983.	VII-13
2	Evolution of fogwater loadings over the course of the 7 January 1983 fog event.	VII-14
3	Evolution of the sulfate equivalent fraction in the fogwater and in the aerosol at Bakersfield during December 1982 - January 1983.	VII-15
4	Fog and aerosol sampling network (winter 1983-1984).	VII-16
5	Aerosol sampling set-up.	VII-17
6	Fogwater concentrations and liquid water contents at four sites during the 7 January 1984 fog.	VII-18
7	Average fogwater loadings at four sites for the 7 January 1984 fog.	VII-19
8	Evolution of the sulfate equivalent fraction in the McKittrick fogwater during December 1983 - January 1984.	VII-20
Appendix VIII		
1(a)	Equilibrium concentrations of S(IV) with and without CH_2O present for two temperatures and two pH values. 10°C is typical of Los Angeles area fog and cloudwater. 10 ppb is an upper limit for 24-hour average CH_2O concentrations.	VIII-9
1(b)	Equilibrium concentrations of S(IV) with and without CH_2O present for two temperatures and two pH values. 0°C is typical of Bakersfield fog. 10 ppb is an upper limit for 24-hour average CH_2O concentrations.	VIII-9
2(a)	Concentrations of CH_2O in equilibrium with 10 ppb CH_2O in the gas phase with and without adduct formation for two temperatures and two pH values. 10°C is typical of Los Angeles area fog and cloudwater. 10 ppb is an upper limit for 24-hour average CH_2O concentrations.	VIII-10
2(b)	Concentrations of CH_2O in equilibrium with 10 ppb CH_2O in the gas phase with and without adduct formation for two temperatures and two pH values. 0°C is typical of Bakersfield fog. 10 ppb is an upper limit for 24-hour average CH_2O concentrations.	VIII-10

LIST OF FIGURES (continued)

<u>Figure</u>		<u>Page</u>
3(a,b)	S(IV) vs. CH ₂ O in fog- and cloudwater. Bakersfield (A), Los Angeles area stratus clouds (B). The line indicates equal concentrations of S(IV) and CH ₂ O.	VIII-11
4	"Excess" S(IV) vs. measured S(IV) in Bakersfield fog-water samples. "Excess" S(IV) is the difference between measured S(IV) and "free" S(IV) (see text). The dashed line indicates equal values for excess and measured S(IV) (i.e., no free S(IV)).	VIII-13
5	S(IV) vs. CH ₂ O in Bakersfield samples at the time of collection and after one month of storage at 4°C without preservatives. The line indicates equal concentrations of S(IV) and CH ₂ O.	VIII-14
Appendix IX		
1	Schematic showing main processes affecting pollutant deposition in a Los Angeles pine forest.	IX-34
2	Profile of southwestern Mount Wilson slope showing location of sampling site.	IX-35
3	Ionic balances for cloudwater samples of 1982 and 1983.	IX-36
4	Concentrations of nitrate versus sulfate measured in cloudwater samples of 1982 and 1983.	IX-37
5	Histogram of pH frequency of cloudwater samples (both seasons); volume-weighted average [H ⁺] for rainfalls are also shown.	IX-38
6	Free acidity (i.e., [H ⁺]) versus sum of nitrate and sulfate concentrations measured in cloudwater samples of 1982 and 1983.	IX-39
7	Ambient aerosol compositions for June 10-11, 1983.	IX-40
8(a-c)	(a) Concentration, (b) LWC, and (c) solute loading for sequential cloudwater samples on June 12, 13, and 17, 1982.	IX-41
9	Same as Figure 8 for samples on June 11 and 12, 1983.	IX-42
10(a-c)	LWC measurement data for June 11, 1983 for three methods: (a) OPC size spectra, (b) CO ₂ laser transmissometer, and (c) RAC collection rate.	IX-43

LIST OF FIGURES (continued)

<u>Figure</u>		<u>Page</u>
Appendix X		
1(a,b)	(a) Typical urban aerosol size distribution profile. (b) Expected shift in the size distribution profile as a result of fog formation.	X-2
2	Caltech rotating arm collector.	X-3
3	Model rotating arm collector used in calibration experiment.	X-5
4	Calibration experiment set-up.	X-6
5	Collection efficiency of model collector vs. generalized Stokes number, for greased and ungreased impaction surfaces.	X-6
6	Collected water per m ³ of air sampled vs. liquid water content.	X-7
Appendix XI		
1	Dependence of k_{obsd} on pH for the oxidation of S(IV) by hydrogen peroxide at 15°C.	XI-2
2	Dependence of $\bar{k}_{obsd}[S(IV)]$ on the concentration of acetic acid for the oxidation of S(IV) by H ₂ O ₂ at pH 4.45; [S(IV)] = 10.0 and 20.0 mM for each point: (a) 6, (b) 15, (c) 21, (d) 30°C.	XI-3
Appendix XII		
1	Dependence of the observed pseudo-first order rate constant, k_{obsd} , on [S(IV)] at pH 2.5.	XII-2
2	Dependence of the observed pseudo-first order rate constant, k_{obsd} , on [CH ₂ O] _t at pH (-log [H ⁺]) 0.0, 0.3, 0.6, and 1.0.	XII-3
3	Dependence of the observed pseudo-second order rate constant, $k_{obsd}/[CH_2O]_t$, on [H ⁺] ⁻¹ over the pH range 0-1.	XII-3

LIST OF FIGURES (continued)

<u>Figure</u>		<u>Page</u>
4	Dependence of the observed pseudo-second order rate constant, $k_{obsd}/[CH_2O]_t$, on $[H^+]^{-1}$ over the pH ($-\log [H^+]$) range 2.5 to 3.4.	XII-3
5	Dependence of $k_{obsd}[H^+]/[CH_2O]_t$ on the concentration of chloroacetate and formate buffers.	XII-3
6	Dependence of $k_{obsd}/\alpha_1[CH_2O]_t (= v/[HSO_3^-][CH_2O]_t)$ on pH ($-\log [H^+]$).	XII-4
7	Dependence of $k_{obsd}/\alpha_1[CH_2O]_t (= v/[HSO_3^-][CH_2O]_t)$ on $K_{a2}/[H^+]$ over the pH ($-\log [H^+]$) range 2.5 - 3.4.	XII-4
8(a,b)	(a) Temperature dependencies of the intrinsic rate constant, k_1 , for the nucleophilic addition of bisulfite ion to formaldehyde. (b) Temperature dependencies of the intrinsic rate constant, k_2 , for the nucleophilic addition of sulfite ion to formaldehyde.	XII-5
9(a,b)	(a) Structures postulated for the activated complexes formed by the nucleophilic addition of bisulfite. (b) Structures postulated for the activated complexes formed by the nucleophilic addition of sulfite to formaldehyde.	XII-6
Chapter II		
1(a-d)	Cummulative bar diagrams for the major and minor chemical constituents in Los Angeles fog, clouds, rain, and mist.	II-3
2(a)	Evolution of fogwater concentrations over the course of a fog event at Bakersfield on 1-6 to 1-7-83.	II-5
2(b)	Fogwater and aerosol loadings of NH_4^+ , NO_3^- , SO_4^{2-} , and H^+ (fogwater) measured at Bakersfield during the period of 12-30-82 to 1-15-83.	II-6
3(a)	Frequency distribution of the pseudo first-order rate constant for S(VI) in-fog production, $k(\% \text{ hr}^{-1})$.	II-8
3(b)	Evolution of the sulfate equivalent fraction in the fogwater and in the aerosol at Bakersfield during the period 12-30-82 to 1-15-84.	II-9
4(a-d)	(a & b) Plots of observed aqueous phase S(IV) concentrations versus observed formaldehyde concentrations (c & d) Calculated equilibrium relationships for total aqueous phase S(IV) as functions of P_{SO_2} and P_{CH_2O} .	II-12

LIST OF FIGURES (continued)

<u>Figure</u>		<u>Page</u>
5(a,b)	Profile of concentration versus time of total sulfite in the fogwater and of the individual contributions to the total sulfate of sulfate aerosol and different S(IV) oxidants. (b) Profile of pH versus time. Liquid water content is 0.1 g m^{-3} , $T = 10.0^\circ\text{C}$.	II-17
6	Profiles versus time of the concentration of the major ions in fogwater given a typical LWC vs. time profile.	II-18
7	Histogram of pH frequency of cloudwater samples at Henninger Flats for 1982 and 1983.	II-20
8(a-c)	Concentration (a), LWC (b), and solute loading (c) for sequential cloudwater samples on June 12, 13, and 17, 1982.	II-21
9	Collection efficiency of model collector vs. generalized Stokes number for greased and ungreased impaction surfaces.	II-24

LIST OF TABLES

<u>Table</u>	Appendix I	<u>Page</u>
1	Description of sampling sites.	I-14
2	Source concentrations of particulate matter.	I-15
3	Liquid water-weighted average fogwater concentrations.	I-16
4	Source contributions to fogwater loading.	I-18
5	Equivalent ratios in coastal fogs.	I-19
6	Chemical equilibria of the $\text{NaCl-H}_2\text{SO}_4\text{-HNO}_3\text{-H}_2\text{O}$ system.	I-20
Appendix II		
1	Description of conditions during and before fog sample collection.	II-3
2	Concentration ranges for major and minor ions, sulfite, and formaldehyde observed during fog events.	II-4
3	Ranges of selected trace-metal concentrations in fog samples.	II-5
4	Equilibrium constants applicable to S(IV) and aldehyde chemistry.	II-9
5	Summary of fog and cloud water compositions	II-11
Appendix III		
1	Fog water composition in Southern California: observed concentration ranges [12-14].	III-2
2	Theoretical rate expressions obtained from the Bäckström mechanism for various termination steps.	III-4
3	Empirical rate laws reported by various investigators for the metal catalyzed autoxidation of SO_2 .	III-5
4	Theoretical rate expressions obtained from the Hayon et al. and Schmittkunkz mechanisms.	III-5
5	Rate expressions for limiting cases of the Bassett and Parker mechanism.	III-7
6	Empirical rate laws for Mn^{2+} -catalyzed autoxidation of S(IV) in aqueous solution.	III-8

LIST OF TABLES (continued)

<u>Table</u>		<u>Page</u>
7	Empirical rate laws for Fe^{3+} -catalyzed autoxidation of S(IV) in aqueous solution.	III-8
8	Empirical rate laws for Cu^{2+} -catalyzed autoxidation of S(IV) in aqueous solution.	III-11
9	Empirical rate laws for Co(III)/Co(II)-catalyzed autoxidation of S(IV).	III-11
10	Empirical rate laws for the oxidation of S(IV) by hydrogen peroxide.	III-18
11	Empirical rate laws for the oxidation of S(IV) by ozone.	III-20
12	Comparison of stability constants for metal-sulfite and -sulfate complexes at 25.0 C.	III-24
13	Equilibria and thermodynamic data considered in fog water model.	III-26
14	Atmospheric conditions for the fog events simulated by the model.	III-28

Appendix IV

1	Henry's Law and aqueous-phase equilibria relevant to the droplet chemistry.	IV-2
2(a,b)	(a) Kinetic expressions for the aqueous phase oxidation reactions of S(IV) to S(VI) and N(III) to N(V). (b) Reaction stoichiometries for reactions in Table 2(a).	IV-3
3	Composition of the air mass (trace gases and condensation nuclei) prior to fog formation at a polluted site.	IV-4
4	Scavenging of gases by fog droplets under conditions of Table 3.	IV-5
5	Scavenging of gases by fog droplets under conditions of Table 3.	IV-7

Appendix V

1	Fog/Smog Episodes.	V-3
---	--------------------	-----

Appendix VI

1	Fogwater concentrations at Bakersfield, California.	VI-4
2	SO_2 oxidation rates in the atmosphere	VI-10

LIST OF TABLES (continued)

<u>Table</u>		<u>Page</u>
Appendix VII		
1	SO ₂ oxidation rates in the atmosphere.	VII-11
2	Fogwater concentrations at McKittrick, California.	VII-12
Appendix VIII		
1	Atmospheric formaldehyde concentrations at selected sites.	VIII-2
2	Summary of reactions involved in the formation of aldehydes from hydrocarbon precursors.	VIII-2
3	Summary of reactions involved in aldehyde destruction.	VIII-3
4	Emissions of SO ₂ , NO _x , and reactive hydrocarbons in airsheds surrounding the sampling sites.	VIII-5
5	Concentration of S(IV) and CH ₂ O in fog- and cloudwater samples collected in California.	VIII-6
6	Concentrations of S(IV) and CH ₂ O on an air volume basis in fog- and cloudwater samples collected in California.	VIII-7
7	Equilibria and thermodynamic data.	VIII-7
Appendix IX		
1	Median and range of concentrations for cloudwater samples at Henninger Flats: 1982 and 1983.	IX-28
2	Chemical loading in aerosol samples at Henninger Flats: 1983	IX-29
3	Wet deposition - Henninger Flats - October 1982 to July 1983.	IX-30
4	Bulk deposition - Henninger Flats - May-July 1983	IX-32
5	Chemical composition of cloudwater removed from pine needles at Henninger Flats: 1982 and 1983.	IX-33
Appendix X		
1	Fogwater collectors reported in the literature.	X-2

LIST OF TABLES (continued)

<u>Table</u>		<u>Page</u>
	Appendix XI	
1	Kinetic data for the oxidation of S(IV) by hydrogen peroxide in the absence of buffer at 15°C.	XI-3
2	Kinetic data for the oxidation of S(IV) by hydrogen peroxide in the presence of buffers at 15°C.	XI-3
	Appendix XII	
1	Kinetic data for the reduction of S(IV) and formaldehyde in aqueous solution.	XII-2

CHAPTER I

A. RESEARCH OBJECTIVES

As a result of our initial Air Resources Board contract, "Characterization of Reactants, Reaction Mechanisms and Reaction Products Leading to Extreme Acid Rain and Acid Aerosol Conditions in Southern California," we discovered that fog water collected in Los Angeles and Bakersfield had higher concentrations of major chemical components than previously observed in atmospheric water droplets. The pH of fog water was found to be in the range of 2.2 to 4.0 with values around 3.0 typical. In light of these highly interesting findings, we felt that more research was needed to document the occurrence of acid fog in urban and non-urban areas. Of special interest was the interrelationship between smog and fog. In the Los Angeles Basin and the Southern San Joaquin Valley smog-derived aerosol particles were predicted to serve as suitable condensation nuclei for the formation of fog, and in turn as the fog droplets evaporate they should provide highly reactive surface sites for the catalytic conversion of SO_2 during the day following a fog event. Further research on fog chemistry and physics was planned to allow us to test various hypotheses about the primary reaction pathways for accumulation of acidity, nitrate, sulfate and ammonium ion in atmospheric water droplets. Since submicron water droplets are difficult to characterize in situ, fog and cloud water represent ideal systems for the characterization of heterogeneous reactions.

Specific research objectives were as follows:

1. To elucidate the fundamental mechanisms for the accumulation of acidity, sulfate, nitrate and ammonia in atmospheric water droplets.
2. To establish with a reasonable degree of certainty that an interrelationship between smog-derived aerosol and fog exists on a diurnal basis.
3. To document the occurrence of acid fog in other likely locations such as Santa Cruz, San Francisco, San Nicholas Island, Morro Bay, San Diego, and Santa Barbara.
4. To determine the relative role of below cloud-scavenging versus in situ transformation processes in clouds for the accumulation of acidity in raindrops.
5. To characterize the surface flux during non-precipitation moisture deposition such as mist, fog and dew.
6. To construct and calibrate refined fog water collection devices.
7. To develop a laser transmissometer for the measurement of liquid water content.
8. To improve and to employ analytical methods for the measurement of H_2O_2 , S(IV), and aldehydes in atmospheric water droplets.
9. To determine the fine aerosol composition before and after a fog event.
10. To apply suitable analytical methodologies for the analysis of gas phase HNO_3 and NH_3 before, during and after a fog event.
11. To develop physical, thermodynamic, and kinetic models for fog, cloud, and rain water chemistry.

B. SUMMARY OF MAJOR ACCOMPLISHMENTS, OBSERVATIONS, AND CONCLUSIONS

1. Fogwater collected at sites in the South Coast Air Basin was consistently acidic, with pH values typically ranging from 2 to 4. The highest acidities were observed during smog episodes. The main contributors to the acidity were nitric and sulfuric acids, with a typical equivalent ratio of 3:1. Secondary sulfate and nitrate aerosol accounted for over 80% of the fogwater loading.
2. Fogwater collected at non-urban coastal sites was usually acidic (pH range 3 to 7). Impact of emission centers on distant coastal locations was documented. The low alkalinity of marine atmospheres make them particularly susceptible to acidification. Oxidation of oceanic dimethylsulfide could be a natural source of sulfuric acid.
3. Stratus clouds collected at 2500' MSL over the Los Angeles Basin were consistently acidic, pH range 2 to 4. Cloudwater concentrations were in the same range as those observed in the basin itself.
4. Fogwater collected in the Southern San Joaquin Valley was not consistently acidic; pH values ranged from 2.5 to 7.5. Millimolar concentrations of sulfate were typically observed, but high ammonia emissions from livestock and cropland neutralized the acid input. Visalia, which is some distance from the major emission sources, had alkaline fogwater (pH 6 - 7.5). McKittrick, located in an oil field with little surrounding agricultural activity, had acidic fogwater (pH 2.5 - 4.5).

5. Liquid water content was the major factor affecting ionic concentrations in fogs. As the fog formed, droplet growth diluted the droplets; as the fog dissipated, the droplets became more concentrated.
6. Evidence was found for the major processes responsible for the acidification of fogwater: (i) the scavenging of acidic precursor aerosol, (ii) the scavenging of gaseous nitric acid, and (iii) oxidation of reduced sulfur components to sulfate. Conversion of $\text{SO}_2(\text{g})$ to sulfate in fogwater does not appear to proceed faster than $10\% \text{ hour}^{-1}$ and therefore cannot account for the high acidities observed at the beginning of fog events; however, sulfate production in the precursor air parcel can lead to sulfuric acid fog condensation nuclei.
7. Modeling of fogwater chemistry indicated that the high acidities observed can be explained by either of the three processes listed above. The main aqueous-phase S(IV) oxidants were found to be hydrogen peroxide, ozone, and oxygen (catalyzed by trace metals). Aqueous-phase production of nitrate was found to be unimportant.
8. The rotating arm collector designed in our laboratory and used to sample fogwater was fully characterized. Evaporation of droplets during all stages of collection was shown to be negligible. Experimental calibration indicated a lower size cut of 15-20 microns. Field data show an overall liquid water collection rate of about 60%. A field intercomparison of fogwater collectors used by various investigators confirmed that our sampler collects representative samples.

9. A screen collector (lower size cut 2 microns, sampling rate $20 \text{ m}^3 \text{ min}^{-1}$) was designed and used in the spring of 1984. Side-by-side comparison indicates that samples collected with this collector and with the rotating arm have similar concentrations.
10. Concentrations of S(IV) in fogwater were far in excess of those expected to be in equilibrium with ambient $\text{SO}_2(\text{g})$. Elevated formaldehyde concentrations suggest the formation of a formaldehyde-S(IV) complex; kinetic and model studies have shown that this complex is very stable and that its formation leads to high aqueous-phase S(IV) concentrations.
11. Extensive Bakersfield fogwater data indicated an important removal to the ground of pollutants scavenged by the fog droplets. This was ascribed to the short residence time of the supermicron fog droplets in the atmosphere. In a stagnant atmosphere this deposition was suspected to alleviate build-up of suspended particles. On the mountain slopes surrounding the Los Angeles Basin, such non-precipitating wet deposition was shown to be a significant source of overall pollutant deposition.
12. Concentrations of NH_4^+ , NO_3^- and SO_4^{2-} in urban fogwater samples are routinely on the order of 10^{-3} M .

13. The relative importance of NO_3^- and SO_4^{2-} reflects their emission pattern in the vicinity. Nitrate exceeds SO_4^{2-} by a factor of 2-3 in Los Angeles where vehicle emissions of NO_x are significant. Sulfate equals or exceeds nitrate in the Southern San Joaquin Valley where emissions from oil-production facilities are important.
14. Concentrations of S(IV) and CH_2O in fog and cloudwater on the order of 10^{-4} M are routinely found in urban areas. Peak values are about 10^{-3} M.
15. The solute loading (mass/ m^3 air) in fog is comparable to that in the aerosol.
16. The $\text{NO}_3^-/\text{SO}_4^{2-}$ ratio in fog is higher than in the dry aerosol proceeding the fog, which suggests that gaseous HNO_3 is incorporated into the fog.
17. Deposition from fog by sedimentation or impaction may be comparable to rainfall deposition at some mountain sites. Trees are very efficient collectors and are often bathed with impacted fog. Cloudwater impacting on LA mountain-slope vegetation routinely has a pH close to 3, which may be injurious to sensitive species.
18. In addition to formaldehyde, fog- and cloudwater contain a variety of higher aldehydes. Acetaldehyde and propanal (or acrolein) often have concentrations comparable to formaldehyde.
19. Low molecular weight carboxylic acids are present in fog and cloudwater at about 10^{-4} M. Formic and acetic acid dominate.

CHAPTER II

II. OVERVIEW, RESULTS, AND DISCUSSION

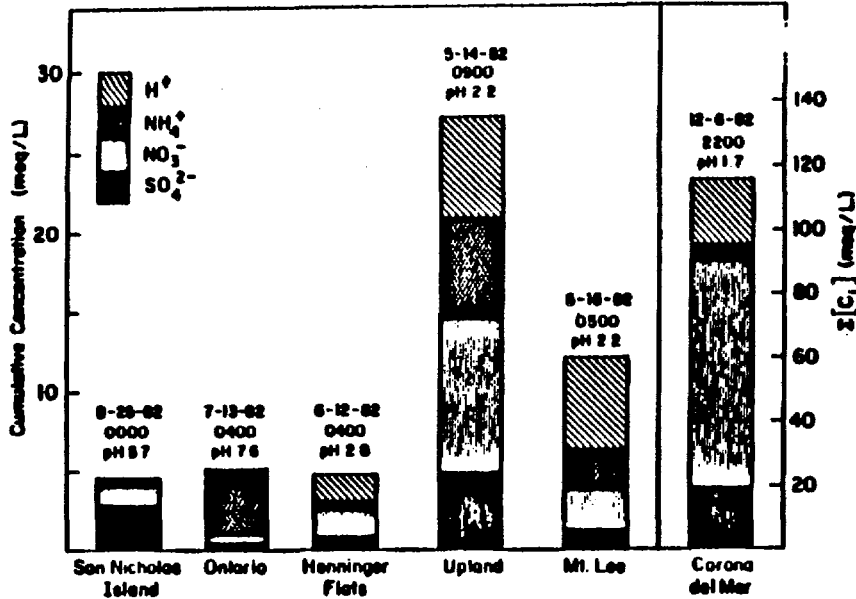
Sulfur dioxide (SO_2) and nitrogen oxides (NO_x) are oxidized to sulfate and nitrate aerosols either homogeneously in the gas phase or heterogeneously in atmospheric microdroplets and hydrometeors (Calvert et al., 1978; Middleton et al., 1980; Moeller, 1980; Cass and Shair, 1984; Schwartz, 1984). Gas-phase production of nitric acid appears to be the dominant source of aerosol nitrate because the aqueous phase reactions of $\text{NO}_x(\text{aq})$ are slow at the nitrogen oxide partial pressures typically encountered in the atmosphere (Schwartz, 1984; Schwartz and White, 1981). Conversely, field studies indicate that the relative importance of homogeneous and heterogeneous SO_2 oxidation processes depends on a variety of climatological factors such as relative humidity and the intensity of solar radiation (Cass and Shair, 1984; Cass, 1977; Gartrell et al., 1963; Smith and Jeffrey, 1975; Cox, 1974).

Cass (1977) has shown that the worst sulfate pollution episodes in Los Angeles occur during periods of high relative humidity and when the day begins with low clouds or fog in coastal areas, while Cass and Shair (1984) have reported that nighttime conversion rates (5.8%/hr) for SO_2 in the Los Angeles sea breeze/land breeze circulation system are statistically indistinguishable from typical daytime conversion rates (5.7%/hr) for the month of July. Zeldin et al. (1976) have reported a high correlation between relative humidity and sulfate when a marine layer covers the Los Angeles Basin. They surmized that marine layers provide an ideal climate for the conversion of sulfur dioxide to

sulfate. On certain days Zeldin et al. found high concentrations of both ozone and sulfate. A typical high sulfate-ozone day was described as a day with nighttime and early morning stratus clouds that enhance sulfate formation, followed by a sunny afternoon with sufficient radiation for the production of ozone by photochemical reactions. On these days the inversion strength was ≥ 7 °C with inversion bases between 250 and 750 m MSL. These results suggest that fog and low lying clouds may play an important role in the diurnal production of sulfate in the Los Angeles basin during certain times of the year. Results of these investigations with the data of Gartrell et al. (1963), Cox (1974), Smith and Jeffrey (1975), Dittenhoeffer and dePena (1978), Enger and Hogstrom (1979), Wilson and McMurry (1981), McMurry et al. (1981), Hegg and Hobbs (1981; 1983), Daum et al. (1984), and Jacob et al. (1984a) indicate that aqueous-phase oxidation of SO_2 is a significant pathway for the formation of acidic sulfate in the atmosphere.

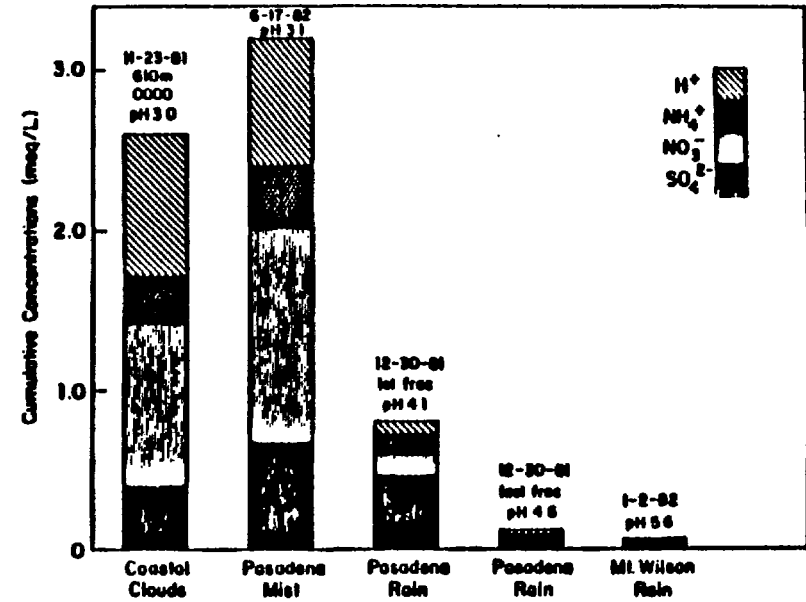
As part of our current research effort, we have characterized the chemistry of fog, cloud, dew, and rain at selected locations in California (Waldman et al., 1982, Jacob and Hoffmann, 1983; Munger et al., 1983; Jacob et al., 1984a). We have reported in the open literature that fog and cloud water often have extremely low pH values (e.g. $1.7 \leq \text{pH} \leq 4$) and extremely high concentrations of sulfate, nitrate, ammonium ion, and trace metals. A representative set of values reported by Waldman et al. (1982) and Munger et al. (1983) are illustrated in Figure 1. Of special interest are the high values observed for SO_4^{2-} , NO_3^- , S(IV), CH_2O , Fe, Mn, Pb and Cu in the fog water droplets. These values and their time-dependent changes (Jacob et al., 1984a) (Figure 2.) indicate that fogs provide a very reactive

Sites With Elevated Concentrations



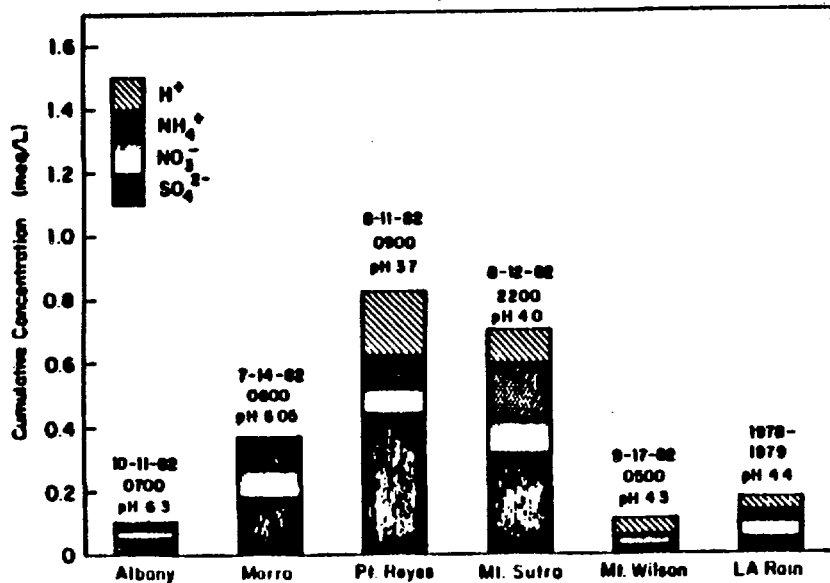
(a)

Comparative Concentrations



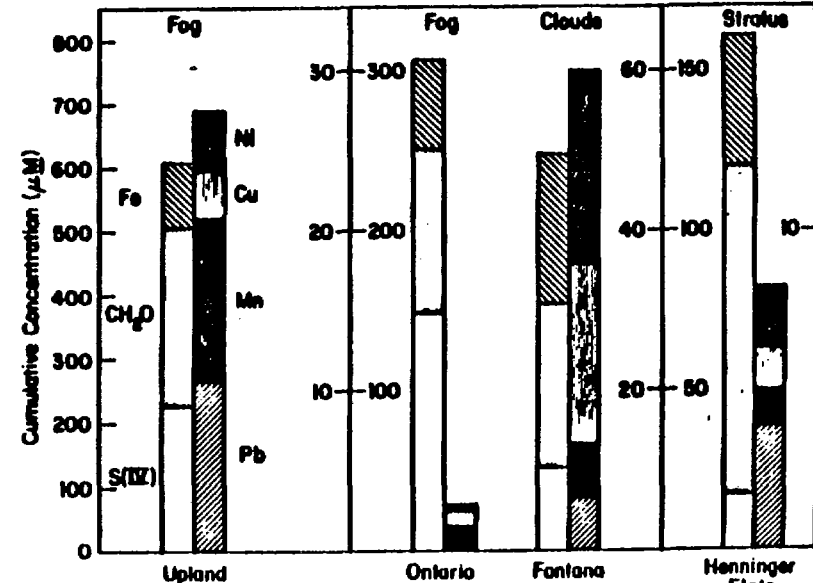
(b)

Moderately Clean Sites



(c)

Concentrations of Secondary Components



(d)

Figure 1a-d. Cumulative bar diagrams for the major and minor chemical constituents in Los Angeles fog, clouds, rain, and mist.

environment for the accumulation of HNO_3 and H_2SO_4 . Concomitant incorporation of NH_3 gas and calcareous dust into the droplet phase neutralizes some of the acidity. In the pH domain typically encountered in fogs and clouds (pH 2-7), absorption of $\text{SO}_2(\text{g})$, $\text{HNO}_3(\text{g})$, $\text{H}_2\text{O}_2(\text{g})$, and $\text{NH}_3(\text{g})$ is thermodynamically favorable because of their relatively high Henry's Law coefficients.

Because of their similarity to clouds with respect to physical characteristics, fogs are likely to reflect the same chemical processes occurring in clouds and to some degree in aqueous microdroplets. Cloud- and fog-water droplets are in the size range of 2 to 50 μm whereas deliquescent haze aerosol will be in the range of 0.01 to 1 μm . On the other hand, raindrops are approximately 100 times larger than cloud and fog droplets (e.g., 0.1 to 3 mm). In Los Angeles we have found that fog water was more concentrated in the primary constituents than the overlying cloud water which was in turn more concentrated than rain water during overlapping periods of time (see Figure 1a-d). Furthermore, Hegg and Hobbs (1981) have observed sulfate production rates in cloud water over Western Washington ranging from 4 to 300% hr^{-1} and pH values from 4.3 to 5.9. In a later study (1982), they reported even higher sulfate production rates in wave clouds (2 to 1,900 % hr^{-1}) over a pH range of 4.3 to 7.0. The sulfate production rate measured with respect to SO_2 in ambient air appeared to increase with an increase in pH. Martin (1983) has shown that the results of Hegg and Hobbs can be interpreted kinetically in terms of the open phase oxidation of S(IV) by O_3 in aqueous solution. Schwartz and Newman (1983) argued subsequently that because the inherent uncertainties in the conversion rates reported by Hegg and Hobbs were unduly large, the reported conversion rates were

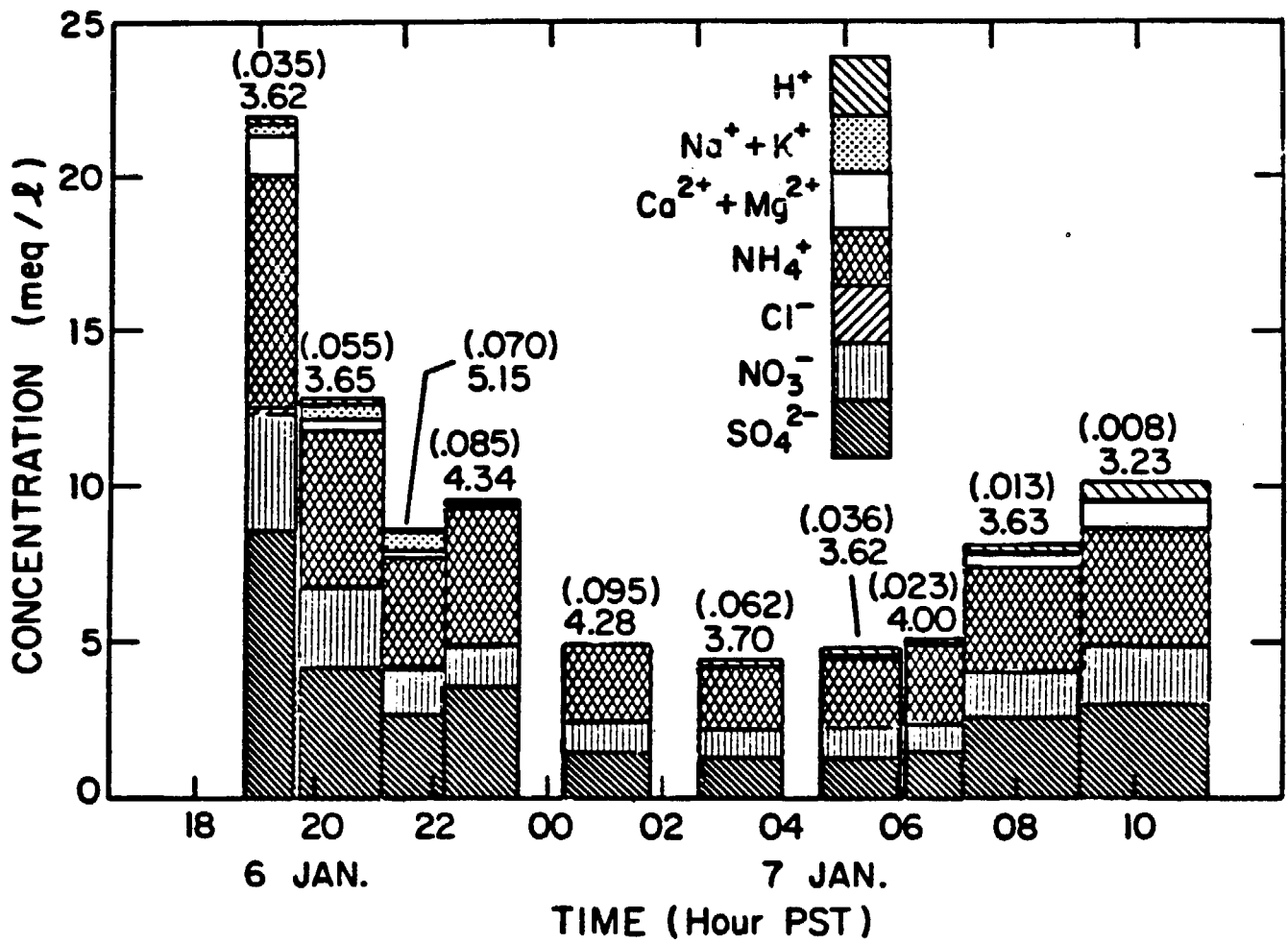


Figure 2a. Evolution of fogwater concentrations over the course of a fog event at Bakersfield on 1-6 to 1-7-83. Fogwater pH and average liquid content (LWC in g m^{-3}) is indicated on the top of each data bar.

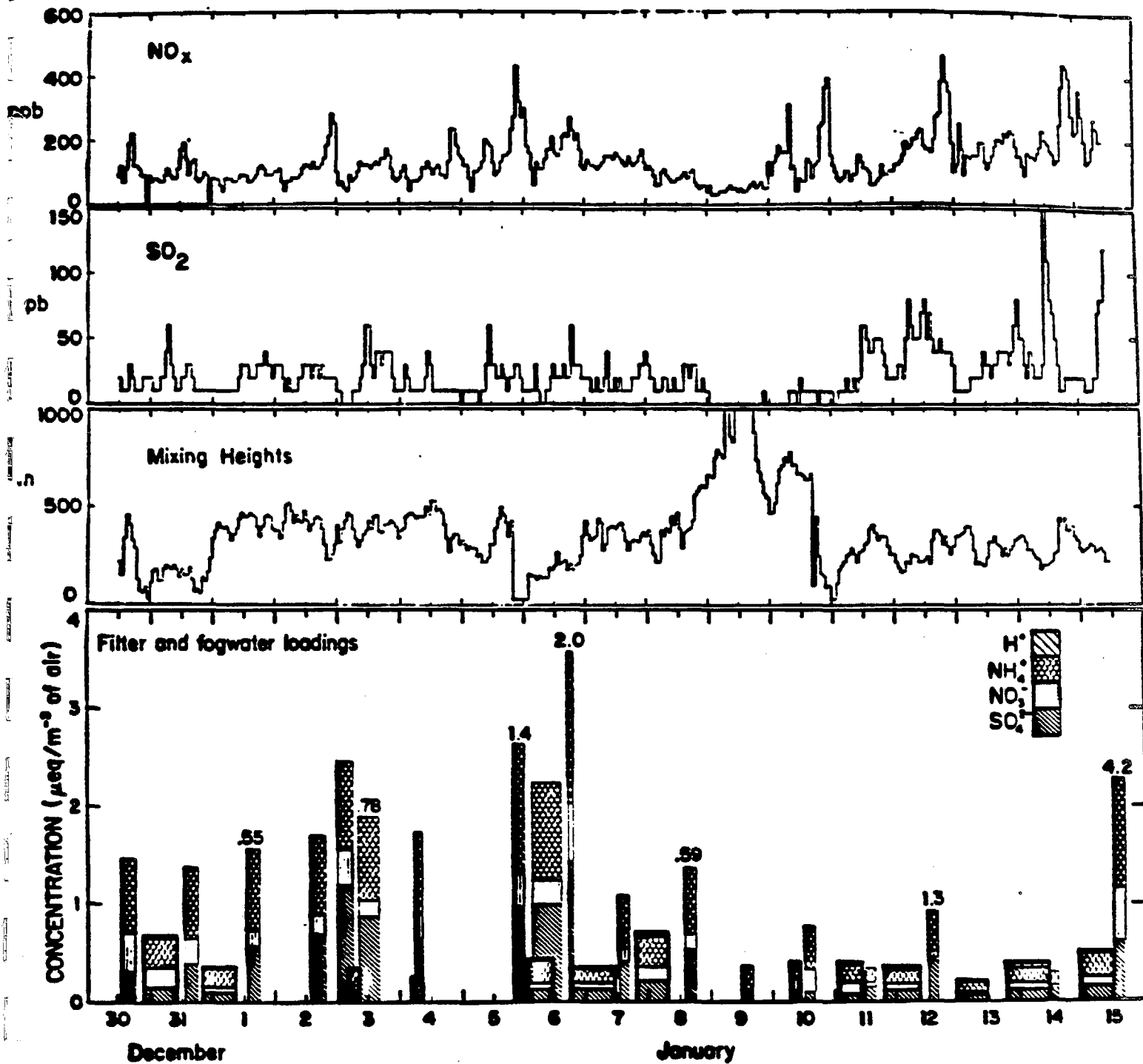


Figure 2b. Fogwater (in bold) and aerosol loadings of NH_4^+ , NO_3^- , SO_4^{2-} , and H^+ (fogwater) measured at Bakersfield during the period of 12-30-82 to 1-15-83. When measured, gaseous NH_3 concentrations (ppb, 1ppb = $0.044 \mu\text{moles m}^{-3}$ at 1.0°C) are indicated on top of the data bars. Mixing heights are given in meters above ground level.

statistically indistinguishable from zero (i.e., the reported data included negative conversion rates due to apparent sulfate loss with respect to time.) Similar observations were made by our research group (Jacob et al., 1984a,b) during "Tule" fog episodes in the San Joaquin Valley in the winters of 1982-1983 and 1983-1984. In Bakersfield, we found S(IV) conversion rates to be as high as 8%/hr at 0°C; however, a significant number of negative conversion rates were also observed such that the mean conversion rate was statistically indistinguishable from zero (Figure 3). Ancillary evidence, such as the increase in the sulfate equivalent fraction of the aerosol during the course of a pronounced stagnation episode supports the general notion of in situ sulfate production during fog and haze episodes in the San Joaquin Valley (Figure 3b). The observation of negative sulfate production rates indicates the relative importance of advection and mass transport in determining the observed fog and cloud water chemistry at a particular time and location. Current research efforts have been designed to address these problems.

Calvert (1984) has pointed out that gas-phase reactions of SO_2 with ozone (O_3), hydroxyl radical (OH^\bullet), and hydroperoxyl radical (HO_2^\bullet) are too slow to account for the aforementioned rates of sulfate production. Consequently, the catalytic autoxidation of SO_2 in deliquescent haze aerosol and hydrometeors has been proposed as a viable non-photolytic pathway for the rapid formation of sulfuric acid in humid atmospheres (Hegg and Hobbs, 1978; Beilke and Gravenhorst, 1978; Penkett et al., 1979b; Kaplan et al., 1981; Martin 1984). In addition, hydrogen peroxide (H_2O_2) and ozone have been given serious consideration as

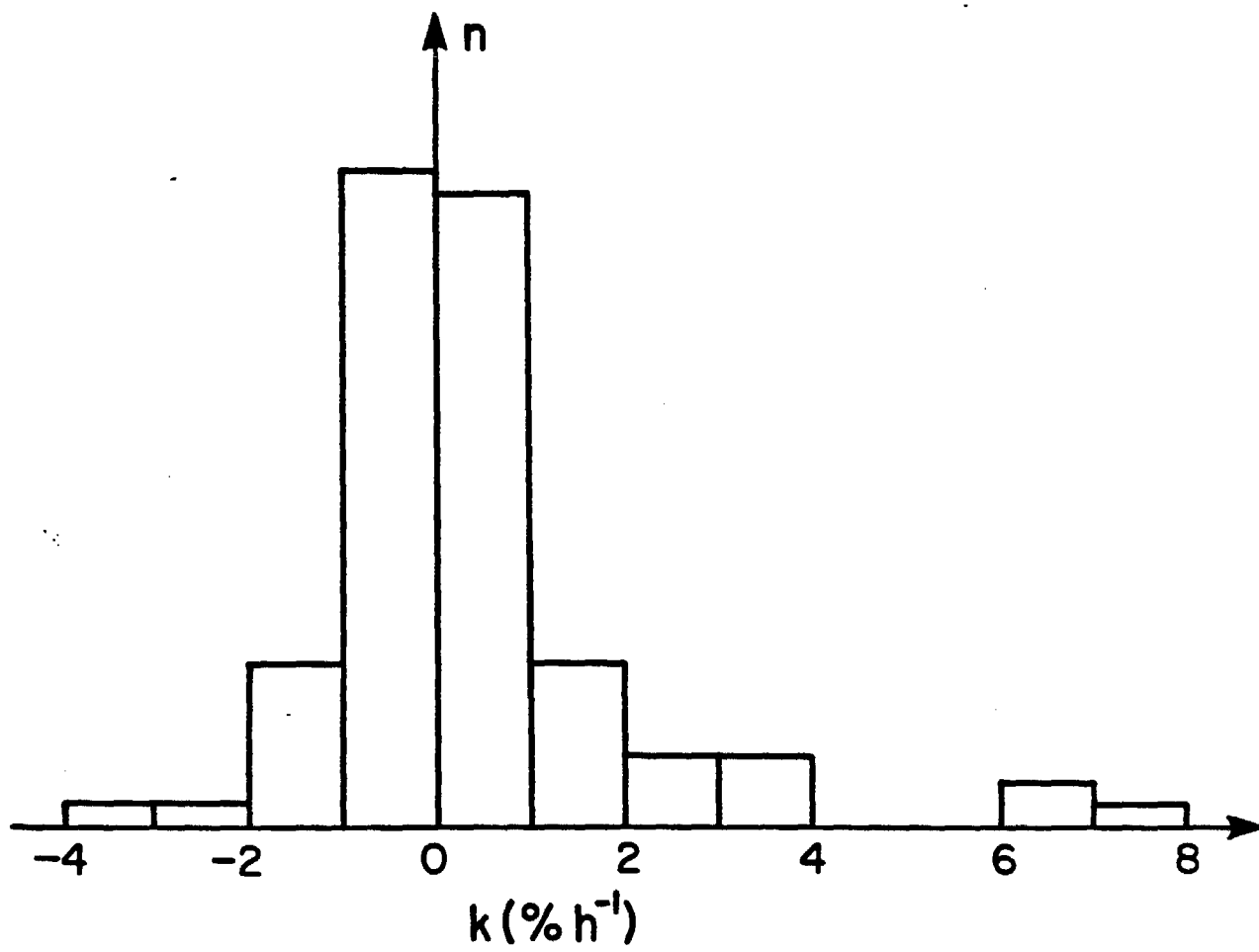


Figure 3a. Frequency distribution of the pseudo first-order rate constant for S(VI) in-fog production, k (% hr^{-1}). Data from $n = 80$ fogwater samples collected at Bakersfield during the period of 12-30-82 to 1-15-83.

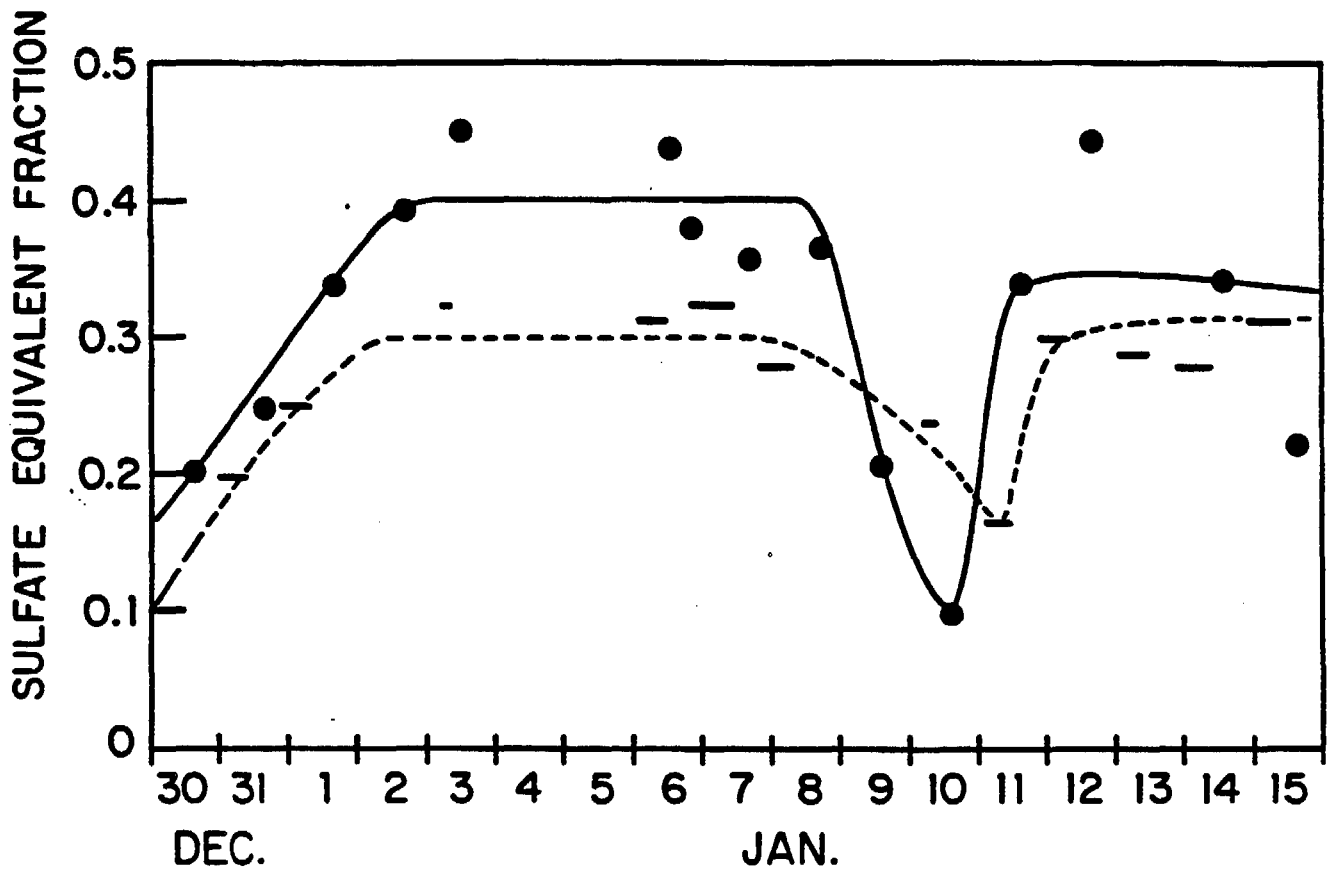


Figure 3b. Evolution of the sulfate equivalent fraction in the fogwater(-) and in the aerosol (•) at Bakersfield during the period 12-30-82 to 1-15-84. Lines have been added to show trends.

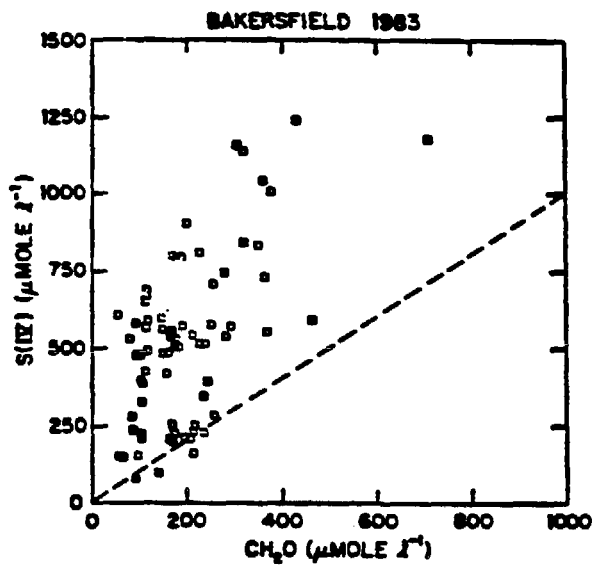
important aqueous-phase oxidants of dissolved SO_2 as discussed by Martin (1984). Oxidation by H_2O_2 seems to be most favorable under low pH conditions ($\text{pH} \leq 4$) because of a rapid rate of reaction and a negative pH-dependence that favors the facile conversion of HSO_3^- to sulfate. In comparison, the metal-catalyzed autoxidation and reaction of S(IV) with O_3 tend to proceed more slowly with decreasing pH (Martin et al., 1981).

Limiting factors in the autoxidation pathways are the total concentration of the active metal catalyst and its equilibrium speciation as a function of pH. Los Angeles fog water contains high concentrations of iron, manganese, copper, nickel and lead, as shown in Figure 1d. Of these metals, Fe, Mn and Cu are expected to be the most effective catalysts for the reaction of S(IV) with molecular oxygen (Jacob and Hoffmann, 1983; Martin, 1984; Hoffmann and Jacob, 1984). Observed concentrations of Fe and Mn in fog of $400 \mu\text{M}$ and $15 \mu\text{M}$, respectively, were not unusual (Munger, et al., 1983). Calculations based on the rate laws presented by Martin (1984) indicate that metal-catalyzed autoxidation may contribute significantly to the overall sulfate formation rate in atmospheric droplets, particularly in the range of Fe and Mn concentrations observed in urban fog (Jacob and Hoffmann, 1983; Hoffmann and Jacob, 1984).

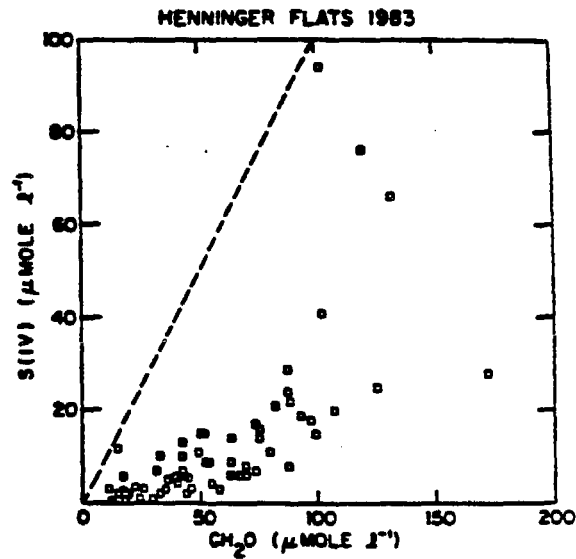
Carbonyl compounds, aldehydes and ketones, influence liquid-phase sulfur dioxide chemistry through their reactions with SO_2 to form stable α -hydroxyalkanesulfonates. Aldehydes are ubiquitous contaminants in the atmosphere. They exist at especially high concentrations ($24\text{-}58 \mu\text{g m}^{-3}$) in urban environments where vehicular emissions are a significant or even dominant source (Grosjean, 1982; NRC, 1981). In addition, aldehydes are generated via numerous pathways from a variety of

precursors present in both clean and polluted atmospheres. These include the oxidation of alkanes and alkenes by OH^\bullet and O_3 . Aldehydes are highly reactive species that decompose rapidly through photolytic and free-radical reactions. For example, the half-life of gaseous formaldehyde, $\text{CH}_2\text{O}(\text{g})$, in the atmosphere is fairly short (2-3 hours). However, dissolution of CH_2O and hydration to form methylene glycol, $\text{CH}_2(\text{OH})_2$, protects it from photolysis. Consequently, atmospheric droplets offer an ideal environment for sulfonic acid production.

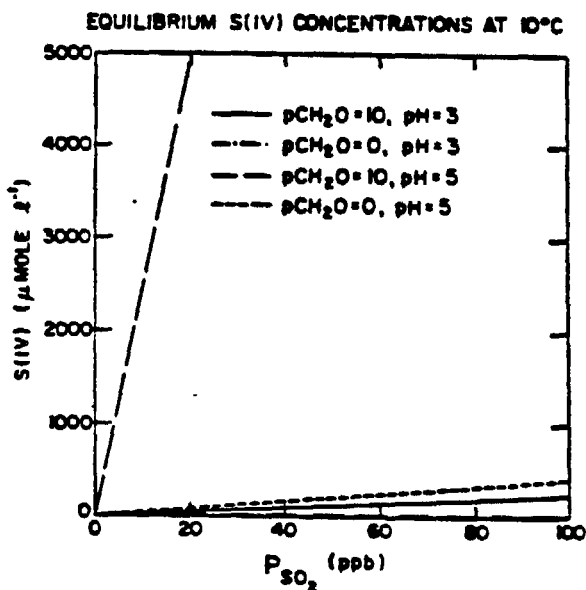
Field measurements have detected formaldehyde at concentrations of greater than $100 \mu\text{M}$ in fog- and cloud-water samples collected in Southern California (Munger et al., 1983; Grosjean and Wright, 1983; Richards et al., 1983; Munger et al., 1984) (see Figure 4a and b). The concentrations of acetaldehyde, propionaldehyde, propenal (acrolein), n-butanal, n-pentanal, n-hexanal, and benzaldehyde occasionally approached or exceeded that of CH_2O (Grosjean and Wright, 1983). Recent work in our laboratory has shown that formaldehyde, acetaldehyde, and propanal are present in urban fog water samples at roughly equal concentrations along with smaller amounts of higher aldehydes. In addition we have shown that for the low-molecular weight aldehydes the corresponding carboxylic acids are also present and that the aldehydes may be slowly oxidized upon standing to their respective carboxylic acids. Furthermore, the presence of CH_2O and H_2O_2 in conjunction with $\text{S}(\text{IV})$ at levels higher than those predicted by gas/liquid solubility equilibria suggests that hydroxymethanesulfonate (HMSA) production stabilizes a fraction of $\text{S}(\text{IV})$ with respect to oxidation (Richards, et al., 1983). Equilibrium calculations using available thermodynamic and kinetic data for the reaction of SO_2 and CH_2O demonstrate that



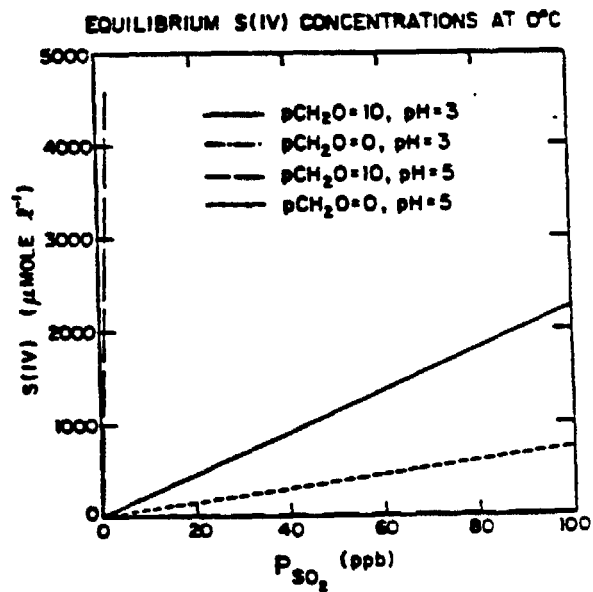
(a)



(b)



(c)

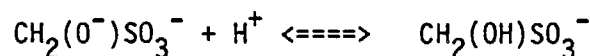
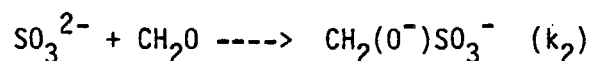
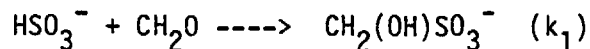
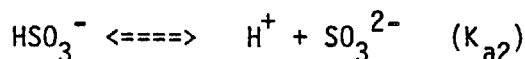
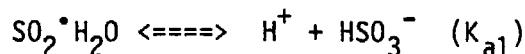
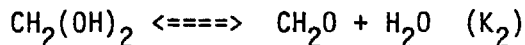


(d)

Figure 4a-d. (a & b) Plots of observed aqueous phase S(IV) concentrations versus observed formaldehyde concentrations. Dashed line indicates a one-to-one correspondence. (c & d) Calculated equilibrium relationships for total aqueous phase S(IV) as functions of P_{SO_2} and P_{CH_2O} .

elevated concentrations of S(IV) in fog water cannot be achieved without consideration of sulfonic acid production, HORHSO_3^- (Munger et al., 1984) (see Figure 4c and d).

Carbonyl-bisulfite addition products are highly stable in aqueous solution at low pH, but they undergo facile dissociation under alkaline conditions. The kinetics of hydroxymethanesulfonate production under pH conditions characteristic of fog and cloud water has been studied in our laboratory. Boyce and Hoffmann (1984) found that the formation of HMSA over the pH range 0.0 to 3.5 occurs by parallel reaction pathways involving nucleophilic addition of HSO_3^- and SO_3^{2-} to the carbonyl C-atom of formaldehyde as follows:



where $k_1 = 7.90 \times 10^2 \text{ M}^{-1} \text{ s}^{-1}$ and $k_2 = 2.48 \times 10^7 \text{ M}^{-1} \text{ s}^{-1}$ at 25°C. Under more weakly acidic conditions (pH > 4), the dehydration of methylene

glycol (equation K₂) may become rate-determining. Application of the rate constants and activation energy parameters obtained in the laboratory to the analysis of the field measurements discussed above indicates that HMSA formation may account for the occurrence of S(IV) at elevated concentrations. However, in acid conditions the reaction time is much longer, which indicates that the HMSA may be present when the fog forms (Munger et al., 1984). Examination of preliminary kinetic data obtained for other aldehyde/sulfur(IV) reaction systems suggests that the mechanism outlined above can be generalized to describe the formation of a wide variety of α -hydroxyalkanesulfonates.

In order to develop a comprehensive physiochemical description of the complex SO₂ reaction network in atmospheric droplets, rate laws, mechanisms and activation energies are being determined for the various pathways of sulfur dioxide transformation in aqueous solution. However at this time complete information has been assembled in only a very few cases. The mechanism of S(IV) oxidation by hydrogen peroxide is fairly well understood (Halperin and Taube, 1952; Hoffmann and Edwards, 1975; Penkett et al., 1979b; Martin and Damschen, 1981; McArdle and Hoffmann, 1983; Kunen et al., 1983;). The reaction proceeds by nucleophilic displacement of water by H₂O₂ on bisulfite ion to form peroxymonosulfite anion (HOOSO₂⁻), which rearranges to sulfate under the influence of specific and general acid catalysis (Mader, 1958; Penkett et al., 1979b; McArdle and Hoffmann, 1983). The significance of this latter feature for open atmospheric systems has been discussed by Jacob and Hoffmann (1983), Hoffmann and Jacob (1983), McArdle and Hoffmann (1983), Schwartz (1984), and Martin (1984). The mechanism of reaction between O₃ and S(IV) has not been clearly defined. Nevertheless, there is a general

consensus among several investigators as to the rate, rate law and pH-dependence of the "uncatalyzed" reaction (Larson et al., 1978; Harrison et al., 1982; Maahs, 1983; Martin, 1984). Most likely, the production of sulfate involves a free-radical chain sequence of steps in which sulfate radical (SO_3^-) and peroxymonosulfite radical (SO_5^-) are intermediates.

For the metal-catalyzed autoxidation of S(IV), there is considerable ambiguity about the mechanism(s) of reaction. First-row transition-metal species can catalyze the reaction of aquated sulfur dioxide and O_2 through four distinctly different pathways as described by Hoffmann and Boyce (1983). These mechanisms include: i) thermally-initiated free radical chain processes involving a sequence of one-electron transfer steps, ii) heterolytic pathways in which formation of an inner-sphere metal-sulfite-dioxygen complex occurs as a prelude to two-electron transfer, iii) heterogeneous catalysis through complexation of HSO_3^- and/or SO_3^{2-} at the surface of metal oxides and oxyhydroxides in suspension, and iv) photochemical oxidation initiated by the absorption of light by S(IV), metal cations, metal-oxide semiconductors, and/or specific metal-sulfite complexes. Hoffmann and Jacob (1984) have compared the theoretical kinetic expressions for each type of mechanism with the empirical rate data obtained in experimental studies of the catalytic autoxidation of SO_2 .

Quantitative analysis of different reaction pathways for the transformation of aquated sulfur dioxide in atmospheric droplet systems has been a major objective of the research conducted in the principal investigator's laboratory for the last four years. Available thermodynamic and kinetic data for the aqueous-phase reactions of SO_2

have been incorporated into a dynamic model of the chemistry of urban fog that has been developed by Jacob and Hoffmann (1983). The fog water model developed by them is a hybrid kinetic and equilibrium model that considers the major chemical reactions likely to take place in atmospheric water droplets. Model results have verified that extremely high acidity may be imparted to fog water droplets by condensation and growth on acidic nuclei or by in situ S(IV) oxidation. Based on both kinetic and equilibrium considerations the important oxidants in the aqueous phase were found to be O_2 catalyzed by Fe(III) and Mn(II), H_2O_2 , and O_3 (See Figures 5 and 6). The results of the model calculations show that metal-sulfite complexation (both with and without electron transfer) and α -hydroxyalkylsulfonate formation enhance water droplet capacity for SO_2 , but did not slow down the net S(IV) oxidation rate leading to fog acidification. Nitrate production in the aqueous phase was found to be dominated by scavenging of $HNO_3(g)$. Highly acidic fog water appears to form predominantly from condensation on highly acidic haze aerosol (i.e. fog condensation nuclei) or scavenging of acidic gases; in these cases (i.e. pH 1.7 fog at Corona del Mar), in situ S(IV) oxidation leads to little further acidification of the fog water. In field situations, the ultimate acidity level in fog depends upon the degree of neutralization of free acidity by ammonia or by scavenged alkaline aerosol. In Los Angeles more ammonia is available further inland from the coast. This may explain in part why higher fog water acidities are found along the coast than at inland sites. Similar observations have been made in the Southern San Joaquin Valley.

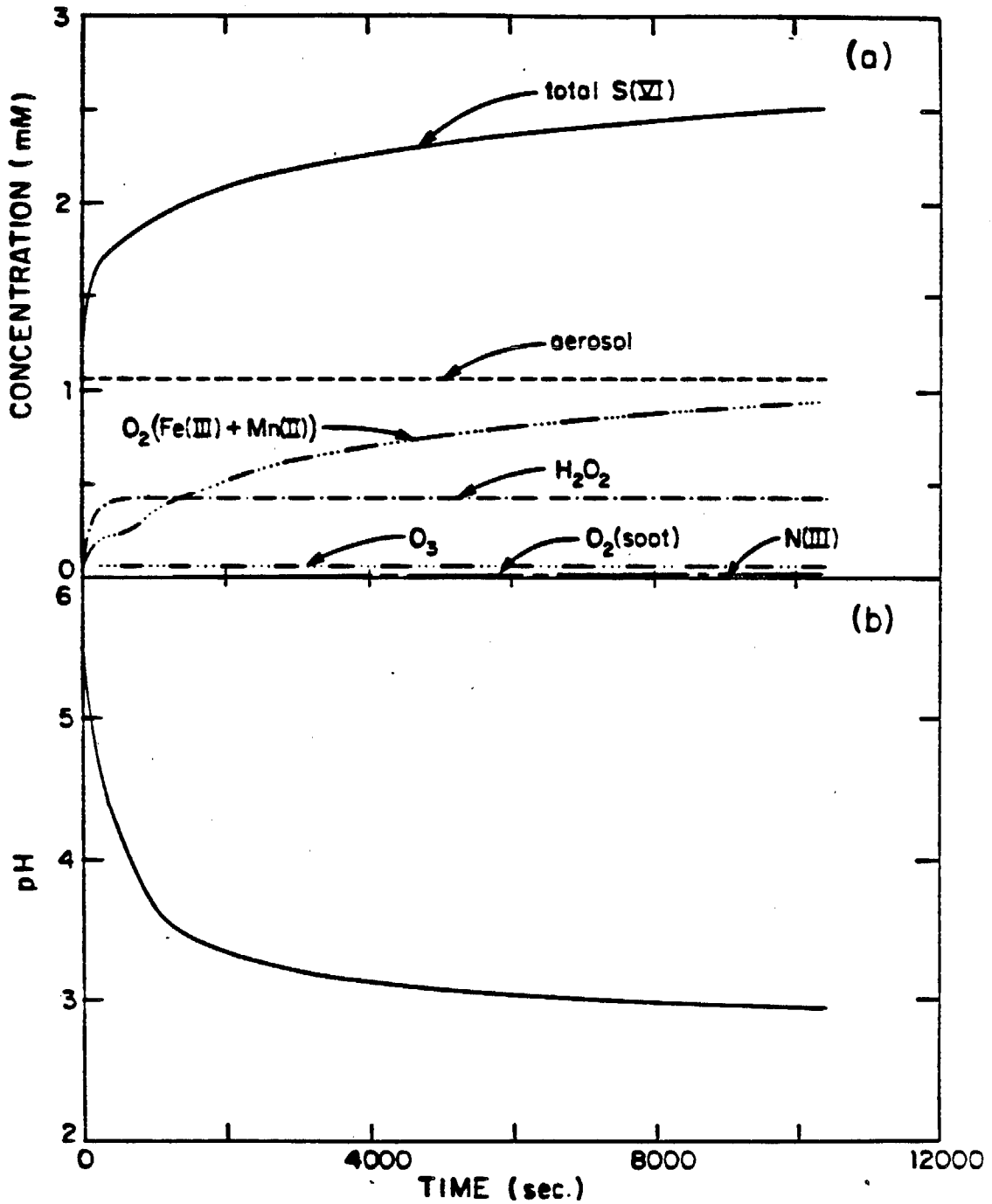


Figure 5. (a) Profile of concentration versus time of total sulfite in the fogwater and of the individual contributions to the total sulfate of sulfate aerosol and different S(IV) oxidants. (b) Profile of pH versus time. Liquid Water Content is 0.1 g m^{-3} , $T = 10.0^\circ\text{C}$.

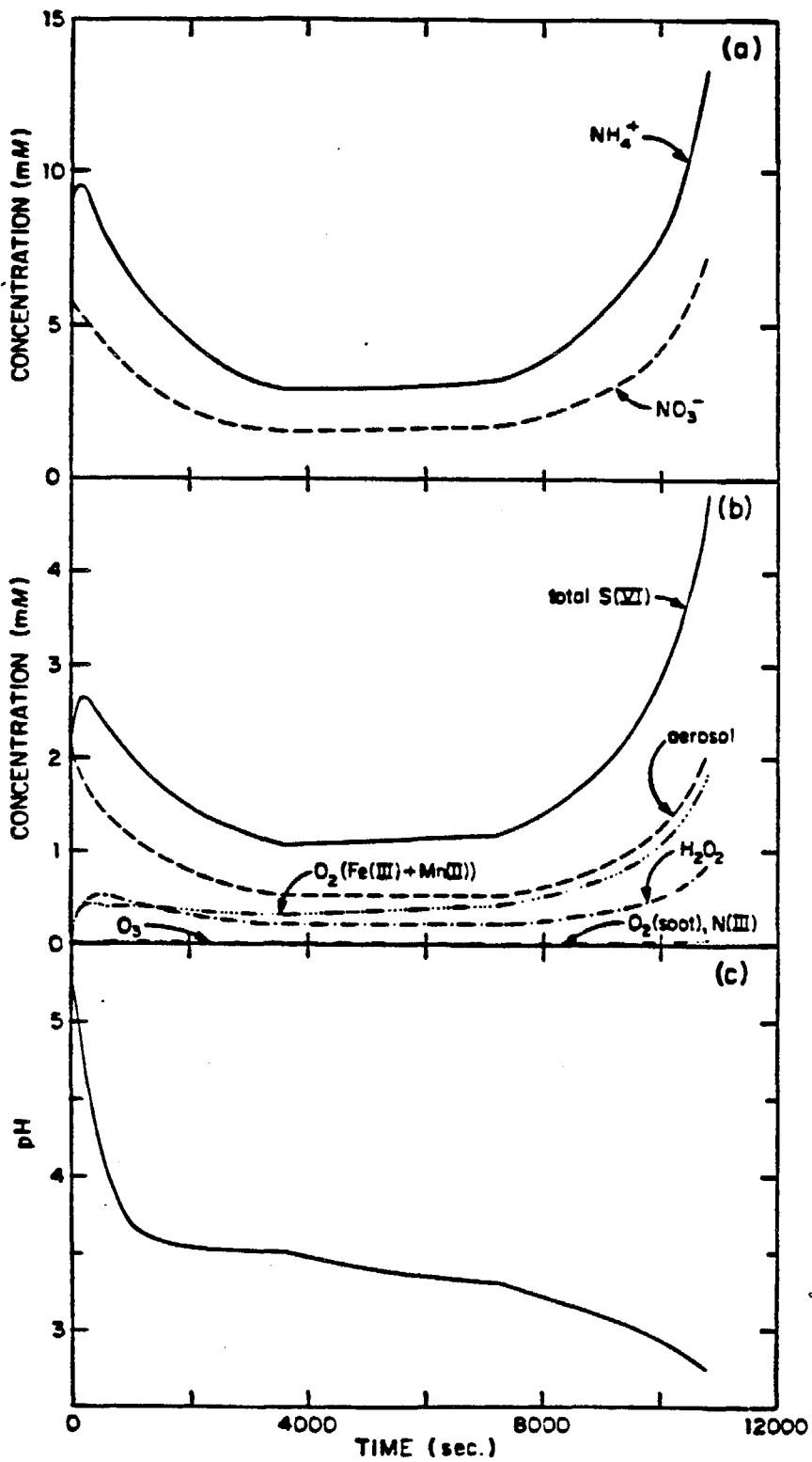


Figure 6. Profiles versus time of the concentration of the major ions in fogwater given a typical LWC vs. time profile.

Waldman et al. (1984) have been studying the chemistry and microphysics of intercepted cloudwater on Los Angeles area mountain slopes. In 1982 and 1983, the observed pH values of the cloudwater ranged from 2.06 to 3.87 with the median value below pH 3 (see Figure 7). The equivalent ratio of nitrate to sulfate in cloudwater at Henninger Flats (elevation 750 m) was close to two, while at the same site the ratio in rainwater was approximately one. Similarly, the nitrate/sulfate ratio observed in dry aerosol was lower than that observed in cloudwater; the additional nitrate found in cloudwater appears to be derived from the scavenging of gaseous nitric acid (see Figure 8).

Cloud droplet capture in the form of intercepted fog appears to be a seasonally important sink for pollutant emissions in the LA Basin. At Henninger Flats up to 50% of the total wet deposition of H^+ , NO_3^- , and SO_4^{2-} may be due to cloud interception; low intensity springtime drizzle accounted for 20% of the deposition measured in precipitation. The intercepted cloudwater that deposited on pine needles was collected and analyzed. The acidity of the water dripping from trees was very similar to that of the suspended cloudwater. The concentrations of major chemical components were found to be significantly greater than in the overlying cloudwater. The additional solute in the drippings is thought to be derived from previously deposited material and the evaporated residue of intercepted cloudwater. Even after rainfall had removed most of the accumulated residue, the concentrations of major cations such as Ca^{2+} and K^+ showed relative increases compared to suspended cloudwater samples. These increases may be attributed in part to ion-exchange of H^+ for K^+ and Ca^{2+} from the pine needles (Tukey, 1970). The potential

STRATUS CLOUDWATER pH FREQUENCY HENNINGER FLATS : 1982 & 1983

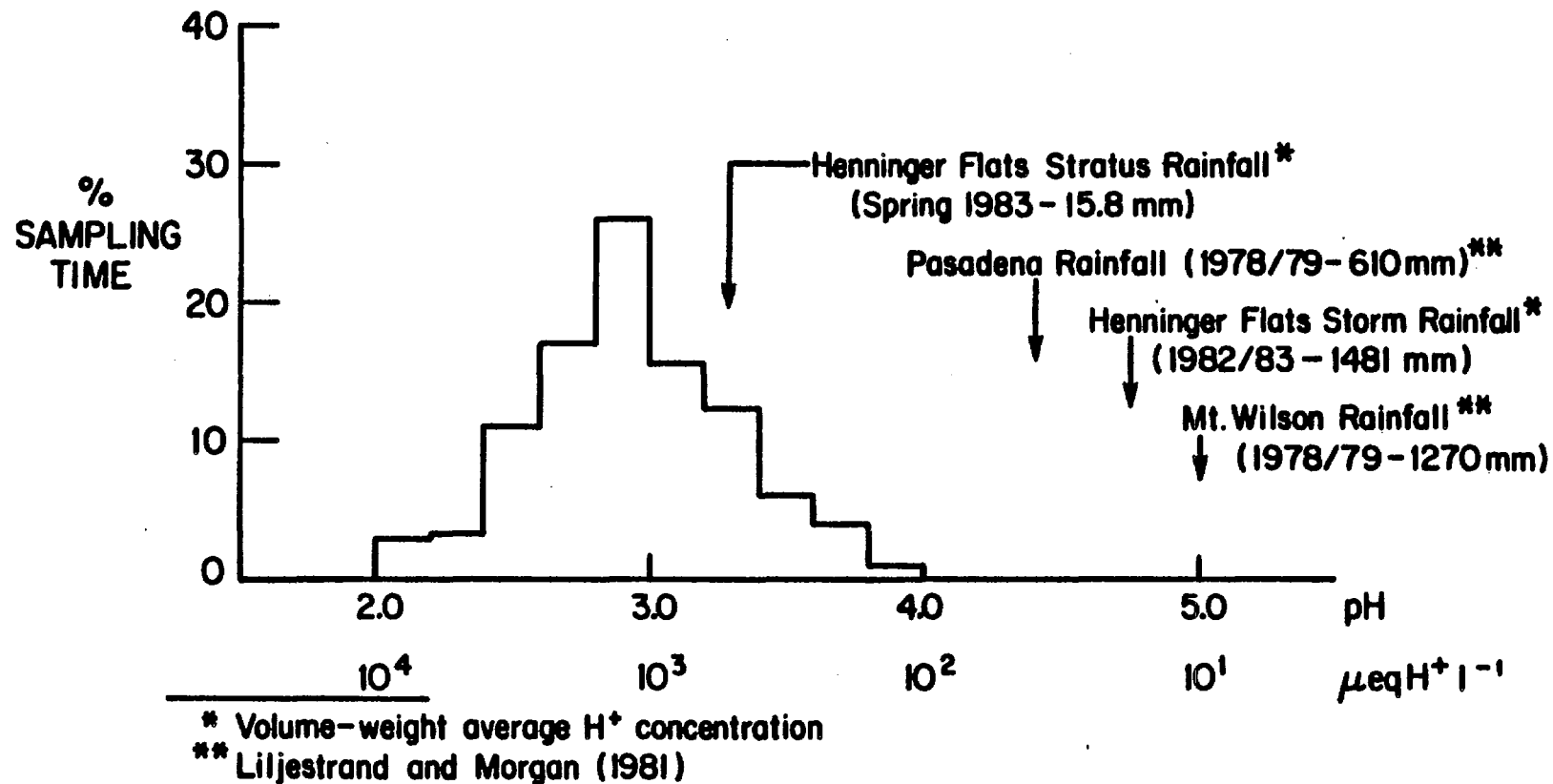


Figure 7. Histogram of pH frequency of cloudwater samples at Henninger Flats for 1982 and 1983; volume-weighted average [H⁺] for rainfall is indicated with arrows.

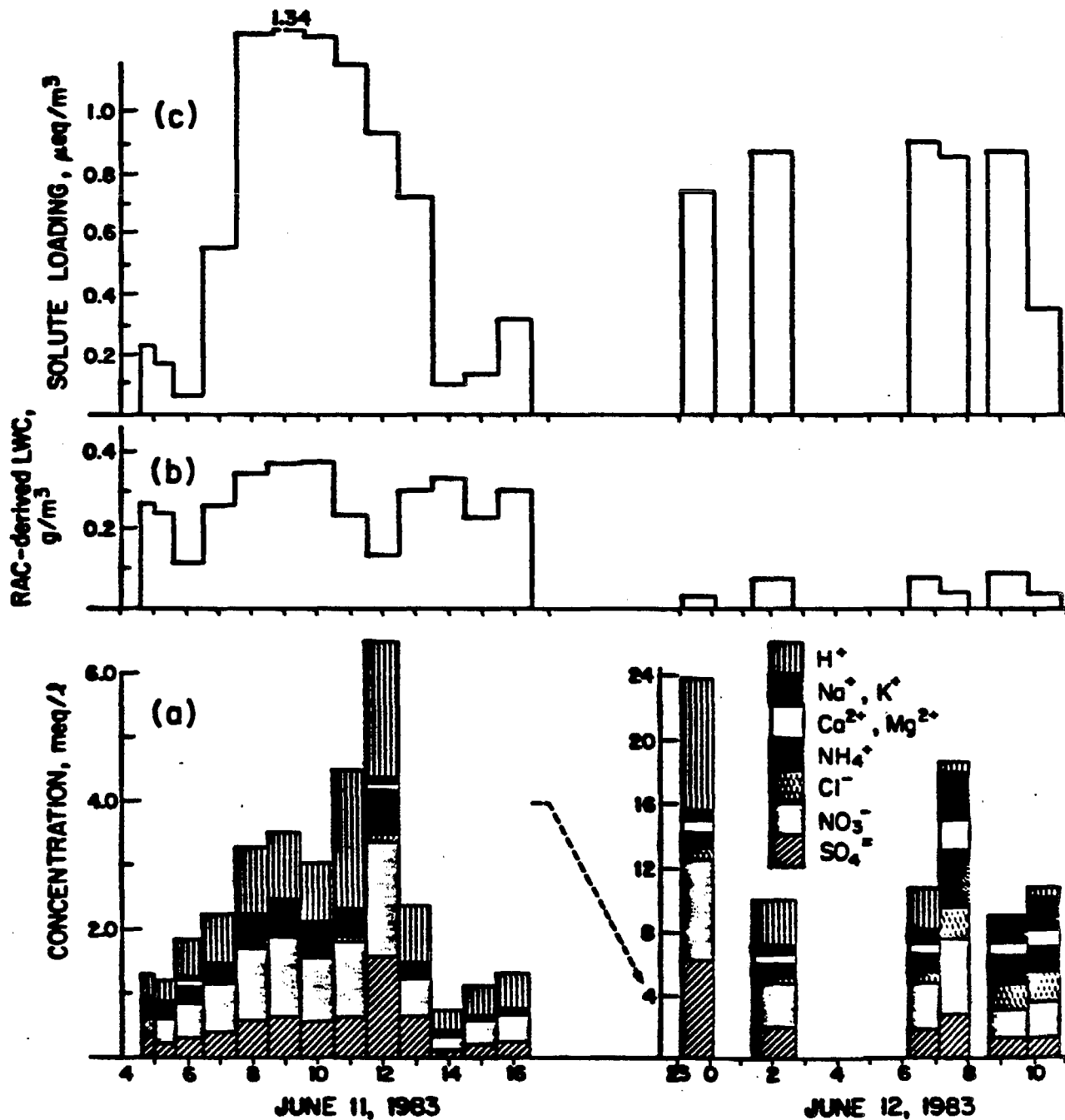


Figure 8. Concentration (a), LWC (b), and solute loading (c) for sequential cloudwater samples on June 12, 13, and 17, 1982. Measurable drizzle occurred prior to sampling on June 17; note the drop in solute loading and the change in scale (a).

for harm to sensitive plant tissue appears to be high given prolonged exposure to the severe microenvironments observed on the slopes of the San Gabriel Mountains and in the Angeles National Forest.

During the last year the Caltech rotating arm collector (RAC) was calibrated using a scale model rotating arm device and a chemically tagged monodisperse aerosol. Jacob et al. (1984c) have characterized the performance of the rotating arm collector in great detail. The rotating arm collector was designed to meet the following criteria:

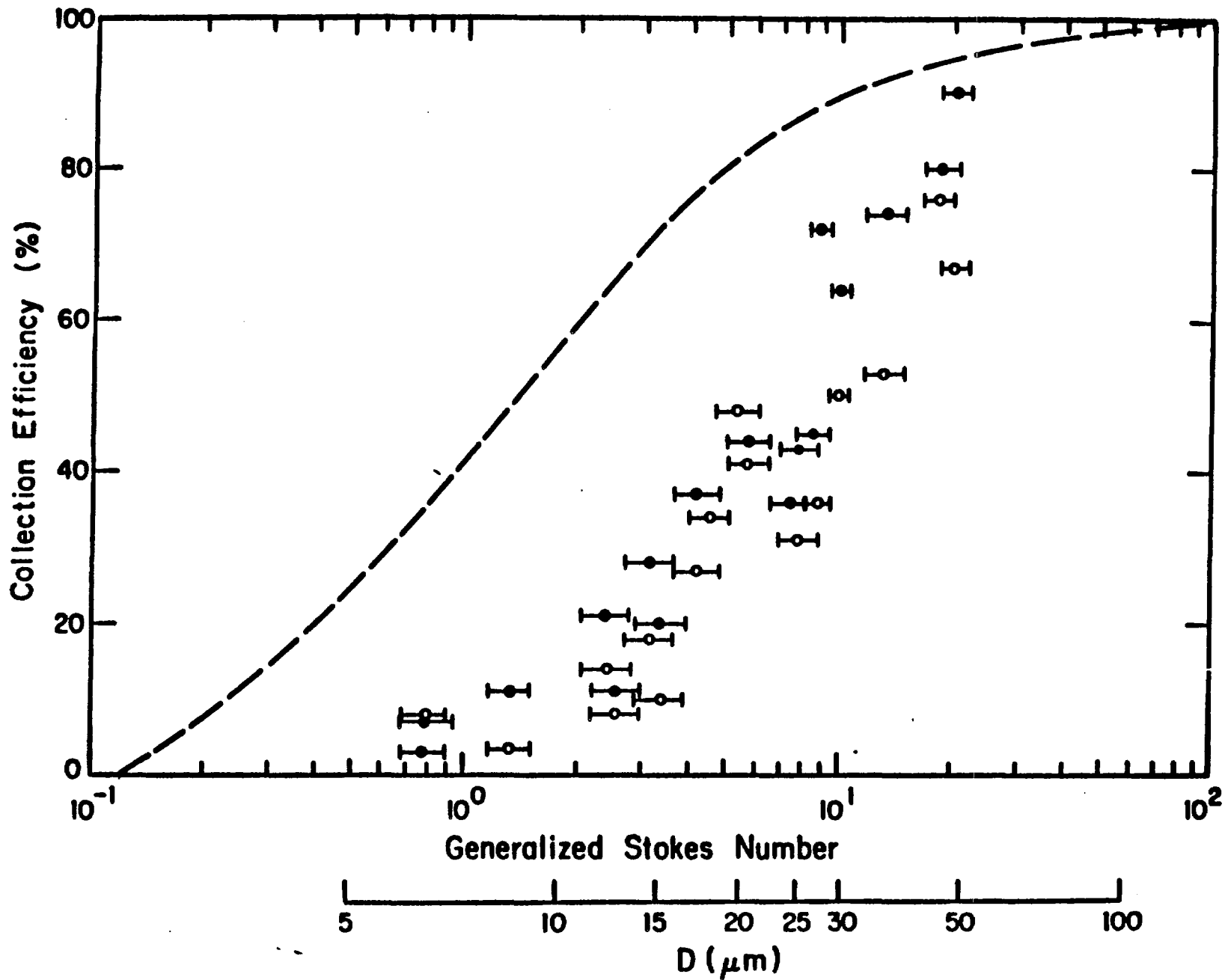
1. The aerodynamic heating associated with the flow of air towards the impactor surface must be small enough not to cause droplet evaporation.
2. The collected droplets must be rapidly sheltered from the changing air masses to prevent evaporation and chemical contamination.
3. The lower size cut must be sharp and in the range of 1-10 μm , and no sampling biases must be introduced for the droplets up to at least 50 μm .
4. The sampling rate must be high enough to collect sufficient amounts of sample for chemical analysis while allowing a reasonable time resolution.

These criteria were met with the exception of criteria 3. Jacob et al. (1984c) found that the scale model version of the RAC had a particle size cut of 20 μm rather than the desired 1-10 μm cut (see figure 9). The RAC performs well in preserving the chemical integrity of the collected droplets and provides a high sampling rate; however, it has the drawback that it does not collect efficiently the smaller droplets in the fog. This has not proved to be a significant problem in that preliminary data suggest that there is not appreciable variation in

chemical composition of fog-water droplets with size (Hering and Blumenthal 1984). Changes in the collector geometry, such as streamline shaping to reduce drag, would produce a smaller size cut. Jet impactors and screen collectors are being evaluated as an alternative to rotating arm collectors.

In June of 1983, five different types of fog/cloud water collectors were compared under field conditions at Henninger Flats. Collectors designed by AeroVironment(AV), Caltech(CIT), the Desert Research Institute(DRI), Global Geochemistry(GGC), and the State University of New York(SUNY)-Albany were operated simultaneously. The mass and pH of the samples collected were measured on site while the detailed chemical analyses were performed by an independent laboratory, Rockwell International. Results of the intercomparison study, sponsored by the Coordinating Research Council, showed that the Caltech and DRI collectors performed the best over the broadest range of conditions (Hering and Blumenthal, 1984). At low liquid water content ($< 0.03 \text{ g m}^{-3}$), the SUNY-Albany rotating string collector, the DRI jet impactor, and the Caltech rotating arm collector had reasonable collection rates with the Caltech collector the highest. The Global Geochemistry mesh collector and the AeroVironment rotating rod collector were not effective in low LWC conditions. With respect to sulfate, nitrate, and pH values obtained under a wide variety of conditions over 38 hours of fog, the Caltech and DRI collectors showed the most consistency and closest agreement. The SUNY-Albany and the AeroVironment collectors showed the greatest deviations from the median values. For example the slope of the observed $[\text{SO}_4^-]$ vs. median $[\text{SO}_4^-]$ over the range of

Figure 9. Collection efficiency of model collector vs. generalized Stokes number for greased(•) and ungreased(o) impaction surfaces.



concentration from 100 to 2000 μM for the SUNY, Caltech, DRI, AeroVironment, and Global Geochemistry collectors, respectively, were 0.69(SUNY), 0.95(CIT), 0.91(DRI), 1.66(AV), and 1.21(GGC). The high values for the AV and GGC collectors indicate that concentration effects due to evaporation are significant problems in these collectors. The low values for the SUNY collector may be attributed to preferential collection of very large droplets by settling. In the case of nitrate correlations, the slopes of the observed concentrations vs. the median values for the same sequence of collectors were found to be 0.83(SUNY), 0.94(CIT), 0.93(DRI), 2.43(AV), and 1.17(GGC). When identical RAC's were placed at different locations at Henninger Flats the results correlated quite well. There appeared to be no statistical difference between the separated collectors (Hering and Blumenthal, 1984).

Details of the results and interpretations summarized above are presented in the Appendices I-XII. Research sponsored either fully or in part by the California Air Resources Board has led to the publication of the following papers:

Waldman, J. M., J. W. Munger, D. J. Jacob, R. C. Flagan, J. J. Morgan and M. R. Hoffmann. "Chemical Composition of Acid Fog." Science 217, 677-680 (1982).

Munger, J. W., D. J. Jacob, J. M. Waldman and M. R. Hoffmann. "Fogwater Chemistry in an Urban Atmosphere." J. Geophys. Res. 88, 5109-5121 (1983).

Hoffmann, M. R. and S. D. Boyce. "Catalytic Autoxidation of Aqueous Sulfur Dioxide in Relationship to Atmospheric Systems." in Trace Atmospheric Constituents: Properties, Transformations and Fates, S. E. Schwartz, ed., Adv. Environ. Sci. Technol. 12, 147-189 (1983).

Jacob, D. J. and M. R. Hoffmann. "A Dynamic Model for the Production of H^+ , NO_3^- , and SO_4^{2-} in Urban Fog." J. Geophys. Res. 88, 6611-6621 (1983).

McArdle, J. V. and M. R. Hoffmann. "Kinetics and Mechanism of the Oxidation of Aqueous Sulfur Dioxide by Hydrogen Peroxide at Low pH." J. Phys. Chem., 87, 5425 (1983).

Jacob, D. J., R. C. Flagan, J. M. Waldman, and M. R. Hoffmann, "Design and Calibration of a Rotating Arm Collector for Ambient Fog Sampling." in Precipitation Scavenging, Dry Deposition, and Resuspension, H. R. Pruppacher et al., eds. Elsevier, New York, pp.125-136 (1983).

Waldman, J. M., J. W. Munger, D. J. Jacob, and M. R. Hoffmann, "Fogwater Composition in Southern California." in Precipitation Scavenging, Dry Deposition, and Resuspension, H. R. Pruppacher et al., eds. Elsevier, New York, pp.137-148 (1983).

Jacob, D. J. and M. R. Hoffmann. "The Chemistry of Nighttime Urban Fog." in Precipitation Scavenging, Dry Deposition, and Resuspension, H. R. Pruppacher et al., eds. Elsevier, New York, pp.149-159 (1983).

Munger, J. W., J. W. Waldman, D. J. Jacob, and M. R. Hoffmann. "Vertical Variability and Short-term Temporal Trends in Precipitation Chemistry." in Precipitation Scavenging, Dry Deposition, and Resuspension, H. R. Pruppacher et al., eds. Elsevier, New York, pp.275-282 (1983).

Hoffmann, M. R., "Acid Fog." Environ. Sci. Tech. 17, 117A-120A, (1983); 18, 61-64 (1984)

Hoffmann, M. R. and D. J. Jacob. "Kinetics and Mechanisms of the
II-26

Catalytic Oxidation of Dissolved Sulfur Dioxide in Aqueous Solution: An Application to Nighttime Fog Water Chemistry." in Acid Precipitation: SO₂, NO and NO₂ Oxidation Mechanisms: Atmospheric Considerations, J. G. Calvert, ed., Butterworth Publishers, Stoneham, MA pp. 101-172 (1984).

Munger, J. W., D. J. Jacob and M. R. Hoffmann. "The Occurrence of Bisulfite-Aldehyde Addition Products in Fog and Cloudwater." J. Atmos. Chem., 1, 335-350 (1984).

Boyce, S. D. and M. R. Hoffmann, "Kinetics and Mechanism of the Formation of Hydroxymethanesulfonic Acid at Low pH." J. Phys. Chem. 88, 4740-4746 (1984).

Jacob, D. J., J. M. Waldman, J. W. Munger, and M. R. Hoffmann, "A Field Investigation of Physical and Chemical Mechanisms Affecting Pollutant Concentrations in Fog Droplets." Tellus, 36B, 272-385 (1984).

Jacob, D. J., R. T. Wang, and R. C. Flagan, "Fogwater Collector Design and Characterization," Environ. Sci. Tech. 18, 827-833 (1984).

Jacob, D. J., J. W. Munger, J. M. Waldman, and M. R. Hoffmann, "Aerosol Composition in a Stagnant Air Mass Impacted by Dense Fogs." Proc. 77th Annual Meeting of the Air Pollution Control Association, San Francisco, CA (paper 24.5) (1984).

Waldman, J. M., J. W. Munger, D. J. Jacob, and M. R. Hoffmann, "Chemical Characterization of Stratus Cloudwater and Its Role as a Vector for Pollutant Deposition in a Los Angeles Pine Forest." accepted for publication, Tellus (1985).

Jacob, D. J., J. M. Waldman, J. W. Munger, and M. R. Hoffmann, "Chemical Composition of Fogwater Collected Along the California Coast." accepted for publication, Environ. Sci. Tech. (1985).

CHAPTER III

III. FUTURE RESEARCH

Over the last three years we have made significant advancements in our understanding of the acidification of haze aerosol, fog, stratus clouds, and hydrometeors and of the roles each play in the acid deposition phenomenon in California. However many problems still need to be addressed and fundamental questions need to be answered before we would be at a stage to advise the Air Resources Board and the local Air Quality Management Districts in terms of possible pollution control strategies to reduce the levels of acid fog and acid deposition. Some of the key problems and questions that need to be addressed in the future are as follows:

- 1. Fogwater and ground-based cloudwater collectors need to be refined and automated in order to make them more suitable for long-term research and for routine monitoring by regulatory agencies.**

We have sampled fogwater with a rotating arm collector designed at Caltech. Our publication, "Fogwater Collector Design and Characterization" (APPENDIX X) discusses in detail the characteristics of this instrument. The rotating arm collector has proven to be a rugged, reliable device, and we have strong evidence that it collects fairly representative fogwater samples (Hering and Blumenthal, 1984). However, the current design presents several problems: (i) the

instrument is difficult to automate (ii) the lower size cut is higher than theoretically predicted (iii) and its operation causes some concern in regard to safety. At this point in our fog and cloud sampling program, we need to design and construct an optimized instrument. The primary aim of future research should be to provide the CARB and other regulatory agencies with a reliable automated sampler to be used for routine monitoring of fogwater chemistry, much in the same way as the acid rain monitoring program currently under way. A second aim is to allow us to expand our fogwater sampling networks while limiting the manpower required.

2. The temporal and areal variations of fogwater chemistry need to be established within well-defined geographical areas. With the exception of the winter of 1983-84 in the Southern San Joaquin Valley, we have little knowledge about the evolution and extent of acid fog in specific locales such as the Los Angeles Basin or the Santa Barbara Channel area.

With the exception of the winter of 1983-1984 in the Southern San Joaquin Valley, our sampling efforts have been limited to a single site during a particular fog episode. In order to fully understand the spatial and temporal variations of the chemical composition of fogwater, we need to be situated at multiple sites during a specific event in a given location. Results from our intercomparison study of last summer have shown that two identical collectors placed within 50 meters of each other gave virtually identical results (Hering and Blumenthal, 1984); however, we anticipate that more significant variations will be seen as the distance of separation between collectors is increased. We have noted in part that the acidity of fogwater in the LA Basin appears to be

the greatest along the coast. As fog is collected further inland we find that the acidity is generally less even though the overall chemical composition is similar. This has been attributed to the greater availability of ammonia inland than along the coast. Similar variations were observed during the same event in the Southern San Joaquin Valley (Jacob et al., 1984b) this past winter. In the SJV, the overall concentrations and acidity of the fog were the greatest close to the sources of SO_2 and NO_x ; further away from the sources the acidity levels and overall concentrations were significantly lower while the ammonium ion concentrations were increased.

The locations in California that are most likely to be affected by the "acid fog" problem are the coastline, along which fogs are frequent seasonal occurrences, and the near coastal mountain slopes. Oberlander(1956) has observed that impaction of fog droplets on trees provides most of the water input to the soil in the San Francisco peninsula. During the summer, coastal stations may report over 50% foggy days (deViolini, 1974). These fogs are often coupled with land breeze/sea breeze systems, which recirculate several times the same air parcels over the shoreline (Cass and Shair,1984). Tracer studies in the Santa Barbara Channel (Reible et al.,1984) have shown that emissions from offshore as well as onshore sources may reside several days along the coast. Other areas impacted by frequent fogs are the San Joaquin Valley during the winter months and the eastern edge of the Los Angeles Basin(Riverside/San Bernardino) during the months of August and September. The Riverside/San Bernardino area should prove to be interesting in that fogs occur there during a time of the year when the smog levels in Los Angeles are generally at a peak.

3. What role do the carboxylic acids and sulfonic acids play in fog acidification and S(IV)/SO₂ transport?

In order to ascertain the exact role of carboxylic and sulfonic acid in the hydrometeor acidification process we must be able to quantify these acids and their conjugate bases on a routine basis. To date no specific methods for hydroxyalkanesulfonic acids have been reported in the literature, however, both alkane and aromatic sulfonates have been determined by chromatographic methods. Normal ion chromatography has been used to separate methanesulfonate and other C1-C8 alkanesulfonates and substituted benzenesulfonates (Williams, 1982; Saltzman et al., 1983); conductivity was used for detection of these compounds. Ion-pair reversed-phase liquid chromatography (IPRP LC) with UV detection has been widely used to separate aromatic sulfonates (Kraak and Huber, 1974; Wahlund, 1975, Terweij-Groen and Kraak, 1977; Rotsch and Pietrzyk, 1980; Prandi and Venturini, 1981; Lagerstrom, 1982). Dionex has recently described a technique referred to as mobile phase ion chromatography (MPIC) for separation of both aromatic and alkyl sulfonates. This method uses polymer based stationary phases rather than silica based materials used in RPIP LC and conductivity detection after eluent suppression. Both methods of separation use quaternary amines as ion-pairing agents in the mobile phase. In order to separate hydroxyalkanesulfonates it is important to prevent them from breaking down to the aldehyde and bisulfite from which they formed. This is possible by maintaining pH in the range where the sulfonates are most stable; Dasgupta et al. (1980) report that hydroxymethanesulfonate is most stable at pH 4. Because hydroxyalkanesulfonates are not UV absorbing conductivity detection is required.

Attempts should be made to detect hydroxyalkanesulfonates by either ion chromatography or MPIC on the model 2020i Ion Chromatograph.

Ion-exclusion chromatography or normal ion chromatography can be used to determine weak acids. In ion exclusion chromatography the column excludes strong acid anions, which elute in the void volume, and weaker acids are separated according to their dissociation constants. In our previous work with this method we have determined that formic and acetic acid are the dominant acids in fog, with a small contribution from propanoic acid and an unknown. Keene et al. (1983) used this method to determine formic and acetic acid in rainwater. The resolution of formic and acetic acid is less than ideal on the Dionex ICE column, however, without use of impractically high concentrations of HCl as eluent. The suppressor columns, which bind Cl^- as a silver salt can not be regenerated, and must be replaced after several hours of operation. Weak acids can also be separated by normal ion chromatography using weak eluents (dilute HCO_3^- or $\text{B}_2\text{O}_7^{2-}$) (Dionex, Applications Note 10). This method would facilitate detection of methanesulfonic acid if it is present in fogwater (Saltzman et al., 1983). Aliquots should be preserved with chloroform (Keene et al., 1983) immediately after collection for reliable organic acid determination.

Our preliminary work suggests that in selected California environments such as the SJV substantial contributions to acidity may arise from the formation of sulfonic acids and secondarily from carboxylic acids (APPENDIX XII).

4. What role does dew play as a sink for atmospheric acidity?

Fogs or its counterpart aloft, clouds, have a consequential impact on atmospheric processes; however, as a ground level phenomenon, fog may

be too infrequent or localized to play an important role in the deposition of pollutants, except on the mountain slopes and the immediate coastal areas. Dew, on the other hand, is a phenomenon which is noted frequently at night throughout the coastal plain as well as inland valleys and mountains. Dew forms on surfaces which cool by long-wave radiation to a temperature below the ambient dewpoint temperature. In Southern California, this is promoted on a routine basis by the prevailing meteorological conditions: clear nighttime skies, moderate to calm winds, and a nearby source of moisture.

The role of dew in modifying the deposition of pollutant species is largely an unknown and needs to be explored more fully. Measurements of dew flux are far from routine; data on dew composition are even more rare. Yaalon and Ganor (1968) found dew composition in Israel to be similar to precipitation at that site. The range of pH for samples was 6.6 to 8.1. Calcium, carbonate and sulfate dominated the ionic composition. Brimblecombe and Todd (1977) measured sodium and potassium concentrations in the 100 micromolar range for dew collected from grass. The K^+/Na^+ ratio for dew collected on actual grass was 3 times greater than for plastic grass surfaces, but it was one-tenth the ratio for dry blade extractions in distilled water, indicating an intermediate impact of foliar leaching on dew composition. Anderson (1979), using pH paper, reported a range for dew pH of 5.0 to 6.7 for dew on grass and glass surfaces. He also noted that a relationship seemed to exist between measured dew pH (increasing) and minimum, nighttime temperature (decreasing).

From these and more general consideration, it is likely that dew occurrence may be important in mediating the impacts that pollutant

deposition has on receptor surfaces. There are several means by which it can be expected to impact deposition:

i) (effect on particle deposition efficiency) Surface wetness is acknowledged to greatly reduce particle rebound and resuspension and, thus, increases dry depositional flux to collection surfaces.

ii) (dissolution of pollutant gases such as SO_2 , HNO_3 and NH_3) The film of dew furnishes a sink for soluble gases. Such dissolution would be dependent on the pH of the aqueous solution, governed by preexistent solute.

iii) (dissolution and transformation of previously deposited material) The repetitive wetting and evaporation of collection surfaces provides the accumulated material opportunity for further aqueous transformation. For example, neutralization would tend to retard volatilization of nitric acid, as would oxidation of dissolved S(IV) compounds. Also, reactions with the surface material have important consequences to vegetation, structures, and automobiles in the urban environment.

iv) (impact on thermal and moisture flux at ground level and on turbulence) It has been shown that dew occurrence delays or inhibits of fog formation. Dew depletes the atmospheric humidity. Both these effects reduce to growth of hygroscopic aerosol and would be expected to diminish particle sedimentation.

5. Do correlations exist among the standard air quality measurements

and the resultant fogwater characteristics?

Fogwater monitoring, while still far from routine, has been performed at a wide variety of locations and times of year in the Southern California (Waldman et al., 1982; Munger et al., 1983; Jacob et al., 1984c). From the available data, qualitative correlations of precursor air quality and pollutant transport with fogwater composition are apparent. These have provided simplistic though useful understandings of their relationship. Most airborne pollutants are readily scavenged by water droplets, especially particulate nitrate and sulfate and soluble gases such as ammonia, nitric acid, and formaldehyde. Thus, fogs and clouds serve as short-lived sinks for airborne pollutants, altering their chemical and physical dynamics, and redistributing them.

On one hand, physical-chemical modeling offers a means for mechanistic prediction of ambient fog acidities and chemical dynamics. However, air quality data routinely available may not support the application of a model in all cases. Detailed study of air quality indicators, meteorological parameters, and trajectory analyses with regard to fog- and cloudwater data would be of great value. While it remains obvious that polluted air leads to polluted fogs, it may be possible to correlate routinely monitored indices with the extent and intensity of smog-into-fog (and fog-into-smog) transformations.

Such research would entail multidisciplinary study of gas-phase, aerosol, and droplet processes plus synoptic and mesoscale meteorology. It would provide refinement of our initial observations. The development of this type of analysis on a regional basis would be particularly useful to air pollution control agencies which have hitherto

been unfamiliar with and unable to address pollution aspects of fogs and clouds in coastal California.

IV. REFERENCES

- Anderson, D. E. (1979) The Acidity of Atmospheric Precipitation, Dew, and Fog, Publ. No. 79-183 Meteorology Program, University of Maryland, College Park, MD.
- Barrett, E. W., Parungo, F. P., and Pueschel, R. F. (1979) Cloud modification by urban pollution: A physical demonstration, Meteorol. Rdsch. 32, 136-149.
- Basset, M. and Seinfeld, J. H. (1983) Atmospheric equilibrium model of sulfate and nitrate aerosols, Atmos. Environ. 17, 2237-2252.
- Beilke, S. and Gravenhorst, G. (1978) Heterogeneous SO₂-Oxidation in the Droplet Phase, Atmos. Environ. 12, 231-239.
- Bird, R. B., Stewart, W. E., and Lightfoot, E. N. (1960) Transport Phenomena, John Wiley & Sons, New York, 780 pp.
- Boyce, S. D. and Hoffmann, M. R. (1984) Kinetics and mechanism of the formation of hydroxymethanesulfonic acid at low pH, J. Phys. Chem. (in press).
- Brimblecombe, P. and Todd, I. J. (1977) Sodium and potassium in dew, Atmos. Environ. 11, 649-650.
- Brown, H. W. (1983) An analysis of air flow over the Southern California Bight and northern San Diego County on January 8 1983, Meteorological Summary, San Diego Air Pollution Control District, private communication.
- Brown, R. and Roach, W. T. (1976) The physics of radiation fog: II-a numerical study, Quart. J. Roy. Met. Soc. 102, 335-354.
- Brun, R. J., Lewis, W., Perkins, P. J., Serafini, J. S. (1955) NACA Report 1215.
- California Air Resources Board (1979) Emission Inventory: 1974, Emission Inventory Branch, Sacramento, CA.
- California Air Resources Board (1982a) Emissions Inventory, California Air Resources Board, Sacramento, California.
- California Air Resources Board (1982b) Air Quality Aspects of the Development of Offshore Oil and Gas Resources, California Air Resources Board Sacramento, CA.
- Calvert, J. G. (ed) (1984) Acid Precipitation, Butterworth Publishers, Boston, MA.
- Calvert, J. G. and Su, F., Bottenheim, J. W. and Strausz, O. P. (1978) Mechanisms of Homogeneous Oxidation of Sulfur Dioxide in the Troposphere, Atmos. Environ. 12, 197-226.

- Calvert, J. G., Su, F., Bottenheim, J. W. and Strausz, O. P. (1978) Mechanisms of Homogeneous Oxidation of Sulfur Dioxide in the Troposphere, Atmos. Environ. 12, 197-226.
- Cass, G. R. (1975) Dimensions of the Los Angeles SO₂/sulfate problem, Memo 15, Environ. Qual. Lab., Calif. Inst. Technol., Pasadena, CA.
- Cass, G. R. (1977) Methods for Sulfate Air Quality Management with Applications to Los Angeles, Methods for Sulfate Air Quality Management with Applications to Los Angeles, Ph.D. Thesis, California Institute of Technology, Pasadena, CA.
- Cass, G. R. (1981) Sulfate air quality control strategy design, Atmos. Environ. 15, 1277-1249.
- Cass, G. R. and Shair, F. H. (1984) Sulfate accumulation in a sea breeze/land breeze circulation system, J. Geophys. Res. 89D, 1429-1438.
- Cooper, J. A. and Watson, J. G. (1980) Receptor oriented methods of air particulate source apportionment, J. Air Pollut. Cont. Assoc. 30, 1116-1125.
- Cox, R. A. (1974) Particle formation from homogeneous reactions of sulfur dioxide and nitrogen dioxide, Tellus 26, 235-240.
- Dasgupta, P. K. (1981) Determination of atmospheric sulfur dioxide without tetrachloromercurate(II): Further refinements of a pararosaniline method and field application, J. Air Pollut. Cont. Assoc. 31, 779-782.
- Dasgupta, P. K., DeCesare, K., and Ullrey, J. C. (1980) Determination of atmospheric sulfur dioxide without tetrachloromercurate(II) and the mechanism of the Schiff reaction, Anal. Chem. 52, 1912-1922.
- Daum, P. H., Schwartz, S. E., and Newman, L. (1984) Acidic and related constituents in liquid water stratiform clouds, J. Geophys. Res. 89D, 1447-1458.
- Davidson, C. I. and Friedlander, S. K. (1978) A filtration model for aerosol dry deposition: application to trace metal deposition from the atmosphere, J. Geophys. Res. 83, 2343-2352.
- Davidson, C. I., Miller, J. M., and Pleskow, M. A. (1982) The influence of surface structure on predicted particle dry deposition to natural grass canopies, Water, Air, Soil Pollut. 18, 25-43.
- Davies, C. N. and Subari, M. (1982) Aspiration above wind velocity of aerosols with thin-walled nozzles facing and at right angles to the wind direction, J. Aerosol Sci. 13, 59-71.
- DeViolini, R. (1974) Climatic Handbook for Point Mugu and San Nicolas Island. Part I: Surface Data, Available from National Oceanographic and Atmospheric Administration, Asheville, NC.

- Dittenhoefer, A. C. and dePena, R. G. (1978) A study of production and growth of sulfate particles in plumes from a coal-fired power plant, Atmos. Environ. 12, 297-306.
- Enger, L. and Hogstrom, U. (1979) Dispersion and Wet Deposition of Sulfur from a Power Plant Plume, Atmos. Environ. 13, 797-810.
- Fortune, C. R. and Dellinger, B. (1982) Stabilization and analysis of S(IV) aerosols in environmental samples, Environ. Sci & Technol. 16, 62-66.
- Friedlander S. K. (1977) Smoke, Dust, and Haze, John Wiley, New York, 317 pp.
- Fung, K. and Grosjean D. (1981) Determination of nanogram amounts of carbonyls as 2,4-dinitrophenylhydrazones by high-performance liquid chromatography, Anal. Chem. 53, 168-171.
- Galloway, J. N., Likens, G. E., Keene, W. C., and Miller, J. M. (1982) The composition of precipitation in remote areas of the world, J. Geophys. Res. 87, 8771-8786.
- Gartrell, J. E., Thomas, J. W. and Carpenter, S. B. (1963) Atmospheric Oxidation of SO₂ in Coal-Burning Power Plant Plumes, Amer. Ind. Hyg. Assoc. Quart. 24, 254-262.
- Grosjean, D. (1982) Formaldehyde and other carbonyls in Los Angeles ambient air, Environ. Sci. & Tech. 16, 254-262.
- Grosjean, D. and Wright, B. (1983) Carbonyls in urban fog, ice fog, cloudwater, and rainwater, Atmos. Environ. 17, 2093-2096.
- Halperin, J. and Taube, H. (1952) The Transfer of Oxygen Atoms in Oxidation-Reduction Reactions. IV. The Reaction of Hydrogen Peroxide with Sulfite, Thiosulfate and of Oxygen, Manganese Dioxide and Permanganate with Sulfite, J. Am. Chem. Soc. 74, 380-382.
- Harrison, H., Larson, T. V. and Monkman, C. S. (1982) Aqueous Phase Oxidation of Sulfites by Ozone in the Presence of Iron and Manganese, Atmos. Environ. 16, 1039-1041.
- Hegg, D. A. and Hobbs, P. V. (1978) Oxidation of Sulfur Dioxide in Aqueous Systems with Particular Reference to the Atmosphere, Atmos. Environ. 12, 241-253.
- Hegg, D. A. and Hobbs, P. V. (1981) Cloudwater chemistry and the production of sulfates in clouds, Atmos. Environ. 15, 1597-1604.
- Hegg, D. A. and Hobbs, P. V. (1982) Measurements of sulfate production in natural clouds, Atmos. Environ. 16, 2663-2668.
- Hegg, D. A. and Hobbs, P. V. (1983) Sulfate Production in Natural Clouds, Atmos. Environ. 16, 2663-2668.

- Hering, S. V. and Blumenthal, D. L. (1983) Field comparison of fog/cloud water collectors: Preliminary results, Proc. APCA Specialty Conference on the Meteorology of Acid Deposition Oct. 1983, Hartford, CN, APCA.
- Hering, S. V. and Blumenthal, D. L. (1984) Sampler Intercomparison Study , Final Report (Draft) to Coordinating Research Council, Atlanta, GA , March 1984.
- Hoffman, Jr., W. A., Lindberg, S. E., and Turner, R. R. (1980) Precipitation acidity: the role of forest canopy in acid exchange, J. Environ. Qual. 9, 95-100.
- Hoffmann, M. R. (1984) Comment on acid fog, Environ. Sci. Technol. 18, 61-64.
- Hoffmann, M. R. and Boyce, S. D. (1983) Catalytic Autoxidation of Aqueous Sulfur Dioxide in Relationship to Atmospheric Systems, Trace Atmospheric Constituents: Properties, Transformations and Fates, S. E. Schwartz, ed. Adv. Environ. Sci. Technol. 12, 147-189.
- Hoffmann, M. R. and Edwards, J. O. (1975) Kinetics and Mechanism of the Oxidation of Sulfur Dioxide by Hydrogen Peroxide in Acidic Solution, J. Phys. Chem. 79, 2096-2098.
- Hoffmann, M. R. and Jacob, D. J. (1984) Kinetics and mechanisms of the catalytic oxidation of dissolved sulfur dioxide in aqueous solution: An application to nighttime fog-water chemistry , in Acid Precipitation, edited by J. G. Calvert, Butterworth Publ., Boston, MA.
- Hoffmann, M. R. and Shair, F. H. (1983) The Evolution of aerosol loadings during wintertime stagnation episodes in the southern San Joaquin Valley, A proposal to the California Air Resources Board Sacramento, California.
- Holz, E. (1982) , California State Science Fair Winner, personal communication.
- Jacob, D. J. and Hoffmann, M. R. (1983) A dynamic model for the production of H^+ , NO_3^- , and SO_4^{2-} in urban fog, J. Geophys. Res. 88C, 6611-6621.
- Jacob, D. J., Waldman, J. M., Munger, J. W. and Hoffmann, M. R. (1984a) A field investigation of physical and chemical mechanisms affecting pollutant concentrations in fog droplets, Tellus , (in press).
- Jacob, D. J., Munger, J. W., Waldman, J. M., and Hoffmann, M. R. (1984b) Aerosol composition in a stagnant air mass impacted by dense fogs: Preliminary results, 77th Annual meeting of the Air Pollution Control Assoc. San Francisco CA, June 24-29, Paper 24.5.
- Jacob, D. J., Wang, R-F. T., and Flagan, R. C. (1984c) Fogwater collector design and characterization, Environ. Sci. & Technol., in press.
- Kaplan, D. J., Himmelblau, D. M. and Kanaoka, C. (1981) Oxidation of Sulfur Dioxide in Aqueous Ammonium Sulfate Aerosols Containing Manganese as a Catalyst, Atmos. Environ. 15, 763-773.

- Katayama, B. and Price, D. R. (1983) Santa Barbara Channel Outer Continental Shelf Petroleum Production Emission Inventory Draft Report, Ventura County Air Pollution Control District, Ventura, CA.
- Katz, U. (1981) A droplet impactor to collect liquid water from laboratory clouds for chemical analysis, Desert Research Institute, unpublished manuscript, Reno, NV.
- Keene, W. C., Galloway, J. N., and Holden, J. N. (1983) Measurement of weak acidity in precipitation from remote areas of the world, J. Geophys. Res. 88C, 5122-5130.
- Keith, R. W. (1980) A Climatological/Air Quality Profile: California South Coast Air Basin, South Coast Air Quality Management District, El Monte, CA, November 1980.
- Kraak, J. C. and Huber, J. F. K. (1974) Separation of acidic compounds by high-pressure liquid-liquid chromatography involving ion-pair formation, J. Chromatog. 102, 333-351.
- Kunen, S. M., Lazrus, A. L., Kok, G. L. and Heikes, B. G. (1983) Aqueous Oxidation of SO₂ by Hydrogen Peroxide, J. Geophys. Res. 88, 3671-3674.
- Kuwata, K., Uebori, M., Yamasaki, H., and Yoshio, K. (1983) Determination of aliphatic aldehydes in air by liquid chromatography, Anal. Chem. 55, 2013-2016.
- Lagerstrom, P.-O. (1982) Separation of structurally related aromatic sulphonic acids and sulphates in synthesis mixtures by ion-pair liquid chromatography, J. Chromatog. 250, 43-54.
- Lala, G. G., Mandel, E., and Jiusto, J. E. (1975) A numerical evaluation of radiation fog variables, J. Atmos. Sci. 32, 720-728.
- Larson, T. V., Horike, N. R. and Halstead, H. (1978) Oxidation of Sulfur Dioxide by Oxygen and Ozone in Aqueous Solution: A Kinetic Study with Significance to Atmospheric Processes, Atmos. Environ. 12, 1597-1611.
- Legg, B. J. and Price, R. I. (1980) The contribution of sedimentation to aerosol deposition to vegetation with a large leaf area index, Atmos. Environ. 14, 305-309.
- Leith, D. and Mehta, D. (1973) Cyclone performance and design, Atmos. Environ. 7, 527-549.
- Likens, G. E., Edgerton, E. S., and Galloway, J. N. (1983) The composition and deposition of organic carbon in precipitation, Tellus 35B, 16-24.
- Maahs, H. G. (1983) Measurements of the Oxidation Rate of Sulfur(IV) by Ozone in Aqueous Solution and Their Relevance to SO₂ Conversion in Nonurban Tropospheric Clouds, Atmos. Environ. 17, 341-345.
- Mader, P. M. (1958) Kinetics of the hydrogen peroxide-sulfite reaction in alkaline solution, J. Am. Chem. Soc. 80, 2634-2639.

- Marple, V. A. and Liu, B. Y. H. (1974) Characteristics of laminar jet impactors, Environ. Sci. & Technol. 8, 648-654.
- Martin, L. R. (1983) Comment on Measurements of Sulfate Production in Natural Clouds, Atmos. Environ. 17, 1603-1604.
- Martin, L. R. (1984) Kinetic Studies of Sulfite Oxidation in Aqueous Solution, in Acid Precipitation, edited by J. G. Calvert, Butterworth Publishers, Stoneham, MA, 63-100.
- Martin, L. R. and Damschen, D. E. (1981) Aqueous Oxidation of Sulfur Dioxide by Hydrogen Peroxide at Low pH, Atmos. Environ. 15, 1615-1622.
- Martin, L. R., Damschen, D. E. and Judeikis, H. S. (1981) Sulfur Dioxide Oxidation Reactions in Aqueous Solution, EPA Report 600/7-81-085, 31 pp.
- McArdle, J. V. and Hoffmann, M. R. (1983) Kinetics and mechanism of the oxidation of aquated sulfur dioxide by hydrogen peroxide at low pH, J. Phys. Chem. 87, 5425-5429.
- McCrae, G. J., Goodin, W. R., and Seinfeld, J. H (1982) Mathematical Modelling of Photochemical Air Pollution, Final Report to the California Air Resources Board, Sacramento, California.
- McMurry, P. H., Rader, D. J. and Smith, J. L. (1981) Studies of Aerosol Formation in Power Plant Plumes. I. Parameterization of Conversion Rate for Dry, Moderately Polluted Ambient Conditions, Atmos. Environ. 15, 2315-2329.
- Middleton, P., Kiang, C. S. and Mohnen, V. A. (1980) Theoretical Estimates of the Relative Importance of Various Urban Sulfate Aerosol Production Mechanisms, Atmos. Environ. 14, 463-472.
- Mohnen, V. A. (1980) Cloud water collection from aircraft, Atmos. Technol. 12, 20-25.
- Moller, D. (1980) Kinetic model of atmospheric oxidation based on published data, Atmos. Environ. 14, 1067-1076.
- Monteith, J. L. (1957) Dew, Q. J. Roy. Met. Soc. 83, 322-341.
- Munger, J. W., Jacob, D. J., Waldman, J. M., and Hoffmann, M. R. (1983) Fogwater chemistry in an urban atmosphere, J. Geophys Res. 88C, 5109-5121.
- Munger, J. W., Jacob, D. J., and Hoffmann, M. R. (1984) The occurrence of bisulfite-aldehyde addition products in fog- and cloudwater, J. Atmos. Chem. , (in press).
- Nagamoto, C. T., Parungo, F., Reinking, R., Pueschel, R., and Gerish, T. (1983) Acid clouds and precipitation in eastern Colorado, Atmos. Environ. 17, 1073-1082.

- Nash, T. (1953) The colorimetric estimation of formaldehyde by means of the Hantzsch reaction, Biochem. J. 55, 416-421.
- National Research Council (1981) Formaldehyde and Other Aldehydes, National Academy Press, Washington D. C., 340 pp.
- Oberlander, G. T. (1956) Summer fog precipitation on the San Francisco peninsula, Ecology 37, 851-852.
- Penkett, S. A., Jones, B. M. R. and Eggleton, A. E. J. (1979a) A Study of SO₂ Oxidation in Stored Rainwater Samples, Atmos. Environ. 13, 139-147.
- Penkett, S. A., Jones, B. M. R., Brice, K. A. and Eggleton, A. E. J. (1979b) The Importance of Atmospheric Ozone and Hydrogen Peroxide in Oxidizing Sulfur Dioxide in Cloud and Rainwater, Atmos. Environ. 13, 123-137.
- Perschke, H. and Broda, E. (1961) Determination of very small amounts of hydrogen peroxide, Nature 190, 257-258.
- Petrenchuk, O. P. and Aleksandrov, N. N. (1966) Ob otenske effektivnosti ulavlivanii oblach nykh kapel samoletnym, Glavnoi Geofiz. Observ., Leningrad Trudy 185, 126-132.
- Pickering, K. E. and Jiusto, J. E. (1978) Observations of the relationship between dew and radiation fog, J. Geophys. Res. C5, 2430-2436.
- Prandi, C. and Venturini, T. (1981) Retention behaviour of aromatic sulfonic acids in ion-pair reversed-phase column liquid chromatography, J. Chromatog. Sci. 19, 308-314.
- Pruppacher, H. R. and Klett, J. D. (1978) Microphysics of Clouds and Precipitation, Reidel, Amsterdam, 714 pp.
- Pueschel, R. F., Barrett, E. W., Wellman, D. L., and McGuire, J. A. (1981) Cloud modification by man-made pollutants: Effects of a coal-fired power plant on cloud drop spectra, Geophys. Res. Lettr. 8, 221-224.
- Reible, D. D., Ouimette, J. R., and Shair, F. H. (1982) Atmospheric transport of visibility degrading pollutants into the California Mojave desert, Atmos. Environ. 16, 599-613.
- Reible, D. D., Shair, F. H., Smith, T. B., and Lehman, D. E. (1984a) The origin and fates of air pollutants in California's San Joaquin Valley I. Winter, Atmos. Environ., (in press).
- Reible, D. D., Shair, F. H., and Lehman, D. E. (1984b) Tracer investigations of atmospheric transport and dispersion in the Santa Barbara Channel area of Southern California, Atmos. Environ., (submitted).
- Reitz, E. B. (1980) The stabilization of small concentrations of formaldehyde in aqueous solutions, Analyt. Lett. 13, 1073-1084.
- Richards, L. W., Anderson, J. A., Blumenthal, D. L., McDonald, J. A., Kok, G. L., and Lazrus, A. L. (1983) Hydrogen peroxide and sulfur(IV) in Los Angeles cloudwater, Atmos. Environ. 17, 911-914.

- Rotsch, T. D. and Pietrzyk, D. J. (1980) Ion-interaction in high performance liquid chromatography of benzenesulfonic acids on amberlite XAD-2, Anal. Chem. 52, 1323-1327.
- Russell, A. G., McRae, G. J. and Cass, G. R. (1983) Mathematical modeling of the formation and transport of ammonium nitrate aerosol, Atmos. Environ. 17, 949-964.
- Saltzman, E. S., Savoie, D. L., Zika, R. G., and Prospero, J. M. (1983) Methanesulfonic acid in the marine atmosphere, J. Geophys. Res. 88C, 10897-10902.
- Scherbatskoy, T. and Klein, R. M. (1983) Response of spruce and birch foliage to leaching by acidic mists, J. Environ. Quality 12, 189-195.
- Schwartz, S. E. (1984) Gas-Aqueous Reactions of Sulfur and Nitrogen Oxides in Liquid-Water Clouds, Acid Precipitation edited by J. G. Calvert, Butterworth Publishers, Boston, MA.
- Schwartz, S. E. and Freiberg, J. E. (1981) Mass-transport limitation to the rate of reaction of gases in liquid droplets: Application to oxidation of SO₂ in aqueous solutions, Atmos. Environ. 15, 1129-1144.
- Schwartz, S. E. and Newman, L. (1983) Comment on Measurements of Sulfate Production in Natural Clouds, Atmos. Environ. 17, 2629-2632.
- Schwartz, S. E. and White, W. H. (1981) Solubility equilibria of the nitrogen oxides and oxyacids in dilute aqueous solution, Adv. Env. Sci. Eng. 4, 1-45.
- Sehmel, G. A. (1980) Particle and gas dry deposition: a review, Atmos. Environ. 14, 983-1011.
- Smith, F. B. and Jeffrey, G. H. (1975) Airborne Transport of Sulphur Dioxide from the U.K., Atmos. Environ. 9, 643-659.
- Smith, R. V. and Erhardt, P. W. (1975) Nash determination for formaldehyde in the presence of bisulfite, Anal. Chem. 47, 2462,2454.
- Smith, T. B., Lehman, D. E., Reible, D. D. and Shair, F. H. (1981) The origin and fate of airborne pollutants within the San Joaquin Valley, Final report to the California Air Resources Board Sacramento, California.
- Solorzano, L. (1967) Determination of ammonia in natural waters by the phenol-hypochlorite method, Limnol. Oceanogr. 14, 799-801.
- Stelson, A. W. (1982) Thermodynamics of aqueous atmospheric aerosols, Ph.D. thesis, California Institute of Technology, Pasadena, California.
- Terwiej-Groen, C. P. and Kraak, J. C. (1977) Ion-pair phase systems for the separation of carboxylic acids, sulphonic acids, and phenols by high pressure liquid chromatography, J. Chromatog. 138, 245-266.

- Tukey, Jr., H. B. (1970) The leaching of substances from plants; Ann. Rev. Plant Physiol. 71, 305-324.
- Unger, C. D. (1984) Analysis of meteorological and air quality data associated with the occurrence of fogwater with high acidity in the Los Angeles Basin, California Air Resources Board Memo, Sacramento, CA.
- Wahlund, K.-G. (1975) Reversed-phase ion-pair partition chromatography of carboxylates and sulphonates, J. Chromatog. 115, 411-422.
- Waldman, J. M., Munger, J. W., Jacob, D. J., Flagan, R. C. Morgan, J. J., and Hoffmann, M. R. (1982) Chemical composition of acid fog, Science 218, 677-680.
- Waldman, J. M., Munger, J. W., Jacob, D. J., and Hoffmann, M. R. (1984) Chemical characterization of stratus cloudwater and its role as a vector for pollutant deposition in a Los Angeles pine forest, Water, Air and Soil Pollut., submitted.
- Wallin, J. R. (1967) Agrometeorological aspects of dew, Agric. Meteor. 4, 85-102.
- Wattle, B. J., Mack, E. J., Pilie, R. J., and Hanley, J. T. (1984) The Role of Vegetation in the Low-level Water Budget in Fog, Report 7096-M-1 Arvin/Calspan Advanced Technology Center, Buffalo, NY.
- Wedding, J. B., McFarland, A. R., and Cermack, J. E. (1977) Large particle collection characteristics of ambient aerosol samplers, Environ. Sci. Technol. 11, 387-390.
- Williams, R. J. (1982) The separation of ionic organosulfur compounds by ion chromatography, J. Chromatog. Sci. 20, 560-565.
- Wilson, J. C. and McMurry, P. H. (1981) Studies of Aerosol Formation in Power Plant Plumes. I. Secondary Aerosol Formation in the Navajo Generating Station Plume, Atmos. Environ. 15, 2329-2339.
- Yaalon, D. H. and Gaynor, E. (1968) Chemical composition of dew and dry fallout in Jerusalem, Israel, Nature 217, 1139-1140.
- Zeldin, M. D., Davidson, A., Brunelle, M. F., and Dickinson, J. E. (1976) A Meteorological Assessment of Ozone and Sulfate Concentrations in Southern California, Evaluation and Planning Division Report 76-1 Southern California Air Pollution Control District, El Monte, CA.
- Zika, R. G., Saltzman, E. S., Chameides, W. L., and Davis, D. D. (1982) H₂O₂ levels in rainwater collected in South Florida and the Bahama Islands, J. Geophys. Res. 87, 5015-5017.

APPENDIX I

CHEMICAL COMPOSITION OF FOGWATER COLLECTED ALONG THE CALIFORNIA COAST.

Daniel J. Jacob, Jed M. Waldman, J. William Munger, and Michael R. Hoffmann*.

Environmental Engineering Science, W. M. Keck Engineering Laboratories, California Institute of Technology, Pasadena, California, 91125.

submitted to Environmental Science and Technology

September 1984

ABSTRACT.

Fogwater collected at both urban and non-urban coastal sites in California was found to be consistently acidic. The highest acidities (pH values down to 2) occurred at sites in the Los Angeles basin or downwind. Concentrations of acid-neutralizing constituents in coastal air were found to be very low, so that fogs were acidic even under relatively clean conditions. Chloride loss relative to its sea salt contribution was observed at sites furthest from anthropogenic sources.

INTRODUCTION.

Recent investigations of fogwater chemical composition in the Los Angeles basin (1, 2) have revealed high ionic concentrations and, often, very high acidities (pH values typically in the range of 2 to 4). Comparable acidities have been observed in low stratus clouds collected by aircraft over the basin (3) and sampled on the slopes of the surrounding mountains (4). These high acidities have raised concern regarding potential damage to materials, vegetation (5), crops (6), and public health (7). Laboratory data indicate that conversion of SO_x to sulfate can proceed rapidly at the concentrations found in urban fog droplets (8) and in the precursor haze aerosol (9). Field studies have proposed evidence for aqueous-phase sulfate production in the atmosphere (10,11,12,13).

Fogs are frequent seasonal occurrences along the California coast. During the summer, coastal stations may report over 50% foggy days (14). These fogs are often coupled with land breeze/sea breeze systems, which recirculate the same air parcels several times across the shoreline (13). Tracer studies in the Santa Barbara Channel (15) have shown that emissions from offshore and coastal sources may reside several days along the coast. These humid, poorly ventilated conditions favor pollutant build-up and sulfate production.

As part of an extensive fog sampling program in California, we have collected fogwater at a number of coastal sites. Coastal fogs may be a major cause of sulfate pollution episodes in Southern California (16). Further, because impaction of fog droplets can be a significant source of water input to the coastal vegetation (17), the

chemical composition of the fogwater has important local implications for acid deposition. Recent interest in these problems has been stirred by federal plans to encourage oil exploration and production in the outer continental shelf off California (18).

SAMPLING SITES AND METHODS.

Fogwater was sampled with a rotating arm collector (19) at eight coastal sites and one island site (Figure 1). The sites, and conditions during sampling, are described in Table 1. Samples were collected over intervals ranging from 30 minutes to 2 hours, and were analyzed for major ions and metals following the protocol described in ref. 1. Concentrations of Na^+ , K^+ , Ca^{2+} , and Mg^{2+} were determined by atomic absorption spectroscopy on filtered aliquots; at some sites (Del Mar, Long Beach, Lennox, Morro Bay) we analyzed both filtered and unfiltered aliquots and did not observe significant differences in concentrations.

Determination of anions by ion chromatography revealed unidentified peaks eluting just before chloride in fogwater samples collected at some urban sites. When chloride concentrations were low, a positive interference from these peaks was noted; chloride concentrations reported are then an upper bound of true chloride concentrations and are indicated as such. The unidentified peaks were likely due to organic acids (20,21). We have measured formate and acetate at concentrations around 10^{-4}M in fog samples (J. W. Munger, unpublished results).

The contributions of different source types to the fogwater

chemical composition were determined from an emission matrix for primary California aerosol (Table 2). Concentrations of fly ash and automobile exhaust were calculated from the concentrations of vanadium and lead, respectively. Contributions from sea salt, soil dust, and cement dust were obtained by a balance on sodium, iron, and calcium, after subtraction of fly ash and automobile exhaust contributions. Because concentrations of the different elements analyzed in a sample spread over a wide range, we found that this apportionment method gave more reliable results than a least-squares fit of all elemental concentrations to the emission matrix (22). Secondary sulfate was calculated by subtraction of primary contributions from the total sulfate concentration. All nitrate was assumed to be of secondary origin.

RESULTS AND DISCUSSION.

Fogwater concentrations. Table 3 gives liquid water-weighted average fogwater concentrations for each event; the detailed data set is available elsewhere (25). Contributions from the different source types are given in Table 4 in terms of fogwater loadings, which we define as the mass of material in fogwater per m^3 of air. Liquid water contents were estimated from the collection rate of our rotating arm collector, assuming a 60% overall collection efficiency (19). A number of methods have been used in field investigations to measure liquid water contents in fogs, but none has been reliably calibrated, and a field intercomparison has revealed systematic biases between different methods (4). Although the absolute error on

our liquid water content estimates cannot be ascertained at this time, we are satisfied that differences in the collection rate closely follow actual differences in the liquid water content (4).

In Table 5, elemental ratios in fogs are compared to those for sea salt. The observed Na/Mg ratios were close to that for sea salt; exceptions were the Long Beach, Lennox, and San Marcos sites, where sea salt constituted only a small fraction of the total loading and significant soil dust contributions of Na and Mg were apparent. Calcium and sulfate were partly of marine origin, but usually had larger contributions from dust (calcium) and secondary production (sulfate). The K/Na ratios were close to that for sea salt at Del Mar, San Nicholas Island, and Pt. Reyes; soil dust was an important source of potassium at other sites.

The sites in and around the Los Angeles basin were by far the most affected by anthropogenic sources (Table 4). The large contribution from automobile exhaust in the fog samples collected at Lennox can be attributed to the nearby freeway and airport traffic. The sulfate-to-nitrate equivalent ratio at Long Beach Harbor was much higher than that usually observed in the Los Angeles basin (0.2-0.5); non-sea salt (NSS) sulfate concentrations in the basin are known to peak in the Long Beach Harbor because of oil burning by ships (10).

The fogs on 7 and 18 December 1981 at Lennox and 7 December 1983 at Corona del Mar occurred during severe sulfate pollution episodes in the Los Angeles basin. Average fogwater pH values below 3 were observed on those nights. On the day following the Corona del Mar event, all coastal stations of the South Coast Air Quality Management District recorded their highest 24-hour sulfate concentrations for

1982, ranging from 23 to 37 $\mu\text{g m}^{-3}$. The prevailing southward transport of pollutants on the night 6-7 December, 1982 (26) explains the extremely high acidities observed at Corona del Mar; a second sample (1 ml) collected as the fog dissipated had a pH = 1.69 (a value which was later confirmed in the laboratory).

High ionic concentrations and acidities were also found in samples collected at Del Mar on 8 January 1983 (Figure 2). The NW winds blowing over Del Mar at the beginning of the sampling period carried pollutants from Los Angeles which had been transported offshore by weak NE winds the previous morning (27). A developing land breeze led to flow reversal between 1900 and 2000 PST and advection over the site of inland air from suburban San Diego County.

Sea salt concentrations dropped considerably as the land breeze developed; contributions from anthropogenic sources also decreased, although less, as the Los Angeles air was replaced by cleaner air.

Fogwater collected at San Marcos Pass (low stratus), Morro Bay, Mt. Sutro, and Pt. Reyes contained much less nitrate, NSS sulfate, and automobile exhaust than fogwater collected in the Los Angeles basin or downwind. However, except at Morro Bay, all samples were acidic; fogwater pH ranged from 4.21 to 4.69 at San Marcos Pass, and from 3.60 to 5.00 at Pt. Reyes. Significant concentrations of metals and NSS calcium at all sites show that the air sampled was of partly continental origin even under onshore wind conditions. This has previously been observed in aerosol collected elsewhere along the California coast (28). Fogwater collected at Pt. Reyes under offshore wind conditions (12 Aug. 1983) contained less sea salt, more soil dust, and more automobile exhaust than fogwater collected on

other nights under the more usual N-NW wind conditions.

Nitrate and NSS sulfate loadings at San Nicholas Island were higher than those at other non-urban sites, even though impact of Los Angeles pollutants is very unlikely under the wind conditions observed on that night. High concentrations of metals and NSS calcium indicated that the air over the island was of mixed marine/continental origin. The relatively high fly ash and low automobile exhaust loadings suggest that the high acidity could be due to advection by NNW winds of a plume from oil drilling operations off Pt. Conception or emissions from the Morro Bay power plant; dilution of the plume would be limited by the low mixing heights and slow horizontal dispersion over the ocean (15). Transport from the Pt. Conception area over San Nicholas Island has been previously documented (29).

The acidity of coastal fogs in California. Fogwater was often extremely acidic in and around the Los Angeles basin; elsewhere, relatively high "background" nitrate and NSS sulfate concentrations apparently led to ubiquitous acidic conditions along most of the California coastline. Pollutant transport with slow dispersion along the coast has been well documented (13, 15), and has been attributed to the dominant NW wind, the sea-breeze/land-breeze circulation system, the low surface roughness of the ocean, and the persistent strong inversions.

Acidities in non-urban coastal fogs were comparable to those found in fogs sampled in the inland San Joaquin Valley of California, where much higher nitrate and sulfate loadings were observed (30).

The non-neutralized fraction of the acidity,

$[H^+]/([NO_3^-]+[(NSS)SO_4^{2-}])$, was typically less than 10% in San Joaquin Valley fogs (30); in comparison, the non-neutralized fraction of the acidity was on the average 25% at San Marcos Pass, 31% at Mt. Sutro, and 48% at Pt. Reyes.

Obviously, there is little alkalinity available in the coastal air to neutralize acid inputs. Ammonia was found to be the main acid-neutralizing component in San Joaquin Valley fogs (30). An excess of ammonia ($H = 50 \text{ M atm}^{-1}$, $K_b = 1.7 \times 10^{-5} \text{ M}$ at 10°C) maintains fogwater pH above 5. Fogwater below pH 5, as found along the coast, cannot support gaseous ammonia at equilibrium; ammonia is then expected to be nearly 100 % scavenged by the fog droplets. The relatively low ammonium fogwater concentrations (as compared to nitrate and sulfate concentrations) show that alkalinity from ammonia is lacking in coastal air. Soil dust is an alternate source of alkalinity, but the small amount present in the droplets (Table 4) limits the extent of H^+ -neutralizing ion-exchange surface reactions. These reactions would mostly involve the cations Ca^{2+} and Mg^{2+} , but as mentioned previously we found these ions to be mostly dissolved. Alkalinity from scavenged soil dust was therefore exhausted.

The low nitrate concentrations observed at Pt. Reyes and Mt. Sutro on 10-13 August, 1982 suggest a source of acidity especially rich in H_2SO_4 . Two likely sources are emission from ships and oxidation of dimethylsulfide volatilized from the ocean surface. Non-sea salt sulfate concentrations of $0.1 - 1 \text{ ug m}^{-3}$ over the Pacific Ocean have been attributed to the oxidation of dimethylsulfide (31), and oceanic dimethylsulfide production has been

found to be maximum near coasts (32). Rapid photooxidation of alkyl sulfides in a sunlight-irradiated chamber has been reported (33). This source of sulfate could therefore possibly be a major contributor to the acidity at non-urban coastal sites in California.

Volatilization of HCl(g) from sea salt nuclei. A number of investigators of marine aerosols have observed chloride loss relative to its expected sea salt contribution (34,35). These investigators report chloride losses ranging from 0% (no loss) up to 100%. Chloride loss proceeds by incorporation of a strong acid in sea salt-containing aerosol, resulting in pH-lowering and volatilization of HCl(g). The strong acids can be HNO₃ (34) or H₂SO₄ (35,36). Displacement by NO₂(g) on NaCl(s) has been found to be effective at ppm concentrations of NO₂ (37).

Table 6 is a summary of thermodynamic data regarding the main reactions involved. If the sea salt particle is solid, the reaction may proceed by adsorption of HNO₃(g) and sublimation of HCl(g) from surface NaCl crystals, or by coagulation of sea salt aerosol with sulfuric acid or bisulfate droplets. Above the deliquescence point, volatilization of HCl(g) is given by the position of equilibrium (3). Both H₂SO₄ and HNO₃ added to a NaCl(aq) aerosol will displace HCl, but HNO₃ is less efficient than H₂SO₄ because it is only slightly less volatile than HCl. Hitchcock et al. (35) infer from field data that HSO₄⁻ does not displace Cl⁻; however, equilibria (3) and (5) indicate that a substantial fraction of chloride could be released to the gas phase at the liquid water contents typical of haze (10⁻³ g m⁻³).

Although volatilization of HCl(g) proceeds effectively in acid haze, reaction (3) indicates that fog, even acidic, cannot support HCl(g) . This is because of the higher liquid water contents, and because acidities in fogs are not as high as those reached in haze. If chloride was lost in the precursor aerosol, it could still be recovered in the fog by scavenging of HCl(g) . Chloride deficiency with respect to its sea salt contribution in the fog therefore requires loss of chloride from the precursor aerosol followed by removal of the resulting HCl(g) from the air parcel during transport prior to droplet activation.

The fogs sampled in our study were acidic, and chloride loss in the precursor aerosol would be expected. However, measured chloride concentrations were in excess of the sea salt contribution at most of our sites; this would be due to (i) anthropogenic sources of chloride, (ii) organic acids interfering with chloride in analysis. Significant chloride loss was observed in 1 sample from Del Mar (18%), all samples from San Nicholas Island (12%-35%), and 4 samples from Pt Reyes (10%-28%). Therefore, chloride loss was observed in the fogwater only at those sites where long transport of acids over the ocean was involved. Transport may have led to separation of HCl(g) from the nuclei, possibly by removal of HCl(g) to the ocean surface. Because of its high reactivity with surfaces, HCl(g) should deposit faster than NaCl aerosol.

CONCLUSION.

Fogwater samples collected at both urban and non-urban sites along the coast of California were consistently acidic. Apart from sea salt, the main constituents were sulfuric and nitric acids (partially neutralized by ammonia). Extremely high acidities (pH values down to 2) were observed at sites in the Los Angeles basin or downwind. The acid-neutralizing capacities were found to be much lower in the coastal air than in inland areas of Southern California, and insufficient to neutralize even low acid inputs at non-urban sites. Chloride loss in fogwater was observed at sites affected by acids advected from distant sources, even though hydrochloric acid volatilized by pH-lowering of the precursor sea salt aerosol would be scavenged upon fog formation. A possible explanation is that HCl(g) deposits faster than NaCl over ocean surfaces.

ACKNOWLEDGEMENTS. We thank the organizations who provided us with sampling sites: the U.S.Navy, the National Park Service, the South Coast Air Quality Management District, the San Luis Obispo and San Diego Air Pollution Control Districts. This research was funded by the California Air Resources Board (contract No. A2-048-32).

LITERATURE CITED.

- (1) Munger, J.W.; Jacob, D.J.; Waldman, J.M.; Hoffmann, M.R.
J. Geophys. Res. 1983, 88, 5109-5123
- (2) Brewer, R.L.; Ellis, E.C.; Gordon, R.J.; Shepard, L.S. Atmos. Environ.
1983, 17, 2267-2271
- (3) Richards, L.W.; Anderson, J.A.; Blumenthal, D.L.; McDonald, J.A.;
Kok, G.L.; Lazrus, A.L. Atmos. Environ. 1983, 17, 911-914
- (4) Waldman, J.M.; Munger, J.W.; Jacob, D.J.; Hoffmann, M.R. submitted
to Tellus
- (5) Scherbatskoy, T.; Klein, R.M. J. Environ. Quality 1983, 12, 189-195
- (6) Granett, A.L.; Musselman, R.C. Atmos. Environ. 1984, 18, 887-891
- (7) Hoffmann, M.R. Environ. Sci. Technol. 1984, 18, 61-63
- (8) Martin, L.R. in "Acid Precipitation", J.G. Calvert ed.,
Butterworth, Boston, 1984 p.63-100
- (9) Crump, J.G.; Flagan, R.C.; Seinfeld, J.H. Atmos. Environ.
1983, 17, 1277-1289
- (10) Cass, G.R. Atmos. Environ. 1981, 15, 1227-1249
- (11) Hegg, D.A.; Hobbs, P.V. Atmos. Environ. 1982, 16, 2663-2668
- (12) Daum, P.H.; Schwartz, S.E.; Newman, L. in "Precipitation
Scavenging, Dry Deposition, and Resuspension", H.R. Pruppacher
et al. ed., Elsevier, New York 1983, p.31-44
- (13) Cass, G.R.; Shair, F.H. J. Geophys. Res. 1984, 89, 1429-1438
- (14) deViolini, R. 1974 Techn. Publ. TP/74/1, Pacific Missiles Range,
Pt. Mugu, CA 1974
- (15) Reible, D.D.; Shair, F.H.; Lehrman, D.E. manuscript in preparation

- (15) Zeldin, M.D. et al. Evaluation and Planning rpt. 76-1, Southern California Air Pollution Control District, El Monte, CA, Aug. 1976
- (17) Azevedo, J.; Morgan, D.L. Ecology 1974, 55, 1135-1141
- (18) California Air Resources Board 1982 "Air quality aspects of the development of offshore oil and gas resources", Sacramento, CA
- (19) Jacob, D.J.; Wang, R.-F.T.; Flagan, R.C. Environ.Sci.Technol. 1984 (in press)
- (20) Nagamoto, C.T.; Parungo, F.; Reinking, R.; Poeschel, R.; Gerish, T. Atmos.Environ. 1983, 17, 1073-1082
- (21) Keene, W.C.; Galloway, J.N. Atmos. Environ. 1984 (in press)
- (22) Friedlander, S.K. Environ.Sci.Technol. 1973, 7, 235-240
- (23) Cooper, J.A.; Watson, J.G., Jr. J. Air Poll. Control Assoc. 1980, 30, 1116-1125
- (24) Weast, R.C. ed. 1975 "Handbook of Chemistry and Physics" 56th ed., p.F-199.
- (25) Jacob, D.J. 1984 Ph.D. thesis, California Institute of Technology, Pasadena, CA .
- (26) Unger, C.D. "An analysis of meteorological and air quality data associated with the occurrence of fogwater with high acidity in the Los Angeles basin", July 18, 1984 memorandum, California Air Resources Board, Sacramento, CA
- (27) Brown, H.W. 1983 "An analysis of air flow over the Southern California bight and northern San Diego county on January 8, 1983", San Diego Air Pollution Control District, San Diego, CA.
- (28) Whitby, K.T.; Sverdrup, G.M. Adv.Environ.Sci.Technol. 1980, 9, 477-517

- (29) Rosenthal, J.; Battalino, T.E.; Hendon, H.; Noonkester, V.R.
Techn. Publ. TP/79/33, Pacific Missiles Test Center, Pt. Mugu,
CA, 1979
- (30) Jacob, D.J.; Waldman, J.M.; Munger, J.W.; Hoffmann, M.R. *Tellus* (in
press)
- (31) Saltzman, E.S.; Savoie, D.L.; Zika, R.G.; Prospero, J.M.
J. Geophys. Res. 1983, 88, 10897-10902
- (32) Andreae, M.O.; Raemdonck, H. Science (Washington, D.C.)
1983, 221, 744-747
- (33) Grosjean, D. Environ. Sci. Technol. 1984, 18, 460-468
- (34) Martens, C.S.; Welosowski, J.J.; Harriss, R.C.; Kaifer, R.
J. Geophys. Res. 1973, 78, 8778-8792
- (35) Hitchcock, D.R.; Spiller, L.L.; Wilson, W.E. Atmos. Environ.
1980, 14, 165-182
- (36) Eriksson, E. Tellus 1960, 12, 63-109
- (37) Finlayson-Pitts, B.J. Nature 1983, 306, 676-677
- (38) Latimer, W.D. "The oxidation states of the elements and their
potentials in aqueous solutions" 2nd ed. Prentice-Hall, New
York, 1952.

Table 1. Description of sampling sites.

<u>Site</u>		<u>Conditions during sampling</u>		
		<u>Inversion base</u> ^(a)	<u>Temp.</u> ^(b)	<u>Surface wind</u> ^(b)
		(m)	(°C)	(m s ⁻¹)
Del Mar	Coastal lagoon, residential surroundings. Collector set on ground, 800 m from shore.	surface	11	moderate NW shifting to moderate E
Corona del Mar	Residential area. Collector set on pier.	260	11	calm
Long Beach Harbor	Industrial area, ships. Collector set on dock, 10 m from water.	220	10	calm
Lemox	Industrial and residential area. Los Angeles Int'l Airport is 2 km NW, major freeway is 500 m E. Ocean is 4 km W. Collector set on roof of 1-story building.	surface	12	1NE
		surface	14	1SE
		220	10	calm
			(7 Dec. 1981)	
			(18 Dec. 1981)	
			(7 Jan. 1983)	
San Nicholas Island	U. S. Navy base, 100 km offshore. No impact from local sources. Collector set at 50 m elevation, 400 m from shore.	150	14	5 NNW
San Marcos Pass	Mountain pass in coastal range, 700m elevation. No nearby sources.	1800	8-15	2S
Morro Bay	Rural town at the base of major power plant. Agriculture, ranches. Some local traffic. Collector set 500 m from shore, on roof of 1-story building.	450	11	0-2 SW
Mt. Sutro	250 m elevation hill in San Francisco. Radio towers, no local traffic. Ocean is 5 km W.	570	12	1 W
Pt. Reyes	National Seashore, no nearby sources. Collector set at tip of peninsula, 10 m elevation, 50 m from shore.	600	12	10-15 N
			(9 Aug. 1982)	
		420	11-12	10-15 N
			(10 Aug. 1982)	
		1800	12-14	10-15 N
			(11 Aug. 1982)	
		240	11-14	2 SE
			(12 Aug. 1982)	

(a) measured by the National Weather Service at San Diego, Los Angeles, Vandenberg AFB, or Oakland.
 (b) measured at the site.

Table 2. Source concentrations of particulate matter^(a).

	sea salt	soil dust	% mass cement dust	fuel oil fly ash	automobile exhaust
Na	30.6	2.5	0.4	5	0 ^(b)
S	2.6	0.1 ^(b)	0.1 ^(b)	15 ^(b)	2 ^(b)
Ca	1.16 ^(c)	1.5	46.0	1.3	0.02 ^(b)
V	9×10^{-7}	0.006	0	7	0
Fe	0	3.2	1.09	6	0.4
Pb	10^{-5}	0.02	0	0.07	40

(a) data from ref. 22 unless otherwise specified.

(b) ref. 23

(c) ref. 24

Table 3. Liquid water-weighted average fogwater concentrations.

Site	Date ^(a)	n	pH	μeq l ⁻¹									μM l ⁻¹		
				H ⁺	Na ⁺	K ⁺	NH ₄ ⁺	Ca ²⁺	Mg ²⁺	Cl ⁻	NO ₃ ⁻	SO ₄ ²⁻	S(IV) ^(b)	CH ₂ O ^(b)	L ^(c)
Del Mar	9 Jan. 83 1840-2300	5	2.85	1410	511	9	781	49	130	614 ^(d)	1850	469	66	78	0.24
Corona del Mar	7 Dec. 82 2100-2300	1	2.16	6920	725	71	2860	197	188	1050	7900	1290	NA	NA	0.11
Long Beach	6 Jan. 83 0400-0500	2	4.90	12.7	62	12	759	45	26	221 ^(d)	252	487	NA	71	0.25
Lennox ^(e)	7 Dec. 81 2305-0840	8	2.96	1100	65	12	1610	111	42	178 ^(d)	2210	926	80	196	0.30
	18 Dec. 81 2315-0045	3	2.66	2190	131	30	1280	127	48	150 ^(d)	2780	1280	NA	178	0.14
	6 Jan. 83 0000-0430	5	3.63	237	41	8	464	39	18	68 ^(d)	365	126	34	68	0.17
San Nicholas Island	26 Aug. 82 2115-0755	7	3.86	138	6060	148	452	450	1500	5330	1580	1080	11	15	0.052
San Marcos Pass ^(f)	20 Aug. 83 2340-1200	14	4.49	32.1	10	3	97	3	4	19	74	55	2	8	0.43
Porro Bay	14 Jul. 82 0500-0900	2	6.17	0.67	746	64	107	120	221	1200	114	214	6	7	0.14
Pt. Sutro	13 Aug. 82 2125-2225	1	3.99	102	648	52	183	93	170	851	87	319	NA	NA	0.056
Pt. Reyes	9 Aug. 82 2200-0000	1	3.60	251	3520	91	327	242	890	3040	526	1280	10	19	0.054
	10 Aug. 82 0230-1115	3	4.48	33.4	3146	72	95	153	782	4576	38	463	4	2	0.081
	11 Aug. 82 0200-1155	7	3.88	132	498	12	59	27	118	645	36	208	5	3	0.13
	12 Aug. 82 0340-0815	6	4.69	20	42	1.6	43	3	10	57	6	54	5	3	0.19

a) date is that of the a.m. samples, or that of the morning following the fog. Time is local time.

(b) averages for S(IV) and CH₂O may be based on incomplete data sets.

(c) average liquid water content (g m⁻³), calculated from the total volume collected.

d) [Cl⁻] may be overestimated due to interference from organic acids during analysis. At Del Mar, this uncertainty is significant only for the last three samples (see text).

(e) 1981 events at Lennox have been previously reported by Munger et al. (1983).

(f) stratus cloud.

Table 3 (continued)

Site	n	-----ug l ⁻¹ -----					
		Fe	Mn	Pb	Cu	Ni	V
Del Mar	4	354	36	310	NA	111	6
Long Beach	2	96	22	152	NA	17	1
Lennox							
7 Dec. 1981	7	1440 ^(a)	37	1180	34	10	6
18 Dec. 1981	3	1330	51	NA	NA	NA	13
6 Jan. 1983	5	315 ^(b)	127	447	NA	25 ^(c)	5
San Nicholas Island	5	431	93	49	49	99	8
San Marcos Pass	9	22	3	23	12	6	NA
Morro Bay	1	192	21	11	57	21	3
Mt. Sutro	1	160	10	24	50	28	NA
Pt. Reyes							
9 Aug. 1982	1	484	67	67	87	209	NA
10 Aug. 1982	3	276	12	21	36	66	NA
11 Aug. 1982	4	301	10	38	151	59	NA
12 Aug. 1982	5	265	7	26	48	17	NA

NA: not analyzed.

Metal concentrations were not determined in the Corona del Mar fog.

(a) average from 6 samples

(b) average from 2 samples

(c) average from 4 samples

Table 4. Source contributions to fogwater loading.

Site	mass loading ($\mu\text{g m}^{-3}$)						
	sea salt	secondary nitrate	secondary sulfate	soil dust	cement dust	fuel oil fly ash	automobile exhaust
Del Mar	9.0	28	4.9	2.8	0.27	0.023	0.21
Corona del Mar	6.1	54	6.6		0.80		
Long Beach	1.2	3.9	5.8	0.58	0.45	0.0036	0.095
Lennox							
7 Dec. 1981	0.80	30	10	8.6	1.1	0.019	0.62
18 Dec. 1981	1.2	25	9.0	5.7	0.74	0.027	
6 Jan, 1983	0.51	3.9	1.0	1.8	0.26	0.012	0.20
San Nicholas Island	23	5.2	4.3	0.55	0.42	0.0074	0.0064
San Marcos Pass	0.34	1.9	1.1	0.27	0.047		0.023
San Pedro Bay	7.5	1.1	1.2	0.97	0.55	0.0086	0.0055
St. Sutro	2.7	0.30	0.74	0.22	0.16		0.0033
Pt. Reyes							
9 Aug. 1982	14	1.8	2.7	0.74	0.21		0.0090
10 Aug. 1982	17	0.16	0.95	0.79	0.038		0.0034
11 Aug. 1982	5.2	0.28	1.1	1.6	0.020		0.014
12 Aug. 1982	0.54	0.074	0.47	1.6	0.0049		0.013

Mass loadings defined as the mass of material in fogwater per m^3 of air. Numbers given are averages for each event. Contributions from soil dust, fly ash, or exhaust were not determined when the concentrations of their respective tracers (Fe, V, Pb) was missing. When Fe data was missing, all NSS Ca was attributed to cement dust.

Table 5. Equivalent ratios in coastal fogs.

Site	Mg ²⁺ /Na ⁺	Cl ⁻ /Na ⁺	Ca ²⁺ /Na ⁺	SO ₄ ²⁻ /Na ⁺	K ⁺ /Na ⁺
Del Mar	0.25	1.2	0.096	0.92	0.018
Corona del Mar	0.26	1.4	0.27	1.8	0.098
Long Beach	0.42	3.6	0.73	7.9	0.20
Lennox					
7 Dec. 1981	0.65	2.7	1.7	14	0.19
18 Dec. 1981	0.36	1.1	0.96	9.7	0.23
6 Jan. 1983	0.43	1.6	0.95	3.04	0.21
San Nicholas Island	0.25	0.91	0.074	0.34	0.024
San Marcos Pass	0.40	1.96	0.33	5.64	0.265
Morro Bay	0.30	1.61	0.16	0.29	0.086
Mt. Sutro	0.26	1.31	0.14	0.49	0.080
Pt. Reyes					
9 Aug. 1982	0.25	0.86	0.069	0.36	0.026
10 Aug. 1982	0.25	1.45	0.049	0.15	0.023
11 Aug. 1982	0.24	1.30	0.054	0.42	0.025
12 Aug. 1982	0.24	1.37	0.063	1.29	0.039
sea salt	0.23	1.17	0.043	0.12	0.021

Table 6. Chemical equilibria of the NaCl-H₂SO₄-HNO₃-H₂O system.

	<u>Reaction</u>	<u>Equilibrium constant</u>
1.	HNO ₃ (g) + NaCl(s) = HCl(g) + NaNO ₃ (s)	3.4 X 10 ⁰
2.	2NO ₂ (g) + NaCl(s) = NOCl(g) + NaNO ₃ (s)	2.2 X 10 ³
3.	H ⁺ (aq) + Cl ⁻ (aq) = HCl(g)	5.6 X 10 ⁻⁷
4.	H ⁺ (aq) + NO ₃ ⁻ (aq) = HNO ₃ (g)	4.3 X 10 ⁻⁷
5.	H ⁺ (aq) + SO ₄ ²⁻ (aq) = HSO ₄ ⁻ (aq)	7.8 X 10 ¹

Equilibrium constants calculated at 298K from free enthalpies of formation (38).

FIGURE CAPTIONS.

Figure 1. Fogwater sampling sites (■).

Figure 2. (a) Fogwater concentrations at Del Mar. pH values and liquid water contents (g m^{-3} , in parentheses) are indicated on top of each data bar. (b) Source contributions to the fogwater loading at Del Mar; contributions from soil dust, fly ash, and exhaust were not determined for the last sample.

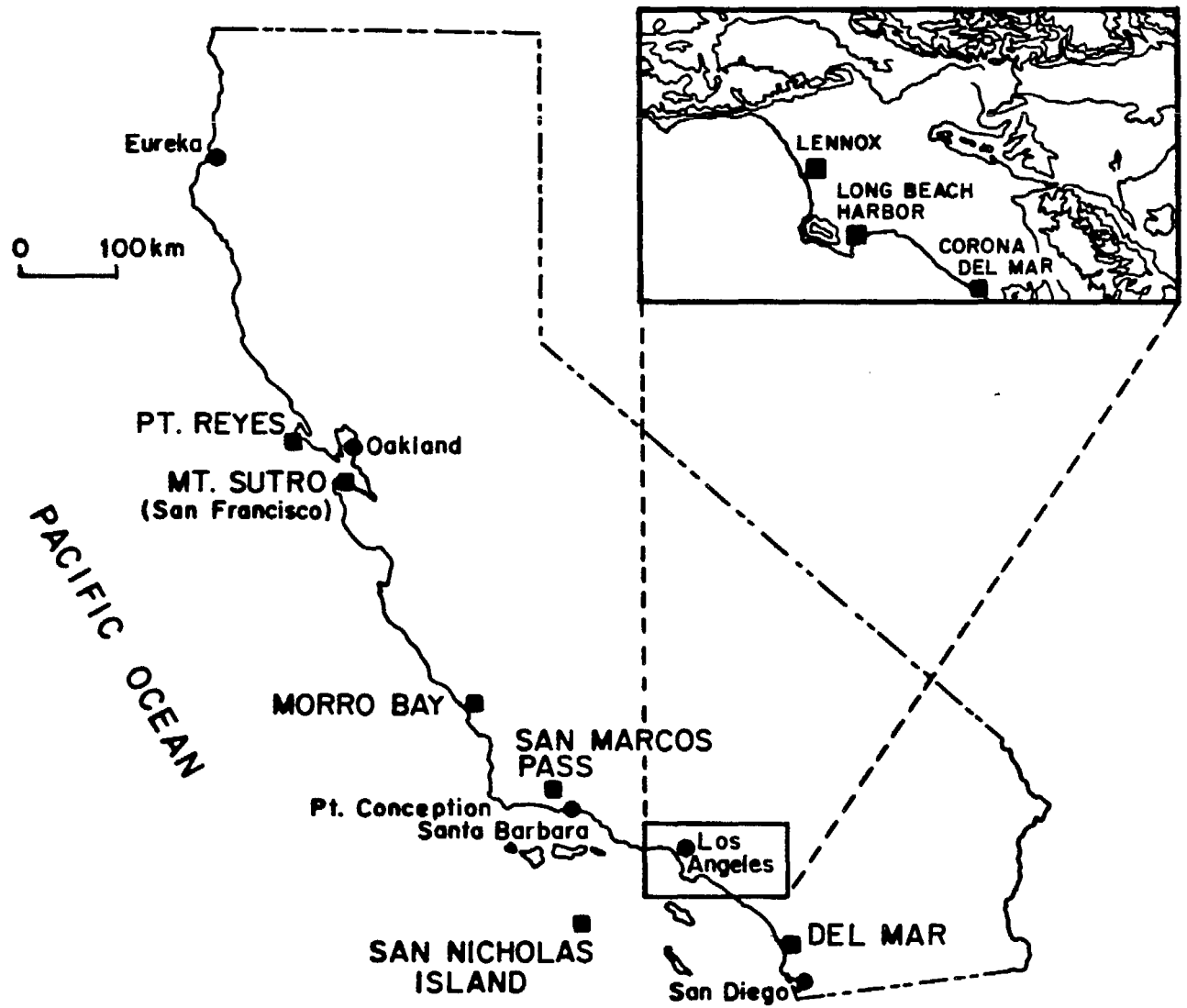


Figure 1

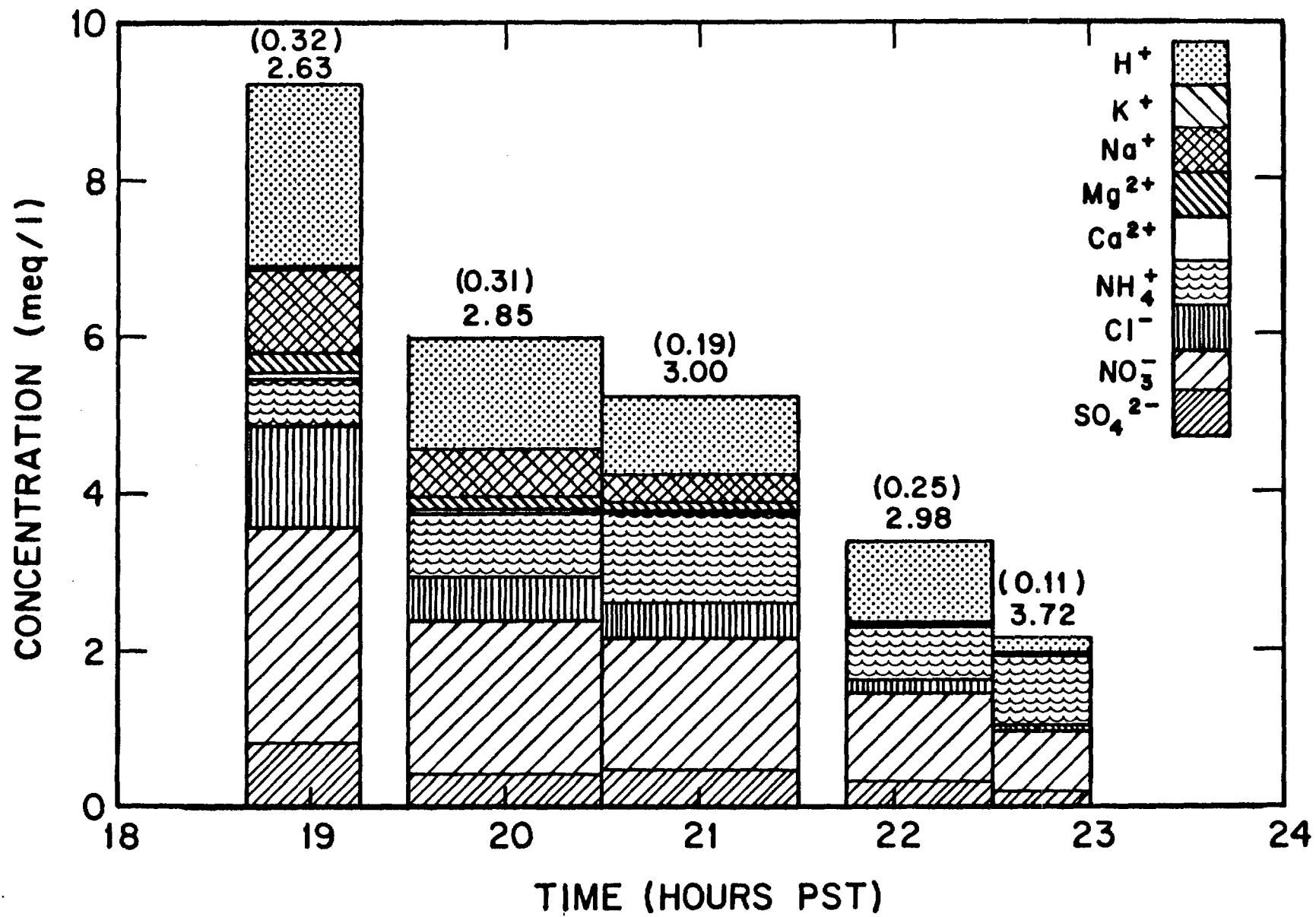


Figure 2a

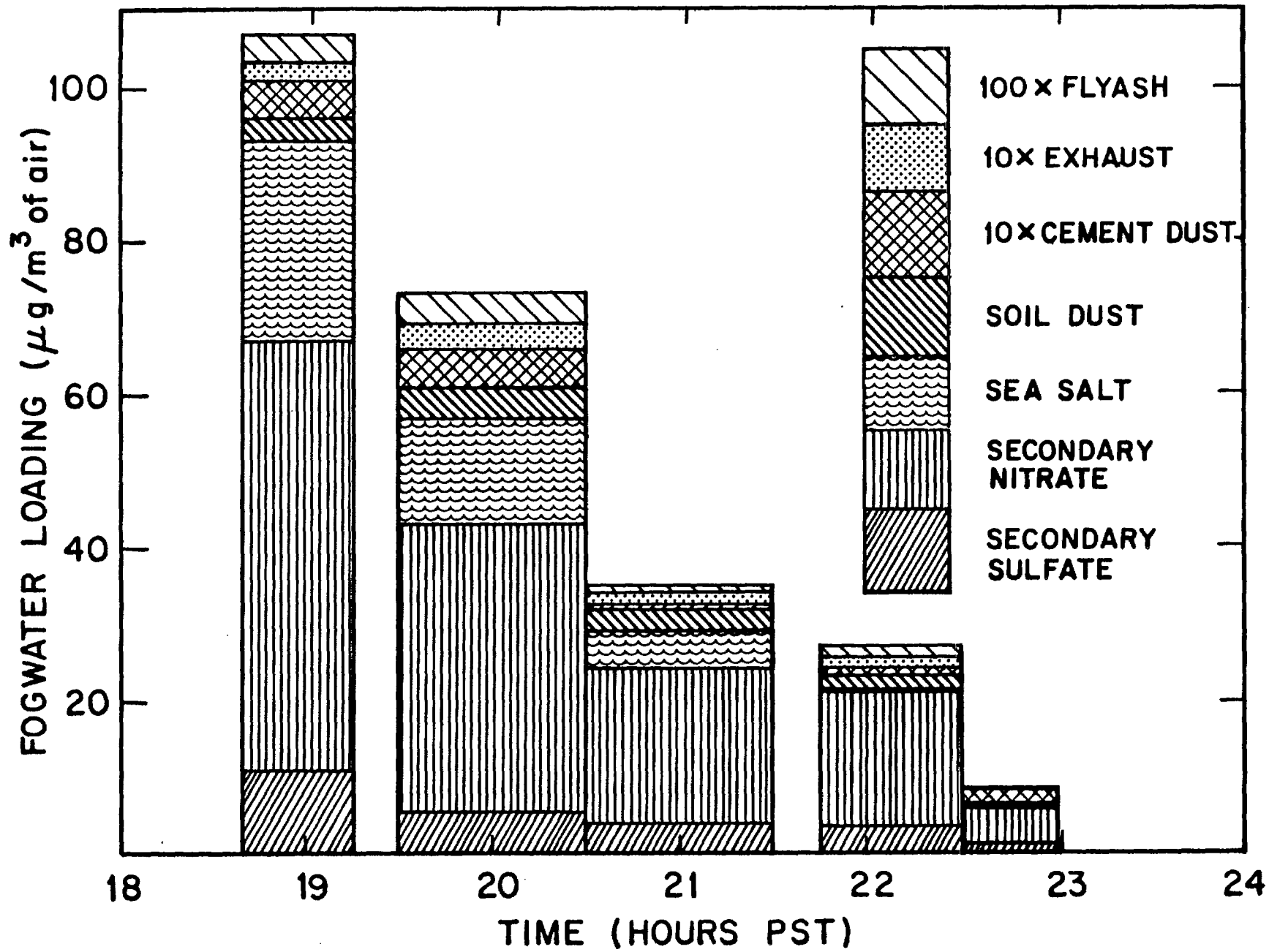


Figure 2b

APPENDIX II. Fogwater Chemistry in an Urban Atmosphere

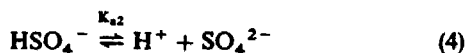
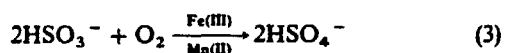
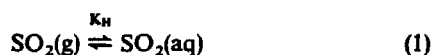
J. WILLIAM MUNGER, DANIEL J. JACOB, JED M. WALDMAN, AND MICHAEL R. HOFFMANN

W. M. Keck Laboratories, California Institute of Technology, Pasadena, California 91125

Analyses of fogwater collected by inertial impaction in the Los Angeles basin and the San Joaquin Valley indicated unusually high concentrations of major and minor ions. The dominant ions measured were NO_3^- , SO_4^{2-} , NH_4^+ , and H^+ . Nitrate exceeded sulfate on an equivalent basis by a factor of 2.5 in the central and coastal regions of the Los Angeles basin but was approximately equal in the eastern Los Angeles basin and the San Joaquin Valley. Maximum observed values for NH_4^+ , NO_3^- , and SO_4^{2-} were 10.0, 12.0, and 5.0, meq l^{-1} , while the lowest pH observed was 2.2. Iron and lead concentrations of over 0.1 mM and 0.01 mM, respectively, were observed. High concentrations of chemical components in fog appeared to correlate well with the occurrence of smog events. Concentrations in fogwater were also affected by the physical processes of condensation and evaporation. Light, dissipating fogs routinely showed the highest concentrations.

INTRODUCTION

Laboratory [Schwartz, 1983; Martin, 1983; Hoffmann and Jacob, 1983] and field [Cass and Shair, 1980; Cox, 1974; McMurry et al., 1981; Smith and Jeffery, 1975; Wilson and McMurry, 1981] studies have indicated that droplet-phase chemistry is important in SO_2 oxidation. Droplet-phase oxidation of SO_2 occurs, in part, via the following reactions



In Los Angeles, Cass [1975] observed a correlation between the occurrence of high sulfate aerosol levels during the afternoon and the presence of coastal fog and low clouds in the morning. The mean SO_2 to SO_4^{2-} conversion rate during July in Los Angeles is $6\% \text{ hr}^{-1}$ [Cass, 1981], whereas gas-phase reactions can account for, at most, conversion rates of $4.5\% \text{ hr}^{-1}$ [Sander and Seinfeld, 1976]. Morgan and Liljestrand [1980] reported that light misting rainfalls emanating from low stratus clouds in Los Angeles resulted in pH values as low as 2.9 with correspondingly high SO_4^{2-} and NO_3^- concentrations. Waldman et al. [1982] have previously reported pH values near 2.2 in urban fog. Furthermore, Hegg and Hobbs [1981] have reported S(IV) to S(VI) conversion rates of 4.0 to $300\% \text{ hr}^{-1}$ in wave clouds over western Washington.

In addition to its importance as a chemical reaction site, fog may exert a significant influence on scavenging and deposition, on human health, and on vegetation. Fog forms in the ground layer where gases and aerosols are most concentrated. Because fog droplets are approximately 100 times smaller than rain drops, they should be more concentrated than rain, and mass transfer should not limit the kinetics of fog droplet reactions [Schwartz, 1983; Baboolal et al., 1981].

In light of these results and the expectation that fog droplets (or the fine aerosol remaining after fog has evaporated) are sites

for rapid conversion of SO_2 to SO_4^{2-} we began a study to characterize the chemical composition of fogwater. Because of the physical similarity to clouds, fog is expected to exhibit the same chemical processes occurring in clouds and, to some degree, aquated submicron aerosols. Information about the chemistry of fogwater may be applicable to the broader questions about ambient acid formation and acidic precipitation. The role of fog in the nocturnal chemistry of SO_2 has been examined by Jacob and Hoffmann [1983].

METHODS

Fogwater was collected with a rotating arm collector (RAC), which was modified from an original design reported by Mack and Pilie [1975]. A 67.5-cm-long, Teflon-coated steel tube with 10×0.95 cm slots milled into opposite sides at each end of the tube is rotated at 1700 rpm with a 1.5-HP induction motor. This rotation imparts a relative velocity of ~ 50 m/s to the slots. Droplets impact in the slots and are driven by centrifugal force into 30-ml polyethylene bottles attached at the ends of the arms. During operation, the pivot of the arm is 1.4 m above ground level. Based upon changes in particle-size distributions measured with a laser optical particle counter during operation in a cloud chamber, the RAC was determined to have a lower-size cut of $\sim 8 \mu\text{m}$ [Jacob et al., 1982]. The bulk of liquid water in fogs is contributed by droplets larger than $8 \mu\text{m}$, but droplets smaller than $8 \mu\text{m}$ may be more concentrated than those that are actually collected. Consequently, the concentration of species in fogwater may be slightly underestimated. With this design, up to 2 ml min^{-1} of fogwater has been collected during dense fog and 0.1 to 1.0 ml min^{-1} during lighter fog. Collection efficiency under these conditions is estimated to be greater than 80%, based on laboratory calibration. We are currently working on a fog sampler with a lower-size cut in order to characterize the chemistry of the smaller fog droplets.

SITE DESCRIPTIONS

Figure 1 indicates the sites at which fogwater was collected. The Pasadena site, which is located on the roof of a four-story building on the Caltech campus, is in a predominantly residential neighborhood 25 km north of downtown Los Angeles. There are no major pollutant sources in the immediate vicinity. The Lennox site was selected because of its close proximity to both industrial and mobile pollutant sources and its high frequency of marine fog in late autumn: it is situated on the roof of a one-story building at a busy intersection within 100 m of a

Copyright 1983 by the American Geophysical Union.

Paper number 3C0293.

0148-0227/83/003C-0293\$05.00

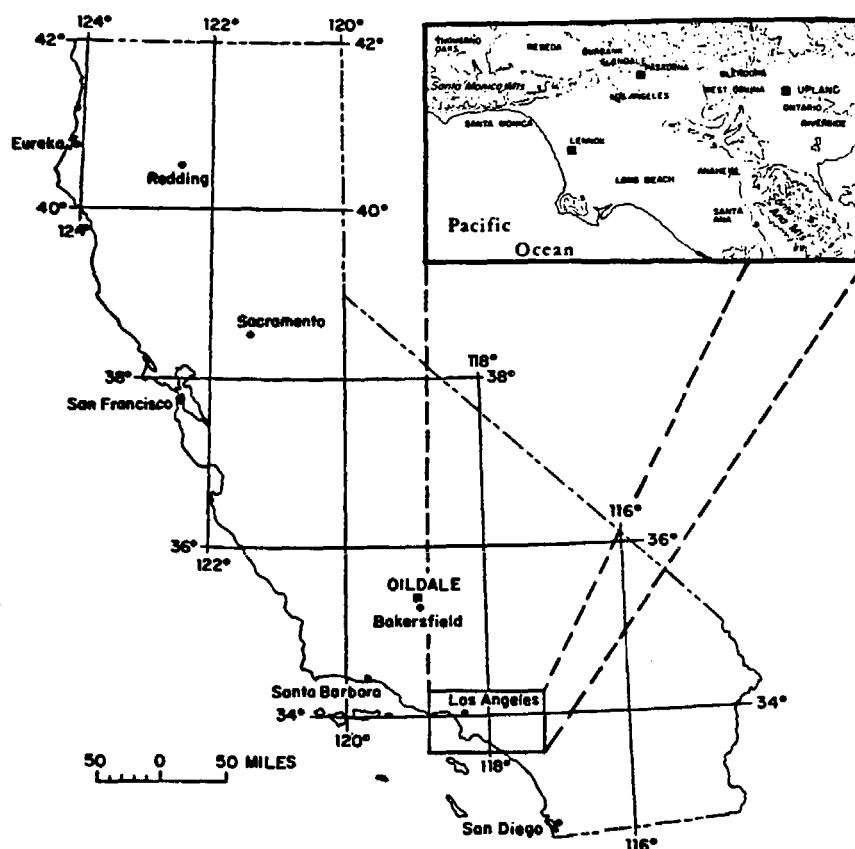


Fig. 1. Map of fog sampling sites in Southern California. Los Angeles area sites are indicated on the inset.

major freeway and 6 km from the ocean. Major point sources near the Lennox site include an oil refinery, power plant, Los Angeles International Airport, and several other industrial facilities.

The Oildale site, near Bakersfield, is in an area with higher sulfur emissions from secondary oil recovery operations and is subject to extensive fog ('Tule fog'), which persists throughout the San Joaquin Valley during the early winter. The sampler was placed on the roof of an air-quality monitoring station (about 4 m aboveground). Upland is 60 km NE of downtown Los Angeles. A steel plant and several other heavy industries are located within 30 km of this site, which is also on the roof of an air-quality monitoring station in a residential area.

FOG PATTERNS

In Los Angeles, fog generally occurs during two distinct periods: November through January and April through June. At the two inland sites, Pasadena and Upland, fog occurs sporadically in the night and early morning throughout the fog seasons. Fogs along the coast tend to form repeatedly for several nights, lifting for only part of the day. In the San Joaquin Valley, fog forms for extended periods during the early winter months and often persists throughout the day.

ANALYTICAL METHODS

The sample-handling and analytical protocol is illustrated in Figure 2. Analysis of the sample began as soon as collection ended; measurement of pH and separation of preserved aliquots was completed within 30 min. In the field, samples were stored over ice, then refrigerated when brought back to the

laboratory; pH was determined in the field with a Radiometer PHM 80 meter. Sulfite was preserved by addition of CH_2O at pH 4 to form hydroxymethanesulfonic acid (HMSA) [Dasgupta *et al.*, 1980; Fortune and Dellinger, 1982]; 3,5-diacetyl-1,4-dihydropyridine (DDL) formed by reaction of formaldehyde and acetyl acetone in the presence of NH_4^+ [Nash, 1953] is stable for at least 7 days [Rietz, 1980]. Sulfite is known to interfere with this reaction [Nash, 1953], but no correction was made. Addition of HNO_3 to achieve a concentration of 0.16 M was used to stabilize an aliquot for trace-metal analyses. Beginning with the Oildale samples, aliquots were filtered through 0.4- μm Nuclepore membranes in the field. Because of extremely high cation and anion concentrations in fogwater, samples usually had to be diluted before analysis. With sample dilution, complete analyses of volumes as small as 5 ml was practicable.

Major cations were determined on a Varian AA5 atomic absorption spectrophotometer by using an air-acetylene flame. Lanthanum was added to the entire aliquot used for AAS in order to release calcium and magnesium. Ammonium was determined by the phenol-hypochlorite method [Solórzano, 1967]. Anions were determined by ion chromatography (IC), using a 3-mM NaHCO_3 /2.4-mM Na_2CO_3 eluent. Aliquots of sample were spiked to give the same $\text{HCO}_3^-/\text{CO}_3^{2-}$ concentration as the eluent in order to eliminate the water dip that interferes with F^- and Cl^- peaks. Galloway *et al.* [1982] suggest that low molecular weight carboxylic acids are present in rainwater. Considering the high aldehyde concentrations observed in fogwater, it is likely that the corresponding acids are present as well. If present, these acids would be a positive interference with fluoride. The absorbance of DDL formed

FOG SAMPLE-HANDLING PROTOCOL

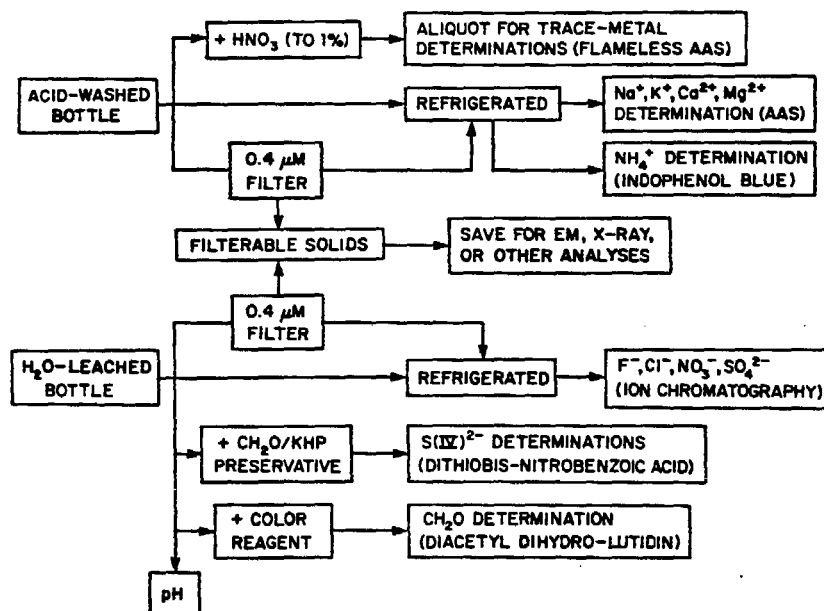


Fig. 2. A schematic flow diagram indicating fog sample-handling protocol and analytical procedures.

from CH_2O was measured at 412 nm on a Beckman Acta III spectrophotometer.

The preserved solution for S(IV) was injected into the IC and eluted with 1 mM KHP [Dasgupta *et al.*, 1980]. Because the F^- and Cl^- peaks coeluted with the hydroxymethanesulfonate (HMSA) using this eluent, the S(IV) in the samples could not be directly quantified. Instead, S(IV) was taken as the difference between the SO_4^{2-} concentration in the preserved aliquot and the SO_4^{2-} concentration in the unpreserved aliquot, measured by the usual IC methods. The first value would be SO_4^{2-} only, the second would be the sum of SO_4^{2-} and SO_3^{2-} . After

December 7, S(IV) was measured by a colorimetric method, using 5,5'-Dithiobis-(2-nitrobenzoic acid) DTNB [Humphrey *et al.*, 1970]. Trace metals were determined by flameless atomic absorption (Varian AA6 equipped with a CRA 90 or Perkin-Elmer 360 with a HGA 2100). Gas-phase concentrations of SO_2 , NO_x , O_3 were made continuously at the Lennox, Upland, and Oildale sites by conventional instrumental methods.

RESULTS

Table 1 describes the conditions before and during the fog sampling. Samples from Pasadena were collected both after

TABLE 1. Description of Conditions During and Before Fog Sample Collection

Site	Date	Sampled Interval, hr	Conditions During Fog	Prior Conditions
Pasadena	November 15, 1981	2040-0115	Light wind SSW-N; sampled beginning to end of fog.	Fair, good air quality.
Pasadena	November 23, 1981	2320-0130	Light S-SE wind; 14°-12°C; fog thickened to near drizzle; sampled beginning to end of fog.	Hazy and smoggy.
Lennox	December 7, 1981	2305-0840	Light westerly wind; traffic volume and ambient pollutants began to increase at 0530; missed first hour of fog, sampled until fog lifted.	Previous night foggy, smoggy during day, NO_x alert called ($\text{NO}_x = 0.8$ ppm).
Lennox	December 18, 1981	2315-0043	Light westerly wind; sampled from beginning of fog; fog persisted until morning.	Previous night foggy; high NO_x levels during day.
Pasadena	December 20, 1981	745-845	Light northerly wind; 10°C; fog began before 0700; sampled until fog lifted.	Previous day was fair.
Oildale	January 14, 1982	0200-0750	Light southerly wind; 3°-4°C, thin fog.	Overcast all of preceding day; dense fog on previous night.
Pasadena	January 17, 1982	2130-2200	Sample collected as fog dissipated.	Smog and haze during the afternoon.
Upland	May 14, 1982	0630-0910	Light and variable wind, 12°C, thin fog.	Low clouds and ground haze throughout night.

TABLE 2. Concentration Ranges for Major and Minor Ions, Sulfite, and Formaldehyde Observed During Fog Events.

Location	Number of Samples in event	Date	pH	H ⁺	Na ⁺	K ⁺	NH ₄ ⁺	Ca ²⁺	Mg ²⁺	$\mu\text{eq l}^{-1}$						SO ₃	CH ₂ O, mg/l
										F ⁻	Cl ⁻	NO ₃ ⁻	SO ₄ ²⁻	SO ₃	CH ₂ O, mg/l		
Pasadena	4	Nov. 15, 1981	5.25-4.74	5.6-55	12-496	4-39	370	19-360	7-153	120	56-280	130-930	62-380	—	—	—	
Pasadena	4	Nov. 23, 1981	4.85-2.92	14-1200	320-500	33-53	1290-2380	140-530	89-360	180-410	480-730	1220-3250	481-944	150-180	3.1-3.5	—	
Lennox	8	Dec. 7, 1981	5.78-2.55	2-2820	28-480	6-156	1120-4060	49-4350	17-1380	115-395	111-1110	820-4560	540-2090	30-250	4.6-12.8	—	
Lennox	3	Dec. 18, 1981	2.81-2.52	1550-3020	80-166	19-40	950-1570	73-190	43-99	180-500	90-197	2070-3690	610-1970	—	—	—	
Pasadena	1	Dec. 20, 1981	3.75	178	51	373	1773	217	78	242	161	1000	450	—	—	—	
Oildale	3	Jan. 14, 1982	3.07-2.90	850-1260	151-1220	39-224	4310-9750	165-1326	20-151	126-242	203-592	3140-5140	2250-5000	440-710	6.1-14.4	—	
Pasadena	1	Jan. 17, 1982	2.25	5625	2180	500	7960	2050	1190	637	676	12000	5060	—	—	—	
Upland	3	May 14, 1982	2.88-2.22	1320-6310	1220-5200	96-482	2329-6312	596-4218	321-1816	168-342	654-1110	4240-10660	2760-4890	446-592	6.1-8.6	—	

clean air days and smoggy days. The fogs in Lennox followed smoggy days. Oildale samples were collected during a period of extensive and persistent fog in the San Joaquin Valley. Samples at Upland were collected after dawn, when the haze that had been present during the night thickened enough to be collected.

The high and low concentrations of major ions, sulfite, and formaldehyde in fogwater during eight fog events are presented in Table 2. Concentrations of most ions in the second set of Pasadena samples, which followed a smoggy day, were higher than in the first Pasadena fog event. At Lennox the concentrations of major ions in fog were even higher than the Pasadena samples. Some of the fog samples from Lennox contained significant amounts of suspended solids. The greatest amount was in the final sample taken from the December 7 fog event during morning rush hour as the fog was dissipating.

The present sampling method does not differentiate between particles within droplets and particles greater than 8 μm that are independent of water droplets. Because the minimum size for activating condensation nuclei in ambient fog is much smaller than the collector cutoff size, most particles collected in fog, with the exception of hydrophobic material, can be assumed to be associated with droplets.

A single fogwater sample collected in Pasadena on January 17 had exceptionally high concentrations. The sulfate and nitrate concentrations were the maximum values observed in any fog. Fogwater collected in Oildale also had very high nitrate and sulfate concentrations as well as the highest NH_4^+ , CH_2O , and S(IV) concentrations. The Upland fog samples were also characterized by high levels of acidity and acidic anions.

Concentrations of trace metals in the fog samples were also elevated, as shown in Table 3. During some of the fog events, metal concentrations varied over an order of magnitude. The usual pattern was for high concentrations at the beginning and end of the event. Lead and iron concentrations exceeded 1.0 mg L^{-1} (0.01 mM) on occasion.

The anion-to-cation ratios were close to unity for most of the samples, but there were discrepancies in some samples. In light of the large dilutions necessary to bring high concentrations down into suitable analytical ranges, the ion balances were reasonable. There were apparent excesses of cations in some of the samples that had large quantities of particles present. Calculation of the ion balance by using the concentrations of cations in filtered aliquots yielded better results. The aliquot for anions was routinely filtered prior to injection into the IC. This does not explain the apparent anion deficiency (or cation excess) in the fogwater samples collected from Oildale. The inclusion of SO_3^{2-} in the anion sum does not completely make up the deficit either, however, sulfite in aliquots from these samples was not measured immediately. Even though preservation techniques were used, sulfite may be underestimated. Considering the high concentrations of aldehydes, it is probable that the corresponding carboxylic acids were present in the fogwater; this would account for some of the apparent anion deficiency. Other factors that may contribute to poor ionic balances are losses of ions to particle surfaces via sorption and formation of adducts and complexes of indeterminate charge.

DISCUSSION

Figure 3 presents the ionic composition of individual fog samples as a function of time. Concentrations of all ions decrease sharply during the first few hours of the fogs in Lennox; however, the ionic proportions do not change appreciably. In most cases, concentrations in the fogwater rose as the fog

TABLE 3. Ranges of Selected Trace-Metal Concentrations in Fog Samples

Site	Date	$\mu\text{g l}^{-1}$				
		Fe	Mn	Pb	Cu	Ni
Pasadena	Nov. 15, 1981	90-2,100	18-160	250-270	1-15	2-21
Pasadena	Nov. 15, 1981	920-1,770	34-56	1,310-2,540	88-140	8-14
Lennox	Dec. 7, 1981	356-23,700	19-810	820-2,400	9-150	2-52
Lennox	Dec. 18, 1981	1,020-2,080	25-81	1,700-2,350	84-1,400	32-54
Pasadena	Dec. 20, 1981	340	42	156	—	—
Oildale	Jan. 14, 1982	240-6,400	97-800	241-366	45-401	124-586
Upland	May 14, 1982	—	430-570	1,690-2,400	156-185	155-213

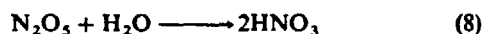
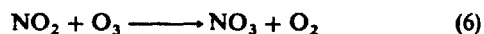
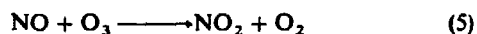
Number of samples per event is the same as for Table 2.

dissipated. The short duration fogs, which were usually very light fogs that resulted in low collection rates, also had high concentrations. Physical processes of droplet growth by accretion of water vapor, followed by evaporation, appear to account for this pattern.

Dilution by droplet growth could take place without any appreciable change in liquid water content (LWC) if the sedimentation rate was high enough to balance the condensation rate. Work by *Roach et al.* [1976] suggests that a significant portion of the liquid water formed during a fog event is lost, presumably to ground surfaces. During the periods over which concentrations were decreasing, collection rates, which are a function of LWC, remained constant. Advection of more dilute fog could account for this as well.

In Figures 4 and 5 the concentration of selected ions, normalized to their initial concentration, are depicted. If physical factors are responsible, the patterns will be nearly identical for ions that are controlled by the same factors or have common sources. The nearly hundredfold increase in Ca^{2+} and Mg^{2+} , and the concomitant drop in H^+ concentration in the final two samples collected in the December 7 fog at Lennox, coincided with morning rush hour traffic, which would generate a large amount of road dust. Concentrations of other ions were increased during that period, as a result of evaporation, but not to the extent that Ca^{2+} and Mg^{2+} increases (25 times their initial concentrations); $[\text{Na}^+]$ and $[\text{Cl}^-]$ increased by a factor of 5, and $[\text{SO}_4^{2-}]$, $[\text{NO}_3^-]$, and $[\text{NH}_4^+]$ returned to their initial concentrations. Acidity was nearly neutralized at the end of this fog event. In association with the increased $[\text{Ca}^{2+}]$ and $[\text{Mg}^{2+}]$, an increase in suspended particles, $[\text{Pb}]$ and $[\text{Fe}]$, was observed at the same time as a rise in CO levels at Lennox, coinciding with the morning traffic. Transfer of gaseous NH_3 into the droplets could account for the increase in $[\text{NH}_4^+]$ and simultaneous drop in $[\text{H}^+]$ during the December 7 Lennox fog event, while the other ions were maintained at constant concentrations. However, if the NH_3 had been present when the fog formed, it would have been immediately scavenged because of its high solubility at low pH. Unless there was a local source for NH_3 , advective transport must be invoked to account for the apparent increase in $[\text{NH}_4^+]$.

In Pasadena, $[\text{H}^+]$ and $[\text{NO}_3^-]$ simultaneously increased while the other ions were decreasing. This may be evidence for the nocturnal formation of HNO_3 via the following reactions [*Graham and Johnston, 1978*]:



Alternatively, the increase in HNO_3 could result from scavenging or diffusion of fine aerosol to the droplets or by advection of fog with higher NO_3^- concentrations.

In nearly all the cases the dominant ions in the fog samples were NO_3^- , SO_4^{2-} , H^+ , and NH_4^+ , which are the major components of secondary aerosol in Los Angeles [*Cass, 1979*]. These ions account for over 90% of the solutes in the initial stages of the Lennox samples. The highest concentrations were observed when the fog was preceded by smoggy days. Because secondary aerosols are effective condensation nuclei [*Barrett et al., 1979*], they will exert a considerable influence on the composition and concentration in fogwater. When the concentration of secondary aerosol is high, the subsequent fogwater will also have high concentrations. The fraction of NO_3^- and SO_4^{2-} neutralized by NH_3 (measured in terms of NH_4^+) will largely determine the free acidity of the fog that first deliquesces. In this connection it is noteworthy that the initial fogwater samples collected at Lennox are the most acidic, and subsequent samples during the event are progressively more neutral, while at Pasadena and Upland the converse is true.

If HNO_3 and NH_3 were present when the fog initially formed, they would be scavenged rapidly as well and influence the fogwater composition [*Jacob and Hoffmann, 1983*]. However, the combination of cooler temperatures and higher humidity before the onset of fog will probably force NH_3 and HNO_3 to condense into the particulate phase [*Stelson and Seinfeld, 1982; Stelson, 1982*], which can be scavenged via nucleation or diffusion as the fog forms.

Figure 6 is a conceptualization of the condensation/evaporation cycle for fog droplets and illustrates the link between fogwater chemistry and the chemistry of smog and haze aerosol. High atmospheric concentrations of aerosol precursors appear to result in highly concentrated fogwater. Likewise, dissipation of highly concentrated fog results in very concentrated and reactive aerosol. The high trace-metal content in fogs would catalyze SO_2 oxidation. This link between fog and the subsequent aerosol can be seen in the correlation reported by *Cass [1975]* between morning fog and high humidity and high aerosol sulfate concentrations in the afternoon.

THE ROLE OF ALDEHYDES IN FOG DROPLETS

Aldehydes are released as primary emissions from combustion sources and are generated photochemically from hydrocarbons [*National Research Council, 1981*]. The peroxide radical is an important byproduct of these reactions. Aldehydes are photochemically destroyed, with $\text{OH}\cdot$ and $\text{HO}_2\cdot$ as byproducts. Intermediates in aldehyde reaction pathways also play a role in the gas-phase reaction networks of SO_2 and NO_x .

Concentrations of formaldehyde as high as 0.5 mM were present in the Los Angeles fogwater samples. Other aldehydes,

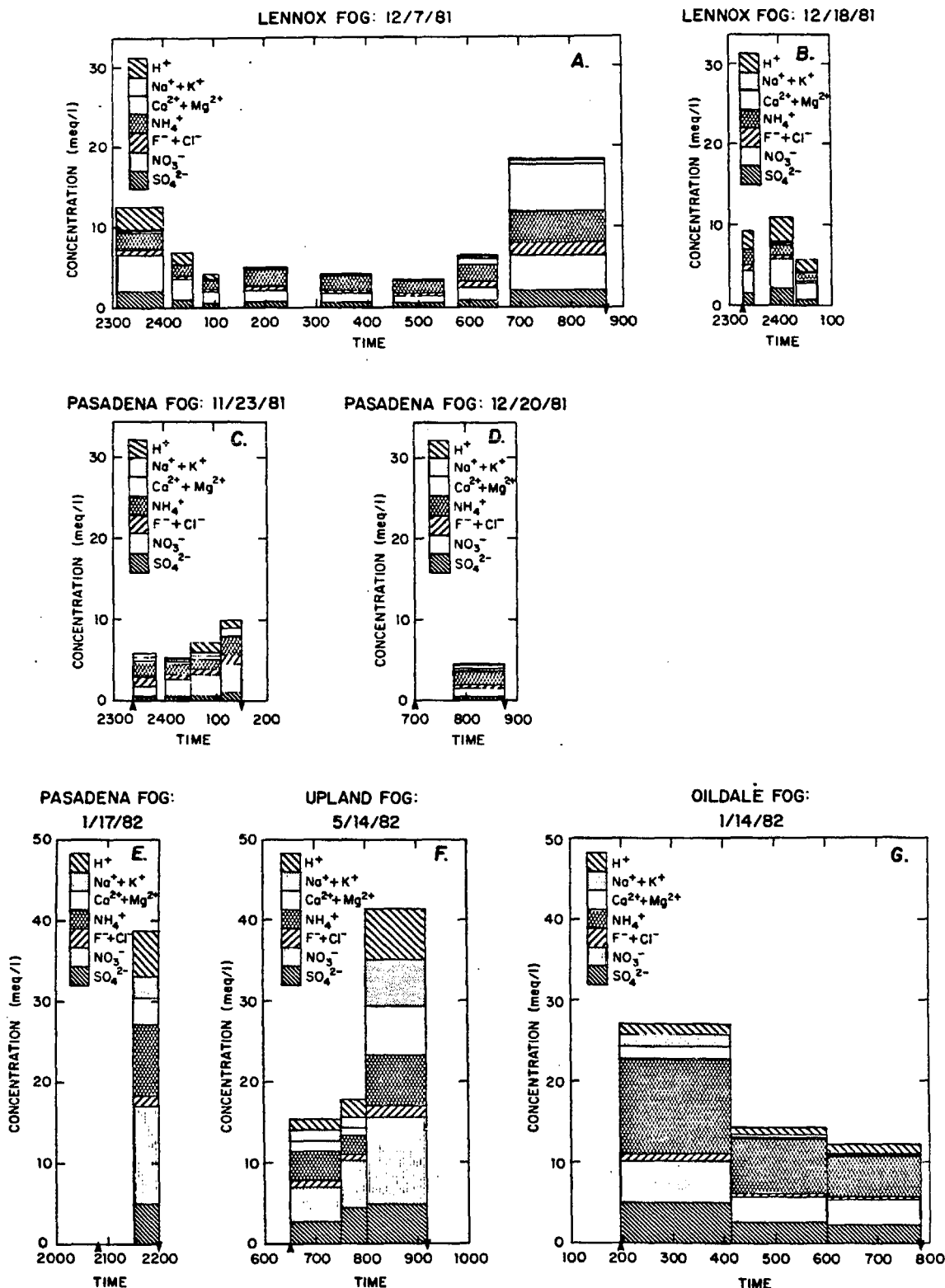


Fig. 3. Ionic composition as a function of time in sequential fog samples. Sampling interval is indicated by the width of each bar. The times of fog formation and dissipation are indicated by arrows.

such as acetaldehyde and benzaldehyde, are present in the Los Angeles atmosphere [National Research Council, 1981; Grosjean, 1982], and their presence in fogwater samples at comparable concentrations has been confirmed by the hydrazone derivative method [Fung and Grosjean, 1981]. Aldehydes react

with HSO₃⁻ according to the following general stoichiometry:



The formation constant for the formaldehyde-bisulfite addition complex, HMSA, has a maximum of about 10⁵ between

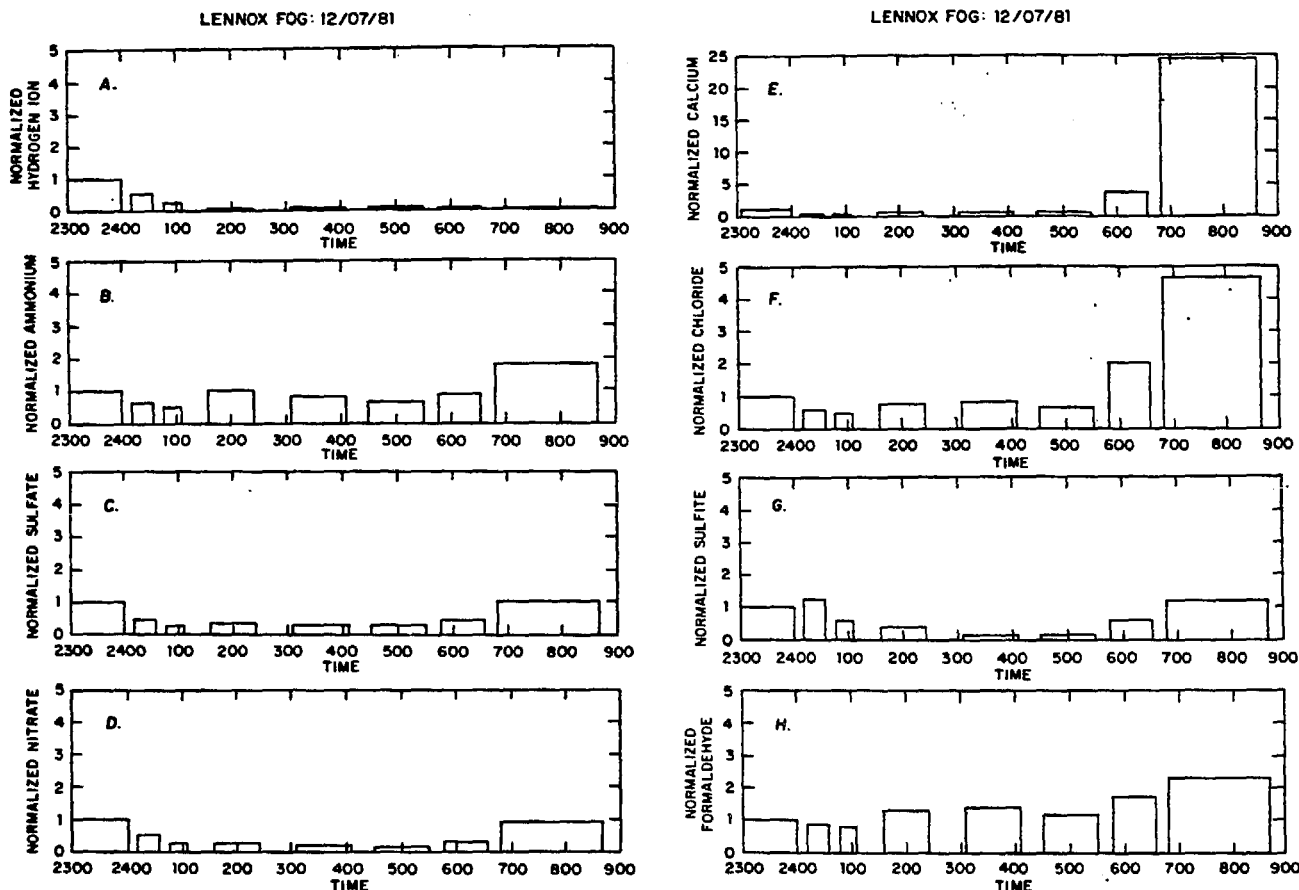


Fig. 4. (a-h) Nondimensional concentrations of individual ions in fog collected on December 7-8, 1981, at the Lennox sampling site. Concentrations are normalized for each component with respect to the concentrations in the initial sample (i.e., $\bar{C}_i = C_i/C_{i,0}$). Note the differences in scale. Sampling interval indicated by the width of each bar. NA indicates that a sample was not analyzed. Magnesium and sodium, which are not shown, were nearly identical to Ca^{2+} and Cl^- , respectively.

pH 4 and 6 and drops to 10^3 at pH 9 [Dasgupta et al., 1980]. Stewart and Donnelly [1932] observed a similar pattern for the formation of the benzaldehyde-S(IV) adduct. They also observed an interaction between temperature and pH. At low pH the temperature dependence of the equilibrium was stronger than at high pH. Low temperature increased the stability of the complex. The molar ratio of formaldehyde to S(IV) in the fog samples ranged from 0.9 to 17. Using Dasgupta's constants, the free S(IV) concentration in the fog ranges from 5% to 60% of the total. The equilibrium partial pressures of SO_2 and CH_2O , required to achieve the S(IV) and CH_2O values measured in the fogwater, were calculated from the following mass balance relationships:

$$[\text{S(IV)}] = [\text{SO}_2(\text{aq})] + [\text{HSO}_3^-] + [\text{SO}_3^{2-}] + \sum_{i=1}^n [\text{R}_i\text{CHOHSO}_3^-] + \sum_{j=1}^m [\text{M}_j\text{SO}_3] \quad (10)$$

$$[\text{R}_i\text{CHO}]_T = [\text{R}_i\text{CHO}] + [\text{R}_i\text{CHOHSO}_3^-] \quad (11)$$

where R_iCHO represents aldehydes forming sulfonic acid adducts, and M_j represents first-row transition metals forming stoichiometric sulfite complexes. Using the appropriate conditional equilibrium expressions for the concentration of the sulfonic acid adducts of CH_2O , CH_3CHO , $\text{C}_7\text{H}_6\text{O}$, and the sulfiteiron(III) complex, and ignoring other S(IV) adducts and

complexes because of their low potential concentrations, gives

$$[\text{S(IV)}] = K_H P_{\text{SO}_2} \left(1 + \frac{K_{a1}}{[\text{H}^+]} + \frac{K_{a1}K_{a2}}{[\text{H}^+]^2} + \frac{K_{a1}K_{a2}\beta}{[\text{H}^+]^2} [\text{Fe(III)}] + \sum_{i=1}^n \frac{K_{a1}}{[\text{H}^+]} [\text{R}_i\text{CHO}] K_{A_i} \right) \quad (12)$$

$$[\text{R}_i\text{CHO}]_T = K_H^i P_{\text{R}_i\text{CHO}} \left(1 + \frac{K_{a1}K_H P_{\text{SO}_2}}{[\text{H}^+]} K_{A_i} \right) \quad (13)$$

$$[\text{Fe(III)}]_T = [\text{Fe(III)}] + [\text{Fe(III)SO}_3^-] \quad (14)$$

where β is the formation constant for an Fe(III) - S(IV) complex; K_H^i is Henry's Law constant for R_iCHO ; K_H is Henry's Law constant for SO_2 ; K_{a1} and K_{a2} are acid dissociation constants; K_{A_i} is the bisulfite adduct formation constant, $P_{\text{R}_i\text{CHO}}$ and P_{SO_2} are partial pressures.

Substitution of the aldehyde and metal mass balances into (12) gives

$$[\text{S(IV)}] = \frac{K_H P_{\text{SO}_2}}{[\text{H}^+]^2} \left[[\text{H}^+]^2 + K_{a1}[\text{H}^+] + \frac{K_{a1}K_{a2}\beta[\text{Fe(III)}]_T[\text{H}^+]^2}{([\text{H}^+]^2 + \beta K_{a1}K_{a2}K_H P_{\text{SO}_2})} + \sum_{i=1}^n \frac{K_{a1}K_{A_i}[\text{H}^+]^2[\text{R}_i\text{CHO}]_T}{([\text{H}^+] + K_{a1}K_{A_i}K_H P_{\text{SO}_2})} \right] \quad (15)$$

The appropriate equilibrium constants are given in Table 4.

In the absence of adduct formation the equilibrium partial pressures of CH_2O calculated from fogwater data range from 16 ppb to 76 ppb, which are reasonable values for the Los Angeles atmosphere [Grosjean, 1982]. Adduct formation would lower the equilibrium partial pressure. The highest values of S(IV) found in some fog samples cannot be completely accounted for by aldehyde and iron-complex equilibria alone. Measured sulfite is 4–5 times higher than the predicted equilibrium value, even with P_{SO_2} as high as 30 ppb at the Los Angeles sites or 50 ppb at Oildale, which are the highest values for those sites. The lower concentrations of S(IV), however, are comparable to the values predicted from equilibrium considerations. Stable organic and inorganic sulfite species in ambient aerosols have been demonstrated to exist [Izatt et al., 1978; Eatough et al., 1978]. Aldehydes may play an important role in the atmospheric chemistry of S(IV) as stabilizers that retard oxidation of S(IV), and possibly as sources of peroxides and free radicals through their photochemistry. More data on the aldehyde content of the atmosphere are necessary to ascertain their role in the heterogeneous chemistry of SO_2 .

NITRATE TO SULFATE EQUIVALENT RATIOS

As is indicated in Figure 7, $[\text{NO}_3^-]$ in Pasadena and Lennox was about 2.5 times $[\text{SO}_4^{2-}]$; at Oildale and Upland the ratio

was closer to 1 : 1. The nitrate to sulfate ratios in fogwater differ markedly from that observed in Los Angeles area rainwater [Liljestrand and Morgan, 1981]. In rainwater the equivalent ratio was less than 1 for coastal and central Los Angeles sites and increased to unity at Riverside at the eastern edge of the basin. Fogwater exhibited the opposite trend: $[\text{NO}_3^-]$ exceeded $[\text{SO}_4^{2-}]$ at the coastal and central Los Angeles sites and decreased to near one at the most inland site (Upland). Beside the differences in their source strengths (NO_x emissions exceed SO_2 emissions by a factor of 2.5 in Los Angeles), there are important differences in the kinetics of their respective oxidations and scavenging processes, as is discussed by Jacob and Hoffmann [1983].

SODIUM CHLORIDE RATIOS

As Figure 8 illustrates, most of the fogwater samples had Na:Cl ratios near that of seawater. There were a few samples with excess Cl^- , which may be due to local sources. The highest excess of Cl^- was found in Lennox fog during morning rush hour, which suggests lead bromochloride salts from automobile emissions as a possible Cl^- source. Those samples also had high [Pb]. Two of the samples with excess Na^+ were collected at the beginning of fog events and may be affected by soil and dust. However, the other samples with excess Na^+ were extremely acidic. Reaction between marine aerosol and acidic gases or aerosol may be volatilizing HCl in the fog or the preceding aerosol as suggested by Eriksson [1960] and Hitchcock [1980]. The resulting fog would be deficient in Cl^- .

COMPARISON TO OTHER DATA

Fog and cloudwater ionic concentrations as high as in some of these samples have been observed previously (see Table 5). At many of the sites, pH values were in the range 3 to 4, but none were as low as the most extreme values for the Los Angeles area fogs. The concentration ranges for the cations Na^+ , K^+ , Ca^{2+} , and Mg^{2+} in other regions overlap with the concentration ranges observed in Southern California. The extreme values reported here, which were found in light fogs and in the Lennox sample that was laden with particles, are somewhat higher. Ammonium concentrations are comparable, but the extreme values observed in this study are about 10 times the maxima for previously reported data. Sulfate concentrations are comparable to other reported values, while nitrate concentrations are considerably higher in the California fogs, which is to be expected because of the dominance of NO_x emissions. Furthermore, high concentrations of HNO_3 , which can be easily scavenged by fogwater, have been measured in the Los Angeles atmosphere [Appel, 1981].

Dense smog as a precursor gave rise to the most highly concentrated fogwater in Los Angeles. Other areas of the world subject to intense air pollution may also prove to have highly concentrated fogwater. Although ionic composition in the 1952 London fog was not measured, approximate calculations based on SO_2 emission rates, measured SO_2 concentrations, droplet residence time, and liquid water content [Wilkins, 1954a, b] gives SO_4^{2-} concentrations of 11 to 46 meq l^{-1} . For comparison, the extreme value measured during the winter of 1981–1982 in Southern California was 5 meq l^{-1} .

IMPLICATIONS

Highly concentrated fogwater can have several important environmental effects. Sedimentation and impaction rates of

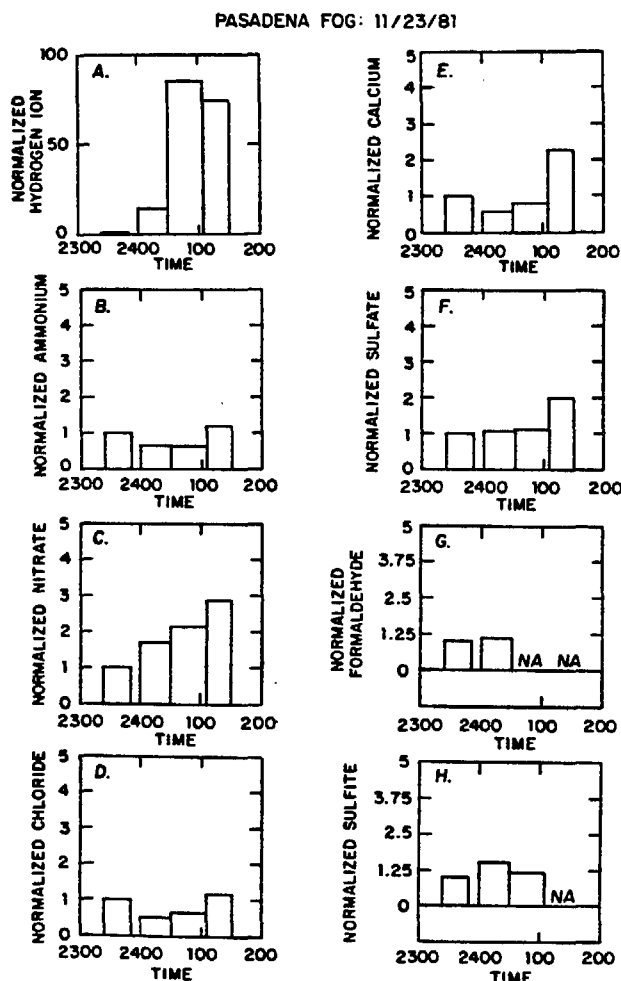


Fig. 5. (a-h) Nondimensional concentrations of individual ions in fog collected on November 23–24, 1981, at the Pasadena sampling site. The normalization procedure and scales are described in Figure 4.

FOG: LINK BETWEEN ATMOSPHERIC AND WATER CHEMISTRY

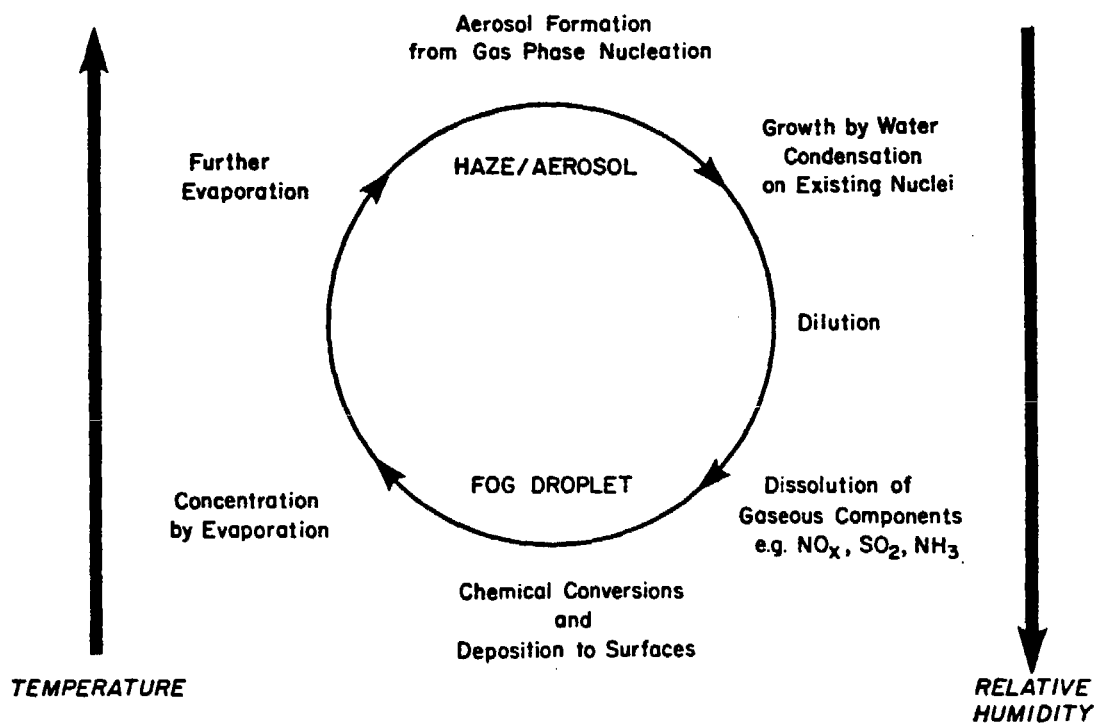


Fig. 6. A schematic diagram depicting the temperature and humidity dependence for fog formation and the apparent link between atmospheric gas phase and water phase chemistry.

TABLE 4. Equilibrium Constants Applicable to S(IV) and Aldehyde Chemistry

	K, M or M atm ⁻¹	ΔH° 298, kcal mol	Reference
$\text{SO}_{2(g)} \overset{K_H}{\rightleftharpoons} \text{SO}_{2(aq)}$	1.245	-6.247	<i>Sillén and Martell [1971]</i>
$\text{SO}_{2(aq)} \overset{K_{a1}}{\rightleftharpoons} \text{H}^+ + \text{HSO}_3^-$	1.290×10^{-2}	-4.161	<i>Sillén and Martell [1971]</i>
$\text{HSO}_3^- \overset{K_{a2}}{\rightleftharpoons} \text{H}^+ + \text{SO}_3^{2-}$	6.014×10^{-8}	-2.23	<i>Sillén and Martell [1971]</i>
$\text{CH}_2\text{O}_{(g)} \overset{K_H}{\rightleftharpoons} \text{CH}_2\text{O}_{(aq)}$	6.3×10^3	—	<i>Ledbury and Blair [1925]</i>
$\text{CH}_2\text{O}_{(aq)} + \text{HSO}_3^- \overset{K_{a1}}{\rightleftharpoons} \text{CH}_2\text{OHSO}_3^-$	$\approx 10^5$	—	<i>Dasgupta et al. [1980]</i>
$\text{Fe}^{3+} + \text{SO}_3^{2-} \overset{\beta}{\rightleftharpoons} \text{FeSO}_3^+$	$\approx 10^{10} - 10^{18}$	—	<i>Carlyle [1971]; Hansen et al. [1976]</i>
$\text{C}_7\text{H}_6\text{O} + \text{HSO}_3^- \overset{K_{a2}}{\rightleftharpoons} \text{C}_7\text{H}_6\text{OHSO}_3^-$	$\approx 10^5$	—	<i>Stewart and Donnally [1932]</i>
$\text{C}_2\text{H}_4\text{O} + \text{HSO}_3^- \overset{K_{a3}}{\rightleftharpoons} \text{C}_2\text{H}_4\text{OHSO}_3^-$	$\approx 10^5$	—	by extrapolation

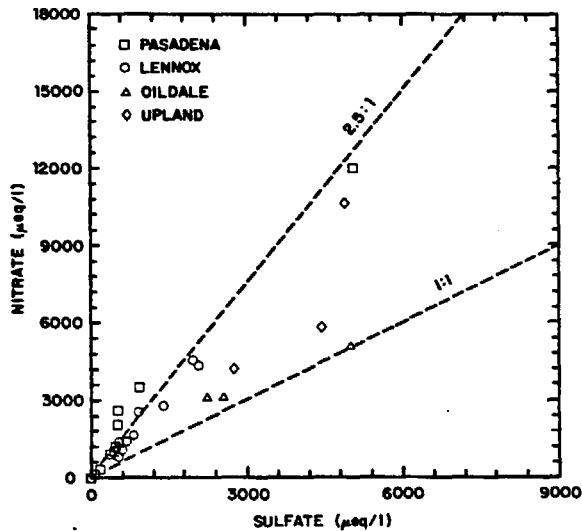


Fig. 7. Plot of nitrate and sulfate equivalent concentrations in fogwater. Dashed lines indicate 2.5 : 1 and 1 : 1 ratios.

fog droplets will be greater than for dry gas and aerosol. Roach *et al.* [1976] have calculated that up to 90% of the liquid water condensed during a fog event may sediment out on the ground. When winds accompany fog, interception of droplets by vegetation is also a major depositional pathway [Schlesinger and Reiners, 1974; Lovett and Reiners, 1982]. Measurement of rain and dry deposition fluxes alone may not adequately account for atmospheric loadings in regions where fog is frequent. Surface wetness from fog deposition may enhance deposition of SO_2

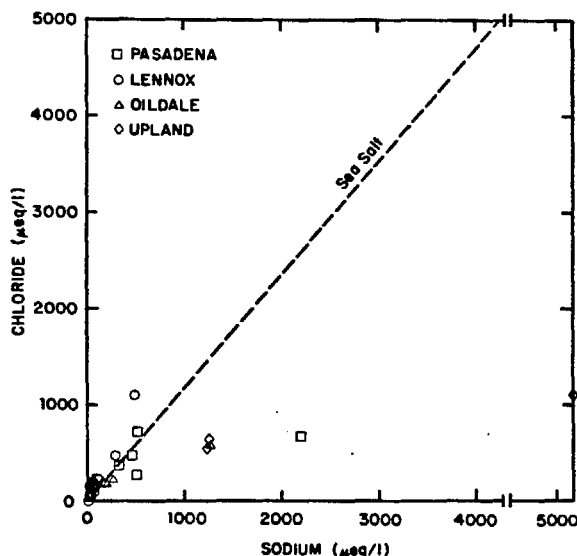


Fig. 8. Plot of sodium and chloride concentrations. Dashed line indicates the NaCl ratio in seawater.

and subsequent oxidation to SO_4^{2-} (with a possible involvement of trace metals) [Lindberg *et al.*, 1979].

Fogwater deposited on leaf surfaces is highly efficient in leaching ions from the leaves [Tukey, 1979] and may result in some plant injury. Experiments with acid mists show plant injury occurring at pH levels around 3 [Jacobson, 1980], which is typical of fogwater in parts of Southern California. Damage to building materials and metal surfaces is also possible from deposition of acidic fog. Corrosion of statuary and building materials has been observed in several locations throughout the world. The role of fog in this damage is not known, although research [Metropolitan Museum of Art, 1979] on the Horses of San Marco (ca. 100 B.C.) in Venice, Italy, indicates that fog and high SO_2 concentrations have resulted in significant damage during the last 50 years.

Historically, fogs have been implicated in a number of severe pollution episodes that caused increased human mortality [Environmental Protection Agency, 1971]. The most notable of these is the infamous London Fog of 1952 [Wilkins, 1954a, b], which caused 4000 excess deaths during the 5-day episode and 12,000 deaths over 4 months. Further research is needed to ascertain whether the fog caused mortality or was merely a consequence of the severe inversion conditions that caused a build up of toxic air pollutants, which were the true agents of mortality. Previous analysis [Larsen, 1970] suggested that these deaths correlated well with the product of gas-phase SO_2 and particle concentrations; however, sulfuric acid mists have been implicated [Wilkins, 1954a, b].

CONCLUSION

Fogwater in Southern California provides a propitious environment for the scavenging of particulate and gaseous forms of S(IV), S(VI), N(V), and N(-III); for the subsequent conversion of S(IV) to S(VI); and for the concomitant production of acidity. Unusually high concentrations of SO_4^{2-} , NO_3^- , NH_4^+ , and H^+ were observed. The highest concentrations were observed during fog events preceded by smoggy days. Acidity caused by NO_3^- and SO_4^{2-} precursors was neutralized to some extent by scavenging of NH_3 and calcareous dust.

The physical processes of condensation and evaporation, along with scavenging and subsequent chemical conversion of reactive gas-phase components, appear to mutually control the temporal trends in fogwater composition. The apparent cyclical relationship between the occurrence of smog and fog in the Los Angeles basin is a manifestation of this phenomenon. The late night and early morning fogs, which form more readily in a particle-laden atmosphere, appear to accelerate and enhance smog production, visibility reduction, and particulate sulfate levels during the subsequent day. This relationship can be dubbed the smog-fog-smog cycle.

Clearly, more research is needed to elucidate the mechanisms by which fog-processed aerosols become highly reactive sites for daytime photochemical transformations. The role of aldehydes and transition metals in the transport and transformation of S(IV) in atmospheric water droplets needs to be explored more intensively. Furthermore, given the millimolar concentrations of some of the metal ions in urban fog, the effect of metal ion catalysts on important chemical transformations (e.g., S(IV) to S(VI)) needs to be considered more carefully in the development of quantitative air quality models for urban airsheds.

TABLE 5. Summary of Fog and Cloud Water Compositions

Location	Date	Type*	pH	$\mu\text{eq l}^{-1}$								Reference	
				SO_4^{2-}	NO_3^-	Cl^-	Na^+	K^+	Ca^{2+}	Mg^{2+}	NH_4^+		
Mt. Washington, N.H.	1930-40	CF	3.0-5.9	4.2-1100		0-34							Houghton [1955]
Nantucket, Mass.	1930-40	MF	—	285-2600		650-5750							Houghton [1955]
Brooklin, Maine	1930-40	F	3.5-6.3	95-770		0-140							Houghton [1955]
SW of London	1960	C†	4.4-7.2	40	19	94	95	13	66	25	22		Oddie [1962]
Germany, Baltic Sea	1955-65	MF†	3.8	1860	900	1740	1500	240	750		2335		Mrose [1966]
Harz Mtn.	1955-65	CF†	5.1	775	450	205	295	85	220		710		Mrose [1966]
nr. Dresden	1955-65	UF†	4.2	3300	380	585			3180		2100		Mrose [1966]
Kiev, USSR	Dec. 1964	C	3.4-5.4	400-2060	17-200	115-325	80-215	30-130	40-535	16-160	235-1300		Petrenchuk and Drozdova [1966]
Mt. Noribura, Japan	July 1963	CF	3.4-4.3	230-1250	50-350	75-230	45-165	55-85			115-260		Okita [1968]
Mt. Tsukaba, Japan	Nov. 1963	CF	5.6-6.5	360-2065	11-75	295-1270	180-435	154			110-965		Okita [1968]
Puerto Rico	Nov.-Dec. 1967	C	4.9-5.4	75-190		150-1975				20-90	35-400		Lazrus et al. [1970]
Nova Scotia	Aug. 1975	MF		54-470		14-235	880-1240	43-50	38-69	42-77	9-72		Mack and Katz [1976]
Coastal California	Sep.-Oct. 1970	MF		77-490	24-235	96-1235	78-945	11-23	9-100	23-175	0-580		Mack et al. [1977]
Whiteface Mtn., N.Y.	Aug. 1976	CF†	3.6-3.9	52-140	140-215	1.7-3.1	2.3-11	13-20	10-20	2.2-6.1	32-89		R. A. Castillo et al. (unpublished manuscript, 1980)
	Aug. 1980	CF	3.2-4.0	32-806	7-192	1-14	1-7	1-6			4-197		Falconer [1981]
Los Angeles, Calif.	Jan. 80	C	4.6-6.8	5-400	0-445	1-760	2-50	1-70			0-230		Hegg and Hobbs [1981]

*Type of sample: F = fog; C = clouds aloft; CF = intercepted clouds; MF = marine fog; UF = urban fog

†Mean values of samples

‡Range of mean values; otherwise range of samples

Acknowledgments. We gratefully acknowledge the financial support of the California Air Resources Board and the invaluable assistance provided by its professional staff. Additional logistical support was provided by the South Coast Air Quality Management District. Special thanks are extended to R. C. Flagan, J. J. Morgan, D. Lawson, and D. Grosjean for their contributions to the success of this research.

REFERENCES

- Appel, B. R., Y. Tokiwa, and M. Haik, Sampling of nitrates in ambient air, *Atmos. Environ.*, **15**, 283-289, 1981.
- Baboolal, B., H. R. Pruppacher, and J. H. Topalian, A sensitivity study of a theoretical model of SO₂ scavenging by water drops in air, *J. Atmos. Sci.*, **38**, 856-870, 1981.
- Barrett, E., F. P. Parungo, and R. F. Pueschel, Cloud modification by urban pollution: A physical demonstration, *Meteorol. Res.*, **32**, 136-149, 1979.
- Carlyle, D. W., A kinetic study of the aquation of sulfite(III) ion, *Inorg. Chem.*, **10**, 761-764, 1971.
- Cass, G. R., Dimensions of the Los Angeles SO₂/sulfate problem, *Memo. 15*, Environ. Qual. Lab., Calif. Inst. Technol., Pasadena, California, 1975.
- Cass, G. R., On the relationship between sulfate air quality and visibility with examples in Los Angeles, *Atmos. Environ.*, **13**, 1069-1084, 1979.
- Cass, G. R., Sulfate air quality control strategy design, *Atmos. Environ.*, **15**, 1227-1249, 1981.
- Cass, G. R., and F. H. Shair, Transport of sulfur oxides within the Los Angeles sea breeze/land breeze circulation system, paper presented at Joint Conference on Application of Air Pollution Meteorology, Am. Meteorol. Soc., New Orleans, March 24-27, 1980.
- Cox, R. A., Particle formation from homogeneous reactions of sulfur dioxide and nitrogen dioxide, *Tellus*, **26**, 235-240, 1974.
- Dasgupta, P. K., K. De Cesare, and J. C. Ullrey, Determination of atmospheric sulfur dioxide without tetrachloromercurate(II) and the mechanism of the Schiff reaction, *Anal. Chem.*, **52**, 1912-1922, 1980.
- Eatough, D. J., T. Major, J. Ryder, M. Hill, N. F. Mangelson, N. L. Eatough, L. D. Hansen, R. G. Meisenheimer, and J. W. Fischer, The formation and stability of sulfite species in aerosols, *Atmos. Environ.*, **12**, 263-271, 1978.
- Environmental Protection Agency, Guide for Air Pollution Avoidance, Appendix B, History of Episodes, *Rep. PH-22-68-32*, pp. 123-135, Washington, D.C., 1971.
- Eriksson, E., The yearly circulation of chloride and sulfur in nature: Meteorological, geochemical, and pedological implications, Part 2, *Tellus*, **12**, 63-109, 1960.
- Falconer, P. D., Cloud Chemistry and Meteorological Research at Whiteface Mountain: Summer 1980, *ASRC Publ. 806*, Atmos. Sci. Res. Center, State Univ. New York, Albany, 1981.
- Fortune, C. R., and B. Dellinger, Stabilization and analysis of sulfur(IV) aerosols in environmental samples, *Environ. Sci. Technol.*, **16**, 62-66, 1982.
- Fung, K., and D. Grosjean, Determination of nanogram amounts of carbonyls as 2,4-dinitrophenylhydrazones by high-performance liquid chromatography, *Anal. Chem.*, **53**, 168-181, 1981.
- Galloway, J. N., G. E. Likens, W. C. Keene, and J. M. Miller, The composition of precipitation in remote areas of the world, *J. Geophys. Res.*, **87**, 8771-8786, 1982.
- Graham, R. A., and H. S. Johnston, The photochemistry of NO₃ and the kinetics of the N₂O₅-O₃ system, *J. Phys. Chem.*, **82**, 254-268, 1978.
- Grosjean, D., Formaldehyde and other carbonyls in Los Angeles ambient air, *Environ. Sci. Technol.*, **16**, 254-262, 1982.
- Hansen, L. D., L. Whiting, D. J. Eatough, T. E. Jensen, and R. M. Izatt, Determination of sulfur(IV) and sulfate aerosols by thermometric methods, *Anal. Chem.*, **48**, 634-638, 1976.
- Hitchcock, D. R., Sulfuric acid aerosols and HCl release in coastal atmospheres: Evidence of rapid formation of sulfuric acid particulates, *Atmos. Environ.*, **14**, 165-182, 1980.
- Hegg, D. A., and P. V. Hobbs, Cloudwater chemistry and the production of sulfates in clouds, *Atmos. Environ.*, **15**, 1597-1604, 1981.
- Hoffmann, M. R., and D. J. Jacob, Kinetics and mechanisms of the catalytic oxidation of dissolved sulfur dioxide in aqueous solution: An application to nighttime fog-water chemistry, in *Acid Precipitation*, vol. 6, edited by J. G. Calvert, Ann Arbor Science Publishers, Ann Arbor, Michigan, 1983.
- Houghton, H. G., On the chemical composition of fog and cloud water, *J. Meteorol.*, **12**, 355-357, 1955.
- Humphrey, R. E., M. H. Ward, and W. Hinze, Spectrophotometric determination of sulfite with 4,4-dithiopyridine and 5,5-dithiobis(2-nitrobenzoic acid), *Anal. Chem.*, **42**, 698-702, 1970.
- Izatt, R. M., D. J. Eatough, M. L. Lee, T. Major, B. E. Richter, L. D. Hansen, R. G. Meisenheimer, and J. W. Fischer, The formation of inorganic and organic S(IV) species in aerosols, in *Proceedings of the 4th Joint Conference on Sensing Environmental Pollutants*, pp. 821-824, American Chemical Society, Washington, D.C., 1978.
- Jacob, D. J., and M. R. Hoffmann, A dynamic model for the production of H⁺, NO₃⁻, and SO₄²⁻ in urban fog, submitted to *J. Geophys. Res.*, 1982.
- Jacob, D. J., R. C. Flagan, J. M. Waldman and M. R. Hoffmann, Design and calibration of rotating-arm collectors for ambient fog sampling, paper presented at 4th International Conference on Precipitation Scavenging, Dry Deposition, and Resuspension, Nov. 29-Dec. 3, Santa Monica, Calif., 1982.
- Jacobson, J. S., Experimental studies on the phytotoxicity of acidic precipitation: The United States experience in *Effects of Acid Precipitation on Terrestrial Ecosystems*, edited by T. C. Hutchinson and M. Havas, pp. 151-160, Plenum, New York, 1980.
- Larsen, R. I., Relating air pollutant effects to concentration and control, *J. Air Pollut. Control Assoc.*, **20**, 214-225, 1970.
- Lazrus, A. L., H. W. Baynton, and J. P. Lodge, Trace constituents in oceanic cloud water and their origin, *Tellus*, **22**, 106-113, 1970.
- Ledbury, W., and E. W. Blair, The partial formaldehyde vapour pressure of aqueous solutions of formaldehyde, Part 2, *J. Chem. Soc.*, **127**, 2832-2839, 1925.
- Liljestrand, H. M., and J. J. Morgan, Spatial variations of acid precipitation in Southern California, *Environ. Sci. Technol.*, **15**, 333-338, 1981.
- Lindberg, S. E., R. C. Harriss, R. R. Turner, D. S. Shriner, and D. D. Huff, Mechanism and rates of atmospheric deposition of selected trace element and sulfate to deciduous forest watershed, *Rep. ORNL/TM-6674*, Oak Ridge Nat. Lab., Oak Ridge, Tenn. 1979.
- Lovett, G. M., and W. A. Reiners, Deposition of cloudwater and dissolved ions to subalpine forests of New England, paper presented at 4th International Conference on Precipitation Scavenging, Dry Deposition, and Resuspension, sponsor, Santa Monica, Calif., Nov. 29-Dec. 3, 1982.
- Mack, E. J., and U. Katz, The Characteristics of Marine Fog Occurring off the Coast of Nova Scotia, *Rep. CJ-5756-M-1*, Calspan Corp., Buffalo, New York, 1976.
- Mack, E. J., U. Katz, C. W. Rogers, D. W. Gaucher, K. R. Piech, C. K. Akers, and R. J. Pilié, An Investigation of the Meteorology, Physics and Chemistry of Marine Boundary Layer Processes, *Rep. CJ-6017-M-1*, Calspan Corp., Buffalo, New York, 1977.
- Mack, E. J., and R. J. Pilié, Fog Water Collector, U.S. Patent 3889532, 1975.
- Martin, L. R., Kinetic studies of sulfite oxidation in aqueous solution, in *Acid Precipitation: SO₂, NO, NO₂ Oxidation Mechanisms: Atmospheric Considerations*, edited by J. G. Calvert, Ann Arbor Science Publishers, Ann Arbor, Mich., 1983.
- McMurry, P. H., D. J. Rader, and J. L. Smith, Studies of aerosol formation in power plant plumes, 1, Parameterization of conversion rate for dry, moderately polluted ambient conditions, *Atmos. Environ.*, **15**, 2315-2329, 1981.
- Metropolitan Museum of Art, *The Horses of San Marco, Venice*, translated from Italian by J. and V. Wilton-Ely, New York, 1979.
- Morgan, J. J., and H. J. Liljestrand, Measurement and interpretation of acid rainfall in the Los Angeles basin, *Rep. AC-2-80*, W. M. Keck Lab. Hydraul. Water Resour., Calif. Inst. Technol., Pasadena, California, 1980.
- Mrose, H., Measurement of pH and chemical analyses of rain-, snow-, and fog-water, *Tellus*, **18**, 266-270, 1966.
- Nash, T., The colorimetric estimation of formaldehyde by means of the Hantzsch reaction, *Biochem. J.*, **55**, 416-421, 1953.
- National Research Council, *Formaldehyde and Other Aldehydes*, National Academy Press, Washington, D. C., 1981.
- Oddie, B. C. V., The chemical composition of precipitation at cloud levels, *Quart. J. R. Meteorol. Soc.*, **88**, 535-538, 1962.
- Okita, T., Concentrations of sulfate and other inorganic materials in fog and cloud water and in aerosol, *J. Meteorol. Soc. Jpn.*, **46**, 120-126, 1968.
- Petrenchuk, O. P., and V. M. Drozdova, On the chemical composition of cloud water, *Tellus*, **18**, 280-286, 1966.
- Rietz, E. B., The stabilization of small concentrations of formaldehyde in aqueous solutions, *Anal. Lett.*, **13**, 1073-1084, 1980.

- Roach, W. T., R. Brown, S. J. Caughey, J. A. Garland, and C. J. Readiness, The physics of radiation fog, 1, A field study, *Quart. J. R. Meteorol. Soc.*, **10**, 313-33, 1976.
- Sander, S. P., and J. H. Seinfeld, Chemical kinetics of homogeneous oxidation of sulfur dioxide, *Environ. Sci. Technol.*, **10**, 1114-1123, 1976.
- Schlesinger, W. H., and W. A. Reiners, Deposition of water and cations on artificial foliar collectors in fir Krummholz of New England mountains, *Ecology*, **55**, 378-386, 1974.
- Schwartz, S. E., Gas-aqueous reactions of sulfur and nitrogen oxides in liquid-water clouds, in *Acid Precipitation: SO₂, NO, and NO₂ Oxidation Mechanisms: Atmospheric Considerations*, edited by J. G. Calvert, Ann Arbor Science Publishers, Ann Arbor, Mich., 1983.
- Sillén, L. G., and A. E. Martell, *Stability Constants of Metal-Ion Complexes, Suppl. 1*, 2nd ed., The Chemical Society, London, 1971.
- Smith, F. B., and G. H. Jeffrey, Airborne transport of sulphur dioxide from the U.K., *Atmos. Environ.*, **9**, 643-659, 1975.
- Solórzano, L., Determination of ammonia in natural waters by the phenylhypochlorite method, *Limnol. Oceanogr.*, **14**, 799-801, 1967.
- Stelson, A. W., Thermodynamics of aqueous atmospheric aerosols, Ph.D. thesis, 127 pp., Calif. Inst. Technol., Pasadena, California, 1982.
- Stelson, A. W., and J. H. Seinfeld, Relative humidity and temperature dependence of the ammonium nitrate dissociation constant, *Atmos. Environ.*, **16**, 983-992, 1982.
- Stewart, T. D., and L. H. Donnally, The aldehyde bisulfite compounds, 2, The effect of varying hydrogen ion and of varying temperature upon the equilibrium between benzaldehyde and bisulfite ion, *J. Am. Chem. Soc.*, **54**, 3555-3558, 1932.
- Tukey, H. B., Jr., The leaching of substances from plants, *Ann. Rev. Plant Physiol.*, **71**, 305-324, 1970.
- Waldman, J. M., J. W. Munger, D. J. Jacob, R. C. Flagan, J. J. Morgan, and M. R. Hoffmann, Chemical composition of acid fog, *Science*, **218**, 677-680, 1982.
- Wilkins, E. T., Air pollution and the London fog of December 1952, *J. R. Sanit. Inst.*, **74**, 1-21, 1954a.
- Wilkins, E. T., Air pollution aspects of the London fog of December 1952, *J. R. Meteorol. Soc.*, **80**, 267-278, 1954b.
- Wilson, J. C., and P. H. McMurry, Studies of aerosol formation in power plant plumes, 2, Secondary aerosol formation in the Navajo generating station plume, *Atmos. Environ.*, **15**, 2329-2339, 1981.

(Received October 4, 1982;
revised February 4, 1983;
accepted February 17, 1983.)

Kinetics and Mechanisms of the Catalytic Oxidation of Dissolved Sulfur Dioxide in Aqueous Solution: An Application to Nighttime Fog Water Chemistry

Michael R. Hoffmann
Daniel J. Jacob

Sulfur dioxide can be oxidized to sulfate aerosols either homogeneously in the gas phase or heterogeneously in atmospheric microdroplets [1-3]. Field studies indicate that the relative importance of homogeneous and heterogeneous processes depends on a variety of climatological factors, such as relative humidity and the intensity of incident solar radiation [4-9].

Cass [5] has shown that the worst sulfate pollution episodes in Los Angeles occur during periods of high relative humidity and when the day begins with low clouds or fog in coastal areas, while Cass and Shair [4] have reported that nighttime conversion rates (5.8%/h) for SO_2 in the Los Angeles sea breeze/land breeze circulation system are statistically indistinguishable from typical daytime conversion rates (5.7%/h) for the month of July. Liljestrand and Morgan [10], in their study of rainfall in the Los Angeles basin, have reported that light, misting precipitation events resulted in low pH values (e.g., pH 2.9) and correspondingly high SO_4^{2-} and NO_3^- concentrations.

Results of these investigations along with the results of other investigators [6-9, 11-13] indicate that aqueous-phase oxidation of SO_2 is a significant pathway for the total transformation of SO_2 .

Waldman et al. [14] characterized the chemistry of winter fogs in the Los Angeles basin; they reported that nighttime fog water has extremely low pH values (e.g., pH 2.2) and extremely high concentrations of sulfate, nitrate, ammonium ion, and trace metals. Observed ranges reported by Waldman et al. [14] are summarized in Table I. Of special interest are the high values observed for SO_4^{2-} , NO_3^- , S(IV), CH_2O , and Fe, Mn, Pb and Cu ions in the fog water droplets. These values

and their time-dependent changes [14] indicate that nighttime fogs provide a very reactive and complex environment for the incorporation and transformation of SO₂ and NO_x to their acidic products, H₂SO₄ and HNO₃. Concomitant incorporation of NH₃ gas and calcereous dust into the droplet phase results in the partial neutralization of the generated acidity. Later sections of this chapter will discuss models for the detailed thermodynamic speciation and possible reaction kinetics that lead to sulfate and nitrate production in these droplet systems.

Because of their similarity to clouds with respect to physical characteristics, fogs are likely to reflect the same chemical processes occurring in clouds and, to some degree, in aqueous microdroplets. Cloud and fog water droplets are in the size range 2–100 μm, whereas aqueous microdroplets will be in the range 0.01–1 μm. On the other hand, raindrops are approximately 100 times larger than cloud and fog water droplets (e.g., 0.1–3 mm). In the Los Angeles study, Waldman et al. [14] found that fog water was more concentrated in the primary constituents than was the overlying cloud water, which was in turn more concentrated than rain water during overlapping periods of time. These results suggest that fog and low-lying clouds may play an important role in the diurnal production of sulfate and nitrate in the Los Angeles basin during certain times of the year when the meteorological conditions are propitious for fog and cloud formation. Furthermore, Hegg and Hobbs [15] have observed sulfate production rates in cloud water over western Washington that ranged from 4.0 to 300%·h⁻¹ and pH values from 4.3 to 5.9. The sulfate production rate appeared to increase with an increase in pH. Similar pH values and sulfate levels were observed in stratus clouds over the Los Angeles basin [15].

Historically, fog events have been correlated with severe pollution episodes in which elevated concentrations of SO₂ and particulate aerosol have been observed [16]. During many of these extended fog periods excess deaths were recorded [17–21]. The London fog of 1952 was particularly bad in this regard. For example, during the London fog of 1952 the daily mass emission rate of SO₂ has been estimated to be 1.82 × 10⁹ g, the affected area to be 1.3 × 10⁹ m², the height of the inversion layer to be 150 m and the liquid water content at 1.23 × 10¹² g [22]. Given the daily observed increase in the gas-phase SO₂ concentration of 0.18 ppm and an established droplet residence time of 0.25 days [18], the sulfate concentration of the fog water can be estimated to be approximately 11.0 meq·L⁻¹ with an apparent conversion rate of 12.5%·h⁻¹. This estimated value can be compared to the sulfate ranges observed in the Los Angeles fog water, which were 0.3–3 meq·L⁻¹. However, the London fog lasted for five days while the Los Angeles fogs of 1981–1982 persisted for no more than eight to ten successive hours.

As pointed out in Chapter 1, gas-phase reactions involving hydroxy radical oxidation of SO₂ are too slow to account for the very high transformation rates. Alternatively, the catalytic autoxidation of SO₂ in aqueous microdroplets has been suggested as a nonphotolytic pathway for rapid production of sulfuric acid in humid atmospheres [22–30]. In addition, H₂O₂ and O₃ have been given serious consideration as the major oxidants of dissolved SO₂ as discussed in Chapters 2 and 4. Oxidation by H₂O₂ seems to be most favorable because of its extremely

Table I. Fog Water Composition in Southern California: Observed Concentration Ranges [12–14]

	Location			
	Pasadena		Los Angeles	
	11-23-81	12-18-81	11-14-82	1981-1982
pH	2.92-4.85	2.52-2.81	2.90-3.07	2.20
NO ₃ ⁻ (μeq·L ⁻¹)	1,220-3,520	2,070-3,690	3,140-5,140	12,000
SO ₄ ²⁻ (μeq·L ⁻¹)	481-944	510-1,970	2,250-5,000	5,060
NH ₄ ⁺ (μeq·L ⁻¹)	1,290-2,380	950-1,570	5,370-10,520	10,520
Fe (μg·L ⁻¹)	920-1,770	1,020-2,080	240-6,600	23,700
Mn (μg·L ⁻¹)	34-56	25-81		812
Pb (μg·L ⁻¹)	1,310-2,540	828-2,400	241-366	2,540
Cu (μg·L ⁻¹)	88-105	9-150	40-400	144
Ni (μg·L ⁻¹)	7.6-13.6	2.3-51.5	125-590	51.5
CH ₂ O (mg·L ⁻¹)	3.1-3.4	3.9-7.6	6.1-14	12.8
SO ₂ ⁻ (μeq·L ⁻¹)	151-235	30-250		250
				54-258

high rate of reaction [31-34] and its pH dependence which favors the reaction at low pH. In comparison, metal-catalyzed autoxidations tend to exhibit decreasing reaction rates with a decrease in pH [27]. Similarly, the reaction rate of O₃ with S(IV) decreases with a decrease in pH.

Limiting factors in the metal-catalyzed pathways will be the total concentration of the active metal catalyst and its speciation as a function of pH. As shown in Table I, Los Angeles fog water has high concentrations of Fe, Mn, Cu, Ni and Pb ions. Of these metals, Fe, Mn and Cu are expected to be the most effective catalysts for autoxidation of S(IV) [27,34]. The highest observed concentrations for Fe and Mn were 424 and 14.8 μM, respectively, while the average Fe and Mn concentrations in Los Angeles fog water were observed to be 51.6 and 1.7 μM, respectively. For comparison, Thornton [35] has reported that the worldwide mean concentrations for Fe in urban, rural and remote rainfall are 4.5, 3.1 and 0.13 μM, respectively. In many calculations of the droplet-phase SO₂ oxidation rate [2,36-39], the assumed Fe concentrations range from 1 to 360 μM and the assumed Mn concentrations range from 1 to 37 μM. At the upper range of the concentration scales, metal-catalyzed reactions may play an important role in the overall SO₂ oxidation rate in light of the rate laws discussed in Chapter 2. The role of metal ion speciation and kinetic models for fog water chemistry will be discussed later in this chapter.

To translate laboratory results on the kinetics of various pathways for SO₂ oxidation in aqueous systems to atmospheric droplet systems, detailed rate laws, mechanisms, activation energies and ionic strength dependencies should be determined. In only very few cases has this complete information been assembled. However, in the case of metal-catalyzed systems, there are numerous discrepancies among investigators concerning the detailed kinetic information [15]. Metal-catalyzed autoxidations can proceed via four distinctly different mechanistic pathways [40]. These include a thermally initiated free-radical chain reaction involving a series of one-electron transfer steps, an inner-sphere metal-sulfite complexation pathway involving a series of two-electron transfers, a surface complexation pathway involving metal oxides and oxyhydroxides in suspension, and photoassisted pathways in which the oxidation is initiated by absorption of light by S(IV), metal ions, metal oxide surfaces or a specific metal-sulfite complex. The details of these different reaction pathways will be discussed in the next section of this chapter.

The mechanism of the oxidation of S(IV) by hydrogen peroxide is fairly well understood [31-33,41,42]. This reaction proceeds via nucleophilic displacement of H₂O₂ on bisulfite (HSO₃⁻) ion and is catalyzed by specific and general acid catalysis. The significance of this latter feature for open atmospheric systems has been discussed in Chapters 2 and 4. On the other hand, the mechanism of the oxidation of sulfite by ozone [32,43] and its various catalytic influences are less well understood. Most likely, the reaction with ozone proceeds via a free radical mechanism involving the sulfite radical and peroxymonosulfite radical species [32]. The details of the polar pathway involving H₂O₂ and the radical pathway involving O₃ will be presented in the next section. This discussion will be followed by presentation of a fog water chemistry model that will incorporate and test the various reaction pathways for an open nonphotolytic system.

A. S(IV) OXIDATION MECHANISMS

1. Metal-Catalyzed Pathways for Oxidation

Reactions of the triplet ground state of molecular oxygen with singlet ground state reductants such as SO₂ proceed slowly because they involve changes in spin multiplicity and a large degree of bond deformation or alteration in the formation of products. In many cases, the reactions of O₂ with organic and inorganic reductants can be accelerated in the presence of transition metal ions and their complexes. In particular, the first-row transition metal ions have been shown to be particularly effective as catalysts for autoxidation [44]. Catalysis by first-row transition metals may occur homogeneously or heterogeneously in the liquid phase. If the catalytic center involves a soluble metal ion or complex, the reaction can be classified as a homogeneous process; however, if the catalytic center involves a metal surface such as an oxide, oxyhydroxide or sulfide solid, then the reaction can be classified as a heterogeneous process in the liquid phase. Transition metal ions such as Co(II), Co(III), Cu(II), Fe(II), Fe(III), Mn(II), Ni(II), V(IV) (as VO²⁺) and their soluble complexes have been shown to be effective homogeneous catalysts [44], while solid surfaces such as Fe₂O₃ [45], TiO₂ [45], CdS [45], ZnO [45], FeOOH [37], Co(OH)₂ [46], V₂O₅ [47], MnO₂ [48] and MnOOH [48] have been shown to be effective heterogeneous catalysts for certain redox reactions.

Numerous attempts have been made to characterize the kinetics and mechanisms of metal-catalyzed autoxidation of S(IV) in aqueous solution; however, these studies have been characterized by inconsistent reaction rates, rate laws and pH dependencies [27,40,44,49]. In this section, postulated mechanisms and their resulting theoretical rate expressions will be examined critically. In general, the homogeneous reaction mechanisms can be broken down into three general categories: (1) free radical chain mechanisms involving a sequence of one-electron transfer steps following a thermal initiation; (2) polar mechanisms involving inner-sphere complexation and two-electron transfer steps; and (3) photoassisted mechanisms. These mechanisms, their rate expressions and the empirical rate laws will be compared for consistency.

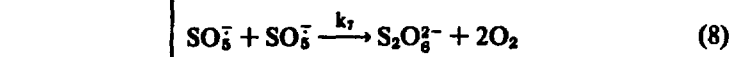
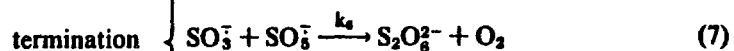
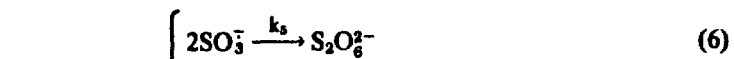
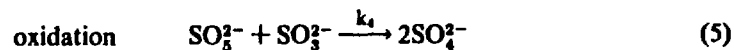
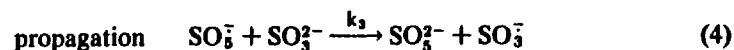
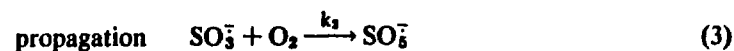
a. Free Radical Chain Reactions

Oxidation of S(IV) in aqueous solution proceeds according to the following simple stoichiometry:



where n varies from 0 to 2 depending on pH. Bäckström [50] proposed that the reaction of Equation 1 involves a chain mechanism in which a metal ion, Mⁿ⁺, of appropriate oxidation state initiates the radical sequence as follows:





where the initiation step involves a one-electron reducible metal ion as the catalytic initiator [for a truly closed catalytic sequence, $\text{M}^{(n-1)+}$ must be oxidized back to M^{n+}], the propagation steps involve SO_3^- , SO_5^- and SO_5^{2-} (peroxymonosulfite ion) as reactive intermediates, the oxidation step is invoked for stoichiometric reasons, and the termination steps result in the production of dithionate, a frequently observed but low-yield product.

Theoretical rate expressions for the overall stoichiometric reaction (Equation 1) (i.e., the summation of Equations 2–5) can be derived readily from the appropriate differential equations describing the total rate of appearance or of disappearance of each species involved in the mechanism provided that the steady-state approximation is used. For example, assuming that the chain mechanism involves Equations 2–5 and Equation 6 as the termination step the following rate expression can be derived [51].

$$-\text{d}[\text{SO}_3^{2-}]/\text{dt} = \text{d}[\text{SO}_3^{2-}]/\text{dt} = k_1[\text{SO}_3^{2-}][\text{M}^{n+}] + k_2(2k_1/k_3)^{0.5}[\text{M}^{n+}]^{0.5}[\text{SO}_3^{2-}]^{0.5}[\text{O}_2] \quad (9)$$

Since the sulfite chain reaction has a chain length of $\sim 50,000$, according to Bäckström [50], the long chain length approximation can be invoked (i.e., $\nu_p/\nu_i \gg 1$ or the ratio of the rate of propagation to the rate of initiation is very large) and Equation 9 can be rewritten as:

$$-\text{d}[\text{SO}_3^{2-}]/\text{dt} = k'[\text{M}^{n+}]^{0.5}[\text{SO}_3^{2-}]^{0.5}[\text{O}_2] \quad (10)$$

where $k' = k_2(2k_1/k_3)^{0.5}$

Different theoretical rate expressions can be obtained if assumptions are made about the nature of the rate-determining propagation step and the corresponding termination step. In addition, the steady-state and the long chain length approxima-

Table II. Theoretical Rate Expressions Obtained from the Bäckström [50] Mechanism for Various Termination Steps^a

Termination Step	Rate Coefficient, <i>k</i>	α	β	γ
k_3	$k_2(2k_1/k_3)^{1/2}$	1/2	1/2	1
k_4	$(2k_1k_2k_3/k_6)^{1/2}$	1/2	1	1/2
k_7	$k_3(2k_1/k_7)^{1/2}$	1/2	3/2	0

^a α , β , and γ represent the reaction orders for the reaction rate given by the generalized rate expression $-\text{d}[\text{SO}_3^{2-}]/\text{dt} = k[\text{M}^{n+}]^\alpha[\text{SO}_3^{2-}]^\beta[\text{O}_2]^\gamma$.

tions for a free radical, closed-sequence catalytic [51,52] process can be used to simplify the algebraic manipulations. Theoretical rate expressions obtained with these procedures are listed in Table II [25,26,37,46,53–60].

The theoretically derived rate expressions can be compared to the empirical rate laws reported by other investigators (Table III). Perusal of this list indicates a considerable lack of agreement among these investigators as to the specific reaction orders; in particular, few empirical rate laws agree with the derived rate expressions shown in Table II. The empirical rate laws observed by Barron and O'Hern [66], Chen and Barron [58] and Bengtsson and Bjerle [60] at constant pH are in general agreement with the third rate expression of Table II. However, later results reported by Sawicki and Barron [59] using a thin-film reactor system contradicted earlier results reported by Barron and co-workers [58,66]. Most often the various investigators concur that the reaction order in oxygen is zero. However, it should be pointed out that an oxygen dependence in many cases was overlooked by using pseudo-order conditions in oxygen or, in other cases, mass-transfer limitations may have resulted in an apparent zero-order oxygen dependency. The first and second rate expressions of Table II show a nonzero reaction order in oxygen and a half-order metal ion dependence, whereas most investigators report a first-order metal ion dependence and a zero-order oxygen dependence. Nonetheless, many of these investigators cite the Bäckström [50] mechanism as a logical sequence of elementary reactions that is adequate to explain their empirical observations. Clearly, in many cases it appears to be inadequate. Finally, a caveat to this comparison is that few investigators used similar analytical and kinetic methodologies and fewer used identical concentration and pH ranges. As a result the lack of agreement is somewhat understandable and may suggest that parallel mechanistic pathways are followed which will result in complicated multiterm rate laws.

In most kinetic studies of the metal catalyzed autoxidation of S(IV), SO_3^- has been identified as the reactive form of S(IV). If this is indeed the case, the apparent pH dependencies in part can be expressed as follows:

$$[\text{S(IV)}] = [\text{H}_2\text{O} \cdot \text{SO}_2] + [\text{HSO}_3^-] + [\text{SO}_3^{2-}] \quad (11)$$

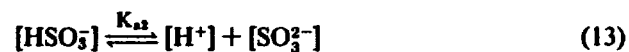
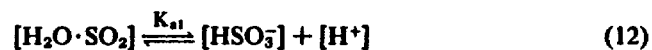
Table III. Empirical Rate Laws Reported by Various Investigators for the Metal Catalyzed Autoxidation of SO_2 .^a

M^{n+}	α	β	γ	Δ	Reference
Mn^{2+}	2	0	0		53
	2	0	0	-1	Chapter 2 ^b
	1	1	0	1	Chapter 2 ^b
	1	1	0	1	54
	≤ 1	≤ 1	0		55
Fe^{3+}	1	1	0		56
	1	1	0	1	37
	1	2	0	1	25
	1	1-2	?	2	26
	1	1	0	-1	Chapter 2
Co^{3+}	2	2	0	1/n	57 ^c
	1	1	0	1/n	57 ^c
	1/2	3/2	0		58
Co^{2+}	1/2	?	2		59
	1/2	3/2	0	-1	60
Cu^{2+}	1	1	1		61
	2	1	1	-1	62
	1/2	1	0	1/n	63 ^c
	1/2	3/2	0		64
	1	1	0	1/2	65
	1/2	3/2	0		66
	1/2	3/2	0		46
	1	1	0		56

^a α , β , γ , and Δ represent the reaction orders for the reaction rate given by the generalized rate expression $-\text{d}[\text{SO}_3^-]/\text{dt} = k[\text{M}^{n+}]^\alpha[\text{SO}_3^-]^\beta[\text{O}_2]^\gamma[\text{H}^+]^\Delta$.

^b Multiterm rate law.

^c Multiterm rate law where $n = 0, 1$ or 2 .



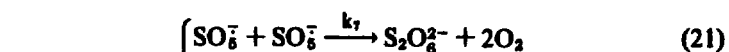
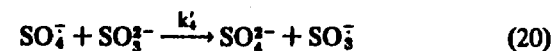
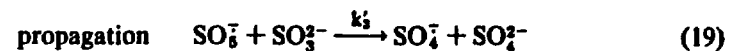
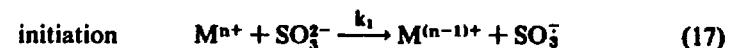
$$[\text{S(IV)}] = [\text{SO}_3^{2-}] \left(\frac{[\text{H}^+]^2}{K_{a1}K_{a2}} + \frac{[\text{H}^+]}{K_{a1}} + 1 \right) \quad (14)$$

$$[\text{SO}_3^{2-}] = [\text{S(IV)}] \left(\frac{K_{a1}K_{a2}}{[\text{H}^+]^2 + K_{a2}[\text{H}^+] + K_{a1}K_{a2}} \right) \quad (15)$$

Substitution into Equation 10 gives

$$\frac{-\text{d}[\text{S(IV)}]}{\text{dt}} = k'[\text{M}^{n+}][\text{S(IV)}]^{0.5}[\text{O}_2] \left(\frac{K_{a1}K_{a2}}{[\text{H}^+]^2 + K_{a2}[\text{H}^+] + K_{a1}K_{a2}} \right) \quad (16)$$

Alternative free-radical mechanisms have been postulated [67,68]. Hayon et al. [67] observed the formation of the sulfate radical ion, SO_4^- , during the flash photolysis and pulse radiolysis of oxygenated sulfite solutions, and they found no firm evidence for SO_3^- . If the flash photolysis experiments employed by Hayon et al. [67] truly give insight into more moderate energetic conditions anticipated in thermal reactions, the following mechanism can be postulated:



This mechanism is similar in many respects to the Bäckström mechanism with the exception of the inclusion of the sulfate radical ion as a reactive propagation intermediate.

Once again, theoretical rate expressions can be derived from the mechanism above using the steady-state approximation, the long chain length assumption, and the assumption that the rate of initiation is equal to rate of termination at steady-state (i.e., $\nu_i = \nu_t$ when $\text{d}[\text{SO}_3^-]/\text{dt} = \text{d}[\text{SO}_4^-]/\text{dt} = \text{d}[\text{SO}_3^{2-}]/\text{dt} = 0$). The resulting equations are listed in Table IV. Regardless of the basic assumptions,

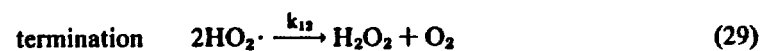
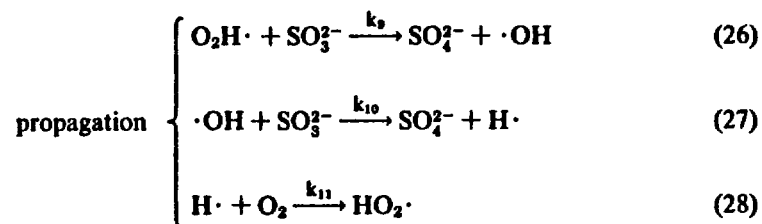
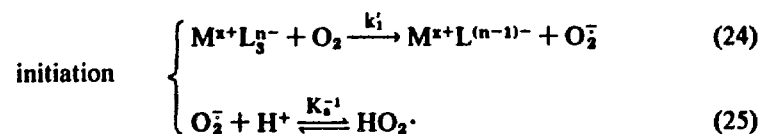
Table IV. Theoretical Rate Expressions Obtained from the Hayon et al. [67] and Schmittkunz [68] Mechanisms^a

Mechanism	Termination Step	Rate Coefficient, k	α	β	γ
Hayon et al.	k_7	$k_7'(2k_1/k_9)^{1/2}$	1/2	3/2	0
Hayon et al.	k_8 or k_9'	$k_8'(2k_1/k_7)^{1/2}$	1/2	3/2	0
Schmittkunz	k_{12}	$k_9(2k_1/k_{12})^{1/2}$	1/2	1	1/2

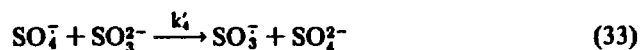
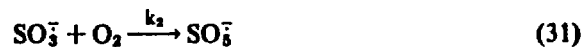
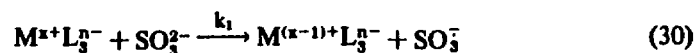
^a α , β , and γ represent the reaction orders for the reaction rate given by the generalized rate expression $-\text{d}[\text{SO}_3^-]/\text{dt} = k[\text{M}^{n+}]^\alpha[\text{SO}_3^-]^\beta[\text{O}_2]^\gamma$.

the mechanism of Hayon et al. [67] yields a single rate expression in which there is a half-order dependence on the metal ion concentration and a three-halves-order dependence on sulfite. The same result is obtained if the k_2 step is assumed to be the rate limiting propagation step.

The mechanism proposed by Schmittkuz [68] postulates two separate chain propagation sequences resulting from two different initiation steps. The first sequence is similar in form to the Bäckström mechanism and the second involves O_2^- , $HO_2\cdot$, $\cdot OH$ and $H\cdot$ as chain carriers. The postulated mechanism is:



here $M^{x+}L_3^{n-}$ is a metal(M)-ligand(L) complex of appropriate charge, $x-n$, and K_a is the acid dissociation constant for the hydroperoxyl radical/superoxide acid-base equilibrium. The second radical pathway involves SO_3^- , SO_4^- and SO_5^- as chain carriers accordingly:



This two-part overall mechanism indicates that there are two transition states and, consequently, a two-term rate law. The rate expression obtained with the methods used above is

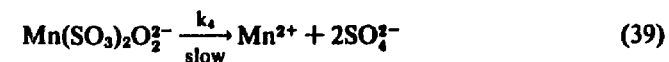
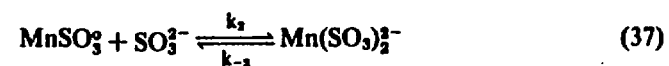
$$d[SO_3^{2-}]/dt = 2k_9(k_1/2k_{12})^{0.5}[M^{x+}L_3^{n-}]^{0.5}[O_2]^{0.5}[SO_3^{2-}] + 2k_4(k_1/2k_4)^{0.5}[M^{x+}L_3^{n-}]^{0.5}[SO_3^{2-}]^{1.5} \quad (35)$$

In this case, pH dependencies in terms of the acid base chemistry of $SO_2(aq)$ have been ignored. A complete analysis valid over broad pH ranges requires consideration of the roles of $SO_2 \cdot H_2O$, HSO_3^- , $SO_2 \cdot H_2O^+$ and $HSO_3\cdot$ as reactive species. Larson et al. [29] used a hybrid mechanism involving two distinct chain propagation sequences with superimposed acid-base equilibria to obtain a rate expression that agreed moderately well with their empirical rate law.

b. Polar Mechanisms Involving Inner Sphere Complexation

Nonradical, polar mechanisms for metal-catalyzed autoxidation of $SO_2(aq)$ have been proposed [25,40,55,56,69]. The common features of the mechanisms include inner-sphere complexation of the catalytic metal by sulfite as a prelude to electron transfer, subsequent binding of dioxygen by the resulting metal-sulfite complex, and finally electron transfer via successive two-electron transfers as opposed to a series of one-electron transfer, chain propagation steps.

Catalytic Effect of Mn^{2+} . Bassett and Parker [69] found that Mn^{2+} salts had a pronounced catalytic effect on the rate of sulfite autoxidation with almost complete suppression of dithionate formation; that the nature of the Mn^{2+} counterion (i.e., SO_4^{2-} or Cl^-) strongly influenced the reaction rate due to competitive complexation; and that a similar catalytic sequence was observed for $Co(II)$ and $Ni(II)$ salts. Based on these observations they proposed the following polar mechanism:



A theoretical rate expression can be derived from this sequence of elementary reactions using the vector method of King and Altman [70]. In this procedure the mechanism is written in a cyclic form that represents the closed nature of the catalytic cycle for the overall reaction. The number of intermediate complexes is readily identified and the concentration of each form of the catalyst can be shown to be proportional to the sums of the terms that are obtained from the

elementary reaction steps which individually or in sequence lead to the specific form of the catalyst. The number of rate constants (or products of individual rate constants and concentrations of species in excess) must be one less than the number of species in a particular cycle. The steady-state approximation is applied to the resultant equations for each reactive intermediate and the final rate expression is obtained by substitution into a designated rate-limiting step. Using this procedure, the following rate expression is obtained:

$$v = -\frac{d[\text{SO}_3^{2-}]}{dt} = \frac{k_4[\text{Mn}^{2+}]_0[\text{SO}_3^{2-}]^2[\text{O}_2]}{K_A + K_B[\text{O}_2] + K_C[\text{SO}_3^{2-}] + K_D[\text{SO}_3^{2-}][\text{O}_2] + K_E[\text{SO}_3^{2-}]^2 + [\text{SO}_3^{2-}]^2[\text{O}_2]} \quad (40)$$

where $K_A = K_1^{-1}K_2^{-1}(K_3^{-1} + k_4/k_3)$
 $K_B = K_1^{-1}k_4/k_2$
 $K_C = K_2^{-1}(K_3^{-1} + k_4/k_3)$
 $K_D = k_4/k_2 + k_4/k_1$
 $K_E = K_3^{-1} + k_4/k_3$
 $[\text{Mn}^{2+}]_0 = \text{initial manganese concentration}$
 $K_1, K_2, K_3 = \text{equilibrium constants for reactions 1, 2 and 3, respectively}$

III-7 This cumbersome expression can be simplified for certain limiting cases if assumptions are made about the magnitude of individual terms, as shown in Table V. It

Table V. Rate Expressions for Limiting Cases of the Bassett and Parker [69] Mechanism*

$$v = -\frac{d[\text{SO}_3^{2-}]}{dt} = \frac{k_4[\text{Mn}^{2+}]_0[\text{SO}_3^{2-}]^2[\text{O}_2]}{K_A + K_B[\text{O}_2] + K_C[\text{SO}_3^{2-}] + K_D[\text{SO}_3^{2-}][\text{O}_2] + K_E[\text{SO}_3^{2-}]^2 + [\text{SO}_3^{2-}]^2[\text{O}_2]}$$

Dominant Term in Denominator	α	β	γ
A	1	2	1
B	1	2	0
C	1	1	1
D	1	1	0
E	1	0	1
$[\text{SO}_3^{2-}]^2[\text{O}_2]$	1	0	0

* $\alpha, \beta,$ and γ represent the reaction orders for the reaction rate given by the generalized rate expression $= d[\text{SO}_3^{2-}]/dt = k[\text{Mn}^{2+}]^\alpha[\text{SO}_3^{2-}]^\beta[\text{O}_2]^\gamma$.

should be emphasized, however, that these limiting cases are idealizations and that intermediate cases generally would be expected.

From laboratory studies of S(IV) oxidation in aqueous aerosols, Matteson et al. [55] reported that the following rate law was adequate to account for their environmental observations under certain conditions:

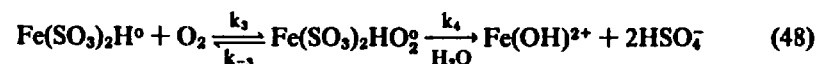
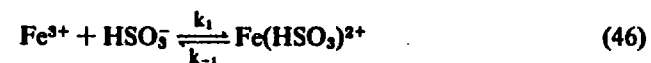
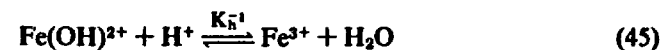
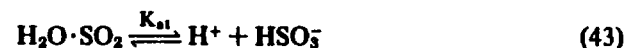
$$v_0 \equiv -\left(\frac{d[\text{H}_2\text{O}\cdot\text{SO}_2]}{dt}\right)_0 = \frac{k[\text{Mn}^{2+}]_0[\text{H}_2\text{O}\cdot\text{SO}_2]_0}{k_1[\text{H}_2\text{O}\cdot\text{SO}_2]_0 + k'[\text{Mn}^{2+}]_0 + K} \quad (41)$$

Here the concentration of S(IV) is expressed as $[\text{H}_2\text{O}\cdot\text{SO}_2]$ to reflect the condition of high acidity employed in the study. Equation 41 can be reduced to

$$v_0 = k''[\text{Mn}^{2+}]_0[\text{SO}_2]_0 \quad (42)$$

for the initial rate when $K \gg k_1[\text{H}_2\text{O}\cdot\text{SO}_2]_0 + k'[\text{Mn}^{2+}]_0$. Indication of such behavior based on aerosol conversion experiments has been observed [22,28]. Similar kinetic behavior has been reported by Ibusuki [54] and in Chapter 2 for low concentrations of S(IV). These results have been summarized in Table VI.

Complexation by Fe(III). Freiberg [71] has proposed a polar catalytic cycle involving inner-sphere complexation of sulfite by Fe(III) as a prelude to electron transfer. His hypothetical mechanism, which was postulated in an effort to obtain an empirical rate law consistent with the experimental data of other investigators (Table VII) is as follows:



Equation 49 represents direct oxidation of S(IV) by 2Fe(III) to produce S(VI).

Table VI. Empirical Rate Laws for Mn²⁺-Catalyzed Autoxidation of S(IV) in Aqueous Solution

Rate ($v = -d[S(IV)]/dt$)	Rate Constant	Conditions	Reference
$v = k[Mn^{2+}][S(IV)][H^+]^{-1}$	$k = 25 s^{-1}$	pH 0-0.2 [S(IV)] < 10 ⁻⁴ M T = 25.0 C	Chapter 2
$v = k[Mn^{2+}][HSO_5^-]$	$k = 5 \times 10^3 M^{-1} \cdot s^{-1}$	pH 3-7.5 T = 25 C	54
$v = k[Mn^{2+}]^2[H^+]^{-1}$	$k = 4.7 s^{-1}$	pH 0-2 [S(IV)] < 10 ⁻⁴ M T = 25 C	Chapter 2
$v = \frac{k_2 k_1 [Mn^{2+}][SO_{2(aq)}]}{k_1 [SO_{2(aq)}] + k_1 k' [Mn^{2+}] + k_2 + k_3}$	$k_1 = 2.4 \times 10^5 \text{ mmol}^{-1} \cdot \text{min}^{-1} \cdot \text{cm}^{-3}$ $k' = n \cdot \text{cm}^3 \cdot \text{m}^{-3}$ $k_2 = 0.22 \text{ min}^{-1}$ $k_3 = 10 \text{ min}^{-1}$	pH < 2 droplet study n = aerosol volume	55
$v_o = \frac{[Mn^{2+}]_o^2 [SO_2]_o^{2.2}}{k_1 [Mn^{2+}]_o^2 + k_2 [SO_2]_o^{2.2}}$	$k_1 = 1.32 \times 10^{-3} M^{-1} \cdot s^{-1}$ $k_2 = 3.2 \times 10^{-4} M^{-1} \cdot s^{-1}$	[Mn ²⁺] _o = 1-100 μM [SO ₂] ~ 10 μM	72
$v = k[Mn^{2+}]^{1.7-2}$	$k \approx 5 - 8 \times 10^2 M^{-1} \cdot s^{-1}$	T = 35 C pH 2.4-3.3	73
$v = k[Mn^{2+}][H^+]^{-1}$	$k = 8 \times 10^{-4} M \cdot \text{min}^{-1}$	T = 10 C pH 1.4-2.0 [S(IV)] = 6 × 10 ⁻⁴ M	74
$v = k_1 [Mn^{2+}]^2 [H^+]^{-1} + k_2 [Fe^{3+}][S(IV)][H^+]^{-1} \times \left(1 + \frac{1.7 \times 10^3 [Mn^{2+}]^{1.5}}{6.31 \times 10^{-6} + [Fe(III)]} \right)$	$k_1 = 4.7 s^{-1}$ $k_2 = 0.82 s^{-1}$ Synergistic term	T = 25 C pH 0-3 [S(IV)] > 10 ⁻⁴ M [Mn ²⁺] = 10 ⁻⁴ M [Fe ³⁺] > 1 μM	Chapter 2

Table VII. Empirical Rate Laws for Fe³⁺ Catalyzed Autoxidation of S(IV) in Aqueous Solution

Rate ($v = -d[S(IV)]/dt$)	Rate Constant	Conditions	Reference
$v = k[Fe(III)][S(IV)][H^+]^{-1}$	$k = 0.82 s^{-1}$	pH 0-3 [S(IV)] > 10 ⁻⁴ M	Chapter 2
$v = k[Fe(III)][S(IV)]$	$k = 100 M^{-1} \cdot s^{-1}$	pH 4-8 [Fe(III)] ~ 1 μM [S(IV)] ~ 1 mM	37
$v = k[Fe(III)][S(IV)] (v = f([H^+]) = [H^+]^{-1})$	$k = 8 \times 10^2 M^{-1} \cdot s^{-1}$ (pH 4) $k = 80 M^{-1} \cdot s^{-1}$ (pH 3)	pH ≤ 4 T = 20 C SO ₂ electrode	26
$v = k[Fe(III)][S(IV)]^2$		pH ≥ 5 T = 20 C SO ₂ electrode	26
$v = k[Fe(III)][S(IV)]^2[H^+]^{-1}$	$k = 40 M^{-1} \cdot s^{-1}$	pH 1.5-3 T = 10 C [Fe(III)] > 10 ⁻⁴ M [S(IV)] > 10 ⁻⁴ M	74
$v = k_1 [Fe^{3+}][H^+]^{-1} \times (1 - k_2 [Fe^{2+}]/2k_3 [O_2])$	No constants reported	Derived from postulated mechanism [Fe(III)] >> [S(IV)] pH ~ 0.6	75
$v = \frac{k_1 [Fe(III)]^2 [SO_3^{2-}]^2}{[Fe(III)][SO_3^{2-}]_o + k_2 [SO_3^{2-}] + k_3 [Fe(III)][SO_3^{2-}]}$	$k_1 = 3.6 \times 10^6 M \cdot s^{-1}$ $k_2 = 2.5 \times 10^{-7} M \cdot s^{-1}$ $k_3 = 4.5 \times 10^5 M \cdot s^{-1}$	T = 10 C μ = 1.2 M pH 1.3-3.3 [Fe(III)] < 10 ⁻³ M [S(IV)] < 10 ⁻³ M	57

Freiberg [71] assumed that Equation 47, the formation of an iron-sulfito complex of 1:2 stoichiometry, was rate-limiting in the catalytic sequence of Equations 43–48. With this assumption, and use of the steady-state hypothesis, Freiberg [71] derived the following overall rate expression:

$$\frac{d[\text{SO}_4^{2-}]}{dt} = \frac{k_1 k_2 (2k_3 k_4 [\text{O}_2] + k_5 [\text{Fe}^{3+}]) [\text{HSO}_3^-] [\text{Fe}^{3+}] [\text{SO}_3^{2-}]}{k_{-1} (k_{-2} + k_3 [\text{O}_2] + k_5 [\text{Fe}^{3+}])} \quad (50)$$

Since

$$[\text{SO}_3^{2-}] = K_{a2} [\text{HSO}_3^-] / [\text{H}^+] = K_{a1} K_{a2} [\text{SO}_2(\text{aq})] / [\text{H}^+]^2 \quad (51)$$

Equation 50 was then expressed as

$$\frac{d[\text{SO}_4^{2-}]}{dt} = \frac{K_T K_{a1}^2 [\text{Fe}^{3+}] [\text{SO}_2(\text{aq})]^2}{[\text{H}^+]^2} \quad (52)$$

where

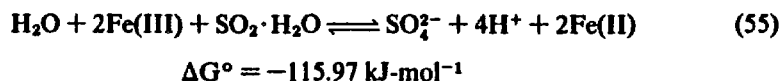
$$K_T = \frac{k_1 k_2 K_{a2} (2k_3 k_4 [\text{O}_2] / k_5 + [\text{Fe}^{3+}])}{k_{-1} [(k_{-2} + k_3 [\text{O}_2]) / k_4] + [\text{Fe}^{3+}]} \quad (53)$$

Equation 50 can be recast in terms of $[\text{SO}_3^{2-}]$ as follows:

$$\frac{d[\text{SO}_4^{2-}]}{dt} = k' [\text{Fe}^{3+}] [\text{SO}_3^{2-}]^2 [\text{H}^+] \quad (54)$$

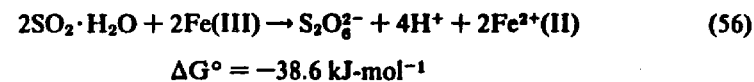
where $k' = K_T / K_{a2}^2$

Since the rate-limiting step (Equation 47) presumably involves the slow substitution of a second SO_3^{2-} to the coordination sphere of $\text{Fe}(\text{H}_2\text{O})_5\text{HSO}_3^{2+}$, there should be no observed kinetic dependence on $[\text{O}_2]$. In addition to a sequence of two-electron transfers involving oxygen as the oxidant, oxidation of S(IV) directly by Fe^{3+} via successive one-electron transfers is predicted thermodynamically (Equation 49) in acidic solution:

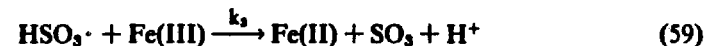
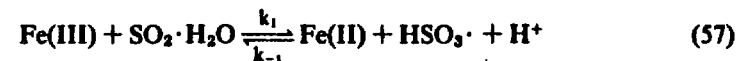


However, due to the extremely slow rate of oxidation of Fe(II) to Fe(III) at low pH [48] a loss of apparent catalytic activity would be predicted if Equation 49 were a predominant pathway in the Fe(III)/ O_2 /SO₂ system, unless Fe(II) also exhibits catalytic activity in a fashion similar to Mn(II), Co(II), Ni(II) and Cu(II).

In addition to direct oxidation of S(IV) by Fe(III) to produce SO_4^{2-} [S(VI)], dithionate $\text{S}_2\text{O}_6^{2-}$ [S(V)] can be produced according to the following stoichiometry:

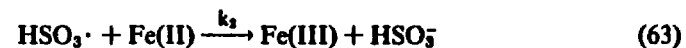


The kinetics of this reaction have been studied by Pollard et al. [76]; they have proposed the following mechanism:



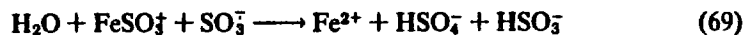
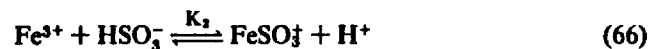
where $k_1 = 2.7 \times 10^{-4} \text{ M}^{-1} \text{ s}^{-1}$

Likewise, Karraker studied direct oxidation of S(IV) by Fe(III) under the conditions of $[\text{Fe}(\text{III})]_0 > [\text{S}(\text{IV})]_0$ and proposed the following mechanism involving initial complexation of Fe(III) by HSO_3^- :



where k_1 and k_2/k_3 were estimated from kinetic data to be 7 min^{-1} and 22, respectively. Further evidence for the formation of discrete iron-sulfito complexes as a prelude to electron transfer has been cited [57,77–80]. Additional work by Carlyle and Zeck [81] suggests that the following noncatalytic mechanism provides a pathway for direct oxidation of S(IV):



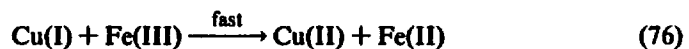
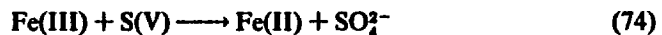
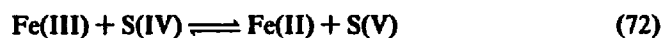


where

$$\frac{-d[\text{S(IV)}]}{dt} = 2k'[\text{Fe(III)}]^2 \quad (70)$$

$$k' = 1.7 \times 10^{-6}[\text{HSO}_3^-]/[\text{H}^+][\text{Fe}^{2+}] + (5.7 \times 10^{-5}[\text{HSO}_3^-]^2/[\text{H}^+][\text{Fe}^{2+}] \times (1/0.19 + [\text{SO}_2])) \quad (71)$$

Catalysis By Cu(II). Direct oxidation of S(IV) by Fe(III) is sensitive to catalysis by Cu(II) [76,81,82]. In general, the catalytic cycle would proceed accordingly:



Equations 72–76 may constitute an important alternative catalytic cycle for oxidation of S(IV) to S(VI). As shown in Table I, fog and cloud water droplets have significant levels of Fe and Cu. At these levels, Cu(II) catalysis of the Fe(III)–S(IV) reaction may contribute to the overall conversion of SO₂ in the droplet phase. According to Carlyle and Zeck [81], the catalytic rate of oxidation of S(IV) is given by:

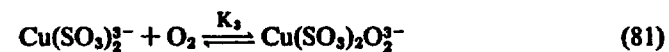
$$\frac{-d[\text{S(IV)}]}{dt} = 2k''[\text{Fe(III)}] \quad (77)$$

where

$$k'' = [\text{Cu}^{2+}][\text{HSO}_3^-][\text{H}^+] \times 1/(14.1[\text{Fe}^{2+}] + 2.2[\text{Cu}^{2+}] + 0.8[\text{Cu}^{2+}]^2/[\text{H}^+]) \quad (78)$$

The reaction sequence of Equations 72–76 is an example of a redox reaction that is accelerated by a catalyst that exists in more than one oxidation state. Catalysis in this case is due to the fact that Equations 75 and 76, which involve the Cu(II)/Cu(I) couple, are fast relative to Equations 72 and 74. The net result is the apparent catalysis of the overall reaction given in Equation 55.

In the case of catalysis by Cu⁺, Lunak et al. [56] proposed that autoxidation of S(IV) proceeds via a two-electron polar pathway as follows:



where $K_1 = 10^{7.85}$
 $K_2 = 10^{7.08}$

The rate law (Table VIII) that results from this mechanism is identical in form to that presented in Equation 40 for catalysis by Mn²⁺.

In the scheme proposed by Lunak et al. [56], Cu²⁺ is reduced rapidly to Cu⁺ by SO₃²⁻; Cu⁺ then acts as the active catalytic center when complexed by excess S(IV) in solution. These investigators established a relative order of catalytic activity as follows:



Unfortunately, Lunak et al. [56] failed to report the pH at which these studies were performed.

The mechanistic interpretation of Lunak et al. [56] is in direct opposition with the kinetic observations and mechanisms proposed by other investigators [46,65,66]. These investigators favor the free radical pathway of Equations 2–8 in which the Cu²⁺/Cu⁺ redox couple acts as an one-electron acceptor



However, using the estimated value of E° (–0.89 V) for the SO₃²⁻/SO₃⁻ redox couple and the E° (0.15 V) for the Cu(II)/Cu(I) couple, it can be shown that Equation 84 is thermodynamically unfavorable, since E_H° for this reaction is –0.74 V (ΔG° = 71 kJ·mol⁻¹) [85]. This fact tends to support the hypothesis that the Cu(II)-catalyzed reaction proceeds via the formation of copper-sulfito complexes,

Table VIII. Empirical Rate Laws for Cu²⁺-Catalyzed Autoxidation of S(IV) in Aqueous Solution

Rate ($\nu = -d[S(IV)]/dt$)	Rate Constant	Conditions	Reference
$\nu = (k_1 + k_2[Cu^{2+}])[SO_3^{2-}]$	$k_1 = 1.3 \times 10^{-2} s^{-1}$ $k_2 = 2.5 \times 10^6 M^{-1} s^{-1}$	pH ₀ = 8.7 [Cu ²⁺] ₀ > 10 ⁻⁹ M Cu(OH) ₂ (s) T = 25 C	65
$\nu = 0.5 k_1[Cu^{2+}]^{1/2}[SO_3^{2-}]^{3/2}$	$k_1 = 1.2 \times 10^3 M^{-1} s^{-1}$	pH 7-9 E _a = 76 kJ·mol ⁻¹ T = 25 C	66
$\nu = 0.5 k_1[Cu^{2+}]^{1/2}[SO_3^{2-}]^{3/2}$		pH 8.5 E _a = 78.2 kJ·mol ⁻¹ T = 25 C [Cu ²⁺] = 1 μM	46
$\nu = k[Cu^{2+}][SO_3^{2-}]/[INHIB]$	$k = 7.3 \times 10^4 M^{-1} s^{-1}$	INHIB = 2-propanal T = 20 C [Cu ²⁺] = 10 μM pH 8.5	56
$\nu = k[Cu^{2+}][SO_3^{2-}]$	$k = 2.3 M^{-1} s^{-1}$ (pH > 12)	pH 4-12 T = 25 C 1-10 M (NH ₄ OH)	83
$\nu = k[Cu^{2+}][SO_3^{2-}]$			84

Table IX. Empirical Rate Laws for Co(III)/Co(II)-Catalyzed Autoxidation of S(IV)

Rate ($\nu = -d[S(IV)]/dt$)	Rate Constant	Conditions	Reference
$\nu = k[Co(II)][SO_3^{2-}][O_2]$	$k = 1.5 \times 10^7 M^{-2} s^{-1}$	T = 20 C pH 8-9.2 [Co(II)] ≤ 0.1 μM [S(IV)] ≤ 0.01 M	61
$\nu = \frac{k_1[Co^{2+}]_0[SO_3^{2-}][O_2]}{1 + k_2[SO_3^{2-}]}$	$k_1 = 1.96 \times 10^9 M^{-2} s^{-1}$ $k_2 = 4.74 \times 10^2 s^{-1}$	T = 20 C pH 8-8.3	86
$\nu = k[Co(H_2O)_6^{3+}]^{1/2}[SO_3^{2-}]^{3/2}$	No constant reported	E _a = 73.15 kJ·mol ⁻¹ pH 9-9.7	58
$\nu = k[Co^{2+}]^{1/2}[SO_3^{2-}]^{3/2}[H^+]^{-1}$	$k \sim 1 \times 10^{-3} s^{-1}$ $k[H^+]^{-1} = 10^3-10^4 M^{-1} s^{-1}$	T = 30-60 C pH 6-7.5 [Co ²⁺] ₀ < 3 μM [S(IV)] ₀ < 1 mM	60
$\nu = k[Co(II)L_4O_2][SO_3^{2-}]$	$k = 1.3 \times 10^1 M^{-1} s^{-1}$	T = 22 C E _a = 112.4 kJ·mol ⁻¹	87
$\nu = k_1[(Co(II)L_4)_2O_2][S(IV)][H^+]^{-1}$	$k_1 = 6.2 \times 10^4 M^{-1} s^{-1}$	T = 25 C μ = 0.5 M pH 0.5-1.3	62

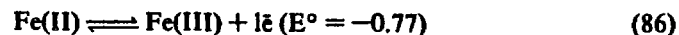
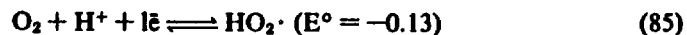


$$E^\circ = -0.9$$

$$\Delta G^\circ = 86.7 \text{ kJ}\cdot\text{mol}^{-1}$$

which react subsequently with oxygen as suggested originally by Titoff [83] and confirmed later by the results of Reinder and Vles [82].

Metal Ion Redox Couples. Metal ion redox couples that would be suitable for 1 e⁻ oxidation of S(IV) to S(V) (i.e., Equation 2) and for initiation of a chain reaction (Equations 2-8), are Co(III)/Co(II) (Table IX), Mn(III)/Mn(II) and V(V)/V(IV) with E° values of 1.82, 1.5 and 1.0 V, respectively [85]. The Fe(III)/Fe(II) couple with an E° of 0.77 V would be insufficient for one-electron production of SO₃⁻. Likewise, initiation of a chain reaction by Equation 24, involving a first-row transition metal redox couple, will be thermodynamically unfavorable as shown below. For example, two appropriate half-reactions:



can be combined to give an initiation step as envisioned by Schmittkuz [68]:

However, from ΔG° it is evident that this is an unfavorable process. Similarly, the other one-electron couples involving the soluble metal ions of Co, Mn, Cu and V are unfavorable for the above free radical initiation step.

c. Catalysis by Specific Metal-Ligand Complexes

Hoffmann and Boyce [40] have studied kinetics and mechanisms of autoxidation of dissolved sulfur dioxide over the pH range of 4.5-11.0 in the presence of Co(II), Fe(II), Mn(II), Cu(II), Ni(II) and V(IV)-4,4',4'',4'''-tetrasulfophthalocyanine complexes. Phthalocyanine ligands are macrocyclic tetrapyrrole compounds similar in structure to porphyrins that readily form square planar complexes in which the metal atoms are located in the plane of the phthalocyanine ring. Certain metal-phthalocyanine complexes, such as cobalt tetrasulfophthalocyanine [Co(II)-TSP] are known to actively bind dioxygen and to serve as reversible oxygen carriers [88,89]. Because of their relationship to naturally occurring organic macromole-

cules, coupled with their high stability, catalytic specificity and oxidase-like activity, metal-phthalocyanine complexes have been shown to be suitable models for studying the catalytic effects of trace metals in aqueous systems [90].

The rate law reported by Hoffmann and Boyce [40] for Co(II)-TSP at pH 6.7 was:

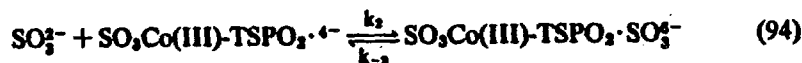
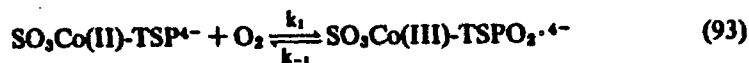
$$-d[S(IV)]/dt = k'[Co(II)-TSP]^{1/2}[S(IV)] \quad (89)$$

and at pH 9.4:

$$-d[S(IV)]/dt = k''[Co(II)-TSP][S(IV)] \quad (90)$$

where $k' = 1.62 M^{-1/2} \cdot s^{-1}$
 $k'' = 1.83 \times 10^3 M^{-1} \cdot s^{-1}$

Based on additional experimental observations and kinetic data reported by Boyce et al. [91], a two-electron transfer, bisubstrate complexation pathway was postulated. The mechanism, which can be classified as an ordered ternary-complex mechanism in the terminology of Laidler and Bunting [92], is as follows:



This general reaction scheme is depicted graphically in Figure 1.

Equation 92 represents the formation of the reactive monomeric catalytic center, $SO_3Co(II)-TSP^{4-}$, from the dominant dimeric form of the catalyst in solution. This sequence of events is consistent with observed spectral changes that

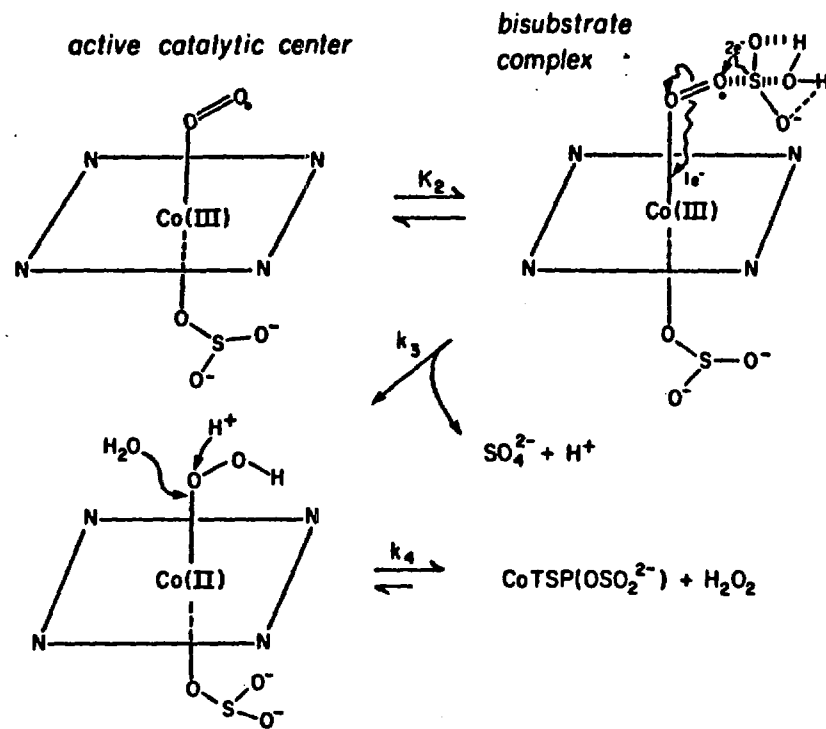


Figure 1. Schematic representation of the proposed catalytic reaction mechanism starting with the Co(II)-TSP sulfite complex as the active catalytic center. Reaction proceeds via the formation of a ternary dioxygen adduct and results in the formation of hydrogen peroxide as an intermediate reduction product of oxygen.

indicate a shift in the dimer-monomer equilibrium (Equation 91) on complexation of the added substrate in an axial coordination position on Co(II) either above or below the plane of the phthalocyanine complex. Complexation of Co(II)-TSP by SO_3^{2-} in an axial coordination site enhances the subsequent complexation of dioxygen as written in Equation 93. Carter et al. [93] studied reversible binding of dioxygen by Co(II) complexes of the general form, $Co(II)-(L)B$, where L is a quadridentate planar ligand and B is an axial ligand, and they concluded that as the π -electron donating ability of B increased the electron density on the cobalt atom would be enhanced; this in turn results in a greater π -bonding electron flow from cobalt to oxygen. Rollman and Chan [94] reported that the imidazole complex of Co(II)-TSP rapidly complexed O_2 , whereas the pyridine complex did not. Similar enhancements of the binding of dioxygen by Co(II)-TSP when complexed by an appropriate axial ligand have been reported [90,95,96]. In addition, studies of the catalytic properties of heme have shown that an axial ligand trans to dioxygen affects both the formation constant and the reversibility of oxygen transfer [89,97].

Electron spin resonance (ESR) studies [94,95] on Co(II)-TSP/O₂ complexes have been shown to be consistent with the formulation of the complex as Co(III)-TSPO₂. The intermediate complex given in Equation 93 is considered to be a mixed-ligand Co(III) complex with a superoxide ion (O₂⁻) and a sulfite ion bound *trans* to one another in axial coordination positions. In the proposed mechanism, the O₂ adduct reacts with an additional SO₃²⁻ ion to form a ternary complex as indicated in Equation 94. This complex, in turn, undergoes a rate-limiting two-electron transfer from the second bound sulfite to the coordinated dioxygen-Co(II) system to form a SO₃ bound to a Co(II)-peroxide complex. The attached SO₃ hydrolyzes rapidly to give a coordinated H₂SO₄, which readily dissociates from the complex. After protonation, the coordinated O₂⁻ is released as H₂O₂. This intermediate H₂O₂ reacts with another molecule of SO₃²⁻ to form SO₄²⁻ via an additional two-electron transfer in the final step. Hydrogen peroxide was identified positively as a reaction intermediate in this system using three different analytical procedures [98-100].

Schutten and Beelen [98] have observed directly the formation and accumulation of H₂O₂ as an intermediate reduction product of O₂ in Co(II)-TSP-catalyzed autoxidation of 2-mercaptoethanol in water. Davies et al. [62] have reported, on the basis of ¹⁸O tracer experiments, that approximately half of the oxygen transferred to sulfite comes from a superoxo-complex, (NH₃)₅Co(III)-O₂-Co(II)NH₃⁵⁺. The other half presumably comes from water. A compatible conclusion as to the origin of oxygen in the oxidized sulfite was reported by Holt et al. [101], who have shown conclusively that the ¹⁸O content of the product sulfate for metal-catalyzed autoxidations of SO₃²⁻ was linearly related to the ¹⁸O content of water, and that at least three of the four oxygen atoms in the sulfate products were isotopically controlled by the solvent water (the remaining atom of oxygen coming from O₂). Finally, Yatsimirskii et al. [87] found strong evidence for complexation of sulfite by the Co(II)-dioxygen complex, Co₂(L-histidine)O₂, as a prelude to electron transfer from S(IV) to O₂. In total, these results are consistent with the mechanism postulated in Equations 91-97.

The theoretical rate expression, that results from the above mechanism, was obtained by standard procedures [92]; it has the form:

$$v = \frac{-d[S(IV)]}{dt} = \frac{k' [SO_3Co(II)-TSP^{4-}]_T [SO_3^{2-}] [O_2]}{K_A + K_B [O_2] + K_C [SO_3^{2-}] + [O_2] [SO_3^{2-}]} \quad (98)$$

where

$$k' = (k_3 k_4) / (k_3 + k_4)$$

$$K_A = [k_4 (k_{-1} k_2 + k_{-1} k_3)] / [k_1 k_2 (k_3 + k_4)]$$

$$K_B = [k_4 (k_{-2} + k_3)] / [k_2 (k_3 + k_4)]$$

$$K_C = (k_3 k_4) / [k_1 (k_3 + k_4)]$$

When the monomer-dimer equilibrium of Equation 91 is considered, Equation 98 can be rewritten as:

$$v = \frac{k' K' [(Co(II)-TSP)_2]^{1/2} [SO_3^{2-}] [O_2]}{K_A + K_B [O_2] + K_C [SO_3^{2-}] + [O_2] [SO_3^{2-}]} \quad (99)$$

where $K' = \beta K_d^{1/2} [SO_3^{2-}]$ when $[SO_3^{2-}]_0 \gg [(Co(II)-TSP)_2]_0$.

Equation 99 can be simplified for the experimental conditions $[O_2] \gg [SO_3^{2-}]$ such that $K_B [O_2] \gg K_A, K_C [SO_3^{2-}]$

$$v \approx \frac{k' K' [(Co(II)-TSP)_2]^{1/2} [SO_3^{2-}]}{K_B + [SO_3^{2-}]} \quad (100)$$

Two extremes can be considered for Equation 100. If $K_B \gg [SO_3^{2-}]$,

$$v \approx k' \beta K_d^{1/2} [(Co(II)-TSP)_2]^{1/2} [SO_3^{2-}] K_B^{-1} \quad (101)$$

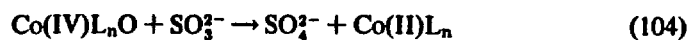
and if $[SO_3^{2-}] \gg K_B$,

$$v \approx k' \beta K_d^{1/2} [(Co(II)-TSP)_2]^{1/2} [SO_3^{2-}] \quad (102)$$

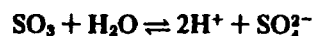
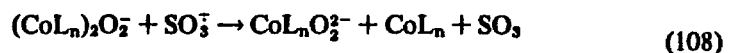
The theoretical rate expressions for the limiting cases given in Equations 101 and 102 can be compared with the experimentally observed rate laws for pH 6.7 (Equation 89) and pH 9.4 (Equation 90). At pH 6.7 a half-order dependence on the catalyst concentration is observed, whereas Equation 101 predicts a half-order dependence on the dimeric form of Co(II)-TSP. Since, at pH 6.7, the dimer is the dominant catalyst species in solution, a half-order dependence on total added catalyst is consistent with the assumption that the monomer is actually the active form. Nonintegral reaction orders arise frequently in polar reactions when the principal reactive species is derived from the dissociation of a dimer [102]. At pH 9.4, a first-order dependence on the catalyst concentration is observed. This result is consistent with the kinetic formulation above if the dimeric form of the catalyst is no longer the dominant species. Cookson et al. [95] see evidence for a shift in the monomer-dimer equilibrium toward the monomer with an increase in pH. If this is the situation, the prior equilibrium can be neglected. Consequently, the theoretical rate expression would show a first-order dependence in catalysts as indicated in Equation 98.

Davies et al. [62] and Yatsimirskii et al. [87] have studied the oxidation of S(IV) by the μ -superoxo dimers, (NH₃)₅Co(III)O₂Co(II)(NH₃)₅⁵⁺ and (L-histidine)₂Co(III)O₂Co(II)(L-histidine)₂. Two mechanisms are possible for these systems. In these mechanisms the μ -superoxo complex, which can be symbolically written as (CoL_n)₂O₂, is the active catalytic center and it reacts either via a two-electron transfer sequence:

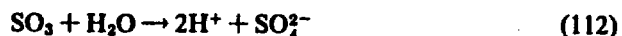
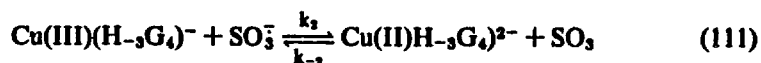
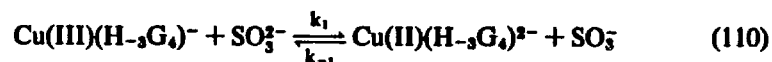




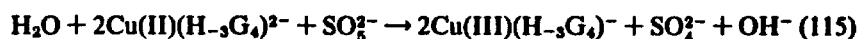
or via a one-electron transfer sequence:



Anast and Margerum [103] have reported that copper(III)-tetraglycine reacts rapidly with sulfite in two reversible one electron steps to give copper(II)-tetraglycine and aquated SO_3 , which hydrolyzes to sulfate as follows:



In the presence of oxygen, Anast and Margerum [113] have proposed that the sulfite radical anion reacts with oxygen to give the peroxymonosulfite radical, SO_3^- , which in turn oxidizes the Cu(II) back to Cu(III)



This mechanism is an example of an induced catalytic reaction in which the Cu(III)/Cu(II)-tetraglycine couple catalyzes the autoxidation of sulfite to sulfate, which can be described by the simple overall stoichiometry of:



Values for k_1 , k_2/k_{-1} and k_{-2}/k_3 were reported to be $3.7 \times 10^4 \text{ M}^{-1}\text{s}^{-1}$, 1.66 and 177 M^{-1} , respectively. In this reaction system, the oxidation of SO_3^{2-} by O_2 promotes an induced oxidation of Cu(II) to Cu(III) via an autocatalytic process in which there is a net gain in $\text{Cu(III)(H}_-3\text{G}_4)^-$ when $\text{Cu(II)(H}_-3\text{G}_4)^{2-}$, O_2 and SO_3^{2-} are present initially.

An induced oxidation mechanism of this type represents a conceptual alternative to a free radical chain sequence (Equations 2-8), even though SO_3^- and $\text{SO}_3^{\cdot-}$ are postulated as reactive intermediates. Induced reactions occur when a relatively fast reaction between two substances ($\text{A} + \text{B} \rightarrow \text{P}$) forces an otherwise slow reaction ($\text{A} + \text{C} \rightarrow \text{P}'$) [103]. According to Edwards [104], the phenomenon of induced reactions provides a method for identifying unstable intermediates in reaction mechanisms; in this particular case, the unstable intermediate would be SO_3^- . Although similar to the free radical scheme of Equations 2-8, the above mechanism involves the regeneration of the initiator, Cu(III), whereas the Bäckström scheme does not.

d. Synergistic Catalysis

Barrie and Georgii [39] and Chapter 2 reported that an apparent synergism exists between Fe^{3+} and Mn^{2+} in the catalytic autoxidation of S(IV). Barrie and Georgii [39] noted that the addition of either Fe^{3+} or Fe^{2+} to an equimolar solution of Mn^{2+} in the presence of S(IV) and oxygen resulted in nonlinear increase in the absorption rate of SO_2 . The net effect of adding iron was to increase the reaction rate tenfold. Chapter 2 examines this apparent synergism in greater detail, and finds that the mixed catalyst system exhibited an overall oxidation rate that was greater than the linear sum of the individual metal-catalyzed rates. This effect was quantitatively described in Chapter 2 with the following multiterm rate law obtained by an empirical force-fit of experimental data:

$$\frac{-d[\text{S(IV)}]}{dt} = k[\text{Mn}^{2+}]^2[\text{H}^+]^{-1} + k'[\text{Fe(III)}][\text{S(IV)}][\text{H}^+]^{-1} + k''[\text{Fe(III)}][\text{Mn}^{2+}][\text{S(IV)}][\text{H}^+]^{-1}/(K + [\text{Fe(III)}]) \quad (117)$$

Existence of a multiple-term rate law indicates that two or more transition states of different composition are involved in parallel in the overall reaction [102,105,106]. Furthermore, each term in the rate law gives the empirical composition and electric charge of the transition state for the rate-determining step for that particular parallel pathway (with the exception of chain mechanisms) [105,106].

With these fundamental rules of kinetics as guidelines, mechanisms for each term in the above rate can be proposed. Neither Chapter 2 nor Barrie and Georgii [39] proposed a hypothetical mechanism for the Fe-Mn synergism; therefore, mechanisms are suggested here for each term.

At the concentration levels used in Chapter 2, catalysis by Mn^{2+} alone exhibits a simple second-order rate law in $[\text{Mn}^{2+}]$ with zero-order dependencies on $[\text{S(IV)}]$

and [O₂] as indicated in Equation 117. A mechanism consistent with the above term would be:



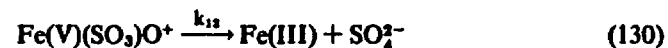
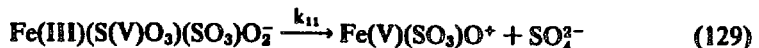
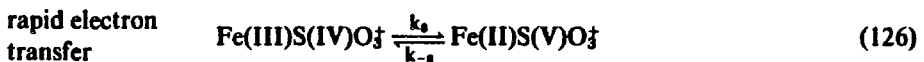
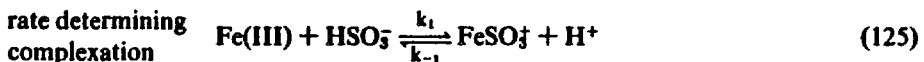
where $k_1/k_{-1} = K_H^* (= 10^{-10.24}$ at $\mu = 0.5 M$ and $T = 25 C$) [107]
 $k_2/k_{-2} = 10^4$ (at $\mu = 0.5 M$ and $T = 25 C$) [107]

With the assumption that Equation 119 constitutes the rate-limiting step in the mechanism and that $k_2 > k_{-2}$, the following rate expression can be derived:

$$\nu_1 = \frac{-d[S(IV)]}{dt} = k_2 K_1 [Mn^{2+}]^2 [H^+]^{-1} \quad (124)$$

This rate expression agrees well with the first term of the empirical rate law.

For the second term of the rate law, the following mechanism can be postulated:



In this mechanism, the first step, which involves the slow complexation of Fe³⁺ by HSO₃⁻ is rate determining; consequently, the theoretical rate expression that results is as follows if it is assumed that [H⁺] ≈ K_{a1} (i.e., ~ pH 2) and k₇ >> k₋₇:

$$\nu_2 = \frac{-d[S(IV)]}{dt} = \frac{k_7 K_{a1}}{2} [Fe^{3+}][S(IV)][H^+]^{-1} \quad (131)$$

where $[S(IV)] = [HSO_3^-] + [H_2O \cdot SO_2]$
 $K_{a1} = [H^+][HSO_3^-]/[SO_2(aq)]$

The overall kinetic coefficient $k_{obs} = k_7 K_{a1}/2$ can be estimated from known kinetic data on ligand substitution [108,109]. Using the water exchange rate constant [110] for Fe³⁺, $k_{ex} \approx 10^2 s^{-1}$ and a calculated ion-pairing constant [111], $K_o \approx 1 M^{-1}$ for the Fe³⁺:HSO₃⁻ ion pair, a value for k₇ (~10² M⁻¹·s⁻¹) can be obtained. At $\mu = 0$, K_{a1} = 0.0123. Using these values, the estimated value of k_{obs} is 0.62 s⁻¹ at T = 25 C, pH 2 and $\mu = 0$. This value can be compared to the value of 0.82 s⁻¹ reported in Chapter 2. However, if k₇ is estimated from the value of the overall second-order rate constant [112] for the complexation of Fe³⁺ by SO₄²⁻ (k₇ ≈ 1 × 10³), the value of k_{obs} would be predicted to be 6.2 s⁻¹ at 25 C, pH 1.8 and $\mu = 0$. These estimates can be made in this fashion because the second-order rate of ligand substitution has been shown to be controlled most often by the water exchange rate of the central metal and to be relatively independent of the nature of the ligand [113].

The third term of the rate law indicates that Fe(III), Mn(II) and S(IV) are brought together in the transition state. One possible mechanism that would result in such a combination involves the formation of a reactive Mn(IV) intermediate from the interaction of the ferryl ion-sulfite complex [114] with Mn²⁺ as follows:



where the rate-limiting step is the two-electron oxidation of Mn(II) by Fe(V). The activation energy for this mechanism should be significantly less than the two previous pathways. This conclusion is consistent with the low apparent activation energy reported by Barrie and Georgii [39] for the synergistic effect of Fe³⁺ on the catalysis by Mn²⁺.

Alternatively, a one-electron oxidation of Mn²⁺ to Mn³⁺ could be envisioned:



This would be followed by a chain sequence (Equations 2-8) initiated by Mn^{3+} :



The redox potential of the Mn^{3+}/Mn^{2+} couple ($E^\circ \leq 1.5$ V) is sufficient to promote the one-electron oxidation of S(IV) to S(V) ($E^\circ \approx 0.9$ V) and truly initiate a radical chain sequence. The rate law for this process would be one of the general forms given in Tables II or IV. This latter mechanistic possibility could readily explain the nonlinear concentration effects observed in Chapter 2 and by Barrie and Georgii [39].

Finally, a third possibility, involving the formation of mixed hydroxy-bridged complexes of Fe(III) and Mn(II), can be considered.



The rate expression obtained from this mechanism would have the following form if complexation of HSO_3^- by the hydroxy-bridged species is assumed to be rate limiting:

$$v = k'[Fe(III)][Mn(II)][S(IV)][H^+]^{-2} \quad (140)$$

Similar expressions involving the concentrations of Fe(III), Mn(II) and S(IV) are obtained for the other mechanisms given above. The rate expression of Equation 140 is not exactly of the form shown in Equation 117, but it does reflect some of the essential features.

2. Photoassisted Catalysis

a. Homogeneous Processes

The catalytic effect of light [50,62,115-125] on autoxidation of dissolved SO_2 has been acknowledged for years as an alternative mode of initiation of the chain reaction sequence given in Equations 2-8. UV irradiation of sulfite/bisulfite systems is thought to produce an aquated electron [62,121] and a sulfite radical ion:



A transient electronic absorption maximum at $\lambda = 700$ nm has been assigned to the solvated electron and a similar transient maximum at $\lambda = 260$ nm has been assigned to the SO_3^- radical ion. The aquated electron decays by reaction with O_2 or HSO_3^- to produce a superoxide ion or sulfite ion and a hydrogen atom, respectively. However, only Lunak and co-workers [126-128] have systematically explored the possibility of metal-catalyzed photooxidation of sulfite, even though the phenomenon of homogeneous metal-assisted photooxidation/reduction processes has been reported previously for Fe(III) and Cu(II)-ligand systems [128-135].

The preliminary work of Lunak and Veprek-Siska [126] has shown a distinct photoassisted catalysis by Fe(III) at wavelengths higher than the cutoff for absorption by sulfite and bisulfite ion in aqueous solution. Quantum yields were shown to depend on the wavelength of irradiation and the concentration of Fe(III) in the system. They have proposed that a quantum of light is absorbed by a ferric-sulfite complex, thereby initiating the catalytic cycle through photoreduction of Fe(III) to Fe(II). In the absence of added Fe(III), the photochemical autoxidation of sulfite above $\lambda = 300$ nm did not proceed to a noticeable extent. A mechanism consistent with their findings would be:



or



After photoinitiation, autoxidation would proceed via a free radical chain after Equation 86 or by inner-sphere electron transfer as shown in Equations 145-147.

Lunak and Veprek-Siska [127] also report that photoinitiated autoxidation of sulfite is influenced by the presence of Mn(II) at trace levels (10^{-8} - 10^{-10} M) and that Cu(II) [125] does not exhibit a photocatalytic effect. On the other hand, Hoffmann and Boyce [40] have reported that cobalt(II)tetrakisulfophthalocyanine catalyzed autoxidation of S(IV) is strongly influenced by visible light in the range

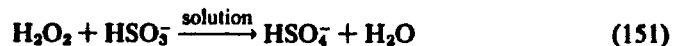
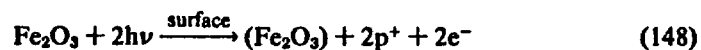
of 300–400 nm. They have interpreted their results in terms of formation of singlet oxygen due to a ligand-to-metal charge transfer absorption.

b. Heterogeneous Processes

A primary source of iron, manganese, zinc, titanium and other metals found in aerosol systems is from combustion of coal. These metals will be released to the atmosphere in their highest oxidation states in the form of metal oxides such as Fe_2O_3 , MnO_2 , ZnO and TiO_2 . Taylor and Flagan [135] and Ouimette and Flagan [136] found direct evidence for significant mass fractions of Fe_2O_3 in submicrometer particle size fractions of fly ash from a coal-fired combustor and from ambient aerosol.

Barrie and Georgii [39] have used average values of Mn and Fe in urban aerosols of 0.2 and 1 $\mu\text{g}/\text{m}^3$, respectively, and an average liquid water content of 0.1 g/m^3 to estimate that the soluble concentration in the aqueous phase is on the order of 10 μM . In making these estimates they assumed that 25% of the total Mn was soluble and 10% of the total iron was soluble. The remaining solid phases are likely to exhibit some catalytic activity [137–141].

Frank and Bard [45] reported that Fe_2O_3 (hematite) surfaces catalyze photoassisted autoxidation of HSO_3^- to HSO_4^- . Irradiation at 400 nm of an oxygenated bisulfite solution with suspended Fe_2O_3 particles resulted in a rapid conversion of S(IV) and S(VI), whereas in the absence of light no conversion of sulfite to sulfate was observed. A sequence of stoichiometric reactions that offers one possible explanation for photoassisted catalysis on a metal oxide (semiconductor) surface is:



where p^+ = charge vacancy created by the photoassisted excitation of an electron from the valence band of the metal oxide to the conduction band

Excited electrons in the conduction band and positive holes in the valence band migrate to the surface (presumably without recombination), where they react, respectively, with oxygen and bisulfite to produce hydrogen peroxide as the reduced product and bisulfate as the oxidized product.

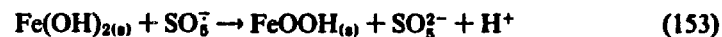
Similar, but less effective, photocatalytic effects have been reported by Frank and Bard [45] for other semiconductor materials such as TiO_2 , CdS and ZnO .

However, results for CdS and ZnO are obscured by the fact that at low pH (pH ~3) these solids dissolve to a certain extent; thus, any apparent photocatalytic effects may be due to dissolved metal species rather than due to inherent properties of the semiconductor material.

Faust and Hoffmann [142] studied photocatalytic autoxidation of HSO_3^- on synthetic Fe_2O_3 suspensions at pH 2.5; they report that the presence of Fe_2O_3 particles results in a slight rate enhancement as compared to the corresponding homogeneous photocatalytic system.

Childs [143] and Childs and Ollis [144] have addressed some of the fundamental considerations that are required to ascertain whether a heterogeneous photoreaction is truly photocatalytic according to Equations 148–151 or stoichiometrically photochemical. In a stoichiometric photochemical reaction, the observed conversion of sulfite to sulfate in irradiated systems may result from (1) direct photoactivation of an adsorbed sulfite on the surface; (2) a surface-prompted reaction of sulfite photoactivated in solution; (3) a noncatalytic reaction of the Fe_2O_3 surface with the adsorbed sulfite; or (4) homogeneous catalysis by Fe(III)/Fe(II) leached from the Fe_2O_3 surface. These questions remain to be resolved in the case of iron-catalyzed systems.

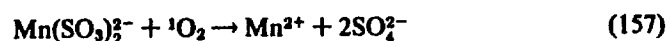
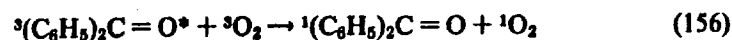
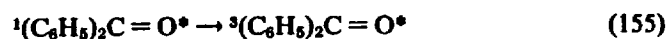
It is apparent [37,58,65,83,86] that the rate of autoxidation of S(IV) is most rapid in the concentration–pH domain where metal hydroxides are the dominant species such as Ni(OH)_2 , Co(OH)_3 , Co_3O_4 , FeOOH , Fe(OH)_3 and Cu(OH)_2 . For example, Brimblecombe and Spedding [37] have proposed that the oxyhydroxides FeOOH ($\alpha\text{-FeOOH}$, $\beta\text{-FeOOH}$, $\gamma\text{-FeOOH}$) would be effective initiators for the production of SO_3^- (since $E^\circ(\text{FeOOH}) = 0.91 \text{ V}$) as follows:



Soot particles have been shown to be effective catalytic surfaces for autoxidation of S(IV) by Brodzinsky et al. [138], Chang et al. [139] and Benner et al. [145] although Cohen et al. [140] reported that the apparent catalysis by ambient fly ash particles was due to Fe(III) leached into aqueous solution. Furthermore, soot and powdered activated carbon surfaces provide moderately effective sites for adsorption of trace metals and these adsorbed metals may in turn be the active catalytic centers.

Ambient soot contains a significant level of polynuclear aromatic hydrocarbons (PAH). Certain PAH have been shown to be photosensitizers for the production of singlet oxygen, which will in turn react electrophilically with an oxidizable substrate rather than through a free radical pathway [146]. A sensitizer, such as PAH, is a molecule that can absorb a quantum of light and then transfer this energy to a second substrate. For example, benzophenone is an efficient producer of $^1\text{O}_2$ ($^1\Delta_g$) [141]:





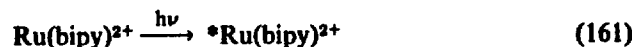
which in turn could oxidize S(IV) to S(VI) by a sequence of two-electron transfers. Energy transfer from an excited triplet state sensitizer to ${}^3\text{O}_2$ (Equation 156) to give ${}^1\text{O}_2$ is a spin-allowed process [146].

Fridovich and Handler [148] have shown that photosensitized dye molecules such as methylene blue and flavin mononucleotide are effective catalysts for autoxidation of S(IV); however, their early work was interpreted in terms of a free radical sequence rather than through production of ${}^1\text{O}_2$ as follows:



Later work by McCord and Fridovich [149] showed that the autoxidation of S(IV) as catalyzed by dimethyl sulfoxide was inhibited by superoxide dismutase. This result indicates that $\text{HO}_2\cdot$ was a likely intermediate. However, in metal-catalyzed reactions, superoxide dismutase had no effect. In light of more recent work [150], the reaction observed by Fridovich and Handler [148] most likely involved the production of ${}^1\text{O}_2$. Srinivasan et al. [150] have shown that irradiated solutions of the dye rose bengal produce both O_2^- and ${}^1\text{O}_2$, which are quickly consumed by SO_3^{2-} at pH 7.8. They have estimated that 77% of the active oxygen generated is ${}^1\text{O}_2$ and 23% O_2^- .

Additional work by Srinivasan et al. [150] has shown that irradiated solutions of $\text{Ru}(2,2'\text{-bipyridyl})^{2+}$ produce O_2^- , which leads to rapid oxidation of S(IV)



Much work remains to be done on photocatalytic systems in aqueous systems to ascertain the role of condensed-phase photochemistry on total S(IV) conversion rates. If photoassisted pathways are shown to be important under ambient condi-

tions, differences between nighttime and daytime conversion rates may have a plausible explanation.

3. Oxidation by Hydrogen Peroxide, Ozone and Nitrous Acid: Catalytic Influences

As indicated in Chapters 2 and 4, hydrogen peroxide appears to be a potentially important oxidant in atmospheric droplets because of its favorable Henry's law constant ($K_H = 1 \times 10^5 \text{ M-atm}^{-1}$), its rapid oxidation of S(IV), and its relative insensitivity to pH changes in an open two-phase system. Hydrogen peroxide is generated in the gas phase by the recombination of hydroperoxyl radicals, in the aqueous phase as an intermediate in metal-catalyzed autoxidations, and at air-water interfaces due to photoinduced redox processes [151]. Measurements by Kok and co-workers [152–155] indicate that steady-state aqueous-phase concentrations can be as high as $50 \mu\text{M}$.

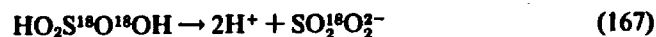
The kinetics of oxidation of S(IV) by H_2O_2 have been studied [31–33,41]. Mader [41] determined that over the pH range of 8–13 the rate of oxidation of S(IV) was characterized by a multiterm rate expression as shown in Table X. The first term accounts for uncatalyzed oxidation, the second term for general acid catalysis, and the third nominally for specific acid and other forms of unspeci-

Table X. Empirical Rate Laws for the Oxidation of S(IV) by Hydrogen Peroxide

Rate ($\nu = -d[\text{S(IV)}]/dt$)	Rate Constant	Conditions	Reference
$\nu = k_0[\text{H}_2\text{O}_2][\text{SO}_3^{2-}] + k_p[\text{H}^+][\text{H}_2\text{PO}_4^-][\text{H}_2\text{O}_2][\text{SO}_3^{2-}] + r_c$	$k_0 = 0.2 \text{ M}^{-1}\text{s}^{-1}$ $k_p = 1.7 \times 10^{10} \text{ M}^{-3}\text{s}^{-1}$ $E_a(k_0) = 63.5 \text{ kJ}\cdot\text{mol}^{-1}$	$T = 25 \text{ C}$ $\mu = 1.0 \text{ M}$ $\text{pH } 7.9\text{--}12.8$	41
$\nu = k[\text{H}^+][\text{H}_2\text{O}_2][\text{S(IV)}] / ([\text{H}^+]/([\text{H}^+] + K_{a2})) + k'[\text{H}_2\text{PO}_4^-][\text{H}_2\text{O}_2][\text{S(IV)}] / ([\text{H}^+]/([\text{H}^+] + K_{a2}))$	$k = 2.7 \times 10^8 \text{ M}^{-2}\text{s}^{-1}$ $k' = 1.3 \times 10^9 \text{ M}^{-2}\text{s}^{-1}$	$T = 12 \text{ C}$ $\mu = 1.0 \text{ M}$ $\text{pH } 4\text{--}8$	31
$\nu = k[\text{H}_2\text{O}_2][\text{HSO}_3^-][\text{H}^+]^{0.7} + k_a[\text{H}_2\text{O}_2][\text{HSO}_3^-][\text{CH}_3\text{CO}_2\text{H}]$ $k_1 = k[\text{H}_2\text{O}_2][\text{H}^+]^{0.7} + k_a[\text{H}_2\text{O}_2][\text{HA}]$	$k = 2.46 \times 10^6 \text{ M}^{-1}\text{s}^{-1}$ (pH 4.6) $k_a = 1.9 \times 10^4 \text{ M}^{-2}\text{s}^{-1}$ $E_a(k_1) = 24.9 \text{ kJ}\cdot\text{mol}^{-1}$ (pH 4.6)	$T = 20 \text{ C}$ $\mu = 0.2 \text{ M}$ $\text{pH } 4\text{--}8$	32
$\nu = \frac{k[\text{H}_2\text{O}_2][\text{HSO}_3^-][\text{H}^+]}{K + [\text{H}^+]}$	$k = 5.6 \times 10^6 \text{ M}^{-1}\text{s}^{-1}$ $K = 0.1 \text{ M}$	$T = 25 \text{ C}$ $\text{pH } 0\text{--}3$ μ (variable)	33
$\nu = \frac{k[\text{H}_2\text{O}_2][\text{H}_2\text{O}\cdot\text{SO}_2]}{K + [\text{H}^+]}$	$k = 8.3 \times 10^4 \text{ M}^{-1}\text{s}^{-1}$ $K = 0.1 \text{ M}$ $E_a = 28 \text{ kJ}\cdot\text{mol}^{-1}$	$T = 25 \text{ C}$ $\text{pH } 0\text{--}3$ μ (variable)	33

fied catalysis. In addition to phosphate buffer catalysis, Mader observed carbonate and arsenate were effective as general acid catalysts. Mader offered no mechanistic interpretation of his kinetic results.

Earlier, Halperin and Taube [42] had suggested that the oxidation proceeded through the formation of a peroxymonosulfurous acid intermediate, which was followed by an intramolecular rearrangement to give sulfate and water. Their conclusions were based on double-isotope labeling experiments that showed that both of the labeled oxygens of $\text{H}^{18}\text{O}^{18}\text{OH}$ were incorporated to the product sulfate, even though the stoichiometry of the reaction requires the net addition of one oxygen atom.



In a subsequent kinetic study of this reaction, Hoffmann and Edwards [31] found definitive evidence for both general acid and specific acid catalysis. They reported the following two-term rate law for the pH range of 4–8:

$$\frac{-d[\text{S(IV)}]}{dt} = k[\text{H}^+][\text{H}_2\text{O}_2][\text{S(IV)}] \left(\frac{[\text{H}^+]}{[\text{H}^+] + K_{a2}} \right) + k'[\text{HA}][\text{H}_2\text{O}_2][\text{S(IV)}] \left(\frac{[\text{H}^+]}{[\text{H}^+] + K_{a2}} \right) \quad (168)$$

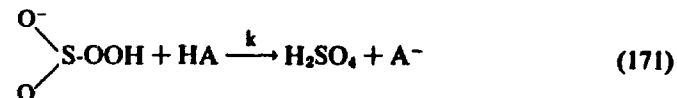
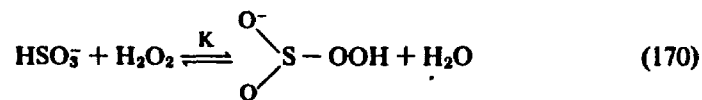
where K_{a2} = second acid dissociation constant

$[\text{S(IV)}]$ = sum of the concentration of sulfite and bisulfite within the pH range of 4–8

HA = weak acids used over this pH range as buffers

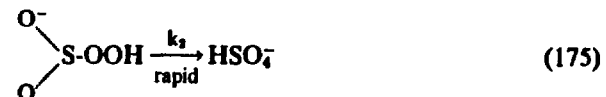
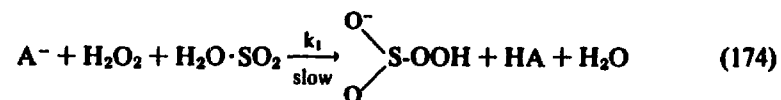
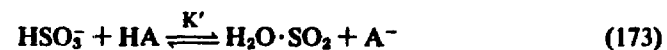
The first term of the rate law reflects the contribution of specific acid catalysis and the second term reflects the contribution of general acid catalysis to the overall rate.

Two alternative mechanisms that are consistent with the observed rate law and the isotopic labeling results of Halperin and Taube [42] are:



where HA = H_3O^+ or a suitable weak acid such as phosphate, citrate, pivalate, acetate or phthalate

According to this mechanism, the reaction occurs via a nucleophilic displacement by H_2O_2 on sulfur of HSO_3^- to form a peroxymonosulfurous acid intermediate (Equation 170), which then undergoes a rate-determining rearrangement to HSO_4^- assisted by H_3O^+ or HA. Alternatively, a mechanism in which there would be an equilibrium protonation of the bisulfite followed by a proton transfer to A^- can be written as:



In this sequence, Equation 174, a termolecular step, in which A^- , H_2O_2 and $\text{H}_2\text{O} \cdot \text{SO}_2$ react to form peroxymonosulfurous acid, is rate-determining. In the first alternative mechanism (Equations 169–171), HSO_3^- is the reactive species of S(IV), and in the second mechanism (Equations 172–175) $\text{H}_2\text{O} \cdot \text{SO}_2$ is predicted to be the reactive species. The work of Martin and Damschen [33] appears to verify that HSO_3^- is in fact the reactive S(IV) species and that the mechanism of Equations 169–171 is valid over a broad range of pH (i.e., 0–8).

Penkett et al. [32] studied peroxide oxidation kinetics over the pH range 4.3–8.2 using acetate, citrate, phosphate and Tris buffers to maintain pH. They confirmed the role of these weak acids as general acid catalysts. However, Penkett et al. report a hydrogen ion dependence of $[\text{H}^+]^{0.7}$ over the pH range of 4–6 as noted in Table X. On the other hand, Martin and Damschen [33] report a first-order dependence on H^+ over the pH range of 1–3 and a reciprocal dependence below pH 1. This switch in pH dependence supports the notion that HSO_3^- is the reactive form of S(IV) in solution.

For the pH range of 1–5, Martin and Damschen [33] expressed the rate

law in a form that is convenient for application to open atmospheric systems as follows:

$$\frac{-d[S(IV)]}{dt} = 8.3 \times 10^5 [H_2O_2][H_2O \cdot SO_2] \quad (176)$$

or

$$\frac{-d[S(IV)]}{dt} = 8.3 \times 10^5 P_{H_2O_2} K_{H,H_2O_2} P_{SO_2} K_{H,SO_2} \quad (177)$$

The concentrations of H_2O_2 and $H_2O \cdot SO_2$ are expressed in terms of the products of their respective Henry's law constants and partial pressures. They also report that the oxidation reaction is apparently insensitive to the effects of metal catalysis (Fe^{3+} and Mn^{2+}) and organic inhibitors (hydroquinone, toluene, pinene and hexene).

However, in the case of H_2O_2 , Fe^{2+} and Cu^{2+} would be the most likely metal ions to exert a catalytic effect on the reaction rate since these metals are well known initiators of the Fenton's reagent reaction [156-158]:



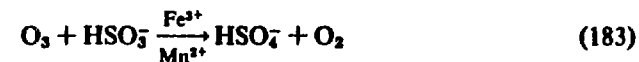
If oxygen were present in the reaction system a free radical pathway could be initiated by Equation 180 and proceed via Equations 3-8 or 18-23. Additional propagation steps can be envisioned to occur as follows:



Future work on the H_2O_2 -S(IV) reaction system should address the possibility of catalysis by Fe(II) and Cu(II).

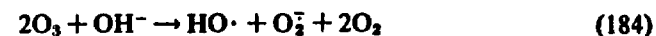
There are few reports of catalytic influences on the oxidation of S(IV) by ozone. Barrie [159] has found that Mn^{2+} promotes the oxidation of S(IV) by ozone in aqueous droplets. In the absence of Mn^{2+} , gas-phase ozone alone failed to enhance SO_2 absorption rates in the aqueous phase. Chapter 2, in the section on ozone oxidation kinetics, reports no apparent catalysis due to Fe^{3+} , Mn^{2+} , VO^{2+} or Cu^{2+} ; however, Harrison et al. [43] reported that additions of Mn^{2+} and Fe^{3+} at concentrations of $10 \mu M$ resulted in enhancements in the observed oxidation rates by factors of approximately 2 and 6, respectively. Addition of competitive complexing agents (phosphate or citrate) inhibits the apparent catalytic process. A maximum in cata-

lytic influence occurred at pH 4.5. This behavior suggests that ferric-sulfito and manganous-sulfito complexes play a role in the oxidation process.



Furthermore, Harrison et al. [43] indicate that the rate of oxidation increases linearly with an increase in Fe^{3+} . These results are summarized in Table XI.

Penkett [160] has proposed the following initiation of a radical mechanism to account for oxidation by ozone:



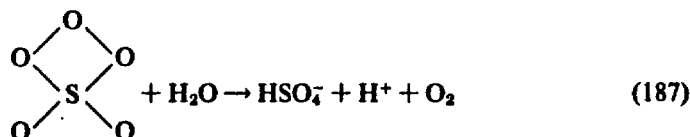
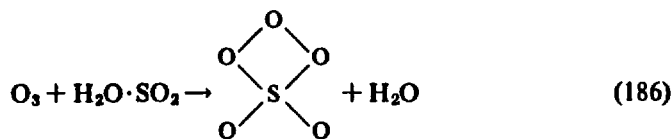
The bisulfite radical of Equation 185 would proceed to react according to Equations 3-8, thereby completing the free radical sequence of the Bäckström mechanism.

Based on isotopic tracer experiments, Espenson and Taube [162] concluded that in acidic solution the reaction between ozone and sulfur dioxide could occur via a simple bimolecular process in which two atoms of oxygen are transferred from ozone to sulfur dioxide or via a radical reaction involving reactive intermediates or via both pathways in parallel. In basic solution, they concluded that the free radical pathway was more likely even though more than one oxygen atom was transferred from ozone to sulfite.

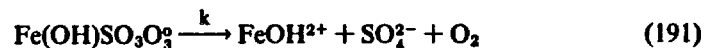
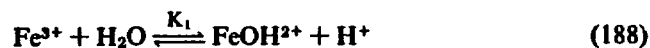
Table XI. Empirical Rate Laws for the Oxidation of S(IV) by Ozone

Rate Law ($\nu = -d[S(IV)]/dt$)	Rate Constant	Conditions	Reference
$= k[O_3][HSO_5^-][H^+]^{-0.5}$	$k = 1.45 \pm 0.7 \times 10^4 M^{-0.5} s^{-1}$	pH 1-5 T = 25 C	32
$= k P_{O_3} K_{H,O_3} [HSO_5^-][H^+]^{-0.1}$	$k = 4.4 \times 10^4 M^{-0.9} s^{-1}$ $K_{H,O_3} = 1.23 M \cdot atm^{-1}$	pH 4-7 T = 25 C	29
$= k[O_3][S(IV)][H^+]^{-0.6}$	$k = 1.9 \times 10^4 M^{-0.6} s^{-1}$	pH 0-3 T = 25 C	Chapter 2
$= k_1[HSO_5^-][O_3] + k_2[SO_3^{2-}][O_3]$	$k_1 = 3.1 \times 10^5 M^{-1} s^{-1}$ $k_2 = 2.2 \times 10^9 M^{-1} s^{-1}$ $E_{a,1} = 46 kJ \cdot mol^{-1}$ $E_{a,2} = 43.9 kJ \cdot mol^{-1}$	pH 0-4 T = 25 C	160
$= k[Fe^{3+}][S(IV)][O_3][H^+]^n$	$k_{obs} = 6.8 \times 10^5 M^{-1} \cdot min^{-1} \cdot ppm^{-1}$	T = 295 K pH 4-6 $[Fe^{3+}] \geq 10 \mu M$	42

If a polar pathway were to occur as suggested by Espenson and Taube [162], a likely mechanism would be as follows:

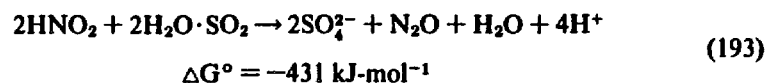
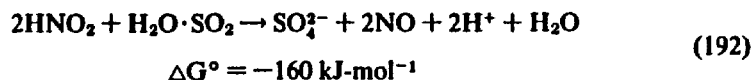


Catalysis by Fe^{3+} and Mn^{2+} may proceed through an initial metal sulfite complex followed by attachment of ozone to form a ternary complex.



Finally, S(IV) in aqueous systems can be oxidized readily by N(III) and N(IV) species in the form of nitrite, nitrous acid and aquated nitrogen dioxide.

Nitrous acid will oxidize S(IV) in acidic solution according to the following stoichiometries:



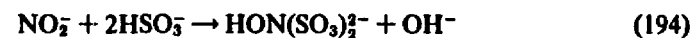
Martin et al. [163] determined that the reaction was first-order in N(III), S(IV) and H^+ , and insensitive to catalysis by Fe^{3+} , Mn^{2+} and VO^{2+} in the absence of O_2 .

$$\frac{-d[\text{S(IV)}]}{dt} = k[\text{HNO}_2]_{\text{T}}[\text{S(IV)}][\text{H}^+] \quad (193)$$

where $[\text{HNO}_2]_{\text{T}} = [\text{HNO}_2] + [\text{NO}_2^-]$
 $k = 142 \text{ M}^{-2} \cdot \text{s}^{-1}$

They found that N_2O was the principal product at low pH.

Oblath et al. [164] found at higher pH (pH 5–7) that hydroxylamine disulfonate formed according to the following stoichiometry:



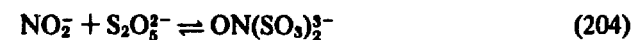
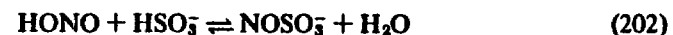
Ross et al. [165] observed that a significant fraction of HNO_2 is converted to NO according to Equation 192 at higher acidities. They found that, in the presence of O_2 , an apparent catalytic cycle involving NO is established. The stoichiometric equations for this sequence are as follows:



Latimer [85] suggested the following mechanism for the reduction of nitrous acid by S(IV):



Oblath et al. [164] suggest the following mechanism:





which involves the formation of a nitrosonium ion, a fairly stable ionic species.

In acid solution, aquated nitrogen dioxide ($\text{N(IV)O}_2(\text{aq})$) readily dimerizes to form nitrogen tetroxide, as reported in Chapter 4 and by Grätzel et al. [166]:



Nitrogen tetroxide, in turn, is a moderately strong oxidizing agent [84] with E° values of +1.07 and +1.03 V, respectively, for the following reactions:



Takeuchi et al. [167] reported that the reaction of S(IV) with $\text{NO}_2(\text{aq})$ proceeds rapidly according to the following stoichiometries and rate laws:



$$\frac{-d[\text{S(IV)}]}{dt} = k_1[\text{NO}_2(\text{aq})][\text{SO}_3^{2-}] \quad (211)$$



$$\frac{-d[\text{S(IV)}]}{dt} = k_2[\text{NO}_2(\text{aq})][\text{HSO}_3^-] \quad (213)$$

where $t = 25^\circ \text{C}$

$$k_1 = 6.6 \times 10^5 \text{ M}^{-1}\text{s}^{-1}$$

$$k_2 = 1.5 \times 10^4 \text{ M}^{-1}\text{s}^{-1}$$

Nash [168] described the role of Fe(II) catalysis in the above reactions in the nanomolar range.

As pointed out in Chapter 4, translation of the above rate laws for closed systems to open atmospheric systems requires that the concentrations of the important gases be expressed in terms of the product of the appropriate Henry's law constant times the observed partial pressures. In the case of HNO_2 and NO_2 , their respective Henry's law constants are 49 and $0.01 \text{ M}\cdot\text{atm}^{-1}$. These moderate values of K_H indicate that the partial pressures of each gas-phase species will determine to a large extent the contribution of the above pathways to the overall rate of S(IV) oxidation.

B. EQUILIBRIUM SPECIATION MODELS

To use the preceding kinetic information reliably in dynamic models of SO_2 transformation in the atmosphere, detailed chemical speciation in aqueous solution for reductant, oxidant and catalysts must be determined. Using data collected on the concentrations of chemical constituents in fog, cloud and rain water, equilibrium speciation models can be developed readily with the aid of the computer programs REDEQL2 and SURFEQL. Both REDEQL2 and SURFEQL are general-purpose programs for computation of multiple, simultaneous chemical equilibria involving acid-base, oxidation-reduction, precipitation-dissolution, complexation-dissociation and adsorption-desorption reactions [169-172]. As an example of the applicability of equilibrium models, we will consider the potential role of iron-sulfite complexes and sulfonic acid derivatives in increasing the apparent capacity of an aqueous droplet system for S(IV); the levels observed in fog and cloud water reported in Table I appear to be above those predicted by the observed partial pressures of SO_2 .

Total S(IV) in the aqueous phase is given by:

$$\text{S(IV)}_T = [\text{SO}_2]_{\text{aq}} + [\text{HSO}_3^-] + [\text{SO}_3^{2-}] \quad (214)$$

$$\text{S(IV)}_T = K_H P_{\text{SO}_2} \left(1 + \frac{K_1}{[\text{H}^+]} + \frac{K_1 K_2}{[\text{H}^+]^2} \right) \quad (215)$$

$$\alpha_0^{-1} = \left(1 + \frac{K_1}{[\text{H}^+]} + \frac{K_1 K_2}{[\text{H}^+]^2} \right) \quad (216)$$

$$\text{S(IV)}_T = K_H P_{\text{SO}_2} / \alpha_0 \quad (217)$$

where K_H = Henry's law constant

K_1 = first acid dissociation constant for $\text{H}_2\text{O}\cdot\text{SO}_2$

K_2 = second acid dissociation constant for $\text{H}_2\text{O}\cdot\text{SO}_2$

Using the appropriate values for K_H , K_1 and K_2 [107], total [S(IV)] can be calculated to be approximately $1 \mu\text{eq}\cdot\text{L}^{-1}$ at 16 ppbv SO_2 and pH 3. However, if the reactions of S(IV) with Fe^{3+} and CH_2O are considered the following expressions are valid:



$$\text{S(IV)}_T = [\text{SO}_2]_{\text{aq}} + [\text{HSO}_3^-] + [\text{SO}_3^{2-}] + [\text{HOCH}_2\text{SO}_3^-] + [\text{FeSO}_3^+] \quad (220)$$

$$S(IV)_T = K_H P_{SO_2} \left(1 + \frac{K_1}{[H^+]} + \frac{K_1 K_2}{[H^+]^2} + \frac{K_1 K_3}{[H^+]} [CH_2O] + \frac{K_4 K_2 K_1}{[H^+]^2} [Fe^{3+}] \right)$$

In this case, for $K_3 = 10^5 M^{-1}$ and $K_4 = 10^{12} M^{-1}$, the $[S(IV)]_T$ will be in the range of 100–600 $\mu eq-L^{-1}$ at 16 ppbv SO_2 and pH 3 if the observed concentrations of CH_2O and Fe are used as initial input values and approximate values for the equilibrium concentrations of CH_2O and Fe^{3+} are determined iteratively.

These computations can be performed readily using SURFEQL. To illustrate the applicability of this modeling approach, a sensitivity analysis on the value for K_4 was performed. Carlyle [77] has reported a value of $K_4 = 10^9$ while Hansen et al. [173] report a value of $K_4 = 10^{16.1}$. The actual value may lie somewhere between these two values.

Metal-sulfite complexes are notably strong compared to the corresponding metal-sulfate species, e.g. $\beta_2(Hg(SO_3)_2^{2-}) = 10^{24}$; $\beta_2(Hg(SO_4)_2^{2-}) = 10^4$. Results are shown in Figure 2. These results suggest that, if $K_4 \geq 10^{10}$, 50% of the total iron in a system initially 0.1 mM in Fe_T will be complexed at $FeSO_3^+$ over the pH range of 2–4. Furthermore, if $K_4 \geq 10^{15}$, the computer model predicts that all of the Fe will be found as the species $FeSO_3^+$. Similar computations can be

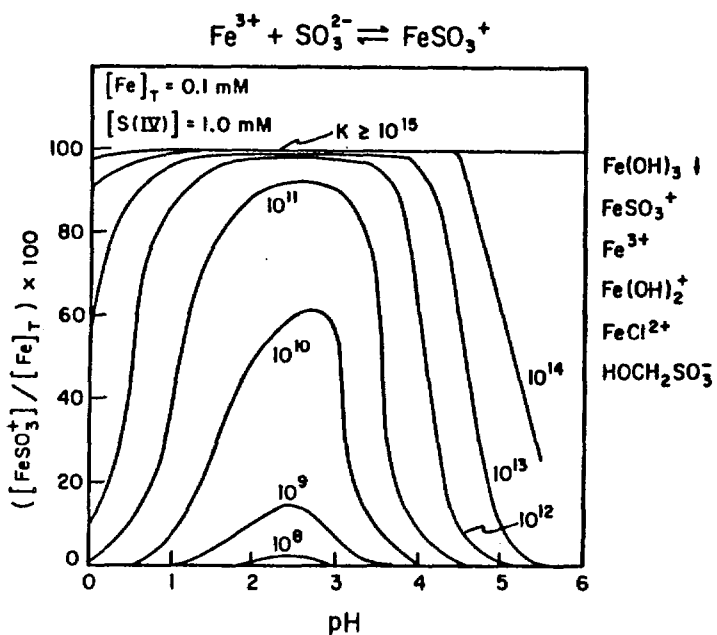


Figure 2. Speciation of Fe(III) vs pH in aqueous solution as a function of the stability constant of $FeSO_3^+$ as determined with SURFEQL. Other species that form are listed on the right side of the figure.

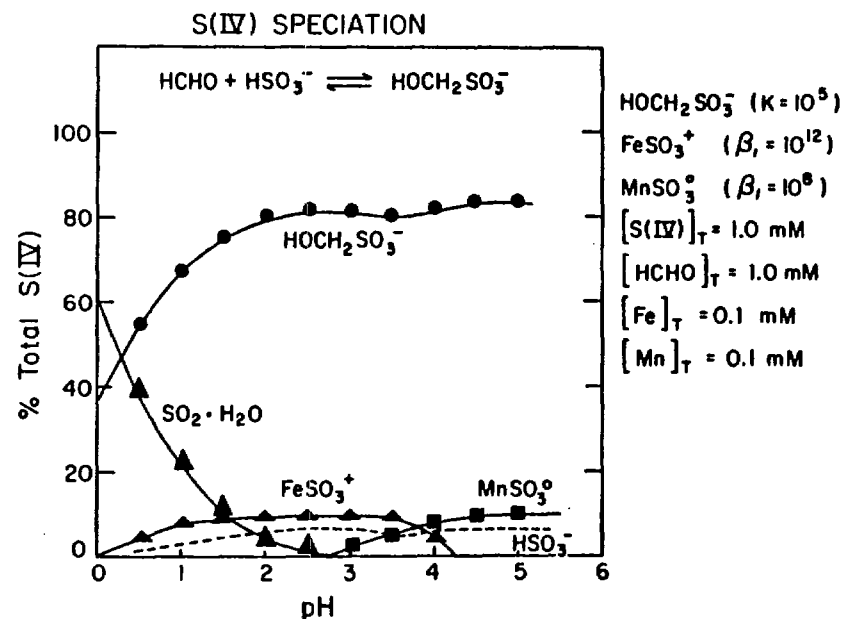


Figure 3. Speciation of S(IV) vs pH for the conditions on the far right of the figure as determined by SURFEQL.

performed on Mn^{2+} and HCHO. Figure 3 shows the total speciation for S(IV) over the pH range of 0 to 6 given the conditions listed on the right side of the figure.

In aqueous aerosol systems, important factors to consider are the nature and roles of dissolved organic molecules that can act as competitive complexing agents for metals. For example, liquid-phase autoxidation of benzaldehyde produces benzoic acid, which can act as a suitable complexing agent (e.g., $pK_{a1} = 3.97$, $\log\beta_{11} = 1.51$ for $Cu(C_7H_6O_2)^+$) and a similar oxidation of 2-hydroxybenzaldehyde to 2-hydroxybenzoic acid produces even a stronger potential ligand (e.g., $pK_{a1} = 2.78$, $\log\beta_{11} = 10.13$ for $Cu(C_7H_6O_4)^+$). The presence of complexing agents of this type and organic reductants will accelerate the dissolution of Fe_2O_3 and MnO_2 , which are the likely sources of soluble iron and manganese in aerosol systems. As shown by Cohen et al. [40], the catalytic activity of soot-derived aerosols correlates well with the total iron released to the liquid phase. To illustrate this effect, oxalic acid/oxalate was added to the computation illustrated in Figure 2 at a concentration of 1.0 mM. Results are shown in Figure 4 for the effect of 1:1, 1:2 and 1:3 ferric oxalate complexes with $\log\beta_1 = 7.5$, $\log\beta_2 = 13.64$ and $\log\beta_3 = 18.49$ on the equilibrium distribution of $FeSO_3^+$. The net effect of the addition of oxalate was to lower the percentage contribution of $FeSO_3^+$ as a function of pH for a given stability constant. This effect is due to competitive complexation.

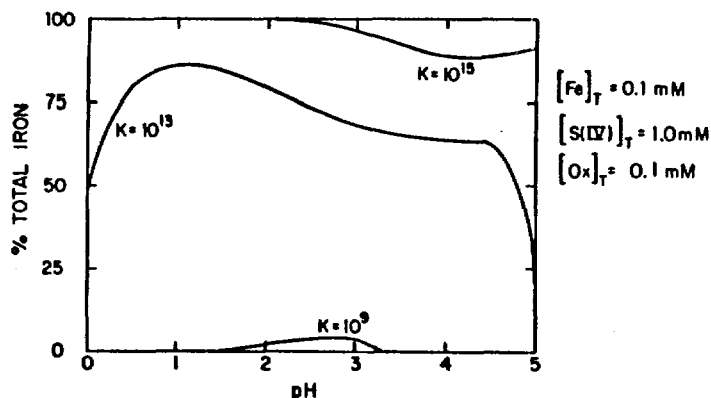


Figure 4. Speciation of Fe(III) perturbed by iron(III)oxalato complexes as a function of pH and stability constant (β_1) of the FeSO_3 .

An additional effect that was not considered here is the possible formation of mixed ligand complexes of Fe^{3+} , S(IV) and oxalate.

As indicated above, certain metal-catalyzed autoxidations of sulfite proceed via the formation of discrete inner-sphere complexes between the reductant, SO_3^{2-} and the catalyst as a prelude to electron transfer. Few metal-sulfite stability constants have been determined because of the thermodynamic instability of sulfite toward oxidation in oxic systems; however, those that have been reported [107] are significantly larger than the corresponding constants for metal-sulfate complexes as shown in Table XII. Sulfite can form complexes by forming a bond either

Table XII. Comparison of Stability Constants* for Metal-Sulfite and -Sulfato Complexes at 25.0 C

Metal	μ	$\log \beta (\text{SO}_3^{2-})$	μ	$\log \beta (\text{SO}_4^{2-})$
Ag^+	0	AgSO_3^- , 5.6	0	AgSO_4^- , 1.3
Cd^{2+}	1.0	$\text{Cd}(\text{SO}_3)_2^{2-}$, 4.2	1.0	$\text{Cd}(\text{SO}_4)_2^{2-}$, 1.6
Hg^{2+}	1.0	$\text{Hg}(\text{SO}_3)_2^{2-}$, 24.1	0.5	$\text{Hg}(\text{SO}_4)_2^{2-}$, 2.4
Ce^{3+}	0	CeSO_3^+ , 8.0	0	CeSO_4^+ , 3.6
Fe^{3+}	0.1	FeSO_3^+ , 18.1 ^b	0	FeSO_4^+ , 4.0
Fe^{2+}			0	FeSO_3^0 , 2.2
UO_2^{2+}	1.0	UO_2SO_3 , 5.3	1.0	UO_2SO_4 , 1.8
Cu^+	1.0	CuSO_3^- , 7.8		
Cu^+	1.0	$\text{Cu}(\text{SO}_3)_2^{2-}$, 8.7		
Cu^{2+}			0	CuSO_4^0 , 2.4

* All constants reported in this table were taken from Smith and Martell [106], except the stability constant for FeSO_3 .

^b Hansen et al. [172].

through sulfur [174,175] or through oxygen [176–178] whereas sulfate is restricted to bond formation through oxygen. Part of the increased metal-sulfite bond stability may be due to the availability of low lying "d" orbitals on sulfur for $p\pi-d\pi$ and $d\pi-d\pi$ metal to ligand backbonding. In addition to this added stability, sulfite can readily form bidentate [179] and bridging complexes with bond formation through two oxygen atoms or through an oxygen and sulfur.

Based on simple linear free energy correlations, reasonable estimates for the stability constants of Fe^{2+} , Mn^{2+} , Cu^{2+} and Ni^{2+} complexes with sulfite can be made using the data given in Table XII. With this information, models for the speciation of fog water (Table I) can be constructed with the aid of SURFEQL. These computations are particularly important in the case of Fe^{3+} since it can exist as a solid ($\text{Fe}(\text{OH})_3$ or FeOOH) over a broad range of pH. Results of a speciation model for the chemical constituents and concentrations listed in Table I are illustrated in Figure 5 for Fe^{3+} , S(IV), Mn^{2+} and Cu^{2+} . Iron(III) above pH 4 is predicted to occur exclusively as amorphous $\text{Fe}(\text{OH})_3$; below pH 4, Fe^{3+} is complexed by SO_3^{2-} ($\log \beta_1 \approx 12$) and by F^- . Only a small fraction of total iron appears as free hexaquo iron(III). This fraction increases at $\text{pH} < 2$.

Copper and manganese speciation are relatively straightforward. At the micro-

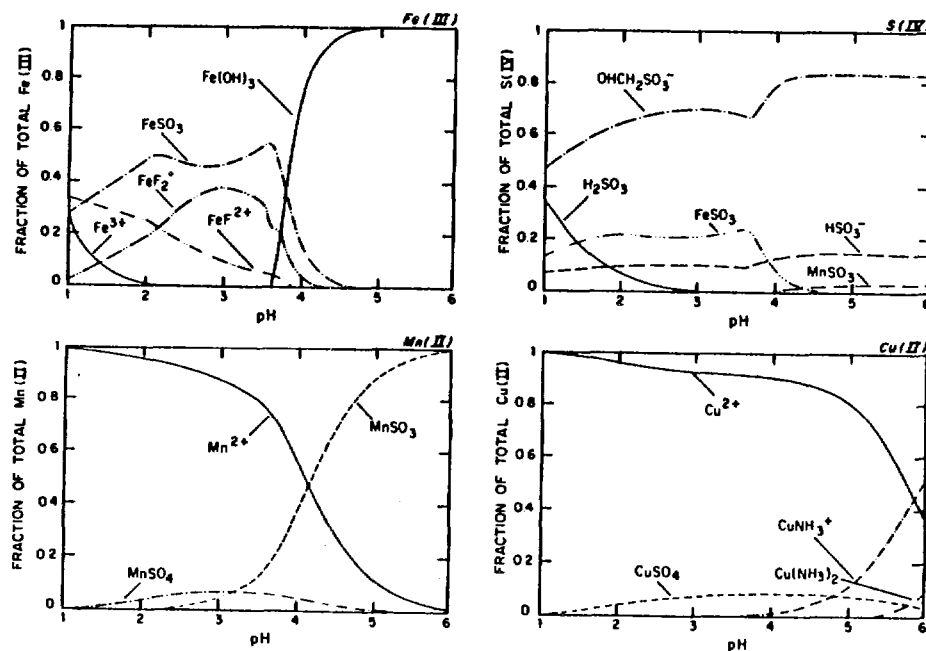


Figure 5. Speciation of Fe(III), S(IV), Cu(II) and Mn(II) in fog water as a function of pH. Input values were the high values for all measured components listed in Table I. ($\log \beta_1 [\text{FeSO}_3] = 12$ and $\log \beta_1 [\text{MnSO}_3] = 8$.)

molar concentration levels given in Table I, both Cu^{2+} and Mn^{2+} occur as soluble species over the pH range 1–6. Copper(II) forms amino complexes to some extent at pH >4. Manganese(II) is found primarily as a sulfite complex ($\log\beta_1 \approx 8$) at pH 4–6 and as a free hexaquo metal at pH <4.

The speciation of S(IV) is of great interest. Bisulfite readily forms sulfonic acid derivatives, α -hydroxyalkanesulfonic acids (also known as bisulfite addition compounds) [180], as indicated in Equation 218, with aldehydes and ketones. Since relatively high levels of formaldehyde ($K_H = 6.3 \times 10^3 \text{ M-atm}^{-1}$) (Chapter 4) and other aldehydes have been found in fog and cloud water in Los Angeles, the formation of these addition complexes must be considered in kinetic or thermodynamic model development. Dasgupta et al. [181] have established a conditional stability constant for the formation of α -hydroxymethanesulfonic acid of approximately $K = 10^{4.8}$ over the pH range 2–6. This constant can be used in the equilibrium computation. Results shown in Figure 5 for S(IV) indicate that the sulfonic acid derivative will be the predominant S(IV) species over a broad range of pH. Of secondary importance below pH 4 are FeSO_3 , HSO_3^- and $\text{H}_2\text{O}\cdot\text{SO}_2$, respectively. The occurrence of S(IV) as stable sulfonic acid derivatives may retard the net oxidation of S(IV) to S(VI). Dasgupta et al. [181] and Fortune and Dellinger [182] have found that addition of CH_2O to sulfite solutions stabilizes S(IV) as hydroxymethanesulfonic acid (HMSO), and that HMSO was not significantly degraded and oxidized to S(VI) for at least one month.

In conclusion, equilibrium speciation models will prove to be an invaluable tool in determining the detailed chemistry of atmospheric water droplets when sufficient time is available for reactions under consideration to be in a steady-state or approximate equilibrium. The kinetic and mass transport limitations for these approximations have been discussed [170,183]. In the next section, the models discussed above will be interfaced with a kinetic model for nighttime fog water chemistry.

III-25

C. FOG WATER CHEMISTRY MODEL

1. Background

Fog and cloud droplets form by condensation of water vapor on the activated cloud condensation nuclei (ACCN) in the atmosphere and grow by accretion of water vapor. The soluble components of the ACCN on which the droplets form dissolve in the droplet and provide an initial chemical loading. As the droplets grow, they absorb gases from the atmosphere, and liquid-phase reactions occur within.

During fall and winter 1981, water from nighttime fogs in the Los Angeles basin were sampled and analyzed (Table I) [14]. The results of this study highlighted the efficiency of fog droplets as scavengers of air pollutants in the boundary layer; extremely high concentrations of sulfate ions, as well as nitrate and ammonium

ions, were routinely found. The Log Angeles basin is a highly polluted region, and the sulfate levels observed could be attributed to (1) scavenging by nucleation of the large primary sulfate ACCN; (2) scavenging by diffusion of the smaller secondary sulfate aerosol particles; and (3) absorption of atmospheric SO_2 and subsequent liquid-phase oxidation to S(VI).

As discussed above, several pathways for the heterogeneous S(IV) \rightarrow S(VI) oxidation scheme must be considered. The most important oxidants appear to be H_2O_2 , O_3 and O_2 catalyzed by the Fe^{3+} and Mn^{2+} present at less-than-millimolar concentrations in the aqueous droplets. Hydrogen peroxide and ozone are both absorbed from the gas phase according to their respective Henry's law equilibria; Fe^{3+} and Mn^{2+} originate from fly ash and soil dust ACCN on which the droplets have condensed. The object of this section is to present a dynamic model for the water chemistry of nighttime urban fogs with which the contributions of the various oxidation mechanisms to the total S(VI) concentrations in fog water can be evaluated.

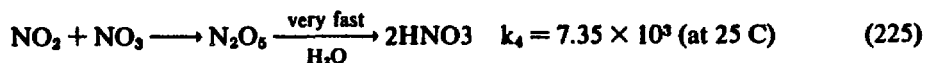
A number of rain and cloud water chemistry models have been proposed in recent years. Adamowicz [184] modeled the chemistry of pure raindrops falling through a well mixed polluted layer with uniform and constant concentrations of SO_2 , CO_2 and NH_3 . He assumed that the aqueous-phase oxidation of S(IV) to S(VI) occurred exclusively through iron-catalyzed oxidation by O_2 according to the kinetic expression of Brimblecombe and Spedding [37]. Mass transfer at the surface of the drop was modeled with two-film theory, which Baboolal et al. [185] have since shown to be unsatisfactory in that it ignores the forced convection inside and outside the falling drop, which greatly enhances the rates of mass transfer. Durham et al. [186] added NO_x to the gas phase and considered O_3 to be the only liquid-phase oxidant, which greatly underestimates S(VI) formation rates. Easter and Hobbs [187] modeled cloud water chemistry by using a wave cloud model, an open atmosphere with trace concentrations of CO_2 , SO_2 and NH_3 , and a rudimentary S(IV) oxidation rate consisting of a simple first-order dependence on sulfite.

In the model presented here, the chemistry is more detailed than in the above models; recent evaluations for reaction mechanisms, rate constants, activation energies and thermodynamic data are used. ACCN chemistry and gas-phase reactions are included to simulate the coupling between gas-phase, liquid-phase and aerosol chemistries. The system is considered closed because of the significant depletion of trace gases due to absorption by the fog droplets, which would make the assumption of an open system very inaccurate. Also, the physical processes relevant to droplet chemistry are examined more rigorously than in the previous models; as shall be shown, restriction of the model to nighttime fogs allows one to account for these physical processes in a simple but fairly realistic manner, whereas in rains and clouds, the large temporal and spatial scales involved make detailed analysis exceedingly difficult. The proposed model is a potentially useful tool for prediction of fog water chemistry, even though the present discussion will mostly be limited to S(IV) aqueous-phase oxidation processes.

2. Model Development

a. Gas-Phase Chemistry

At nighttime the gas-phase chemistry is considerably simplified over that in the daytime because of the absence of sunlight and thus of the associated photochemical reactions. In the absence of OH, O³(P) and CH₃O₂ radicals, which disappear rapidly after sunset, SO₂ gas-phase oxidation is very slow [188] and negligible on the time scales of a fog event. Although oxidation by ozone of organics (especially olefins) may be important, it will not be considered at the present time. Gas-phase chemistry is assumed to be limited to NO_x oxidation, which proceeds through the following mechanism [189,190]:



No data are given for the activation energies of Equations 224 and 225; a doubling of the reaction rates for a 10° C increase in temperature is assumed.

The kinetics of the hydrolysis of N₂O₅, which involves both water vapor and the fog droplets, is not well understood. The essential work in this problem area has been reviewed [191]. Hydrolysis of N₂O₅ appears to occur much faster at the surface of aerosol particles than homogeneously in the gas phase. In the presence of fog droplets the reaction is probably very fast, because of the large droplet surface area and the possibility of heterogeneous hydrolysis. Therefore, this step is assumed to be instantaneous. Reactions 222–225 yield a system of differential equations that is readily solved by a fourth-order Runge-Kutta routine. The overall reaction rate is essentially limited by the slow rate of oxidation of NO₂.

b. Liquid-Phase Chemistry

Droplet chemistry is determined primarily by ACCN chemistry and by absorption and subsequent aqueous-phase reactions of atmospheric gases. Gases are absorbed and react in the droplet according to the equilibria listed in Table XIII. The temperature dependence for all the equilibrium constants in Table XIII is determined by the Van't Hoff equation:

$$\ln K_T = \ln K_{298.15} - \frac{\Delta H^\circ}{R} \left(\frac{1}{T} - \frac{1}{298.15} \right) \quad (226)$$

Table XIII. Equilibria and Thermodynamic Data Considered in Fog Water Model [10, 32, 196, 197]

Reaction	$\Delta G^\circ_{298.15}$ (kcal-mol ⁻¹)	$\Delta H^\circ_{298.15}$ (kcal-mol ⁻¹)	$K_{(aq)}$ (M-atm ⁻¹ or M)
H ₂ O(l) ⇌ H ⁺ + OH ⁻	19.093	13.345	1.008 × 10 ⁻¹⁴
CO ₂ (g) + H ₂ O(l) ⇌ H ₂ CO ₃ (l)	2.005	-4.846	3.390 × 10 ⁻³
H ₂ CO ₃ (l) ⇌ H ⁺ + HCO ₃ ⁻	8.687	1.825	4.283 × 10 ⁻⁷
HCO ₃ ⁻ ⇌ H ⁺ + CO ₃ ²⁻	14.09	3.55	4.687 × 10 ⁻¹¹
NH ₃ (g) ⇌ NH ₃ (l)	-2.41	-8.17	5.844 × 10 ¹
NH ₃ (l) ⇌ NH ₄ ⁺ + OH ⁻	6.503	8.65	1.709 × 10 ⁻⁵
SO ₂ (g) ⇌ SO ₂ (l)	-0.130	-6.247	1.245
SO ₂ (l) ⇌ HSO ₃ ⁻ + H ⁺	2.578	-4.161	1.290 × 10 ⁻³
HSO ₃ ⁻ ⇌ SO ₃ ²⁻ + H ⁺	9.850	-2.23	6.014 × 10 ⁻⁸
HNO ₃ (g) ⇌ H ⁺ + NO ₃ ⁻	-8.92	-17.46	3.460 × 10 ⁵
H ₂ O ₂ (g) ⇌ H ₂ O ₂ (l)		-14.5	7.1 × 10 ⁴
O ₃ (g) ⇌ O ₃ (l)		-5.04	9.4 × 10 ⁻³

It is interesting to note that at the pH commonly encountered in fogs (pH 2–6) all of the gaseous nitric acid and ammonia are absorbed by the droplets because of their acid-base chemistries in the liquid phase. For other gases absorption is limited.

Oxidation of S(IV) in the droplet is allowed to proceed along the major pathways discussed previously. The important oxidants are H₂O₂ and O₃; oxidation by dissolved O₂ may also be important if catalyzed by Fe³⁺ and Mn²⁺, for which the catalytic synergism noted in Chapter 2 is considered. Oxidation by NO_x and by O₂ catalyzed by trace metals other than Fe³⁺ and Mn²⁺ is ignored for the present time.

Speciation of Fe and Mn within the droplets may control their catalytic effectiveness. Fe and Mn are effective catalysts as long as they are dissolved (as free ions or complexes in solution); however, their catalytic properties are totally altered if they occur as solid phases. Surface catalysis may occur, but this possibility will not be considered here. The distribution of Fe and Mn species inside the fog droplets was obtained from typical values for the concentration of all major components of Los Angeles fog water with SURFEQL [172]. The results are shown in Figure 5. Mn²⁺ remains totally in solution at the pH values found in fog water, but Fe³⁺ starts to precipitate as Fe(OH)₃ above pH 4. At pH values above 5 no Fe³⁺ remains in solution; therefore, high pH values quench the iron-catalyzed S(IV) oxidation mechanism. Total soluble Fe³⁺, y, is given by the following relationship:

$$y = *K_{so}[\text{H}^+]^3 \alpha_0 \text{Fe}_T$$

where y is the dissolved fraction of the total iron in the system, $*K_{S0}$ is the solubility product constant for $\text{Fe}(\text{OH})_3$ (S), and α_0 is defined as follows:

$$\alpha_0 = (1 + \beta_1[\text{F}^-]^2 + \beta_2[\text{F}^-] + \beta_3[\text{SO}_3^{2-}] + *K_{11}/[\text{H}^+] + *K_{21}[\text{H}^+]^2)^{-1}$$

For all oxidation reactions the reaction rates and activation energies are chosen from the expressions suggested in Chapter 2 for atmospheric models, with speciation for Fe^{3+} added.

c. Physical Description

The model presented here uses a closed-box approximation. At $t = 0$, under conditions determined by the ambient saturation, size distribution and chemical composition of the CCN, water droplets suddenly form and grow subsequently by accretion of water vapor. Scavenging of the smaller aerosol particles by diffusion to the surface of the droplet is not included in the model.

The possible limitation of S(IV) oxidation reactions by mass transfer has been discussed [185,188,192,193]. Seinfeld [188] indicated that the liquid-phase chemical equilibria of concern are established very quickly and thus do not induce any rate limitations in the system. Schwartz and Freiberg [192,193] showed that, for stationary droplets smaller than $50 \mu\text{m}$, the rate was limited by the chemical oxidation rates. Baboolal et al. [185] extended this analysis by showing that for the few fog water droplets larger than $50 \mu\text{m}$ that exhibit a significant sedimentation velocity (as opposed to the smaller quasistationary droplets), forced convection both inside and outside the droplet enhances significantly the rates of mass transfer as calculated for stationary droplets. Because of this enhancement the diffusion rate still is faster than the S(IV) oxidation rate. Therefore, the chemical changes in fog droplets are most likely limited by the specific reaction rates.

Because fogs are generally localized events and occur on time scales of a few hours, usually under low wind conditions, no consideration of long-term transport of condensing/evaporating droplets was included in the model; also, evolution of the droplet spectrum through coagulation can be neglected since mass transfer does not limit the reaction kinetics. Droplet growth can simply be accounted for by the input of a time-dependent liquid water content (LWC), which is measured experimentally. Thus a reasonable physical description of the system in the model can be limited to the input of temperature and of a time-dependent LWC.

d. Mathematical Formulation

At time $t = 0$, droplets are assumed to suddenly condense in an atmospheric "closed box" containing ACCN and trace atmospheric gases; the instantaneous formation of these droplets is associated with a certain LWC. This LWC may be made to vary with time following either experimental observations or theoretical predictions [194]. In the results presented here, LWC will be taken to be constant. When the droplets form they receive an initial chemical loading from the water-

soluble fraction of the ACCN, immediately absorb atmospheric gases according to Henry's law and the liquid-phase equilibria of Table XIII are established. The concentrations of the species at equilibrium are obtained by solving the electroneutrality equation for a closed system (see appendix for details of the calculation).

Formation of S(VI) in the liquid phase is calculated over small time increments Δt by a forward finite-difference technique:

$$[\text{S(VI)}]_{t+\Delta t} = [\text{S(VI)}]_t + \left(\sum_{\text{ox}} \left(\frac{d[\text{S(VI)}]}{dt} \right)_{\text{ox}} \right) \Delta t \quad (228)$$

After each time step, changes in gas-phase concentrations from fresh emissions and NO_x oxidation are calculated, and the electroneutrality equation is solved to obtain the new equilibrium concentrations for the species in the system.

Time increments are taken as $\Delta t = 2 \times 10^{-4} n$ (minutes) where n is the time step number; this expression allows for a better resolution at the beginning of the fog event, where chemical changes are rapid. The use of smaller time steps did not change the calculation results.

4. Results and Discussion

The model was designed to interpret the results of the 1981-1982 fog sampling program [14] and to shed light on the relative importances of the various liquid-phase S(IV) oxidation mechanisms in ambient fog droplets. The present discussion will be limited to the latter point, in light of the fog water data collected in the Los Angeles basin [14] and the permanent atmospheric chemistry records of the Air Quality Management District.

The following pre-fog nighttime gas-phase concentrations were assumed for all model runs:

- $\text{CO}_2 = 3.3 \times 10^5$ ppb,
- $\text{NO} = 100$ ppb,
- $\text{NO}_2 = 50$ ppb,
- $\text{NH}_3 = 5$ ppb,
- $\text{HNO}_3 = 3$ ppb, and
- $\text{SO}_2 = 20$ ppb.

In cases H and I, different levels and emission rates for NO and NO_2 are considered.

Gas emission sources per liter of basin air were taken to be

- $\delta_{\text{NO}} = 0.1 \text{ ppb} \cdot \text{min}^{-1} \cdot \text{L}^{-1}$,
- $\delta_{\text{NO}_2} = 0.01 \text{ ppb} \cdot \text{min}^{-1} \cdot \text{L}^{-1}$,
- $\delta_{\text{SO}_2} = 0.05 \text{ ppb} \cdot \text{min}^{-1} \cdot \text{L}^{-1}$, and
- $\delta_{\text{NH}_3} = 0.005 \text{ ppb} \cdot \text{min}^{-1} \cdot \text{L}^{-1}$.

Concentrations of gas-phase ozone at night range from 0 to 30 ppb. There is some evidence of nighttime diffusion of ozone from the upper atmosphere down to the boundary layer as ozone is depleted near the ground by gas-phase oxidation reactions [195]; this source term will be ignored for now. Because NO is usually in excess of O₃, the additional ozone would merely oxidize part of the excess NO and thus have little effect on the droplet chemistry.

Hydrogen peroxide levels are poorly documented, and the reliability of the few existing measurements has been questioned; a concentration range of 1-5 ppb will be assumed. Hydrogen peroxide is not considered to be an important oxidant for nighttime gas-phase NO_x chemistry.

A major feature of the Los Angeles fog water as shown in Table I is the high levels of trace metals. The model calculations were performed for the ranges observed, which are 20-200 μeq-L⁻¹ for Fe³⁺ and 1-10 μeq-L⁻¹ for Mn²⁺. For all runs a typical value of 20 was taken for the Fe/Mn ratio in equivalents. Table XIV gives concentration conditions imposed on the model calculations.

Calculations were first made under conditions typical of Los Angeles fog with a temperature of 10° C, a LWC of 1 g-m⁻³, prefog conditions of 1 ppb H₂O₂ and 10 ppb O₃ and trace metal levels in the droplets of 100 μeq-L⁻¹ for Fe and 5 μeq-L⁻¹ for Mn. Synergism between Fe and Mn was considered for S(IV) oxidation, and the ACCN were assumed to be NaCl or some other neutral aerosol. The results of the calculations are shown in Figure 6.

A basic feature of S(IV) nighttime oxidation is that the strong oxidants (H₂O₂ and O₃) are not resupplied to the atmosphere in the absence of the daytime photochemical reactions. As seen in Figure 6, 10 min after fog formation, H₂O₂ and O₃ no longer contribute to S(IV) oxidation because they have been totally depleted from the atmosphere, H₂O₂ by S(IV) liquid-phase oxidation and O₃ by S(IV) liquid-phase oxidation and NO_x gas-phase oxidation. Hydrogen peroxide is an efficient liquid-phase oxidant because it is very soluble in water, has rapid oxidation rates at low pH, and is not depleted at a significant level by gas-phase oxidation reactions. On the other hand, O₃ is poorly soluble; its rate for oxidizing S(IV) drops dramatically as pH decreases; and it reacts quickly with NO in the gas phase to form NO₂. Hydrogen peroxide is thus a very effective oxidant for S(IV) in ambient fog water, whereas oxidation by O₃ is relatively insignificant.

In addition, it is apparent from the model calculations that rapid reaction of O₃ with NO not only prevents liquid-phase S(IV) oxidation by O₃ but also gas-phase NO₂ oxidation by O₃, which is the rate-limiting reaction for the formation of nitric acid at night; thus, there is no nitrate formation during a nighttime fog event (although the fog water may have a high nitrate concentration because of the scavenging of nitrate particles and of the prefog gaseous nitric acid).

Finally, the most striking result of the calculations is the dominating role of metal-catalyzed oxidation, which accounts for more than 90% of the S(VI) formed in the liquid phase four hours after the beginning of the fog event. Unlike H₂O₂ and O₃, there is an infinite supply of O₂, and concentrations of Fe and Mn in Los Angeles fog water are high enough to make O₂ an effective oxidant. Although the corresponding oxidation rates exhibit an inverse dependence on H⁺

Table XIV. Atmospheric Conditions for the Fog Events Simulated by the Model*

Concentrations of Atmospheric Gases (ppb)	Case									
	A	B	C	D	E	F	G	H	I	
H ₂ O	1	1	1	5	1	1	1	1	1	1
O ₃	10	10	10	10	10	10	10	10	10	10
NO	100	100	100	100	100	100	100	100	5	0
NO ₂	50	50	50	50	50	50	50	50	10	0
Aqueous-Phase Metal Concentrations (μeq-L ⁻¹)										
Fe ³⁺	100	20	100	100	100	100	100	100	100	100
Mn ²⁺	5	1	5	5	5	5	5	5	5	5
Sources of NO _x (ppb-min ⁻¹)										
δ _{NO}	0.1	0.1	0.1	0.1	0.1	0.1	0.1	0.1	10 ⁻³	0
δ _{NO₂}	0.01	0.01	0.01	0.01	0.01	0.01	0.01	0.01	10 ⁻⁴	0
ACCN Composition	NaCl	NaOH	NaCl	NaCl						
Synergism, Fe/Mn	Yes	Yes	No	Yes	Yes	Yes	Yes	Yes	Yes	Yes
Temperature (C)	10	10	10	10	25	10	10	10	10	10

* Additional conditions: 330 ppm CO₂, 3 ppb HNO₃, 5 ppb NH₃, 20 ppb SO₂, δ_{NO₂} = 0.05 ppb-min⁻¹, δ_{Mn₂} = 0.005 ppb-min⁻¹ and LWC = 1 g-m⁻³.

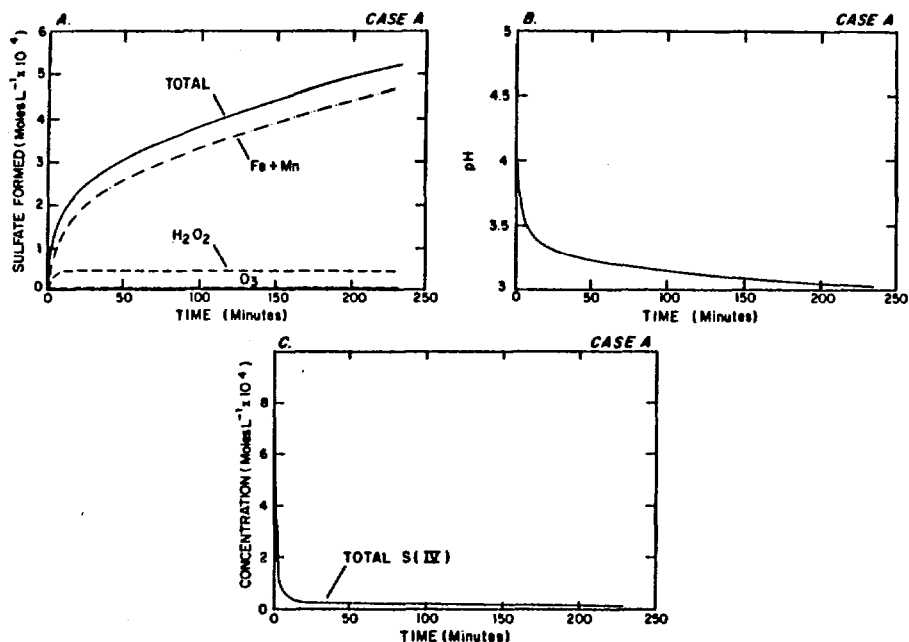


Figure 6. Sulfate formed, pH and total S(IV) for the fog water as a function of time after fog formation, under conditions typical of the Los Angeles atmosphere (case A): 20 ppb SO₂, 10 ppb O₃, 1 ppb H₂O₂ in the pre-fog gas phase, metal aqueous-phase concentrations of 100 μeq-L⁻¹ Fe³⁺ and 5 μeq-L⁻¹ Mn²⁺.

concentration, dissolution of the ferric hydroxide precipitate below pH 4 maintains oxidation rates at a high level at the low pH values characteristic of Los Angeles fog water. Even at the lowest concentrations of metals found in the fog water (Case B, Figure 7) and in the absence of synergism between Fe and Mn catalytic effects (Case C, Figure 7), metal-catalyzed oxidation is still the major source of S(VI) formation.

It should not, however, be concluded from the above results that H₂O₂ is only a minor contributor to S(IV) oxidation. Because no reliable method exists for measuring gas-phase H₂O₂, its levels in the atmosphere are uncertain; at concentrations higher than the 1 ppb considered in Case A it may be an important oxidant. This is illustrated by Case D (Figure 8), where a pre-fog H₂O₂ level of 5 ppb is assumed; the contribution of H₂O₂ to S(IV) oxidation is then important, and dominates oxidation processes until two hours after fog formation. High levels of H₂O₂ also slow down the metal-catalyzed oxidation kinetics because of the abrupt pH drop associated with the rapid quantitative depletion of H₂O₂.

Temperature dependence of the chemical composition of the droplet was studied by raising the temperature in Case A from 10 to 25 C (Case E, Figure 8). At this higher temperature the oxidation rates are higher, but the solubilities

of the gases are lower. These opposite effects make the system rather stable to changes in temperature. Comparing Cases A and E 4 h after fog formation, somewhat more S(VI) has been produced at the higher temperature (700 μmol-L⁻¹ at 25° C vs 520 μmol-L⁻¹ at 10 C) while the pH is slightly lower (2.9 at 10° C vs 3.05 at 25° C). Oxidation of S(IV) by ozone becomes totally unimportant at 25° C, as ozone is even less soluble than at 10 C.

The effect of droplet "background" acidity was investigated by calculating the chemical content of the droplets in Case F of acid ACCN (1 μmol-m⁻³ of HNO₃) and in Case G of basic ACCN (1 μmol-m⁻³ of NaOH). These cases yielded "initial pH values" of 3.03 and 6.50, respectively; the calculated results are shown in Figure 9 (cases F and G). The effects of the pH changes are damped by the slow S(IV) metal catalyzed oxidation rates at low pH, and after 4 h, the pH values are reasonably close at 2.90 and 3.15, respectively. However, six times more sulfate is formed in the initially "basic" droplet. A main feature of this latter case is that the high initial pH allows for a much higher rate of S(IV) oxidation by O₃, which then becomes a major contributor to S(IV) oxidation.

In urban air, the levels of NO at dusk are generally higher than those of

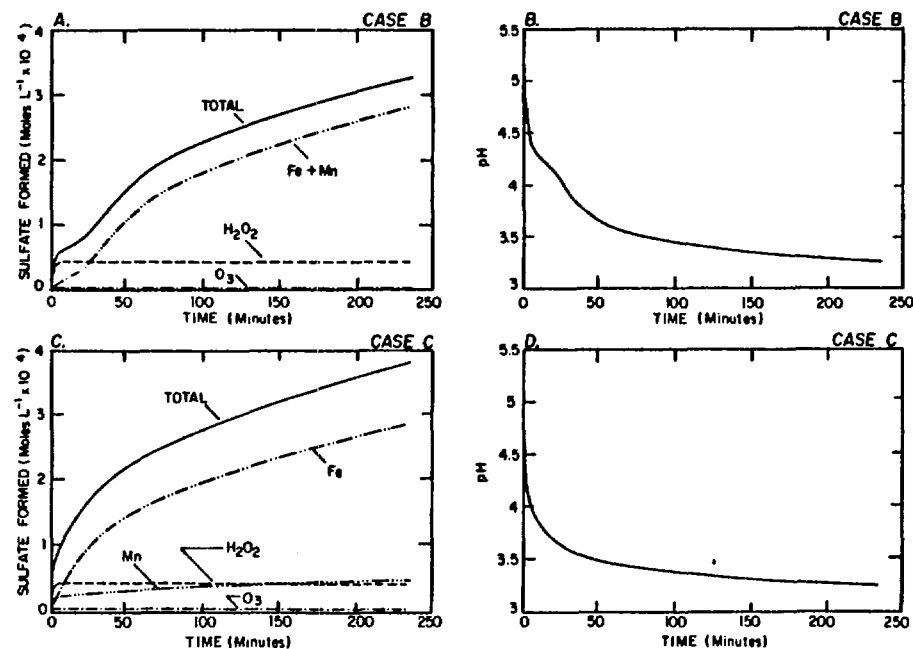


Figure 7. Sulfate formed and pH for the fog water as a function of time after fog formation, when Fe³⁺ = 20 μeq-L⁻¹ and Mn²⁺ = 1 μeq-L⁻¹ (case B) which are the lows observed in the Los Angeles fog water, or when no synergism for iron- and manganese-catalyzed oxidation mechanisms is considered (case C).

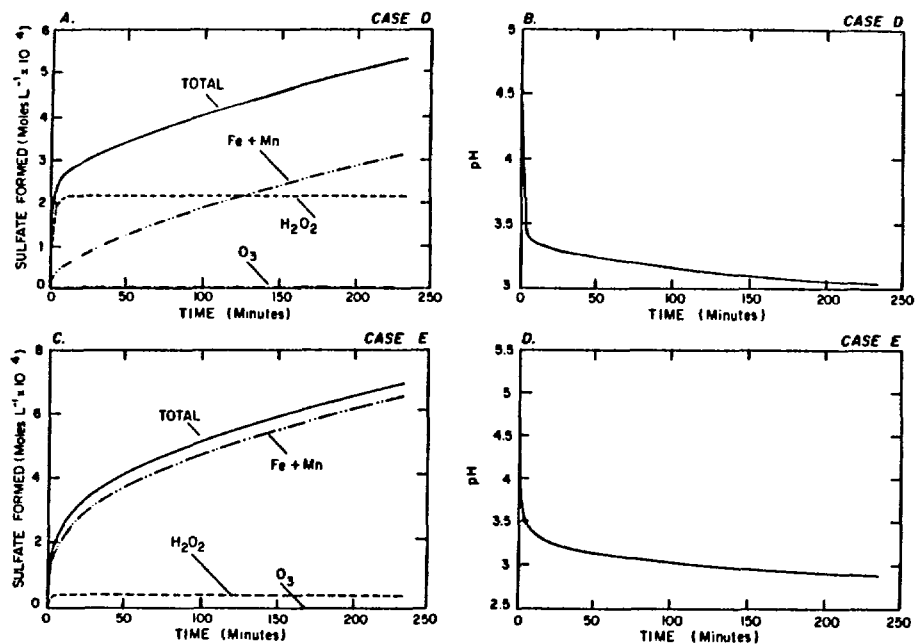


Figure 8. Sulfate formed and pH for the fog water as a function of time after fog formation, when $\text{H}_2\text{O}_3 = 5$ ppb in the pre-fog gas phase (case D), or when the temperature is 25 C (case E).

O_3 , and the gas-phase oxidation of NO by O_3 depletes all the O_3 from the system. However, it may happen that ozone will be in excess of NO; in that case, after the oxidation of all the NO to form NO_2 , there will be ozone available to oxidize both NO_2 in the gas phase to form nitric acid and S(IV) in the liquid phase to form S(VI). Figure 10 illustrates the chemical behavior of the fog under conditions of Case H, where ozone is in excess of NO. Comparing the results to those of Case A, one observes a slight increase in the ozone contribution to the S(IV) liquid-phase oxidation, but mostly a large amount of nitrate formed. After NO is depleted, the slow gas-phase oxidation of NO_2 to HNO_3 thus becomes the dominant pathway for ozone removal from the system. Less sulfate is then formed because of the drop in pH due to the incorporation in the droplet of the nitric acid. It is interesting to note that under conditions of a NO_x -free atmosphere (Case I, Figure 10) one does not observe an increase in the production of S(VI) by ozone as compared to Case H; this shows that production is not limited by competition from gas-phase NO_2 oxidation but rather by the inefficacy of ozone as a liquid-phase oxidant for S(IV) in low pH solutions. It is observed from the model calculations that there is no oxidation of S(IV) by ozone below pH 4 regardless of the NO_2 concentrations.

Overall the results of this dynamic model reveal some important features

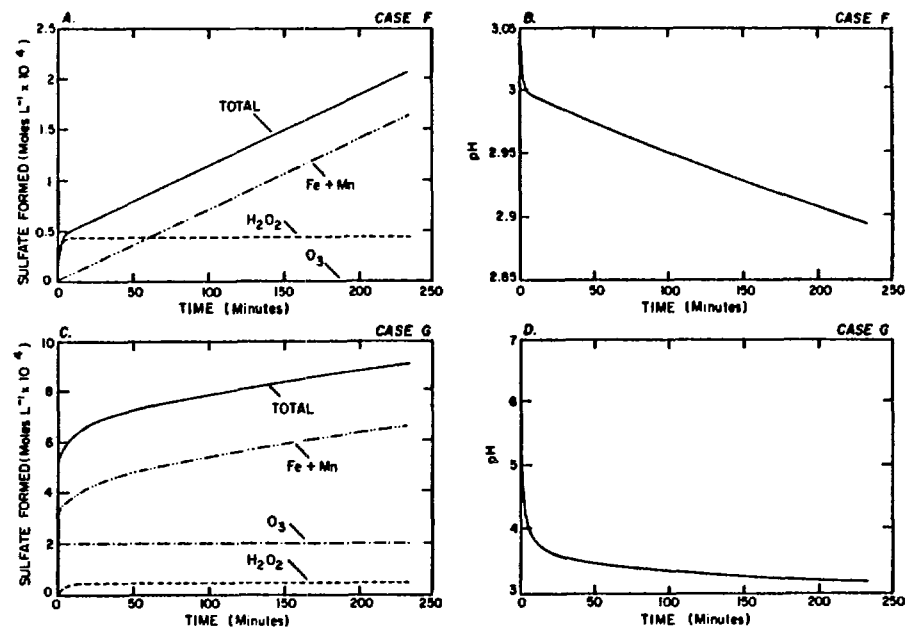


Figure 9. Sulfate formed and pH for the fog water as a function of time after fog formation, when condensation takes place on HNO_3 ACCN (case F), or on NaOH ACCN (case G).

of S(IV) liquid-phase oxidation in the fogwater of polluted atmospheres. They are:

1. The main contributor to S(VI) formation in the aqueous phase at night is metal-catalyzed oxidation of S(IV). This conclusion may be challenged because of the lack of definitive data for H_2O_2 concentrations in the atmosphere, which makes our estimated value of 1 ppb no more than an educated guess; it still appears that metal-catalyzed oxidation is more important in polluted atmospheres than has been hitherto recognized.
2. S(IV) oxidation by ozone is insignificant because of a combination of slow oxidation rates at low pH, poor ozone solubility and depletion of ozone in the gas phase by oxidation of NO.
3. S(IV) oxidation by H_2O_2 is very rapid, but is limited by the amount of H_2O_2 originally present in the system.
4. Precipitation of ferric hydroxide at pH 4, with the accompanying loss (or modification) of its catalytic properties, requires that Fe^{3+} speciation be taken into account in the development of atmospheric water chemistry models.
5. If the level of NO is higher than that of O_3 , there is no nitrate formation in the fog. If it is lower than that of O_3 , O_3 will first oxidize NO very quickly to form NO_2 and then slowly oxidize NO_2 to form NO_3 , which

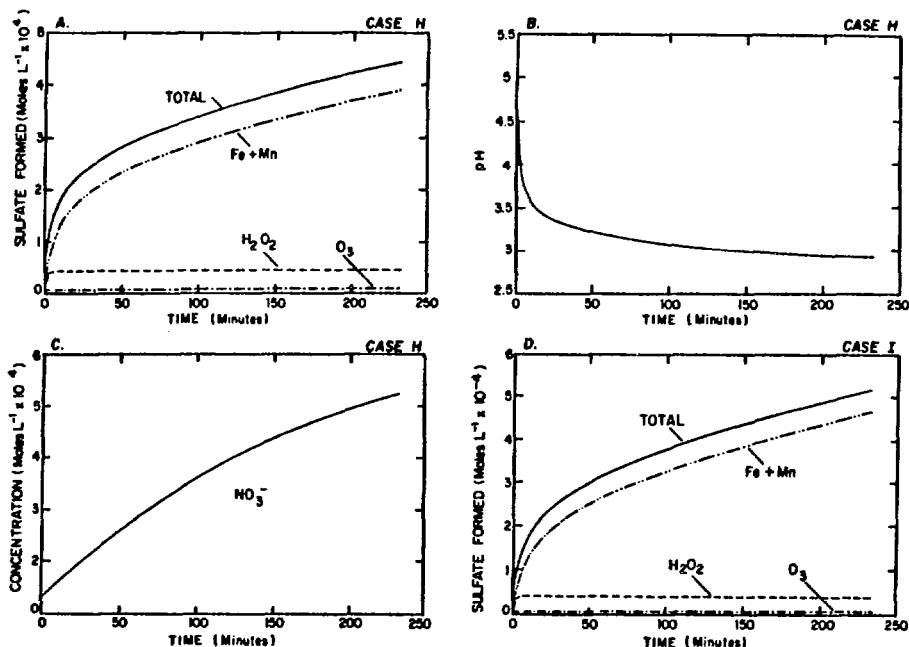


Figure 10. Sulfate formed, pH and nitrate for the fog water as a function of time after fog formation when ozone is in excess of NO (case H), and sulfate formed under conditions of a NO_x-free atmosphere (case I).

will then react to produce nitric acid. The rate of S(IV) oxidation by ozone in such a system is not limited by the amount of NO₂ in the atmosphere but by the pH of the fog water. Below pH 4 it is insignificant.

5. Conclusion

In heavily polluted atmospheric water droplets, such as those found in urban fogs, the model presented here shows that metal-catalyzed S(IV) oxidation is a significant contributor to formation of S(VI) in the liquid phase, and apparently is more important than oxidation by H₂O₂. Under conditions typical of the Los Angeles area, liquid-phase oxidation of S(IV) to S(VI) is found to account for sulfate concentrations in the range of 5 × 10⁻⁴ mole-L⁻¹ 4 h after fog formation. Waldman et al. [14] found sulfate concentrations ranging from 5 × 10⁻⁴ to 2 × 10⁻³ mole-L⁻¹ in the fog. Direct comparison of our calculated values with the field data is difficult, since Waldman et al. did not measure the LWC of the fogs they studied; nevertheless, it appears clearly that absorption of SO₂ followed by liquid-phase oxidation is an important mechanism for explaining the sulfate concentrations in polluted fog water.

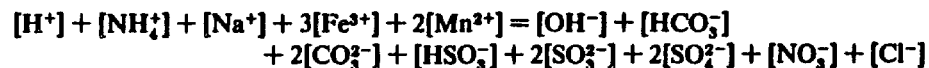
The present model needs to be refined further; the main limitations now are the failure to include organic complexing agents and reductants and the rather simplistic treatment of the formation of complexes. Absorption of formaldehyde followed by formation of its sulfite complex (HOCH₂SO₃⁻) must be considered in an advanced model; including this complex and others requires the use of multidimensional calculation routines such as SURFEQL to obtain the equilibrium concentrations of the species in the droplet.

ACKNOWLEDGMENTS

The authors acknowledge gratefully the financial support of the U.S. Environmental Protection Agency (Grant No. R808086-1) and the President's Fund/Sloan Foundation Grant administered by the California Institute of Technology. They are also grateful to S. Schwartz, J. Seinfeld and G. McRae for their helpful comments.

D. APPENDIX: THE ELECTRONEUTRALITY EQUATION

The ionic species in the fog droplets must satisfy the following electroneutrality equation:



where the iron and manganese complexes have been omitted for now to allow the equation to be solved by the one-dimensional Newton's method. Fe³⁺ and Mn²⁺ are assumed to be introduced in the liquid phase through ACCN containing FeCl₃ and MnCl₂.

In the closed two-phase system considered here the mass balance equation for component A can be written:

$$A_T = \frac{P_A}{RT} + L[A(aq)]$$

where P_A = atmospheric partial pressure of A
 [A(aq)] = concentration of A in the liquid phase (where A may be distributed among different species)
 L = LWC (liters of water per liters of air)
 A_T = total double-phase concentration of A in a liter of air (note that L ≪ 1); a constant for the system

For sulfur(IV), for example,

$$S_T = \frac{P_{SO_2}}{RT} + L([SO_2(l)] + [HSO_3^-] + [SO_3^{2-}])$$

From Table XIII:

$$K_7 = \frac{[SO_2(l)]}{P_{SO_2}}$$

$$K_8 = \frac{[HSO_3^-][H^+]}{[SO_2(l)]}$$

$$K_9 = \frac{[SO_3^{2-}][H^+]}{[HSO_3^-]}$$

which yields

$$[SO_3^{2-}] = \frac{K_7 K_8 K_9 S_T}{[H^+]^2} \left(\frac{1}{\frac{1}{RT} + L \left(K_7 + \frac{K_7 K_8}{[H^+]} + \frac{K_7 K_8 K_9}{[H^+]^2} \right)} \right)$$

In this manner the electroneutrality equation can be rewritten:

$$\begin{aligned} [H^+] + \frac{K_5 K_6 [H^+]}{K_w} \left(\frac{[NH_3]_T}{\frac{1}{RT} + L \left(K_5 + \frac{K_5 K_6 [H^+]}{K_w} \right)} \right) + [Na^+] + 3[Fe^{3+}] + 2[Mn^{2+}] \\ = \frac{K_w}{[H^+]} + \frac{K_2 K_3}{[H^+]} P_{CO_2} + \frac{2K_2 K_3 K_4}{[H^+]^2} P_{CO_2} + \frac{K_7 K_8}{[H^+]} \\ \times \left(\frac{S_T}{\frac{1}{RT} + L \left(K_7 + \frac{K_7 K_8}{[H^+]} + \frac{K_7 K_8 K_9}{[H^+]^2} \right)} \right) \\ + \frac{2K_7 K_8 K_9}{[H^+]^2} \left(\frac{S_T}{\frac{1}{RT} + L \left(K_7 + \frac{K_7 K_8}{[H^+]} + \frac{K_7 K_8 K_9}{[H^+]^2} \right)} \right) \\ + 2[SO_3^{2-}] + \frac{K_{11}}{[H^+]} \frac{[NO_3]_T}{\frac{1}{RT} + \frac{LK_1}{[H^+]}} + [Cl^-] \end{aligned}$$

which is of the form $f([H^+]) = 0$ and is readily solved by Newton's method.

E. REFERENCES

1. Calvert, J.G., F. Su, J.W. Bottenheim and O.P. Strausz. "Mechanisms of Homogeneous Oxidation of Sulfur Dioxide in the Troposphere," *Atmos. Environ.* 12:197-226 (1978).
2. Middleton, P., C.S. Kiang and V.A. Mohnen. "Theoretical Estimates of the Relative Importance of Various Urban Sulfate Aerosol Production Mechanisms," *Atmos. Environ.* 14:463-472 (1980).
3. Möller, D. "Kinetic Model of Atmospheric Oxidation Based on Published Data," *Atmos. Environ.* 14:1067-1076 (1980).
4. Cass, G.R., and F.H. Shair. "Transport of Sulfur Oxides Within the Los Angeles Sea Breeze/Land Breeze Circulation System," in *Proceedings of the Second Joint Conference on Applications of Air Pollution Meteorology* (American Meteorological Society, 1980), pp. 320-327.
5. Cass, G.R. "Methods for Sulfate Air Quality Management with Applications to Los Angeles," PhD Thesis, California Institute of Technology, Pasadena, CA (1977).
6. Cox, R.A. "Particle Formation from Homogeneous Reactions of Sulfur Dioxide and Nitrogen Dioxide," *Tellus* 26:235-240 (1974).
7. McMurry, P.H., D.J. Rader and J.L. Smith. "Studies of Aerosol Formation in Power Plant Plumes. I. Parameterization of Conversion Rate for Dry, Moderately Polluted Ambient Conditions," *Atmos. Environ.* 15:2315-2329 (1981).
8. Smith, F.B., and G.H. Jeffrey. "Airborne Transport of Sulphur Dioxide from the U.K.," *Atmos. Environ.* 9:643-659 (1975).
9. Wilson, J.C., and P.H. McMurry. "Studies of Aerosol Formation in Power Plant Plumes—I. Secondary Aerosol Formation in the Navajo Generating Station Plume," *Atmos. Environ.* 15:2329-2339 (1981).
10. Liljestrand, H.M., and J.J. Morgan. "Spatial Variation of Acid Precipitation in Southern California," *Environ. Sci. Technol.* 15:333-339 (1981).
11. Gartrell, J.E., J.W. Thomas and S.B. Carpenter. "Atmospheric Oxidation of SO₂ in Coal-Burning Power Plant Plumes," *Am. Ind. Hyg. Assoc. Quart.* 24:113-120 (1963).
12. Diffenheoffer, A.C., and R.G. dePena. "A Study of Production and Growth of Sulfate Particles in Plumes from a Coal-Fired Power Plant," *Atmos. Environ.* 12:297-306 (1978).
13. Enger, L., and U. Hogstrom. "Dispersion and Wet Deposition of Sulfur from a Power Plant Plume," *Atmos. Environ.* 13:797-810 (1979).
14. Waldman, J.M., J.W. Munger, D.J. Jacob, R.C. Flagan, J.J. Morgan and M.R. Hoffmann. "Chemical Composition of Acid Fog," *Science* 218:677-680 (1982).
15. Hegg, D.A., and P.V. Hobbs. "Cloud Water Chemistry and the Production of Sulfates in Clouds," *Atmos. Environ.* 15:1597-1604 (1981).
16. "Guide for Air Pollution Avoidance. Appendix B. History of Episodes," PH-22-68-32, U.S. EPA (1971), pp. 123-135.
17. Wilkins, E.T. "Air Pollution and the London Fog of December, 1952," *J. Roy. San. Instit.* 74:1-21 (1954).
18. Wilkins, E.T. "Air Pollution Aspects of the London Fog of December, 1952," *J. Roy. Meteorol. Soc.* 80:267-278 (1954).
19. Holland, W.W. *Air Pollution and Respiratory Disease* (Westport, CT: Technomic Publishing Co., Inc., 1972), pp. 27-51.
20. Friedlander, S.K., and A.L. Ravimohan. "A Theoretical Model for the Effect of an

- Acute Air Pollution Episode on a Human Population," *Environ. Sci. Technol.* 2:1101-1108 (1968).
21. Larsen, R.I. "Relating Air Pollutant Effects to Concentration and Control," *J. Air Poll. Control Assoc.* 20:214-225 (1970).
 22. Cheng, R.T., M. Corn and J.O. Frohlinger. "Contributions to the Reaction Kinetics of Water-Solubles and SO₂ in Air at ppm Concentrations," *Atmos. Environ.* 5:987-1008 (1971).
 23. Beilke, S., and G. Gravenhorst. "Heterogeneous SO₂-Oxidation in the Droplet Phase," *Atmos. Environ.* 12:231-239 (1978).
 24. Dasgupta, P.K., P.A. Mitchell and P.W. West. "Study of Transition Metal-S(IV) Systems," *Atmos. Environ.* 13:775-782 (1979).
 25. Freiberg, J. "Effects of Relative Humidity and Temperature on Iron-Catalyzed Oxidation of SO₂ in Atmospheric Aerosols," *Environ. Sci. Technol.* 8:731-734 (1974).
 26. Fuzzi, S. "Study of Iron(III) Catalyzed Sulphur Dioxide Oxidation in Aqueous Solution over a Wide Range of pH," *Atmos. Environ.* 12:1439-1442 (1978).
 27. Hegg, D.A., and P.V. Hobbs. "Oxidation of Sulfur Dioxide in Aqueous Systems with Particular Reference to the Atmosphere," *Atmos. Environ.* 12:241-253 (1978).
 28. Kaplan, D.J., D.M. Himmelblau and C. Kanaoka. "Oxidation of Sulfur Dioxide in Aqueous Ammonium Sulfate Aerosols Containing Manganese as a Catalyst," *Atmos. Environ.* 15:763-773 (1981).
 29. Larson, T.V., N.R. Horike and H. Halstead. "Oxidation of Sulfur Dioxide by Oxygen and Ozone in Aqueous Solution: A Kinetic Study with Significance to Atmospheric Processes," *Atmos. Environ.* 12:1597-1611 (1978).
 30. Penkett, S.A., B.M.R. Jones and A.E.J. Eggleton. "A Study of SO₂ Oxidation in Stored Rainwater Samples," *Atmos. Environ.* 13:139-147 (1979).
 31. Hoffmann, M.R., and J.O. Edwards. "Kinetics and Mechanism of the Oxidation of Sulfur Dioxide by Hydrogen Peroxide in Acidic Solution," *J. Phys. Chem.* 79:2096-2098 (1975).
 32. Penkett, S.A., B.M.R. Jones, K.A. Brice and A.E.J. Eggleton. "The Importance of Atmospheric Ozone and Hydrogen Peroxide in Oxidizing Sulfur Dioxide in Cloud and Rainwater," *Atmos. Environ.* 13:123-137 (1979).
 33. Martin, L.R., and D.E. Damschen. "Aqueous Oxidation of Sulfur Dioxide by Hydrogen Peroxide at Low pH," *Atmos. Environ.* 15:1615-1622 (1981).
 34. Martin, L.R., D.E. Damschen and H.S. Judeikis. "Sulfur Dioxide Oxidation Reactions in Aqueous Solution," EPA 600/7-81-085, U.S. EPA (1981).
 35. Thornton, J.D. "The Metal and Strong Acid Composition of Rain and Snow in Minnesota: Land Use Effects," MS Thesis, University of Minnesota, Minneapolis, MN (1981).
 36. Overton, J.H., V.P. Aneja and J.L. Durham. "Production of Sulfate in Rain and Raindrops in Polluted Atmospheres," *Atmos. Environ.* 13:355-367 (1979).
 37. Brimblecombe, P., and D.J. Spedding. "The Catalytic Oxidation of Micromolar Aqueous Sulphur Dioxide," *Atmos. Environ.* 8:937-945 (1974).
 38. Middleton, P., C.S. Kiang and V.A. Mohnen. "Theoretical Estimates of the Relative Importance of Various Urban Sulfate Aerosol Production Mechanisms," *Atmos. Environ.* 14:463-472 (1980).
 39. Barrie, L.A., and H.W. Georgii. "An Experimental Investigation of the Absorption of Sulfur Dioxide by Water Drops Containing Heavy Metal Ions," *Atmos. Environ.* 10:743-749 (1976).
 40. Hoffmann, M.R., and S.D. Boyce. "Catalytic Autoxidation of Aqueous Sulfur Dioxide in Relationship to Atmospheric Systems." *Adv. Environ. Sci. Tech.* 12, 148-189 Wiley-Interscience, New York (1983).
 41. Mader, P.M. "Kinetics of the Hydrogen Peroxide-Sulfite Reaction in Solution," *J. Am. Chem. Soc.* 80:2634 (1958).
 42. Halperin, J., and H. Taube. "The Transfer of Oxygen Atoms in Oxidation-Reduction Reactions. IV. The Reaction of Hydrogen Peroxide with Sulfite and Thiosulfate, and of Oxygen, Manganese Dioxide and Permanganate with Sulfite," *J. Am. Chem. Soc.* 74:380-382 (1952).
 43. Harrison, H., T.V. Larson and C.S. Monkman. "Aqueous Phase Oxidation of Sulfites by Ozone in the Presence of Iron and Manganese," *Atmos. Environ.* 16:1039-1041 (1982).
 44. Hoffmann, M.R. "Trace Metal Catalysis in Aquatic Environments," *Environ. Sci. Technol.* 14:1061-1066 (1980).
 45. Frank, S.N., and A.J. Bard. "Heterogeneous Photocatalytic Oxidation of Cyanide and Sulfite in Aqueous Solution at Semiconductor Powders," *J. Phys. Chem.* 81:1484-1488 (1977).
 46. Mishra, G.C., and R.D. Srivastava. "Homogeneous Kinetics of Potassium Sulfite Oxidation," *Chem. Eng. Sci.* 31:969-971 (1976).
 47. Borekov, G.K., R.A. Buyanov and A.A. Ivanov. "Kinetics of Sulfur Dioxide on Vanadium Catalysts," *Kinetika Kataliz* 8:153-159 (1967).
 48. Sung, W., and J.J. Morgan. "Kinetics and Products of Ferrous Iron Oxygenation in Aqueous Systems," *Environ. Sci. Technol.* 14:561-568 (1981).
 49. Beilke, S., and G. Gravenhorst. "Heterogeneous SO₂-Oxidation in the Droplet Phase," *Atmos. Environ.* 12:231-239 (1978).
 50. Bäckström, H. "Der Kettenmechanismus bei der Autoxydation von Natriumsulfittlösungen." *Z. Physik. Chem.* 25B:122-138 (1934).
 51. Moore, J.W., and R.G. Pearson. *Kinetics and Mechanism* (New York: Wiley-Interscience, 1981).
 52. Boudart, M. *The Kinetics of Chemical Processes* (Englewood Cliffs, NJ: Prentice-Hall, Inc., 1968), pp. 246.
 53. Coughanowr, D.R., and F.E. Krause. "The Reaction of SO₂ and O₂ in Aqueous Solutions of MnSO₄," *Ind. Eng. Chem. Fund.* 4:61-66 (1965).
 54. Ibusuki, T. "Manganese(II) Catalyzed Sulfur Dioxide Oxidation in Aqueous Solution at Environmental Concentrations over a Wide Range of pH," *Atmos. Environ.* (in press).
 55. Matteson, J.J., W. Stöber and H. Luther. "Kinetics of the Oxidation of Sulfur Dioxide by Aerosols of Manganese Sulfate," *Ind. Eng. Chem. Fund.* 8:677-684 (1969).
 56. Lunak, S., A. El-Wakil and J. Veprek-Siska. "Autoxidation of Sulfite Catalyzed by 3d Transition Metals and Inhibited by 2-Propanol: Mechanism of Inhibited and Induced Reactions," *Coll. Czech. Chem. Comm.* 43:3306-3316 (1978).
 57. Aubuchon, C. "The Rate of Iron Catalyzed Oxidation of Sulfur Dioxide by Oxygen in Water," PhD Thesis, Johns Hopkins University, Baltimore, MD (1976).
 58. Chen, T.I., and C.H. Barron. "Some Aspects of the Homogeneous Kinetics of Sulfite Oxidation," *Ind. Eng. Chem. Fund.* 11:466-470 (1972).
 59. Sawicki, J.E., and C.H. Barron. "On the Kinetics of Sulfite Oxidation in Heterogeneous Systems," *Chem. Eng. J.* 5:153-159 (1973).
 60. Bengtsson, S., and I. Bjerle. "Catalytic Oxidation of Sulphite in Dilute Aqueous Solutions," *Chem. Eng. Sci.* 30:1429-1435 (1975).

61. Yagi, S., and H. Inoue. "The Absorption of Oxygen into Sodium Sulfite Solution," *Chem. Eng. Sci.* 17:411-421 (1962).
62. Davies, R., A.K.E. Hagopian and A.G. Sykes. "Kinetic and Oxygen-18 Tracer Studies on the Reaction of Sulphite with the Superoxo-Complex $(\text{NH}_3)_5\text{Co}\cdot\text{O}_2\cdot\text{Co}(\text{NH}_3)_5^{2+}$ in Aqueous Media," *J. Chem. Soc. (A)*:623-629 (1969).
63. Linek, V., and J. Mayrhoferova. "The Kinetics of Oxidation of Aqueous Sodium Sulfite Solution," *Chem. Eng. Sci.* 25:787-800 (1970).
64. Mishra, G.C., and R.D. Srivastava. "Kinetics of Oxidation of Ammonium Sulfite by Rapid-Mixing Method," *Chem. Eng. Sci.* 30:1387-1390 (1975).
65. Fuller, E.C., and R.H. Crist. "The Rate of Oxidation of Sulfite Ions by Oxygen," *J. Am. Chem. Soc.* 63:1644-1650 (1941).
66. Barron, C.H., and H.A. O'Hern. "Reaction Kinetics of Sodium Sulfite by the Rapid-Mixing Method," *Chem. Eng. Sci.* 21:397-404 (1966).
67. Hayon, E., A. Treinin and J. Wilf. "Electronic Spectra, Photochemistry, and Autoxidation Mechanism of the Sulfite-Bisulfite-Pyrosulfite Systems. The SO_2^- , SO_3^- , and $\text{SO}_3^{\cdot-}$ Radicals," *J. Am. Chem. Soc.* 94:47-57 (1972).
68. Schmittkuz, H. "Chemilumineszenz der Sulfitooxidation," Dissertation, Naturwissenschaftliche Fakultät, Frankfurt (1963).
69. Bassett, H., and W.G. Parker. "The Oxidation of Sulphurous Acid," *J. Chem. Soc.* (1951), pp. 1540-1560.
70. King, E.L., and C. Altman. "A Schematic Method of Deriving the Rate Laws for Enzyme Catalyzed Reactions," *J. Phys. Chem.* 60:1375-1378 (1956).
71. Freiberg, J. "The Mechanism of Iron-Catalyzed Oxidation of SO_2 ," *Atmos. Environ.* 9:661-672 (1975).
72. Bracewell, J.M., and D. Gall. "The Catalytic Oxidation of Sulfur Dioxide in Solution at Concentrations Occurring in Fog Droplets," paper presented at the Symposium on Physio-chemical Transformation of Sulfur Compounds in the Atmosphere and the Formation of Acid Smogs, Mainz, Germany, 1967.
73. Hoather, R.C., and C.F. Goodeve. "The Oxidation of Sulphurous Acid III. Catalysis by Manganous Sulphate," *Trans. Faraday Soc.* 30:1149-1156 (1934).
74. Neytzell-deWilde, F.G., and L. Taverner. "Experiments Relating to Possible Production of Air Oxidizing Acid Lachur by Autoxidation for the Extraction of Uranium," *2nd U.N. Intl. Conf. Peaceful Uses for Atomic Energy Proc.* 3:303-317 (1958).
75. Karraker, D.G. "The Kinetics of the Reaction Between Sulfurous Acid and Ferric Ion," *J. Phys. Chem.* 67:871-874 (1963).
76. Pollard, F.H., P. Hanson and G. Nickless. "Chromatographic Studies on the Oxidation of Sulphurous Acid by Ferric Iron in Aqueous Acid Solution," *J. Chromatog.* 5:68-73 (1961).
77. Carlyle, D.W. "A Kinetic Study of the Aqation of Sulfitoiron(III) Ion," *Inorg. Chem.* 10:761-764.
78. Lancaster, J.M., and R.S. Murray. "The Ferricyanide-Sulphite Reaction," *J. Chem. Soc.* (1971), pp. 2755-2758.
79. Veprek-Siska, J., D.M. Wagnerova, and K. Eckschlager. "Einäquivalent-Oxydationen. II. Sulfitoxydation Durch Komplexionen," *Coll. Czech. Chem. Comm.* 31:1248-1255 (1966).
80. Veprek-Siska, J., A. Solcova and D.M. Wagnerova. "Einäquivalent-Oxydationen. III. Kinetik der Sulfitoxydation Mittels Pentacyanoaquoferrats(III)," *Coll. Czech. Chem. Comm.* 31:3287-3298 (1966).
81. Carlyle, D.W., and O.T. Zeck, Jr. "Electron Transfer Between Sulfur(IV) and Hexa-aquoiron(III) Ion in Aqueous Perchlorate Solution. Kinetics and Mechanisms of Uncatalyzed and Cu(II)-Catalyzed Reactions," *Inorg. Chem.* 12:2978-2983.
82. Higginson, W.C.E., and J.W. Marshall. "Equivalence Changes in Oxidation-Reduction Reactions in Solution: Some Aspects of the Oxidation of Sulphurous Acid," *J. Chem. Soc.* (1957), pp. 447-458.
83. Reinders, W., and S.I. Vles. "The Catalytic Oxidation of Sulfites," *Rec. Trav. Chem.* 44:249-268 (1925).
84. Titoff, A. "Beiträge zur Kenntnis der Negativen Katalyse in Homogeneous System," *Z. Phys. Chem.* 45:641-683 (1903).
85. Latimer, W. M. *Oxidation Potentials* 2nd ed. (New York: Prentice-Hall, Inc., 1952).
86. Srivastava, R.D., A.F. McMillan and I.J. Harris. "The Kinetics of Oxidation of Sodium Sulphite," *Can. J. Chem. Eng.* 46:181-184 (1968).
87. Yatsimirskii, K., B. Bratushko, I. Yu and I.L. Zatsny. "Kinetics and Mechanism of the Reduction of Molecular Oxygen Coordinated in the Complex $\text{Co}_2(\text{L-histidine})_2\text{O}_2$ by Sodium Sulphite in Aqueous Solution," *Zh. Neorgan. Khimii.* 22:1611-1616 (1977).
88. Abel, E.W., J.M. Pratt and R. Whelan. "Formation of a 1:1 Oxygen Adduct with the Cobalt(II)-Tetrasulphophthalocyanine Complex," *Chem. Commun.* (1971), pp. 449-450.
89. Jones, R.D., D.A. Summerville and F. Basolo. "Synthetic Oxygen Carriers Related to Biological Systems," *Chem. Revs.* 79:139-179 (1979).
90. Hoffmann, M.R., and B.C.H. Lim. "Kinetics and Mechanism of the Oxidation of Sulfide by Oxygen: Catalysis by Homogeneous Metal-Phthalocyanine Complexes," *Environ. Sci. Technol.* 13:1406-1413 (1979).
91. Boyce, S.D., M.R. Hoffmann, P.A. Hong and L.M. Moberly. "Catalysis of the Autoxidation of Aquated Sulfur Dioxide by Homogeneous and Heterogeneous Transition Metal Complexes," in *Acid Rain, Vol. 1, Meteorological Aspects* (Ann Arbor, MI: Ann Arbor Science Publishers, 1983).
92. Laidler, K.J., and P.S. Bunting. *The Chemical Kinetics of Enzyme Action* (Oxford: Clarendon Press, 1973).
93. Carter, J.J., D.P. Rillema and F. Basolo. "Oxygen Carrier and Redox Properties of Some Neutral Cobalt Chelates," *J. Am. Chem. Soc.* 96:392-400 (1974).
94. Rollmann, L.D., and S.I. Chan. "Electron Spin Resonance Studies of Low-Spin Cobalt(II) Complexes. Base Adducts of Cobalt Phthalocyanine," *Inorg. Chem.* 10:1978-1982 (1971).
95. Cookson, D.J., T.D. Smith, J.F. Boas, P.R. Hicks and J.R. Pilbrow. "Electron Spin Resonance Study of the Autoxidation of Hydrazine, Hydroxylamine and Cysteine Catalyzed by the Cobalt(II) Chelate Complex of 3,10,17,24-Tetrasulphophthalocyanine," *J. Chem. Soc.* (1977), pp. 109-114.
96. Przywarska-Bonicecka, H., and K. Fried. "The Influence of Additional Ligands on Autoxidation of Cobalt and Iron 4,4',4",4"-Tetrasulfonated Phthalocyanines," *Roczniki Chemii.* 50:43-52 (1976).
97. Basolo, F., B. M. Hoffmann and J.A. Ibers. "Synthetic Oxygen Carriers of Biological Interest," *Accts. Chem. Res.* 8:384-392 (1975).
98. Schutten, J.H., and T.P.M. Beelen. "The Role of Hydrogen Peroxide During the Autoxidation of Thiols Promoted by Bifunctional Polymer-Bonded Cobalt Phthalocyanine Catalysts," *J. Mol. Catal.* 10:85-97 (1981).

99. Zika, R., and E. Saltzman. "Interaction of Ozone and Hydrogen Peroxide in Water: Implications for Analysis of H_2O_2 in Air," *Geophys. Res. Lett.* 9:213-234 (1982).
100. Egerton, A.C., A.J. Everett, G.J. Minkoff, S. Rudrakanchana and K.C. Salooja. "Some Improvements in the Methods of Analysis of Peroxides," *Anal. Chim. Acta* 10:422-429 (1954).
101. Holt, B.D., R. Kumar and P.T. Cunningham. "Oxygen-18 Study of the Aqueous Phase Oxidation of Sulfur Dioxide," *Atmos. Environ.* 15:557-566 (1981).
102. Frost, A.A., and R.G. Pearson. *Kinetics and Mechanism*. (New York: John Wiley & Sons, Inc., 1961).
103. Anast, J.M., and D.W. Margerum. "Trivalent Copper Catalysis of the Autoxidation of Sulfite. Kinetics and Mechanism of the Copper (III/II) Tetraglycine Reactions with Sulfite," *Inorg. Chem.* 20:2319-2326 (1981).
104. Edwards, J.O. *Inorganic Reaction Mechanisms* (Reading, MA: W.A. Benjamin, Inc., 1965).
105. Edwards, J.O., E.F. Greene and J. Ross. "From Stoichiometry and Rate Law to Mechanism," *J. Chem. Educ.* 45:381-385 (1968).
106. Bunnet, J.F. "From Kinetic Data to Reaction Mechanism," in *Investigation of Rates and Mechanisms of Reactions Part I*, 3rd ed., E.S. Lewis, Ed. (New York: Wiley-Interscience, 1974).
107. Smith, R.M., and A.M. Martell. *Critical Stability Constants, Vol. 4, Inorganic Complexes* (New York, Plenum Press, 1976).
108. Langford, C.H., and H.B. Gray. *Ligand Substitution Processes*. (Reading, MA: W.A. Benjamin, Inc., 1966).
109. Bernasconi, C.F. *Relaxation Kinetics* (New York: Academic Press, Inc., 1976).
110. Taube, H. *Electron Transfer Reactions of Complex Ions in Solution* (New York: Academic Press, Inc., 1970).
111. Fuoss, R.M. "Ion Association III. The Equilibrium Between Ion Pairs and Free Ions," *J. Am. Chem. Soc.* 80:5059-5061 (1958).
112. Davis, G.G., and W.F. Smith. "The Kinetics of the Formation of the Monosulphate Complex of Iron(III) in Aqueous Solution," *Can. J. Chem.* 40:1836-1845 (1962).
113. Basolo, F., and R.G. Pearson. *Mechanisms of Inorganic Reactions* (New York: John Wiley & Sons, Inc., 1967).
114. Groves, J.T. In: *Metal Ion Activation of Dioxygen*, T.G. Spiro, Ed. (New York: John Wiley & Sons, Inc., 1979).
115. Mathews, H.J., and L.H. Dewey. "A Quantitative Study of Some Photochemical Effects Produced by Ultra-Violet Light," *J. Phys. Chem.* 17:211-218 (1912).
116. Mathews, H.J., and M.E. Weeks. "The Effect of Various Substances on the Photochemical Oxidation of Solutions of Sodium Sulfite," *J. Am. Chem. Soc.* 39:635-647 (1917).
117. Mason, R.B., and J.H. Mathews. "The Effect of Ultra-Violet Light on the Oxidation of Sodium Sulfite by Atmospheric Oxygen," *J. Phys. Chem.* 30:414-420 (1926).
118. Alyea, H.N., and L.J. Bäckström. "The Inhibition Action of Alcohols on the Oxidation of Sodium Sulfite," *J. Am. Chem. Soc.* 51:90-109 (1929).
119. Haber, F., and O.H. Wansbrough-Jones. "Über die Einwirkung des Lichtes auf Sauerstofffreie und Sauerstoffhaltige Sulfittlösung," *Z. Phys. Chem.* B18:103-123 (1931).
120. Norman, R.O.C., and P.M. Storey. "Electron Spin Resonance Studies. Part XXXI. The Generation, and Some Reactions of the Radicals SO_3^- , $S_2O_3^-$, S^- and HS^- in Aqueous Solution," *J. Chem. Soc. (B)*:1009-1013 (1971).
121. Dogliotti, L., and E. Hayon. "Flash Photolysis Study of Sulfite, Thiocyanate and Thiosulfate Ions in Solution," *J. Phys. Chem.* 72:1800-1807 (1967).
122. Bäckström, H.L.J. "The Chain Reaction Theory of Negative Catalysis," *J. Am. Chem. Soc.* 49:1460-1472 (1927).
123. Bäckström, H.L.J. "Der Kettenmechanismus bei der Autoxydation von Aldehyden," *Z. Phys. Chem. (Leipzig)* B25:99-121 (1934).
124. Abel, E. "Zur Theorie der Oxydation von Sulfit zur Sulfat durch Sauerstoff," *Monatsch. Chem.* 82:815-834 (1951).
125. Matsuura, A., J. Harada, T. Akehata and T. Shirai. "Rate of Ammonium Sulfite Oxidation in Aqueous Solution," *J. Chem. Eng. Japan* 2:199-203 (1969).
126. Lunak, S., and J. Veprek-Siska. "Photochemical Autoxidation of Sulfite Catalyzed by Iron(III) Ions," *Coll. Czech. Chem. Commun.* 41:3495-3503 (1976).
127. Lunak, S., and J. Veprek-Siska. "Catalytic Effect of Metal Ions on Photochemical Reactions of Molecular Oxygen. III. Photochemical Autoxidation of Sulfite Catalyzed by Manganese(II) Ions," *Reac. Kin. Catal. Lett.* 5:157-161 (1976).
128. Veprek-Siska, J., S. Lunak and A. El-Wakil. "Catalytic Effect of Ferric Ions on the Photoinitiated Autoxidation of Sulfite," *Z. Naturforsch.* 29B:812-813 (1974).
129. Balzani, V., and V. Carassiti. *Photochemistry of Coordination Compounds* (New York: Academic Press, Inc., 1970).
130. Langford, C.H., M. Wingham and V.S. Sastri. "Ligand Photooxidation in Copper(II) Complexes of Nitrotriacetic Acid," *Environ. Sci. Technol.* 7:820-822 (1973).
131. Langford, C.H., and J.H. Carey. "The Charge Transfer Photochemistry of the Hexaquoiron(III) Ion, the Chloropentaaquoiron(III) Ion, and the μ -Dihydroxo Dimer Explored with tert-Butyl Alcohol Scavenging," *Can. J. Chem.* 53:2430-2435 (1975).
132. Lockhart, H.B., Jr., and R.V. Blakeley. "Aerobic Photodegradation of Fe(III)-(Ethylenedinitrilo) Tetraacetate (Ferric EDTA)," *Environ. Sci. Technol.* 12:1035-1038 (1975).
133. Miles, C.J., and P.L. Brezonik. "Oxygen Consumption in Humic-Colored Waters by a Photochemical Ferrous-Ferric Catalytic Cycle," *Environ. Sci. Technol.* 15:1089-1095 (1981).
134. Baker, A.D., A. Casadavell, H.D. Gafney and M. Gellender. "Photochemical Reactions of Tris(oxalato) Iron(III)," *J. Chem. Educ.* (1980), pp. 314-315.
135. Taylor, D.D., and R.C. Flagan. "Aerosols from a Laboratory Pulverized Coal Combustor," in *Atmospheric Aerosol: Source/Air Quality Relationships*, E.S. Macias and P.K. Hopke, Eds., ACS Symp. Ser. No. 167 (Washington, DC: American Chemical Society, pp. 157-172 (1981).
136. Ouimette, J.R., and R.C. Flagan. "Chemical Species Contributions to Light Scattering by Aerosols at a Remote Arid Site," in *Atmospheric Aerosol: Source/Air Quality Relationships*, E.S. Macias and P.K. Hopke, Eds., ACS Symp. Ser. No. 167 (Washington, DC: American Chemical Society, 1981), pp. 125-156.
137. Adamson, A.W., and P.D. Fleischauer. *Concepts of Inorganic Photochemistry* (New York: Wiley-Interscience, 1975).
138. Brodzinsky, R., S.G. Chang, S.S. Markowitz and T. Novakov. "Kinetics and Mechanism for the Catalytic Oxidation of Sulfur Dioxide on Carbon in Aqueous Suspensions," *J. Phys. Chem.* 84:3354-3358 (1980).
139. Chang, S.G., R. Toosi and T. Novakov. "The Importance of Soot Particles and Nitrous Acid in Oxidizing SO_2 in Atmospheric Aqueous Droplets," *Atmos. Environ.* 12:297-306 (1981).
140. Cohen, S., S. Chang, S. Markowitz and T. Novakov. "Role of Fly Ash in Catalytic Oxidation of S(IV) Slurries," *Environ. Sci. Technol.* 15:1498-1502 (1981).

141. Kim, K.K., and J.S. Choi. "Kinetics and Mechanism of the Oxidation of Sulfur Dioxide on α -Fe₂O₃," *J. Phys. Chem.* 85:2447-2450 (1981).
142. Faust, B.C., and M.R. Hoffmann. "Photocatalytic Oxidation of Dissolved Sulfur Dioxide on Fe₂O₃ Surfaces" (in progress).
143. Childs, A.L. "Studies in Photoassisted Heterogeneous Catalysis," PhD Thesis, Princeton University, Princeton, NJ (1981).
144. Childs, L.P., and D.F. Ollis. "Is Photocatalysis Catalytic?" *J. Catal.* 66:383-390 (1980).
145. Benner, W.H., R. Brodzinsky and T. Novakov. "Oxidation of SO₂ in Droplets Which Contain Soot Particles," *Atmos. Environ.* 16:1333-1340 (1982).
146. Colton, F.A., and G. Wilkinson. *Advanced Inorganic Chemistry* (New York: John Wiley & Sons, Inc., 1980).
147. Roberts, J.D., S. Ross and M.C. Caserio. *Organic Chemistry* (Menlo Park, CA: W.A. Benjamin, Inc., 1971).
148. Fridovich, I., and P. Handler. "Detection of Free Radicals in Illuminated Dye Solutions by the Initiation of Sulfite Oxidation," *J. Biol. Chem.* 235:1835-1838 (1960).
149. McCord, J.M., and I. Fridovich. "The Utility of Superoxide Dismutase in Studying Free Radical Reactions," *J. Biol. Chem.* 214:6056-6063 (1969).
150. Srinivasan, V.S., D. Podolski, N.J. Westrick and D.C. Neckers. "Photochemical Generation of O₂⁻ by Rose Bengal and Ru(bpy)₃²⁺," *J. Am. Chem. Soc.* 100:6513-6515 (1978).
151. Zika, R.G. "Photochemical Generation and Decay of Hydrogen Peroxide in Seawater," *Trans. Am. Geophys. Union* 61:1010 (1980).
152. Kok, G.L., T.P. Holler, M.B. Lopez, H.A. Nachtrieb and M. Yuan. "Chemiluminescent Method for Determination of Hydrogen Peroxide in the Ambient Atmosphere," *Environ. Sci. Technol.* 12:1072-1076 (1978).
153. Kok, G.L., K.R. Darnall, A.M. Winer, J.N. Pitts, Jr. and B.W. Gay. "Ambient Air Measurements of Hydrogen Peroxide in the California South Coast Basin," *Environ. Sci. Technol.* 12:1077-1080 (1978).
154. Kok, G.L. "Measurements of Hydrogen Peroxide in Rainwater," *Atmos. Environ.* 14:653-656 (1980).
155. Kok, G.L. "Measurements of Hydrogen Peroxide in Rainwater," *EOS Trans. Am. Geophys. Union* 45:884 (1981).
156. Walling, C. "Fenton's Reagent Revisited," *Accts. Chem. Res.* 12:125-131 (1975).
157. Baxendale, J. H. "Decomposition of Hydrogen Peroxide by Catalysts in Homogeneous Aqueous Solution," *Adv. Catal.* 4:31 (1952).
158. Uri, N. "Inorganic Free Radicals in Solution," *Chem. Rev.* 50:375 (1952).
159. Barrie, L.A. "An Experimental Investigation of the Absorption of Sulfur Dioxide by Cloud and Raindrops Containing Heavy Metals," PhD Thesis, University of Frankfurt (1975).
160. Penkett, S.A. "Oxidation of SO₂ and Other Atmospheric Gases by Ozone in Aqueous Solution," *Nature, Phys. Sci.* 240:105-106 (1972).
161. Erickson, R.E., L.M. Yates, R.L. Clark and D. McEwen. "The Reaction of Sulfur Dioxide with Ozone in Water and Its Possible Atmospheric Significance," *Atmos. Environ.* 11:813-817 (1977).
162. Espenson, J.H., and H. Taube. "Tracer Experiments with Ozone as Oxidizing Agent in Aqueous Solution," *Inorg. Chem.* 4:704-709 (1965).
163. Martin, L.R., D.E. Damschen and H.S. Judeikis. "The Reactions of Nitrogen Oxides with SO₂ in Aqueous Solution," *Atmos. Environ.* 15:191-195 (1981).
164. Oblath, S.B., S.S. Markowitz, T. Novakov and S.G. Chang. "Kinetics of Formation of Hydroxylamine Disulfonate by Reaction of Nitrite with Sulfites," *J. Phys. Chem.* 85:1017-1021 (1981).
165. Ross, D.S., C.L. Gu, G.P. Hum and D.G. Hendry. "Catalytic Oxidation of SO₂ by NO_x in Aqueous Systems" (submitted).
166. Grätzel, M., S. Taniguchi and A. Henglein. "Pulsradiolytisch Untersuchung der NO-Oxydation und des Gleichgewichts N₂O₃ ⇌ NO + NO₂ in Wässriger Lösung," *Ber. Bunsenges. Phys. Chem.* 74:488-492 (1970).
167. Takeuchi, H., M. Ando and N. Kizawa. "Absorption of Nitrogen Oxides in Aqueous Sodium Sulfite and Bisulfite Solutions," *Ind. Eng. Chem. Des. Dev.* 16:303-308 (1977).
168. Nash, T. "The Effect of Nitrogen Dioxide and of Some Transition Metals on the Oxidation of Dilute Bisulfite Solutions," *Atmos. Environ.* 13:1149-1154 (1979).
169. Morel, F.M., and J.J. Morgan. "A Numerical Method for Computing Equilibria in Aqueous Chemical Systems," *Environ. Sci. Technol.* 6:58-67 (1972).
170. Hoffmann, M. R. "Thermodynamic, Kinetic and Extrathermodynamic Considerations in the Development of Equilibrium Models for Aquatic Systems," *Environ. Sci. Technol.* 15:345-353 (1981).
171. Westall, J.C., J.L. Zachary and F.M. Morel. "MINEQL, A Computer Program for the Calculation of Chemical Equilibrium Composition of Aqueous Solutions," Tech. Note 18, Department of Civil Engineering, Massachusetts Institute of Technology, Cambridge, MA (1976).
172. Westall, J.C., and H. Hohl. "A Comparison of Electrostatic Models for the Oxide/Solution Interface," *Adv. Coll. Interface Sci.* 12:265-294 (1980).
173. Hansen, L.D., L. Whiting, D.J. Eatough, T.E. Jensen and R.M. Izatt. "Determination of Sulfur(IV) and Sulfate in Aerosols by Thermometric Methods," *Anal. Chem.* 48:634-638 (1976).
174. Eider, R.C., M.J. Heeg, M.D. Payne, M. Trkula and E. Deutsch. "Trans Effect in Octahedral Complexes. 3. Comparison of Kinetic and Trans Effects Induced by Coordinated Sulfur in Sulfite- and Sulfinatepentaamminecobalt(III) Complexes," *Inorg. Chem.* 17:431-440 (1978).
175. Raston, C.L., A.H. White and J.K. Yandell. "Structural and Kinetic Effects in Cobalt(III) Complexes with Cobalt-Sulfur Bonds. The Crystal Structure of trans-Bis(ethylenediamine)-imidazolesulfitecobalt(III) Perchlorate Dihydrate," *Aust. J. Chem.* 31:993-998 (1978).
176. Magnusson, A., L.G. Johansson and O. Lindqvist. "The Structure of Manganese(II) Sulfite," *Acta Cryst.* B37:1108-1110 (1981).
177. Johansson, L.G., and E. Ljungström. "Structure of Iron(II) Sulfite 2.5 Hydrate," *Acta Cryst.* B36:1184-1186 (1980).
178. Johansson, L.G., and O. Lindqvist. "Manganese(II) Sulfite Trihydrate," *Acta Cryst.* B36:2739-2741 (1980).
179. Baldwin, M.E. "Sulphitobis(ethylenediamine)Cobalt(III) Complexes," *J. Chem. Soc.* (1961), pp. 3123-3128.
180. Bordwell, F.G. *Organic Chemistry* (New York: Macmillan Co., 1963).
181. Dasgupta, P.K., K. DeCesare and J.C. Ullrey. "Determination of Atmospheric Sulfur Dioxide without Tetrachloromercurate(II) and the Mechanism of the Schiff Reaction," *Anal. Chem.* 52:1912-1922 (1980).
182. Fortune, C.R., and B. Dellinger. "Stabilization and Analysis of Sulfur(IV) Aerosols in Environmental Samples," *Environ. Sci. Technol.* 16:62-66 (1982).
183. Pankow, J.F., and J.J. Morgan. "Kinetics for the Aquatic Environment," *Environ. Sci. Technol.* 15:1155-1164, 1306-1313 (1981).
184. Adamowicz, R.F. "A Model for the Reversible Washout of Sulfur Dioxide, Ammonia

- and Carbon Dioxide from a Polluted Atmosphere and the Production of Sulfates in Raindrops." *Atmos. Environ.* 13:105-121 (1979).
185. Baboolal, L.B., H.R. Pruppacher and J.H. Topalian. "A Sensitivity Study of a Theoretical Model of SO₂ Scavenging by Water Drops in Air," *J. Atmos. Sci.* 38:856-870 (1981).
 186. Durham, J.L., J.H. Overton and V.P. Aneja. "Influence of Gaseous Nitric Acid on Sulfate Production and Acidity in Rain," *Atmos. Environ.* 15:1059-1068 (1981).
 187. Easter, R.C., and P.V. Hobbs. "The Formation of Sulfates and the Enhancement of Cloud Condensation Nuclei in Clouds," *J. Atmos. Sci.* 31:1586-1594 (1974).
 188. Seinfeld, J.H. *Lectures in Atmospheric Chemistry*, American Institute of Chemical Engineers Monograph Series 76 (1980).
 189. Graham, R.A., and H.S. Johnston. "The Photochemistry of NO₂ and the Kinetics of the N₂O₅-O₃ System," *J. Phys. Chem.* 82:254-268 (1978).
 190. Baulch, D.L., R.A. Cox, R.F. Hampson, Jr., J.A. Kerr, J. Troe and R.T. Watson. "Evaluated Kinetic and Photochemical Data for Atmospheric Chemistry," *J. Phys. Chem. Ref. Data* 9:295-471 (1980).
 191. Richards, L.W. "Comments on the Oxidation of NO₂ to Nitrate—Day and Night," *Atmos. Environ.* (in press).
 192. Schwartz, S.E., and J.E. Freiberg. "Mass-Transport Limitation to the Rate of Reaction of Gases in Liquid Droplets: Application to Oxidation of SO₂ in Aqueous Solutions," *Atmos. Environ.* 15:1129-1144 (1981).
 193. Freiberg, J.E., and S.E. Schwartz. "Oxidation of SO₂ in Aqueous Droplets: Mass-Transport Limitation in Laboratory Studies and the Ambient Atmosphere," *Atmos. Environ.* 15:1145-1154 (1981).
 194. Rodhe, B. "The Effect of Turbulence on Fog Formation," *Tellus* 14:49-86 (1962).
 195. McRae, G.J. Personal communication.
 196. *Kirk-Othmer Encyclopedia of Chemical Technology*, Vol. 16, 3rd ed., (1981), p. 701.
 197. Beutier, D., and H. Renon. "Representation of NH₃-H₂S, H₂O-NH₃-CO₂-H₂O, and NH₃-SO₂-H₂O Vapor-Liquid Equilibria," *Ind. Eng. Chem. Process. Des. Dev.* 17:220-228 (1978).